

Bangor University

DOCTOR OF PHILOSOPHY

Petrov-Galerkin finite element methods

Dogan, Abdulkadir.

Award date:
1997

Awarding institution:
Bangor University

[Link to publication](#)

General rights

Copyright and moral rights for the publications made accessible in the public portal are retained by the authors and/or other copyright owners and it is a condition of accessing publications that users recognise and abide by the legal requirements associated with these rights.

- Users may download and print one copy of any publication from the public portal for the purpose of private study or research.
- You may not further distribute the material or use it for any profit-making activity or commercial gain
- You may freely distribute the URL identifying the publication in the public portal ?

Take down policy

If you believe that this document breaches copyright please contact us providing details, and we will remove access to the work immediately and investigate your claim.

Download date: 19. Sept. 2024

PETROV-GALERKIN FINITE ELEMENT METHODS

Thesis submitted to University of Wales in support of
the application for the degree of Philosophiæ Doctor

by

ABDULKADIR DOGAN

supervised by

DR. L. R. T. GARDNER

1991 MATHEMATICS SUBJECT CLASSIFICATION: 35Q20, 65N30,
65N35, 76B25.

KEY WORDS: RLW equation, Burgers' Equation, Galerkin, Finite element,
methods, Undular bore, Petrov-Galerkin.

ABDULKADIR DOGAN
School of Mathematics,
University of Wales,
Dean Street,
Bangor,
Gwynedd,
U.K



June 1997

Third party material to be excluded from digitised thesis:

None

**PETROV-GALERKIN FINITE
ELEMENT METHODS
ABDULKADIR DOGAN**

Dedicated

to

*my mother, my father, my wife , my daughter , younger brothers and
younger sister*

Declaration

The work of this thesis has been carried out by the candidate and contains the results of his own investigations. The work has not been already accepted in substance for any degree, and is not being concurrently submitted in candidature for any degree. All sources of information have been acknowledged in the text.

Director of Studies
Dr. L. R. T. Gardner

Candidate
Abdulkadir Dogan

Statement

I hereby grant consent for my thesis, if accepted, to be available for photocopying and inter-library loan and for the title and summary to be made available to outside organisations.

Candidate: _____

Acknowledgements

I would like to thank my supervisor, Dr. L. R. T. Gardner, for his help, encouragement and guidance during the course of this work and the preparation of my thesis, and I would like also to express my gratitude to Dr. G. A. Gardner, for invaluable discussion, comments on mathematics and advice.

It is my pleasure to acknowledge the support and encouragement of my beloved wife, my daughter and all my family, in all stages of the preparation of this thesis.

Thanks go to all friends and the staff with whom I have enjoyed working in Bangor. I am also grateful to all people who have helped me so far.

Finally, thanks are due to the Turkish Government, The Council of Higher Education and University of Nigde for providing me with a maintenance grant. This research would not have been possible without The Council of Higher Education Scholarship which Turkish Government awarded me.

This Thesis was typeset using L^AT_EX.

Summary

The main aim of this work is the study of Petrov-Galerkin finite element methods and their application to the numerical solution of transient non-linear partial differential equations. We use as examples numerical algorithms for the solution of the Regularised Long Wave equation and Burgers' equation.

Firstly the theoretical background to the finite element method is discussed.

In the following chapters finite element methods based on the Petrov-Galerkin approach are set up. Firstly we set up Galerkin's method, and later the least squares method and a Petrov-Galerkin method containing a piecewise constant weight function. The appropriate element matrices are determined algebraically using the computer algebra package Maple. Finally we set out to extend the least squares algorithm to include quadratic B-spline elements.

The numerical algorithms for the RLW equation have been tested by studying the motion, interaction and development of solitary waves. We have shown that these algorithms can faithfully represent the amplitude of a single solitary wave over many time steps and predict the progress of the wave front with small error. In the interaction of two solitary waves the numerical algorithms reproduce the change in amplitudes and the phase advance, and phase retardation caused by the interaction. The development of an undular bore is modelled and we demonstrate that its shape, height and velocity are consistent with earlier results.

Simulations arising from three different initial conditions for Burgers'

time finite elements. The results are compared with published data and found to be consistent. Also, simulations arising from four different initial conditions for Burgers' Equation are studied using a Petrov-Galerkin method with quadratic B-spline finite elements and a piecewise constant weight function. It is demonstrated that the results obtained agree well with earlier work.

The L_2 and L_∞ error norms for all problems are, where possible, compared with published data. We conclude that Petrov-Galerkin methods are eminently suitable for the numerical solution of transient non-linear partial differential equations leading, as we have shown, to very accurate results.

Contents

Acknowledgements	i
Summary	ii
1 Introduction	1
2 Finite Element Methods	3
2.1 Introduction	3
3 A Galerkin Finite Element Scheme For The RLW Equation	10
3.1 Introduction	10
3.2 The finite element solution	11
3.2.1 Stability Analysis	15
3.3 Test problems	16
3.3.1 Conservation laws for the RLW equation	16
3.3.2 Error norms	18
3.3.3 Solitary wave motion	19
3.3.4 Two wave interactions	44
3.4 Discussion	48
4 A Least-Squares Finite Element Scheme For The RLW Equation	49
4.1 Introduction	49
4.2 The finite element solution	50
4.2.1 Stability Analysis	55

4.3	Test problems	56
4.3.1	Solitary wave motion	57
4.4	Modelling an undular bore	78
4.5	Discussion	83
5	A Petrov-Galerkin Algorithm For The RLW Equation	85
5.1	Introduction	85
5.2	The finite element solution	86
5.2.1	Stability Analysis	88
5.3	Validation	89
5.4	Modelling an undular bore	107
5.5	Discussion	121
6	A Least-Squares Finite Element Scheme For Burgers' Equation	122
6.1	Introduction	122
6.2	The finite element solution	123
6.2.1	Stability Analysis	127
6.3	Test problems	128
6.4	Discussion	147
7	A Petrov-Galerkin Finite Element Scheme For Burgers' Equation	148
7.1	Introduction	148
7.2	The finite element solution	150
7.2.1	Stability Analysis	154
7.3	The initial state	155
7.4	Test problems	157
7.5	Discussion	181
8	A Least-Squares Quadratic B-Spline Finite Element Scheme For The RLW Equation	182
8.1	Introduction	182
8.2	The B-spline finite element solution	182

9 General Conclusions	189
Bibliography	192

Chapter 1

Introduction

In Chapter 2, we describe weighted residual methods, Galerkin, Petrov-Galerkin, least square method.

In Chapter 3, a Galerkin Finite Element scheme is set up for The Regularised long Wave Equation. The element matrices are determined algebraically using MAPLE. Assembling the element matrices together and using a Crank-Nicolson difference scheme for the time derivative leads to a set of quasi-linear equations which are solved by a tridiagonal algorithm. The method is tested by calculating how the L_2 and L_∞ error norms change during the motion of a single and double solitary wave and comparing this work with the error found by earlier authors for a similar experiment. Three conservative quantities C_1 , C_2 , C_3 are also computed for simulations using a single solitary wave and double solitary wave as initial condition. Besides this the interaction of two solitary waves, both of small amplitude, are simulated.

In Chapter 4, we set up a numerical algorithm for the solution of the Regularised Long Wave Equation using a least squares finite element method together with a Crank-Nicolson difference scheme for the time derivative which leads to a set of quasi-linear equations which are solved using a tridiagonal algorithm. A linear stability analysis is used to show that the scheme is unconditionally stable. The L_2 and L_∞ error norms have been calculated for single and double solitary wave simulations and compared with the error found by earlier authors. Three conservative quantities C_1 , C_2 , C_3 have been

computed. Lastly the development of an undular bore from an appropriate initial condition is simulated.

In Chapter 5, we set up a Petrov-Galerkin scheme for the Regularised Long Wave Equation using quadratic elements and piecewise constant weight functions.

In chapter 6, we set up a numerical solution of Burgers' Equation using a least squares approach with linear elements. This leads to set of quasi linear equations which can be solved using a tridiagonal algorithm. A linear stability analysis is set up which shows that the scheme is unconditionally stable. We describe simulations arising from three different initial conditions and the results of these experiments are compared with published data. As the analytic solution is expressed in closed form the L_2 and L_∞ error norms are easily calculated. The results of our computations are given in Figures and Tables and are compared with the analytic solutions given by Kakuda and Tosaka.

In Chapter 7, a Petrov-Galerkin scheme using quadratic elements together with a piecewise constant weight function is set up for Burgers' Equation. Similar problems are discussed.

In Chapter 8, a least-squares quadratic B-Spline finite element scheme is set up for the the Regularised Long Wave Equation. A computer program based on this approach is in progress of being developed.

Finally, in Chapter 9 we draw conclusions on this work.

Chapter 2

Finite Element Methods

2.1 Introduction

The term finite element was first used by Clough [31] in 1960. Since its inception, the literature on finite element applications has grown exponentially, [21, 35, 101, 104, 105] and today there are numerous journals which are primarily devoted to the theory and applications of the finite element method [92].

The finite element method is now widely accepted as the first choice numerical method in all kinds of structural engineering applications in aerospace, naval architecture and the nuclear power industry. Applications to fluid mechanics are currently being developed for the study of tidal motion, thermal and chemical transport and diffusion problems, as well as for fluid-structure interactions.

During the nineteen-sixties, research on the finite element method was widely pursued simultaneously in various parts of the world, particularly in the following directions.

a) The method was reformulated as a special case of the weighted residual method.

b) A wide variety of elements were developed including bending elements, curved elements.

c) The method was recognised as a general method for the solution of partial differential equations. Its applicability to the solution of nonlinear and dynamic problems of structures was amply demonstrated as was its extension into other domains such as soil mechanics, fluid mechanics and thermodynamics. Solutions were obtained to engineering problems hitherto thought intractable [36].

In the finite difference approximation of a differential equation, the derivatives in the equation are replaced by difference quotients which involve the values of the solution at discrete mesh points of the domain. The resulting discrete equations are solved, after imposing the boundary conditions, for the values of the solution at the mesh points. Although the finite difference method is simple in concept, it suffers from several disadvantages. The most notable are the inaccuracy of the derivatives of the approximated solution, the difficulty in imposing the boundary conditions along nonstraight boundaries, the difficulty in accurately representing geometrically complex domains, and the inability to employ nonuniform and nonrectangular meshes.

The finite element method overcomes some of the difficulties of the finite difference method because it is based on integral formulations. The geometrical domain of the problem is represented as a collection of finite elements and can be divided into nonuniform and nonrectangular elements if the need arises [92].

Modern finite element integral formulations are mainly obtained by two different procedures: variational formulations and weighted residual formulations [3].

Variational models usually involve finding the nodal parameters that yield a stationary (maximum or minimum) value of a specific integral relation known as a functional. It is well known that the solution that yields a stationary value of the functional and satisfies the boundary conditions, is equivalent to the solution of an associated differential equation known as the Euler equation. If the functional is known, then it is relatively easy to find the corresponding Euler equation.

Most engineering and physical problems are initially defined in terms of a differential equation. The finite element method requires an integral for-

mulation so that one must search for the functional whose Euler equation has been given. Unfortunately, this is a difficult and sometimes impossible task, therefore there is an increasing emphasis on the various weighted residual techniques that can generate an integral formulation directly from the original differential equations.

The generation of finite element models by weighted residual techniques is a relatively recent development. However, these methods are increasingly important in the solution of differential equations.

Let us start with finding an unknown function u which satisfies a certain operator equation:

$$Au = f \quad \text{in } \Omega = (a, b) \quad (2.1)$$

where f is a known function and Ω is the domain of interest. A is a real differential operator of order $2m$ (m is positive). The differential operator A is linear in u and its derivatives appear linearly in A . Otherwise A is nonlinear.

The boundary conditions can contain the derivatives up to $2m - 1$ and at each boundary point there are m boundary conditions. If the boundary conditions involve u and derivatives of order less than m then they are called essential. Otherwise they are natural.

In the weighted residual method the solution u is approximated by the interpolation functions ϕ_j through:

$$u_N = \sum_{j=1}^N c_j \phi_j \quad (2.2)$$

where c_j are unknown parameters to be determined.

The best choice of the approximated functions ϕ_j are polynomials because polynomials are easy to manipulate, both algebraically and computationally. Polynomials are also attractive from the point of view of the Weierstrass approximation theorem which states that any continuous function may be approximated, arbitrarily closely, by a suitable polynomial.

The choice of the approximation ϕ_j is required to satisfy the following conditions: The approximation must

- (a) have geometrical invariance,

- (b) contain a complete polynomial which includes all the lower terms, and
- (c) have sufficient continuity and parameters to represent the solution.

Substitute the approximate solution (2.2) into the operator equation (2.1). This operation defines a residual R_N :

$$R_N = Au - f \quad (2.3)$$

where R_N is a function of the chosen independent functions ϕ_j and the unknown parameters c_j . To determine the unknown parameters c_j using the weighted residual method one can set the integral, over the domain Ω , of the product of the residual and some weight functions ψ_j to be zero:

$$\int_{\Omega} \psi_j R_N dx = 0 \quad j = 1, \dots, N \quad (2.4)$$

where the weight functions, in general, are not the same as the approximation functions ϕ_j . The equation (2.4) can be simplified to the form:

$$\sum_{j=1}^N \left(\int_{\Omega} \psi_i A \phi_j dx \right) c_j = \int_{\Omega} \psi_i f dx$$

or

$$\sum_{j=1}^N A_{ij} c_j = f_i \quad (2.5)$$

where:

$$A_{ij} = \int_{\Omega} \psi_i A \phi_j dx$$

$$f_i = \int_{\Omega} \psi_i f dx$$

For different choices of the weight functions we find different types of the weighted residual technique (2.4).

For $\psi_i \equiv \phi_i$, the weighted residual method (2.4) is called the Galerkin method while the weighted residual approach is called the Petrov-Galerkin method, if $\psi_i \neq \phi_i$.

To find the least square method one determines the parameters c_i by minimising the integral of the square of the residual (2.4):

$$\frac{\partial}{\partial c_i} \int R_N^2 dx = 0$$

or

$$\int \frac{\partial R_N}{\partial c_j} R_N dx = 0 \quad (2.6)$$

The Equation (2.6) can be written in simplified form:

$$\sum_{j=1}^N \left(\int_{\Omega} A\phi_i A\phi_j dx \right) c_j = \int_{\Omega} (A\phi_i) f dx$$

or

$$\sum_{j=1}^N A_{ij} c_j = f_i \quad (2.7)$$

where

$$A_{ij} = \int_{\Omega} (A\phi_i)(A\phi_j) dx$$

$$f_i = \int_{\Omega} (A\phi_i) f dx$$

Another popular method for solving the boundary value problem is the collocation method. The idea behind this approach is to make the residual in Equation (2.3) zero at N selected points in the domain Ω :

$$R_N(x_i) = 0 \quad i = 1, \dots, N \quad (2.8)$$

or

$$\sum_{j=1}^N c_j A\phi_j(x_i) = f(x_i) \quad i = 1, \dots, N \quad (2.9)$$

Equation (2.9) gives a system of N equations in the N unknown parameters c_j which can be solved numerically.

For both variational and weighted residual formulations the following restrictions are generally accepted as a means of establishing convergence of the finite element model as the mesh is increasingly refined: [3]

a) (A necessary criterion) the element interpolation functions must be capable of modelling any constant values of the dependent variable or its

derivatives, to the order present in the defining integral statement, in the limit as the element size decreases.

b) (A sufficient criterion) the element shape functions should be chosen so that at element interfaces the dependent variable and its derivatives, of up to one order less than those occurring in the defining integral statement, are continuous.

The basic ideas introduce certain terms that are used in the finite-element analysis of any problem: [92]

a) Finite-element discretisation. First, the continuous region or line is represented as a collection of a finite number n of subregions, say segments for example. This is called the discretisation of the domain by segments. Each of these segments is called an element. The collection of elements is called the finite-element mesh. One can discretise the domain, depending on the shape of the domain, into a mesh of more than one type of element.

b) Error estimate. There are three kinds of error in a finite-element solution:

- (i) errors due to the approximation of the domain
- (ii) errors due to the approximation of the solution
- (iii) errors due to numerical computation.

c) Number and location of the nodes. The number and location of the nodes in an element depends on

- (i) the geometry of the element
- (ii) the degree of the approximation (i.e., the degree of the polynomials),
- (iii) the variational form of the equation.

d) Assembly of elements. The assembly of elements, in a general case, is based on the idea that the solution is continuous at the interelement boundaries.

e) Accuracy and convergence. The accuracy and convergence of the finite-element solution depends on the differential equation solved and the elements used. The word “accuracy” refers to the difference between the exact solution and the finite-element solution, and the word “convergence” refers to the accuracy as the number of elements in the mesh is increased.

f) The time dependent problems. For time dependent problems, there are

derivatives, to the order present in the defining integral statement, in the limit as the element size decreases.

b) (A sufficient criterion) the element shape functions should be chosen so that at element interfaces the dependent variable and its derivatives, of up to one order less than those occurring in the defining integral statement, are continuous.

The basic ideas introduce certain terms that are used in the finite-element analysis of any problem: [92]

a) Finite-element discretisation. First, the continuous region or line is represented as a collection of a finite number n of subregions, say segments for example. This is called the discretisation of the domain by segments. Each of these segments is called an element. The collection of elements is called the finite-element mesh. One can discretise the domain, depending on the shape of the domain, into a mesh of more than one type of element.

b) Error estimate. There are three kinds of error in a finite-element solution:

- (i) errors due to the approximation of the domain
- (ii) errors due to the approximation of the solution
- (iii) errors due to numerical computation.

c) Number and location of the nodes. The number and location of the nodes in an element depends on

- (i) the geometry of the element
- (ii) the degree of the approximation (i.e., the degree of the polynomials),
- (iii) the variational form of the equation.

d) Assembly of elements. The assembly of elements, in a general case, is based on the idea that the solution is continuous at the interelement boundaries.

e) Accuracy and convergence. The accuracy and convergence of the finite-element solution depends on the differential equation solved and the elements used. The word “accuracy” refers to the difference between the exact solution and the finite-element solution, and the word “convergence” refers to the accuracy as the number of elements in the mesh is increased.

f) The time dependent problems. For time dependent problems, there are

two steps to be followed:

i) The partial differential equations are approximated by the finite element method to obtain a set of ordinary differential equations in time.

ii) The ordinary differential equations in time are solved approximately by finite difference methods to obtain algebraic equations, which are then solved for the nodal values.

The basic steps for the solution of a differential equation using the finite element method is as follows: [92]

a) Divide the given domain into a finite elements. Number the nodes (the points of subdomains where the function is evaluated) and the elements. Generate the geometric properties (such as; coordinates, cross-sectional area, and so on) needed for the problem.

b) Evaluate the element equations by constructing a suitable weighted residual formula of given differential equation using:

$$u = \sum_{i=1}^N u_i \psi_i \quad (2.10)$$

where ψ_i are the chosen interpolation functions.

If we substitute the Equation (2.10) in the chosen weighted residual formula, we will find the formula:

$$\{K^e\}\{u^e\} = \{F^e\} \quad (2.11)$$

c) Assemble the element contributions to find the equation for the whole problem.

d) Impose the boundary conditions of the problem.

e) Solve the overall system of equations.

f) Compute the solution and represent the results in tabular and/or graphical form.

Chapter 3

A Galerkin Finite Element

Scheme For The RLW Equation

3.1 Introduction

The regularised long wave (RLW) equation is solved by Galerkin's method using linear space finite elements. In simulations of the migration of a single solitary wave this algorithm is shown to have good accuracy for small amplitude waves. In addition, for very small amplitude waves (≤ 0.09) it has higher accuracy than an approach using quadratic B-spline finite elements within Galerkin's method. The interaction of two solitary waves is modelled for small amplitude waves.

The RLW equation plays a major role in study of non-linear dispersive waves [19, 89]. There is experimental evidence to suggest that this description breaks down if the amplitude of any wave exceeds about 0.28, since wave breaking is then observed with water waves [89].

The RLW equation has been solved numerically by Eilbeck and McGuire [37] Bona et al [19] and, more recently, by Jain et al [64]. We have studied the RLW equation using Galerkin's method with both cubic [40] and quadratic [46] B-spline finite elements and a least squares technique [83, 84] with space-time linear finite elements [49]. Here we use Galerkin's method

with linear finite elements [83, 84] to construct a numerical solution. We discuss the properties and advantages of this method and compare its accuracy in modelling a solitary wave with that of numerical algorithms described in references [64], [46] and [49]. Finally, the interaction of two solitary waves of small amplitude is studied.

3.2 The finite element solution

We solve the normalised RLW equation

$$U_t + U_x + \epsilon U U_x - \mu U_{xxt} = 0, \quad (3.1)$$

where ϵ , μ are positive parameters and the subscripts x and t denote differentiation. When the RLW equation is used to model waves generated in a shallow water channel the variables are normalised in the following way. Distance x and water elevation U are scaled to the water depth h and time t is scaled to $\sqrt{h/g}$, where g is the acceleration due to gravity. Physical boundary conditions require $U \rightarrow 0$ as $|x| \rightarrow \infty$.

When applying Galerkin's method we minimise the functional [103]

$$\int_0^L [U_t + U_x + \epsilon U U_x - \mu U_{xxt}] W_j dx = 0, \quad (3.2)$$

where W_j is a weight function, with respect to the nodal variables.

A uniform spatial array of linear finite elements is set up $0 = x_0 < x_1 \dots < x_N = L$. A typical finite element of size $\Delta x = (x_{m+1} - x_m)$, mapped by local coordinates ξ , where $x = x_m + \xi \Delta x$, $0 \leq \xi \leq 1$, makes, to integral (3.2), the contribution

$$\int_0^1 [U_t + \frac{1}{\Delta x} U_\xi + \frac{\epsilon}{\Delta x} \hat{U} U_\xi - \frac{\mu}{\Delta x^2} U_{\xi\xi t}] W_j d\xi, \quad (3.3)$$

where to simplify the integral, \hat{U} is taken to be constant over an element. This leads to

$$\int_0^1 [U_t + v U_\xi - b U_{\xi\xi t}] W_j d\xi, \quad (3.4)$$

where

$$b = \frac{\mu}{\Delta x^2},$$

and

$$v = \frac{1}{\Delta x}(1 + \epsilon \hat{U})$$

is taken as locally constant over each element. The variation of U over the element $[x_m, x_{m+1}]$ is given by

$$U^e = \sum_{j=1}^2 N_j u_j, \quad (3.5)$$

where N_1, N_2 are linear spatial basis functions and $u_1(t), u_2(t)$ are the nodal parameters. With the local coordinate system ξ defined above the basis functions have expressions [103]

$$N_1 = 1 - \xi,$$

$$N_2 = \xi.$$

For Galerkin's method we identify the weight functions W_j with the basis functions N_j giving

$$\int_0^1 [U_t + vU_\xi - bU_{\xi\xi t}] N_j d\xi. \quad (3.6)$$

Integrating by parts leads to

$$\int_0^1 [(U_t + vU_\xi) N_j + bU_{\xi t} N_j'] d\xi. \quad (3.7)$$

Now if we substitute for U using Equation (3.5), an element's contribution is obtained in the form

$$\sum_{k=1}^2 \int_0^1 [(N_k \frac{du_k}{dt} + v N_k' u_k) N_j + b N_k' N_j' \frac{du_k}{dt}] d\xi, \quad (3.8)$$

where the prime denotes differentiation with respect to ξ , which in matrix form becomes

$$[A^e + bD^e] \frac{du^e}{dt} + C^e u^e, \quad (3.9)$$

where

$$u^e = (u_1, u_2)^T,$$

are the relevant nodal parameters. The element matrices are

$$A_{jk}^e = \int_0^1 N_j N_k d\xi,$$

$$C_{jk}^e = v \int_0^1 N_j N_k',$$

$$D_{jk}^e = \int_0^1 N_j' N_k',$$

where j, k take only the values 1 and 2. The matrices A^e , C^e and D^e are thus 2x2, and have the explicit forms

$$A^e = \frac{1}{6} \begin{pmatrix} 2 & 1 \\ 1 & 2 \end{pmatrix},$$

$$C^e = \frac{1}{2} v \begin{pmatrix} -1 & 1 \\ -1 & 1 \end{pmatrix},$$

$$D^e = \begin{pmatrix} 1 & -1 \\ -1 & 1 \end{pmatrix},$$

and v given by

$$v = \frac{1}{\Delta x} (1 + \epsilon u_1),$$

is constant over the element.

Formally assembling together contributions from all elements leads to the matrix equation

$$[A + bD] \frac{du}{dt} + [C]u = 0, \quad (3.10)$$

and $u = (u_0, u_1, \dots, u_N)^T$, contains all the nodal parameters. The matrices A, C, D are tridiagonal and row m of each has the following form:

$$A : \frac{1}{6} (1, 4, 1)$$

$$D : (-1, 2, -1)$$

$$C : \frac{1}{2}(-v_{m-1}, v_{m-1} - v_m, v_m)$$

A typical member of (3.10) is

$$\begin{aligned} & \frac{d}{dt} \left[\left(\frac{1}{6} - b \right) u_{m-1} + \left(\frac{2}{3} + 2b \right) u_m + \left(\frac{1}{6} - b \right) u_{m+1} \right] \\ &= \frac{1}{2} v_{m-1} u_{m-1} - \frac{1}{2} (v_{m-1} - v_m) u_m - \frac{1}{2} v_m u_{m+1}, \end{aligned} \quad (3.11)$$

where v_m is given by

$$v_m = \frac{1}{\Delta x} (1 + \epsilon u_m^n).$$

To obtain a numerical solution for this set of ordinary differential equations we can use a Crank-Nicolson approach and centre on $t = (n + \frac{1}{2})\Delta t$ and let

$$\frac{du_m}{dt} = \frac{1}{\Delta t} (u_m^{n+1} - u_m^n), \quad (3.12)$$

$$u_m = \frac{1}{2} (u_m^{n+1} + u_m^n). \quad (3.13)$$

Hence we obtain the recurrence relationship

$$\begin{aligned} & \left(\frac{1}{6} - b - \frac{\Delta t}{4} v_{m-1} \right) u_{m-1}^{n+1} + \left(\frac{2}{3} + 2b + \frac{\Delta t}{4} [v_{m-1} - v_m] \right) u_m^{n+1} \\ & \quad + \left(\frac{1}{6} - b + \frac{\Delta t}{4} v_m \right) u_{m+1}^{n+1} = \left(\frac{1}{6} - b + \frac{\Delta t}{4} v_{m-1} \right) u_{m-1}^n \\ & \quad + \left(\frac{2}{3} + 2b - \frac{\Delta t}{4} [v_{m-1} - v_m] \right) u_m^n + \left(\frac{1}{6} - b - \frac{\Delta t}{4} v_m \right) u_{m+1}^n. \end{aligned} \quad (3.14)$$

The boundary conditions $U(0, t) = 0$ and $U(L, t) = 0$ require $u_0 = 0$ and $u_N = 0$. The above set of quasi-linear equations has a matrix which is tridiagonal in form so that a solution using the Thomas algorithm is possible, however, due to the presence of the non-linear term an inner iteration may be required.

3.2.1 Stability Analysis

The growth factor g of the error ϵ_j^n in a typical Fourier mode of amplitude $\hat{\epsilon}^n$

$$\hat{\epsilon}_j^n = \hat{\epsilon}^n \exp(ijk\Delta x) \quad (3.15)$$

where k is the mode number and Δx the element size, is determined for a linearisation of the numerical scheme.

In the linearisation it is assumed that the quantity U in the nonlinear term is locally constant. Under these conditions the error ϵ_j^n satisfies the same finite difference scheme as the function δ_j^n and we find that a typical member of Equation (3.14) has the form

$$\begin{aligned} & \left(\frac{1}{6} - b - \frac{\Delta t}{4\Delta x}\right)\epsilon_{m-1}^{n+1} + \left(\frac{2}{3} + 2b\right)\epsilon_m^{n+1} \\ & + \left(\frac{1}{6} - b + \frac{\Delta t}{4\Delta x}\right)\epsilon_{m+1}^{n+1} = \left(\frac{1}{6} - b + \frac{\Delta t}{4\Delta x}\right)\epsilon_{m-1}^n \\ & + \left(\frac{2}{3} + 2b\right)\epsilon_m^n + \left(\frac{1}{6} - b - \frac{\Delta t}{4\Delta x}\right)\epsilon_{m+1}^n, \end{aligned} \quad (3.16)$$

where

$$b = \frac{\mu}{\Delta x^2}$$

substituting the above Fourier mode gives

$$(p + iq)\epsilon^{\hat{n}+1} = (p - iq)\epsilon^{\hat{n}}$$

where

$$p = \left(\frac{1}{3} - 2b\right) \cos[k\Delta x] + \left(\frac{2}{3} + 2b\right)$$

and

$$q = \frac{\Delta t}{2\Delta x} \sin[k\Delta x].$$

Writing $\epsilon^{\hat{n}+1} = g\epsilon^{\hat{n}}$, it is observed that $g = \frac{p-iq}{p+iq}$ and so has unit modulus. Hence the linearised scheme is unconditionally stable.

3.3 Test problems

With the boundary conditions $U \rightarrow 0$ as $x \rightarrow \pm\infty$ the solitary wave solution of the RLW equation is [89]

$$U(x, t) = 3c \operatorname{sech}^2(k[x - vt - x_0]), \quad (3.17)$$

where

$$k^2 = \frac{\epsilon c}{4\mu(1 + \epsilon c)},$$

and

$$v = 1 + \epsilon c,$$

is the wave velocity. It is expected that this solution will also be valid for sufficiently wide finite regions.

3.3.1 Conservation laws for the RLW equation

Partial differential equations possess an infinite number of conservation laws. An important state in the development of the general method of solution for the RLW equation is that solutions obey a number of independent conservation laws. Definition [2], pages 21-22.

For the partial differential equation

$$U(x, t, u(x, t)) = 0,$$

where $x \in \mathbf{R}$, $t \in \mathbf{R}$ (real numbers) are temporal and spatial variables and $u(x, t) \in \mathbf{R}$ the dependent variable, a conservation law is an equation of the form

$$\frac{\partial}{\partial t} T_i + \frac{\partial}{\partial x} X_i = 0$$

which is satisfied for all solutions of the equations. Where $T_i(x, t)$ the conserved density, and $X_i(x, t)$, the associated flux, which are in general, functions of x, t, u and the partial derivatives of u ; $\frac{\partial}{\partial t}$ shows the partial derivative with respect to t ; and $\frac{\partial}{\partial x}$ the partial derivative with respect to x . If additionally, u tends to zero as $|x| \rightarrow \infty$ sufficiently rapidly

$$\frac{\partial}{\partial t} \int_{-\infty}^{\infty} T_i(x, y) = 0.$$

Therefore

$$\int_{-\infty}^{\infty} T_i(x, y) = b,$$

where b , a constant, is the conserved density.

For the RLW equation there are only three conservation laws [86],

$$i) \quad C_1 = \int_{-\infty}^{+\infty} U dx,$$

$$ii) \quad C_2 = \int_{-\infty}^{+\infty} [U^2 + \mu(U_x)^2] dx,$$

$$iii) \quad C_3 = \int_{-\infty}^{+\infty} [U^3 + 3U^2] dx.$$

In the simulations of solitary wave motion that follow the invariants C_1 , C_2 and C_3 are monitored to check the conservation of the numerical algorithm.

i) We assume (a) that $U, U_x, U_{xt} \rightarrow 0$ as $x \rightarrow \pm\infty$ and (b) $C_1 = \int_{-\infty}^{+\infty} U dx$ exists. When Equation (3.1) is multiplied by $U^0 = 1$ and then integrated between $x = -R$ and $x = R$, gives

$$\int_{-R}^R U_t dx + [U + \frac{\epsilon}{2}U^2 - \mu U_{xt}]_{x=-R}^{x=R} = 0.$$

Because of (a) the integrated terms vanish in the limit as $R \rightarrow \infty$, and hence we have

$$\int_{-\infty}^{\infty} (U_t) dx = \frac{dC_1}{dt} = 0.$$

Thus C_1 is a constant.

ii) When Equation (3.1) is multiplied by U and then integrated between $x = -R$ and $x = R$, an integration by parts of the final term on the left hand side gives

$$\begin{aligned} & \int_{-R}^R (UU_t + \mu U_x U_{xt}) dx \\ & + [\frac{1}{2}U^2 + \frac{\epsilon}{3}U^3 - \mu U U_{xt}]_{x=-R}^{x=R} = 0. \end{aligned}$$

Because of (a) the integrated terms vanish in the limit as $R \rightarrow \infty$, and hence we have

$$\int_{-\infty}^{\infty} (UU_t + \mu U_x U_{xt}) dx = \frac{1}{2} \frac{dC_2}{dt} = 0.$$

Thus C_2 is a constant.

iii) When Equation (3.1) is multiplied by $U^2 + 2U$ and then integrated between $x = -R$ and $x = R$, an integration by parts gives

$$\int_{-R}^R \left[\left(\frac{1}{3} U^3 \right)_t + (U^2)_t \right] dx \\ + [U^2 + U^3 + \frac{1}{4} U^4]_{x=-R}^{x=R} = 0.$$

Because of (a) the integrated terms vanish in the limit as $R \rightarrow \infty$, and hence we have

$$\frac{d}{dt} \int_{-\infty}^{\infty} \left(\frac{1}{3} U^3 + U^2 \right) dx = \frac{1}{3} \frac{dC_3}{dt} = 0.$$

Thus $C_3 = \text{constant}$.

3.3.2 Error norms

The L_2 and L_∞ error norms

$$\|U^{exact} - U^n\|_2 = [\Delta x \sum_1^N |U_j^{exact} - U_j^n|^2]^{\frac{1}{2}},$$

and

$$\|U^{exact} - U^n\|_\infty = \max_j |U_j^{exact} - U_j^n|,$$

measure the mean and maximum differences between the numerical and analytic solutions.

Table 3.1

Invariants and error norms for single solitary wave
amplitude=0.3, $\Delta x = 0.125$, $\Delta t = 0.1$, $-40 \leq x \leq 60$.

method	time	C_1	C_2	C_3	$L_2 \times 10^3$	$L_\infty \times 10^3$
Galerkin linear elements	0	3.97993	0.810461	2.57901	0.002	0.007
	2	3.98016	0.810532	2.57924	0.060	0.028
	4	3.98039	0.810610	2.57950	0.116	0.054
	6	3.98060	0.810677	2.57972	0.170	0.077
	8	3.98083	0.810752	2.57996	0.224	0.100
	10	3.98105	0.810822	2.58020	0.276	0.120
	12	3.98125	0.810884	2.58041	0.325	0.139
	14	3.98144	0.810947	2.58061	0.370	0.155
	16	3.98165	0.811014	2.58083	0.417	0.171
	18	3.98187	0.811095	2.58110	0.467	0.185
	20	3.98206	0.811164	2.58133	0.511	0.198
Galerkin quadratic [46]	20	3.97989	0.810467	2.57902	0.220	0.086
l.s linear [49]	20	3.98203	0.808650	2.57302	4.688	1.755
f.d [46] [64] cubic	20	4.41219	0.897342	2.85361	196.1	67.35

3.3.3 Solitary wave motion

In all simulations $\epsilon = \mu = 1$. To allow comparison with earlier simulations of the motion of a single solitary wave [46, 49, 64] Equation (3.17) is taken as initial condition at $t = 0$, with range $-40 \leq x \leq 60$, $\Delta x = 0.125$, $\Delta t = 0.1$, $x_0 = 0$ and $c = 0.1$ so that the solitary wave has amplitude 0.3. The simulation is run to time $t = 20$ and the L_2 and L_∞ error norms and the invariants C_1 , C_2 , C_3 , whose analytic values can be found as

$$C_1 = \frac{6c}{k} = 3.9799497,$$

$$C_2 = \frac{12c^2}{k} + \frac{48kc^2\mu}{5} = 0.81046249,$$

$$C_3 = \frac{36c^2}{k} \left(1 + \frac{4c}{5}\right) = 2.5790007,$$

are recorded throughout the simulation: see Table (3.1). In Figure (3.1) the initial wave profile and that at $t=20$ are compared. It is clear that, by $t = 20$, there has been little degradation of the wave amplitude and that any non-physical oscillations that may have developed on the wave are too small to be observed. The distribution of error shown in Figure (3.2) is concentrated near the wave maximum and oscillates smoothly between -2×10^{-4} and $+3 \times 10^{-5}$. Results previously obtained, at time $t = 20$, with quadratic B-spline finite elements, of length $\Delta x = 0.1$, within a standard Galerkin approach [46], with a finite difference scheme based upon cubic spline interpolation functions [46, 64] with space step $\Delta x = 0.1$ and with a least squares method with linear elements [49] are given for comparison in Table (3.1).

This simulation of a solitary wave of amplitude 0.3 leads, at $t = 20$, to an L_∞ error norm with value 0.198×10^{-3} , while the quantities C_1, C_2, C_3 change by less than 0.1%. In a simulation of a solitary wave of amplitude 0.3 the least squares algorithm leads, at $t = 20$, to an L_∞ error norm with value 1.755×10^{-3} , while the quantities C_1, C_2, C_3 change by up to 0.25%. In a corresponding simulation using a B-spline method with quadratic spline elements the error norm at $t = 20$ is only 0.086×10^{-3} and the quantities C_1, C_2, C_3 change by less than $8 \times 10^{-4}\%$.

The difference scheme used by Jain et al [64] is based upon cubic spline interpolation functions. We have implemented this algorithm [46] and find that for a solitary wave of amplitude 0.3 at $t = 20$ the L_∞ error norm has a value of about 68×10^{-3} , it is also found that the quantities C_1, C_2, C_3 increase from the analytic value by about 10%. These errors are considerably higher than those obtained with the present algorithm and conservation is correspondingly poor. We see that for solitary waves of amplitude 0.3 Galerkin's method with linear elements is more accurate than the least squares approach with linear elements but is less accurate algorithm than Galerkin with quadratic splines, while the finite difference scheme is least accurate of all.

In a second simulation the migration of a single solitary wave with the smaller amplitude 0.09 in Tables (3.2) to (3.8) we examine the effect of

various space/time steps. The smaller amplitude 0.09 is modelled using the same range and space/time steps as quoted in [46, 49, 64]. The results given in Table (3.4) are obtained. At time $t = 20$ for single solitary wave in Figure (3.3) is plotted. The analytic values of the invariants are $C_1 = 2.109407$, $C_2 = 0.127302$, $C_3 = 0.388806$. This simulation of a solitary wave of amplitude 0.09 leads to an L_∞ error norm, at $t = 20$, of about 0.20×10^{-3} , while the quantities C_2 , C_3 change by less than 0.03%, C_1 changes by less 0.1%.

With the least squares algorithm [49] the L_∞ error norm, at $t = 20$, is 0.24×10^{-3} , while the quantities C_1 , C_2 , C_3 change by similar amounts to those above. In a corresponding simulation using a B-spline method with quadratic spline elements [46] the error norm at $t = 20$ is 0.432×10^{-3} and while the quantities C_2, C_3 change by less than $8 \times 10^{-4}\%$, C_1 changes by about 0.12%.

With the cubic finite difference scheme [64] it is found that $L_\infty = 4 \times 10^{-3}$ at time $t = 20$ and that the quantities C_1 , C_2 , C_3 increase from the analytic value by about 10% during the course of the experiment. These errors are considerably higher than those obtained with the present algorithm and conservation is poor. We find that the least squares algorithm [49] has the highest mean accuracy and also, for this smaller solitary wave, better conservation than exhibited in Table (3.1).

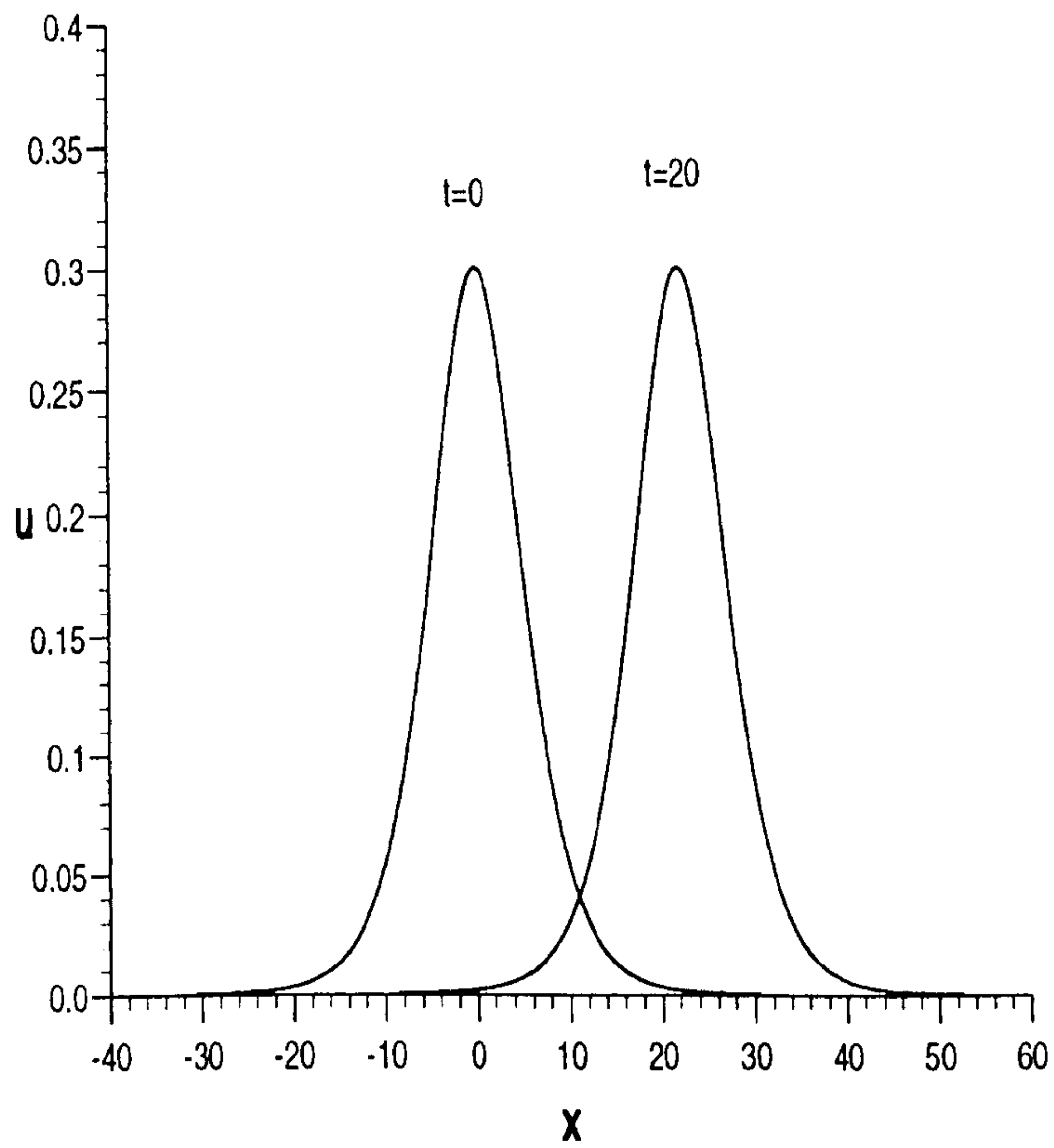


Figure 3.1 Profiles of the solitary wave
at $t = 0$ and $t = 20$.

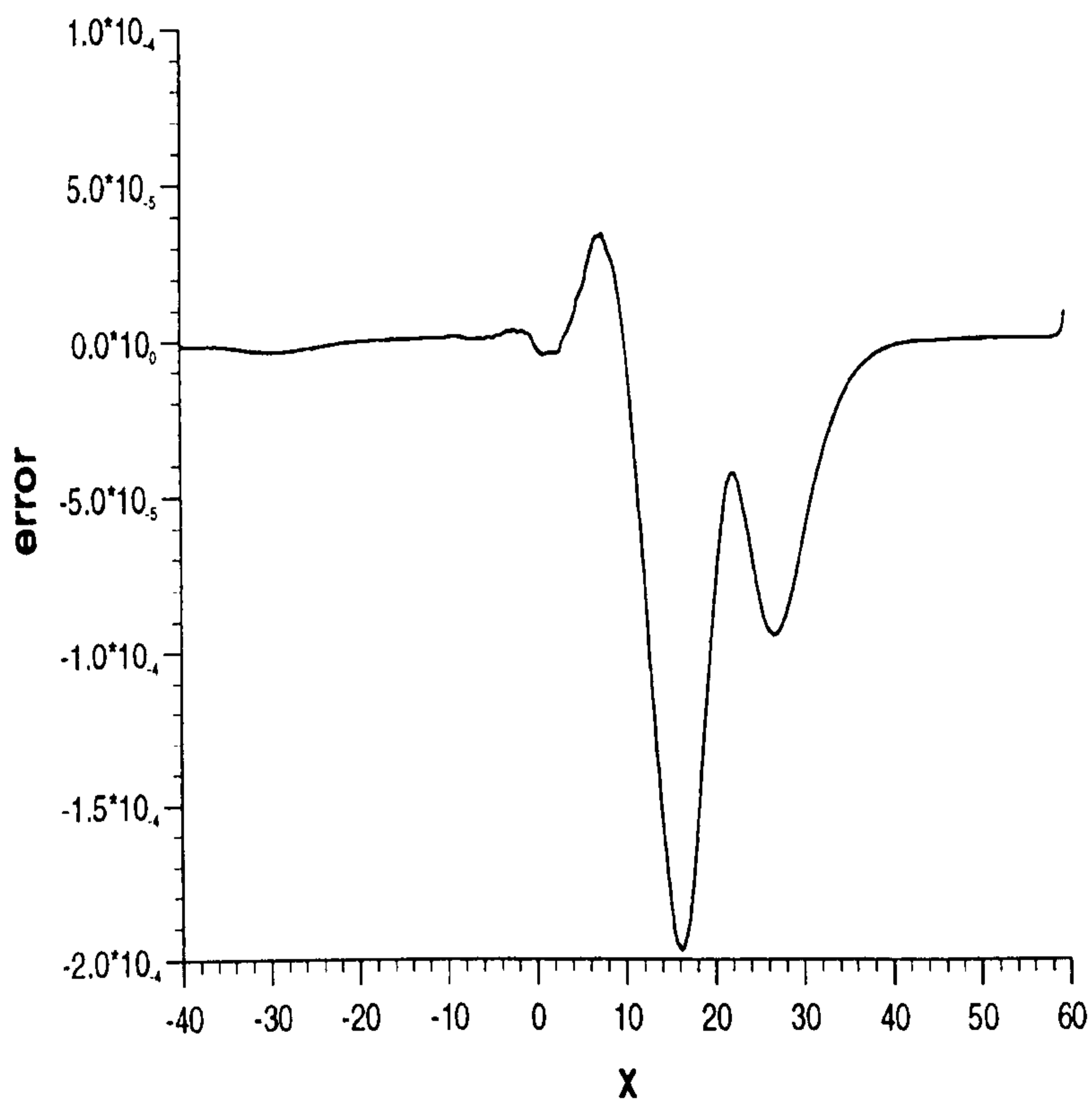


Figure 3.2 The error = exact-
numerical solution at $t = 20$ for the solitary wave in Figure (3.1) plotted on a larger scale.

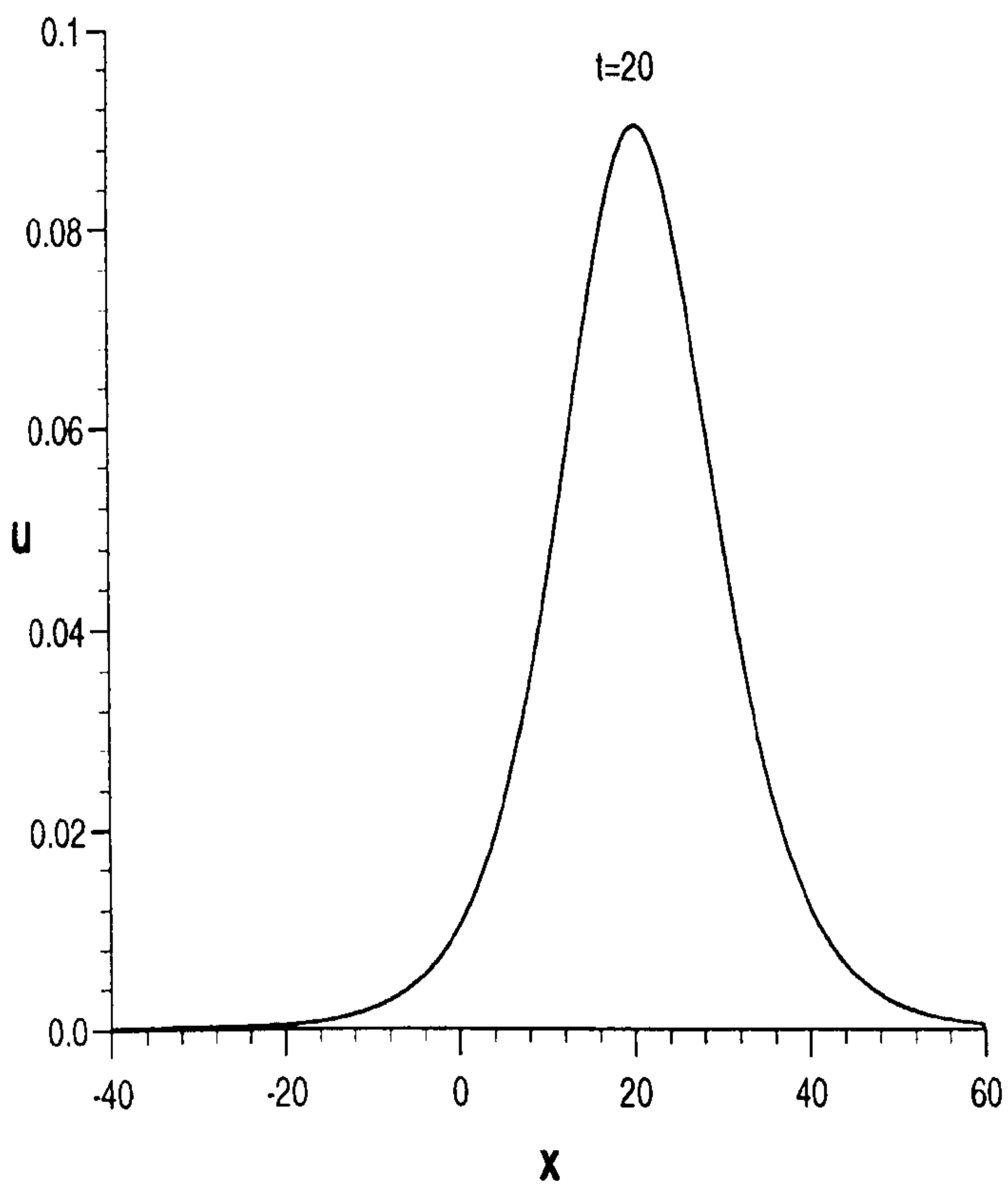


Figure 3.3 Profiles of solitary wave
at $t = 20$, amplitude=0.09, $\Delta x = 0.125$,
 $\Delta t = 0.1$, $-40 \leq x \leq 60$.

Table 3.2

Invariants and error norms for single solitary wave
amplitude=0.09, $\Delta x = 0.025$, $\Delta t = 0.025$, $-40 \leq x \leq 60$.

method	time	C_1	C_2	C_3	$L_2 \times 10^3$	$L_\infty \times 10^3$
Galerkin linear elements	0	2.10705	0.127306	0.388804	0.062	0.390
	2	2.08668	0.124791	0.381033	3.806	1.116
	4	2.06634	0.122321	0.373405	7.567	2.205
	6	2.04607	0.119886	0.365889	11.296	3.314
	8	2.02611	0.117520	0.358587	14.950	4.367
	10	2.00628	0.115196	0.351417	18.557	5.396
	12	1.98650	0.112906	0.344353	22.129	6.413
	14	1.96681	0.110657	0.337420	25.657	7.402
	16	1.94710	0.108446	0.330604	29.145	8.360
	18	1.92752	0.106288	0.323955	32.579	9.316
20	1.90798	0.104180	0.317459	35.953	10.248	

Table 3.3

Invariants and error norms for single solitary wave
amplitude=0.09, $\Delta x = 0.05$, $\Delta t = 0.05$, $-40 \leq x \leq 60$.

method	time	C_1	C_2	C_3	$L_2 \times 10^3$	$L_\infty \times 10^3$
Galerkin linear elements	0	2.10704	0.127304	0.388803	0.088	0.390
	2	2.10818	0.127399	0.389097	0.341	0.274
	4	2.10921	0.127493	0.389391	0.660	0.200
	6	2.11018	0.127590	0.389690	0.984	0.296
	8	2.11111	0.127688	0.389995	1.313	0.393
	10	2.11196	0.127782	0.390284	1.637	0.492
	12	2.11274	0.127877	0.390578	1.957	0.599
	14	2.11339	0.127970	0.390868	2.275	0.708
	16	2.11392	0.128067	0.391165	2.588	0.813
	18	2.11430	0.128169	0.391479	2.902	0.921
20	2.11441	0.128267	0.391784	3.209	1.023	

Table 3.4

Invariants and error norms for single solitary wave
amplitude=0.09, $\Delta x = 0.125$, $\Delta t = 0.1$, $-40 \leq x \leq 60$.

method	time	C_1	C_2	C_3	$L_2 \times 10^3$	$L_\infty \times 10^3$
Galerkin linear elements	0	2.10702	0.127302	0.388804	0.138	0.390
	2	2.10779	0.127303	0.388807	0.116	0.274
	4	2.10840	0.127303	0.388809	0.150	0.193
	6	2.10890	0.127303	0.388809	0.213	0.136
	8	2.10931	0.127303	0.388809	0.283	0.142
	10	2.10963	0.127304	0.388811	0.347	0.148
	12	2.10985	0.127304	0.388812	0.401	0.151
	14	2.10994	0.127304	0.388812	0.445	0.154
	16	2.10986	0.127305	0.388814	0.480	0.155
	18	2.10959	0.127305	0.388815	0.510	0.156
20	2.10906	0.127305	0.388815	0.535	0.198	
Galerkin quadratic [46]	20	2.10460	0.127302	0.388803	0.563	0.432
l.s linear [49]	20	2.10769	0.127260	0.388677	0.347	0.239
f.d [46] [64] cubic	20	2.333	0.140815	0.430052	14.45	3.996

Table 3.5

Invariants and error norms for single solitary wave
amplitude=0.09, $\Delta x = 0.25$, $\Delta t = 0.2$, $-40 \leq x \leq 60$.

method	time	C_1	C_2	C_3	$L_2 \times 10^3$	$L_\infty \times 10^3$
Galerkin linear elements	0	2.10700	0.127302	0.388804	0.195	0.390
	2	2.10773	0.127305	0.388815	0.140	0.274
	4	2.10827	0.127308	0.388827	0.110	0.193
	6	2.10865	0.127312	0.388837	0.105	0.136
	8	2.10893	0.127315	0.388847	0.114	0.096
	10	2.10908	0.127318	0.388858	0.129	0.067
	12	2.10913	0.127321	0.388868	0.142	0.050
	14	2.10905	0.127325	0.388879	0.153	0.051
	16	2.10882	0.127329	0.388889	0.162	0.051
	18	2.10840	0.127332	0.388899	0.169	0.051
20	2.10774	0.127335	0.388908	0.177	0.067	

Table 3.6

Invariants and error norms for single solitary wave
amplitude=0.09, $\Delta x = 0.5$, $\Delta t = 0.4$, $-40 \leq x \leq 60$.

method	time	C_1	C_2	C_3	$L_2 \times 10^3$	$L_\infty \times 10^3$
Galerkin linear elements	0	2.10695	0.127301	0.388804	0.275	0.390
	2	2.10762	0.127308	0.388826	0.199	0.274
	4	2.10805	0.127315	0.388847	0.161	0.193
	6	2.10831	0.127321	0.388868	0.158	0.136
	8	2.10842	0.127328	0.388888	0.174	0.096
	10	2.10843	0.127335	0.388908	0.196	0.067
	12	2.10836	0.127341	0.388929	0.218	0.057
	14	2.10818	0.127348	0.388949	0.240	0.066
	16	2.10788	0.127355	0.388970	0.262	0.075
	18	2.10741	0.127361	0.388990	0.285	0.085
20	2.10671	0.127368	0.389010	0.309	0.094	

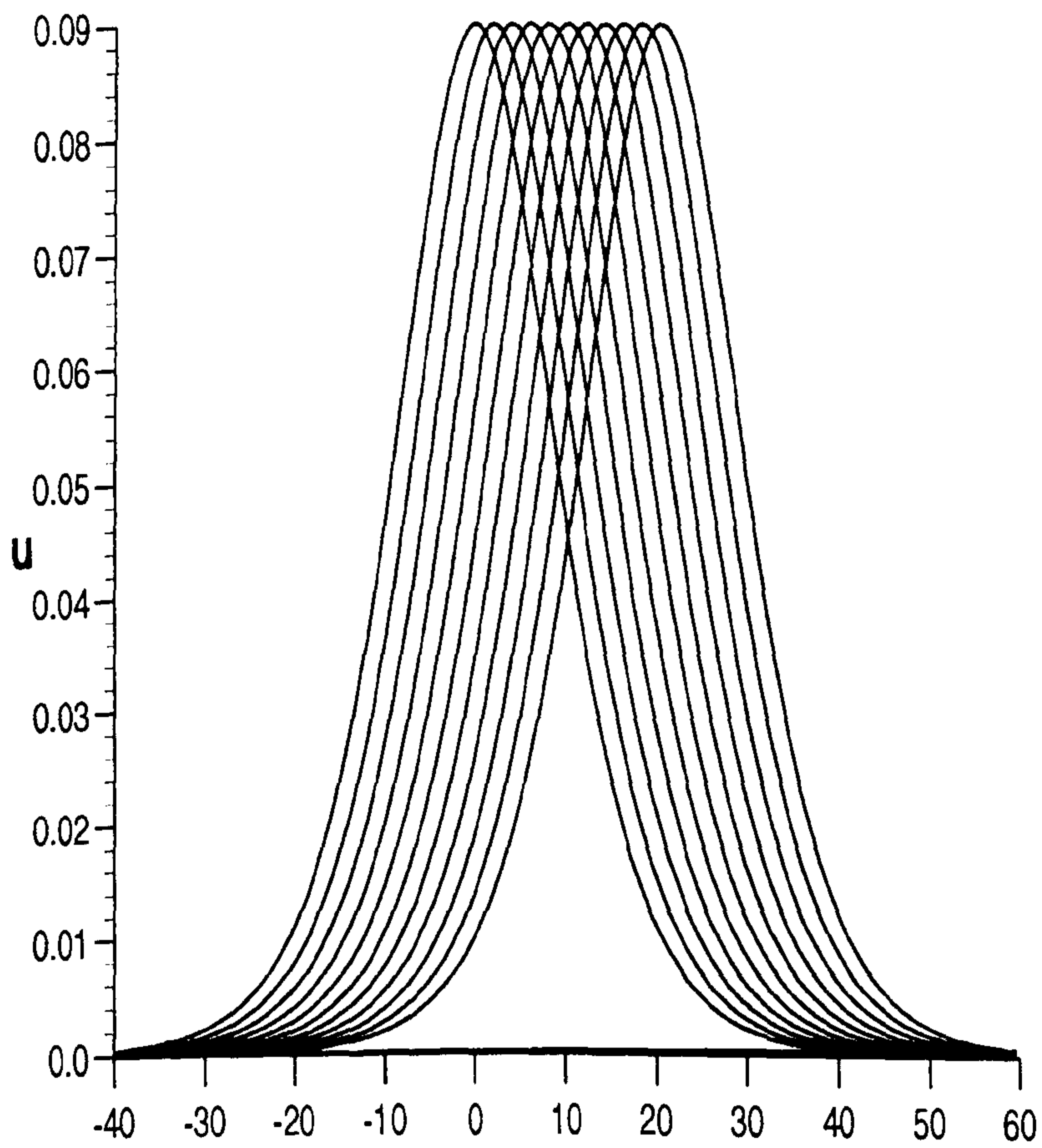


Figure 3.4 Profiles of solitary waves at times from $t = 0$ to $t = 20$, amplitude=0.09, $\Delta x = 0.5$, $\Delta t = 0.4$, $-40 \leq x \leq 60$.

Table 3.7

Invariants and error norms for single solitary wave
amplitude=0.09, $\Delta x = 1.0$, $\Delta t = 0.8$, $-40 \leq x \leq 60$.

method	time	C_1	C_2	C_3	$L_2 \times 10^3$	$L_\infty \times 10^3$
Galerkin linear elements	0	2.10684	0.127300	0.388804	0.390	0.390
	1.6	2.10737	0.127311	0.388838	0.318	0.294
	3.2	2.10772	0.127321	0.388871	0.322	0.222
	4.8	2.10792	0.127332	0.388904	0.373	0.168
	6.4	2.10802	0.127343	0.388937	0.444	0.147
	8.0	2.10805	0.127354	0.388970	0.517	0.146
	9.6	2.10804	0.127364	0.389004	0.588	0.158
	11.2	2.10800	0.127375	0.389037	0.658	0.185
	12.8	2.10792	0.127386	0.389070	0.727	0.212
	14.4	2.10778	0.127397	0.389102	0.797	0.239
16.0	2.10757	0.127407	0.389135	0.869	0.264	
17.6	2.10726	0.127418	0.389168	0.944	0.293	
19.2	2.10681	0.127429	0.389201	1.022	0.317	
20.8	2.10617	0.127439	0.389233	1.105	0.345	

Table 3.8

Invariants and error norms for single solitary wave
amplitude=0.09, $\Delta x = 4.0$, $\Delta t = 0.8$, $-40 \leq x \leq 60$.

method	time	C_1	C_2	C_3	$L_2 \times 10^3$	$L_\infty \times 10^3$
Galerkin linear elements	0	2.10615	0.127281	0.388803	0.779	0.390
	1.6	2.10834	0.127468	0.389380	0.784	0.294
	3.2	2.11035	0.127654	0.389957	1.108	0.291
	4.8	2.11223	0.127841	0.390533	1.534	0.531
	6.4	2.11402	0.128027	0.391109	1.983	0.689
	8.0	2.11575	0.128214	0.391684	2.438	0.775
	9.6	2.11744	0.128400	0.392259	2.890	1.065
	11.2	2.11908	0.128586	0.392833	3.340	1.157
	12.8	2.12069	0.128772	0.393406	3.787	1.293
	14.4	2.12225	0.128957	0.393979	4.230	1.555
	16.0	2.12374	0.129143	0.394551	4.671	1.531
	17.6	2.12513	0.129328	0.395123	5.110	1.807
19.2	2.12639	0.129513	0.395694	5.551	1.970	
20.8	2.12744	0.129698	0.396265	5.997	1.887	

Table 3.9

Error norms for single solitary wave at
 $t = 20$ amplitude=0.09, $-40 \leq x \leq 60$.

Δx	Δt	$L_2 \times 10^3$	$L_\infty \times 10^3$
0.025	0.025	35.9	10.3
0.05	0.05	3.21	1.023
0.125	0.1	0.535	0.198
0.25	0.2	0.177	0.067
0.5	0.4	0.31	0.094
1.0	0.8	1.11	0.345
4.0	0.8	6.00	1.89

Table 3.10

Invariants and error norms for single solitary wave
amplitude=0.09, $\Delta x = 0.05$, $\Delta t = 0.05$, $-80 \leq x \leq 120$.

method	time	C_1	C_2	C_3	$L_2 \times 10^3$	$L_\infty \times 10^3$
Galerkin linear elements	0	2.10940	0.127301	0.388805	0.008	0.002
	2	2.10975	0.127396	0.389098	0.313	0.111
	4	2.11011	0.127494	0.389400	0.625	0.196
	6	2.11047	0.127590	0.389697	0.929	0.293
	8	2.11086	0.127691	0.390009	1.239	0.391
	10	2.111245	0.127791	0.390317	1.551	0.490
	12	2.11159	0.127884	0.390604	1.854	0.596
	14	2.11198	0.127982	0.390909	2.162	0.704
	16	2.11236	0.128077	0.391203	2.463	0.810
	18	2.11275	0.128179	0.391515	2.772	0.917
20	2.11312	0.128274	0.391809	3.072	1.021	

Table 3.11

Invariants and error norms for single solitary wave
amplitude=0.09, $\Delta x = 0.125$, $\Delta t = 0.1$, $-80 \leq x \leq 120$.

method	time	C_1	C_2	C_3	$L_2 \times 10^3$	$L_\infty \times 10^3$
Galerkin linear elements	0	2.10940	0.127301	0.388805	0.000	0.000
	2	2.10941	0.127302	0.388808	0.013	0.008
	4	2.10942	0.127303	0.388809	0.026	0.012
	6	2.10943	0.127304	0.388812	0.037	0.016
	8	2.10943	0.127304	0.388813	0.048	0.019
	10	2.10944	0.127304	0.388814	0.059	0.024
	12	2.10946	0.127305	0.388816	0.069	0.027
	14	2.10946	0.127305	0.388818	0.078	0.032
	16	2.10947	0.127306	0.388819	0.088	0.038
	18	2.10947	0.127307	0.388821	0.097	0.039
20	2.10948	0.127307	0.388822	0.106	0.041	

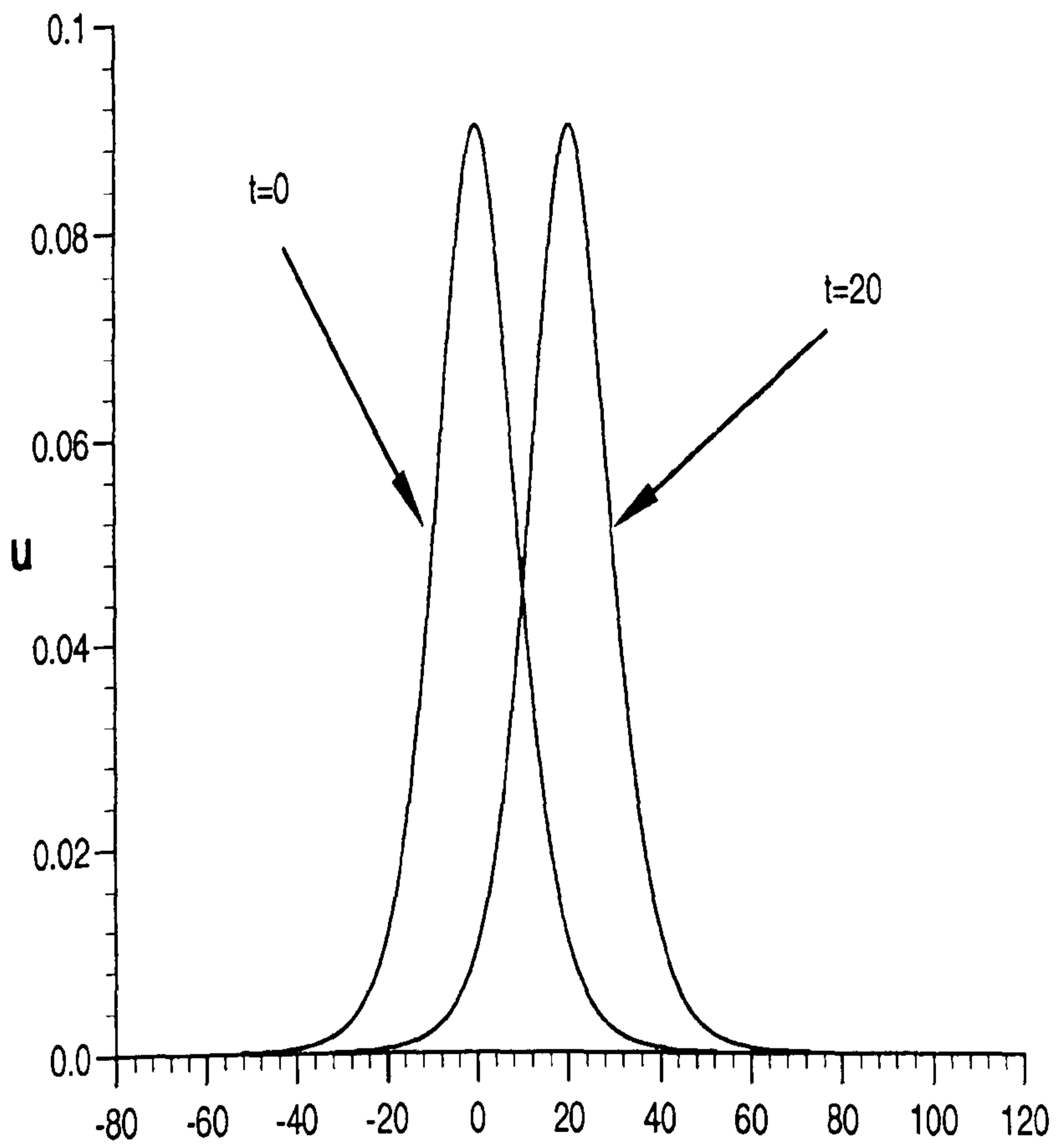


Figure 3.5 Profiles of the solitary wave
at $t = 0$ and $t = 20$ amplitude=0.09,
 $\Delta x = 0.125$, $\Delta t = 0.1$, $-80 \leq x \leq 120$.

Table 3.12

Invariants and error norms for single solitary wave
amplitude=0.09, $\Delta x = 0.25$, $\Delta t = 0.2$, $-80 \leq x \leq 120$.

method	time	C_1	C_2	C_3	$L_2 \times 10^3$	$L_\infty \times 10^3$
Galerkin linear elements	0	2.10940	0.127302	0.388806	0.000	0.000
	2	2.10944	0.127305	0.388816	0.008	0.003
	4	2.10947	0.127308	0.388827	0.016	0.006
	6	2.10950	0.127312	0.388836	0.024	0.009
	8	2.10953	0.127315	0.388847	0.032	0.012
	10	2.10957	0.127318	0.388857	0.040	0.015
	12	2.10960	0.127321	0.388867	0.047	0.018
	14	2.10963	0.127325	0.388878	0.055	0.021
	16	2.10967	0.127328	0.388889	0.063	0.024
	18	2.10970	0.127332	0.388899	0.070	0.026
20	2.10973	0.127335	0.388910	0.078	0.029	

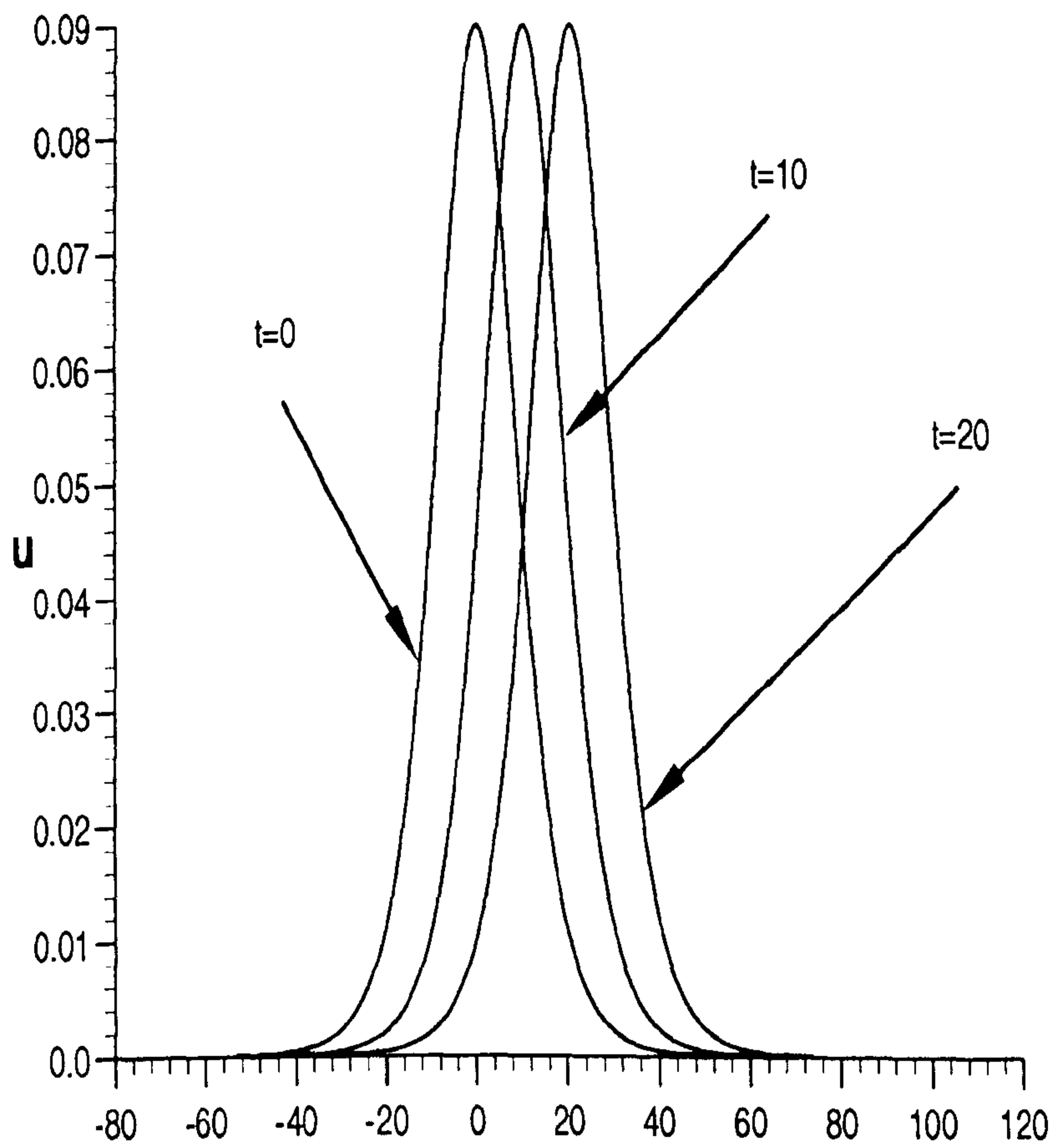


Figure 3.6 Profiles of the solitary wave
at times $t = 0, 10, 20$ amplitude=0.09,
 $\Delta x = 0.25, \Delta t = 0.2, -80 \leq x \leq 120$.

Table 3.13

Invariants and error norms for single solitary wave
 amplitude=0.09, $\Delta x = 0.5$, $\Delta t = 0.4$, $-80 \leq x \leq 120$.

method	time	C_1	C_2	C_3	$L_2 \times 10^3$	$L_\infty \times 10^3$
Galerkin linear elements	0	2.10940	0.127301	0.388806	0.000	0.000
	2	2.10947	0.127308	0.388827	0.027	0.009
	4	2.10954	0.127315	0.388847	0.053	0.019
	6	2.10960	0.127321	0.388868	0.079	0.028
	8	2.10967	0.127328	0.388888	0.105	0.038
	10	2.10973	0.127335	0.388909	0.132	0.047
	12	2.10979	0.127341	0.388929	0.158	0.057
	14	2.10986	0.127348	0.388950	0.183	0.066
	16	2.10993	0.127355	0.388971	0.209	0.075
	18	2.10999	0.127361	0.388991	0.235	0.085
20	2.11005	0.127368	0.389012	0.260	0.094	

Table 3.14

Error norms for single solitary wave at
 $t = 20$, amplitude=0.09, $-80 \leq x \leq 120$.

Δx	Δt	$L_2 \times 10^3$	$L_\infty \times 10^3$
0.05	0.05	3.072	1.021
0.125	0.1	0.106	0.041
0.25	0.2	0.078	0.029
0.5	0.4	0.260	0.094

In Table (3.9) we examine the effect of various space-step/time-step combinations and find that the highest accuracy is obtained with space step 0.25 combined with time step 0.2. The recurrence relationships (3.14) are second order accurate in the space and time step and errors initially decrease as Δt and Δx are made smaller. However since the number of elements grows as the steps Δt and Δx are decreased the number of numerical operations required to solve the matrix recurrence relationships also grows and eventually build up of truncation errors causes the L_2 and L_∞ error norms to increase as shown in Table (3.9). In Figure (3.4) we plot profiles for the solitary wave at times from $t = 0$ until $t = 20$.

As the amplitude of a solitary wave is reduced the pulse broadens and it may be necessary to increase the solution range in order to maintain accuracy. The effect of the doubling the range from $-40 \leq x \leq 60$ to $-80 \leq x \leq 120$ is demonstrated in Tables (3.10) to (3.13). In Table (3.14) the maximum improvement in accuracy is obtained for $\Delta x = 0.25$, $\Delta t = 0.2$ when both error norms are reduced by a factor of about 2.3. We draw for these values in Figure (3.6) at times $t = 0, 10, 20$. In Figure (3.5) is plotted profiles of the solitary wave at $t = 0$ and $t = 20$, amplitude 0.09, $\Delta x = 0.125$ and $\Delta t = 0.1$, with the range $-80 \leq x \leq 120$.

The error norms and invariants for an even smaller solitary wave, amplitude = 0.03, are given in Tables (3.15) to (3.17). With the range $-80 \leq x \leq 120$, $\Delta x = 0.25$ and $\Delta t = 0.2$ we obtain excellent results. Throughout the simulation the L_2 and L_∞ error norms remain less than 5×10^{-5} , while the invariants C_2 and C_3 change by less than $5 \times 10^{-3}\%$ and C_1 changes by about 0.023% by time $t = 20$. The effect of changes in the space and time steps is examined in Table (3.18). The smallest error norms are obtained with the choice $\Delta x = 0.25$ and $\Delta t = 0.2$. In Figure (3.7) is plotted for the solitary wave at $t = 0$ and $t = 20$, amplitude 0.03, with the range $-80 \leq x \leq 120$.

Table 3.15

Invariants and Error norms for single solitary wave
amplitude=0.03, $\Delta x = 0.125$, $\Delta t = 0.1$, $-80 \leq x \leq 120$.

method	time	C_1	C_2	C_3	$L_2 \times 10^3$	$L_\infty \times 10^3$
Galerkin linear elements	0	1.205554	0.024167	0.072938	0.015	0.042
	2	1.205629	0.024167	0.072938	0.020	0.034
	4	1.205693	0.024167	0.072938	0.032	0.028
	6	1.205752	0.024167	0.072938	0.046	0.023
	8	1.205801	0.024168	0.072938	0.059	0.019
	10	1.205842	0.024167	0.072938	0.073	0.018
	12	1.205880	0.024168	0.072938	0.086	0.021
	14	1.205909	0.024168	0.072939	0.099	0.025
	16	1.205935	0.024168	0.072939	0.112	0.029
	18	1.205957	0.024168	0.072939	0.124	0.032
20	1.205968	0.024168	0.072939	0.136	0.035	

Table 3.16

Invariants and Error norms for single solitary wave
amplitude=0.03, $\Delta x = 0.25$, $\Delta t = 0.2$, $-80 \leq x \leq 120$.

method	time	C_1	C_2	C_3	$L_2 \times 10^3$	$L_\infty \times 10^3$
Galerkin linear elements	0	1.205551	0.024167	0.072938	0.021	0.042
	2	1.205627	0.024168	0.072938	0.017	0.034
	4	1.205685	0.024168	0.072938	0.014	0.028
	6	1.205730	0.024168	0.072938	0.013	0.023
	8	1.205766	0.024168	0.072939	0.012	0.019
	10	1.205792	0.024168	0.072939	0.012	0.015
	12	1.205811	0.024168	0.072939	0.012	0.013
	14	1.205823	0.024168	0.072939	0.013	0.010
	16	1.205832	0.024168	0.072939	0.014	0.008
	18	1.205834	0.024168	0.072940	0.014	0.007
20	1.205834	0.024168	0.072940	0.015	0.006	

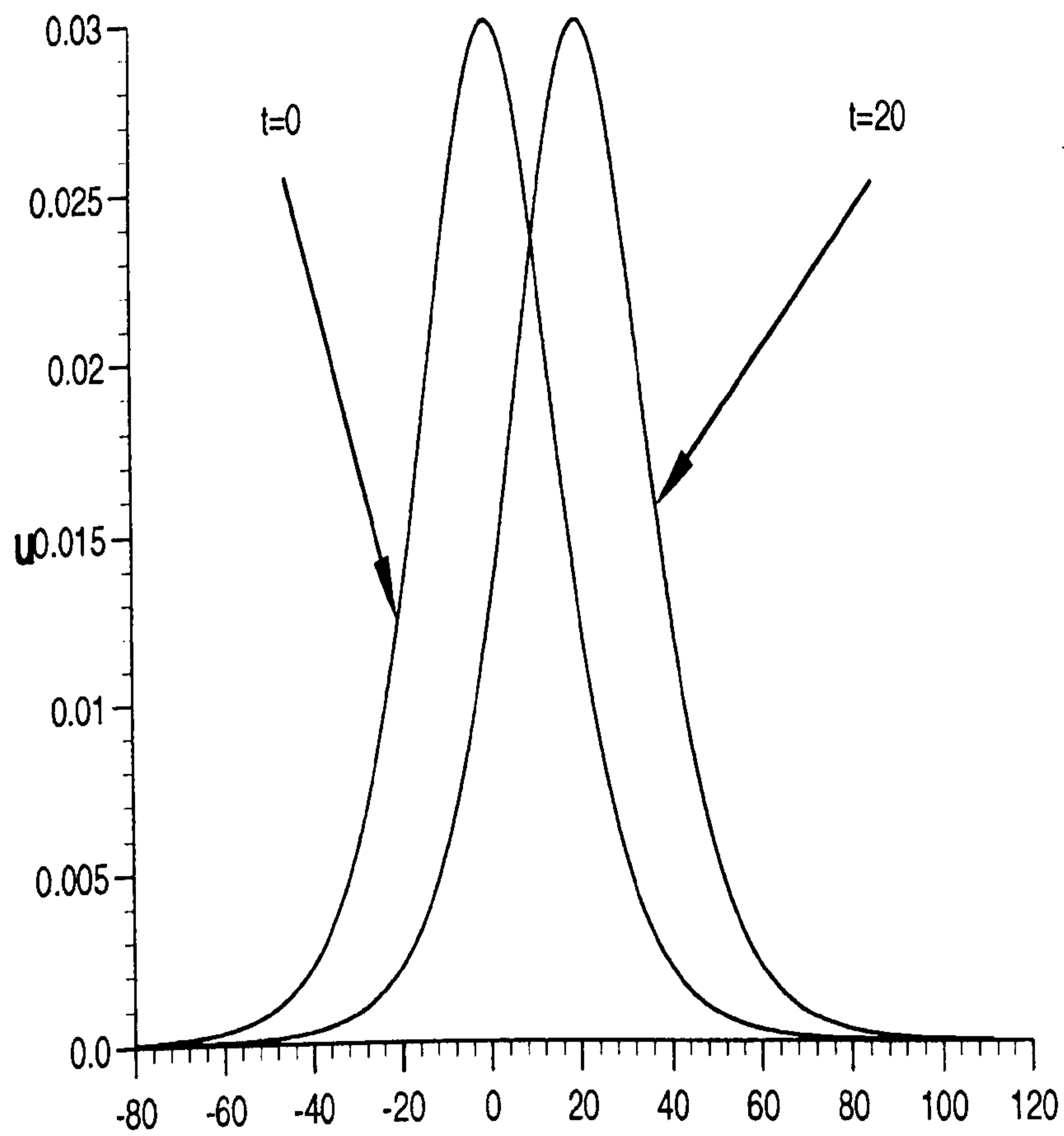


Figure 3.7 Profiles of solitary wave at
 $t = 0$ and 20 amplitude=0.03, $\Delta x = 0.25$,
 $\Delta t = 0.2$, $-80 \leq x \leq 120$.

Table 3.17

Invariants and Error norms for single solitary wave
amplitude=0.03, $\Delta x = 0.5$, $\Delta t = 0.4$, $-80 \leq x \leq 120$.

method	time	C_1	C_2	C_3	$L_2 \times 10^3$	$L_\infty \times 10^3$
Galerkin linear elements	0	1.205545	0.024167	0.072938	0.030	0.042
	2	1.205613	0.024168	0.072938	0.025	0.034
	4	1.205660	0.024168	0.072939	0.025	0.028
	6	1.205690	0.024168	0.072939	0.029	0.023
	8	1.205707	0.024168	0.072940	0.034	0.019
	10	1.205716	0.024168	0.072940	0.038	0.015
	12	1.205722	0.024168	0.072941	0.042	0.015
	14	1.205724	0.024169	0.072941	0.045	0.015
	16	1.205723	0.024169	0.072942	0.047	0.015
	18	1.205720	0.024169	0.072942	0.048	0.015
20	1.205715	0.024169	0.072943	0.050	0.015	

Table 3.18

Error norms for single solitary wave at
 $t = 20$, amplitude=0.03, $-80 \leq x \leq 120$.

Δx	Δt	$L_2 \times 10^3$	$L_\infty \times 10^3$
0.125	0.1	0.136	0.035
0.25	0.2	0.015	0.006
0.5	0.4	0.050	0.015

3.3.4 Two wave interactions

As initial condition we use [19]

$$U(x, t) = 3c_1 \operatorname{sech}^2(k_1[x - v_1 t - x_1]) + 3c_2 \operatorname{sech}^2(k_2[x - v_2 t - x_2]), \quad (3.18)$$

where

$$k_j^2 = \frac{\epsilon c_j}{4\mu(1 + \epsilon c_j)},$$

and

$$v = 1 + \epsilon c_j,$$

evaluated at $t = 0$ produce two solitary waves. Again in these simulations we take $\epsilon = \mu = 1$. The one of the amplitude $3c_1$ sited at $x = x_1$ and that of amplitude $3c_2$ at $x = x_2$. An interaction occurs when the larger is placed to the left of the smaller. We study such an interaction with $c_1 = 0.2$, $x_1 = -177$, $c_2 = 0.1$ and $x_2 = -147$ running the simulation for a time 400 and using the region $-200 \leq x \leq 400$ with $\Delta x = 0.12$ and $\Delta t = 0.1$. Since there is no exact analytic two wave solution, the accuracy of the simulation is guaged by degree of conservation produced by the algorithm. We find that with the space/time step combination 0.12/0.1 the quantities C_1 , C_2 , C_3 show a higher degree of conservation than with the choice 0.05/0.05.

In Table (3.19) the variation of the invariants during the simulation with $\Delta x = 0.12$, $\Delta t = 0.1$ are listed; each changes by less than 0.45%, while Figure (3.9) shows the interaction profile at times from 0 to 400 in steps of 100. Figure (3.8) is plotted Interaction profiles of the solitary waves at times from $t = 0$ until $t = 400$.

Table 3.19

Invariants for interaction of two solitary waves
 amplitudes 0.6 and 0.3, $\Delta x = 0.12$, $\Delta t = 0.1$.

time	C_1	C_2	C_3
0	9.8586	3.2449	10.7788
40	9.8642	3.2456	10.7809
80	9.8683	3.2475	10.7872
120	9.8719	3.2491	10.7928
160	9.8751	3.2506	10.7979
200	9.8786	3.2523	10.8036
240	9.8825	3.2544	10.8109
280	9.8854	3.2557	10.8156
320	9.8883	3.2569	10.8197
360	9.8907	3.2576	10.8220
400	9.8930	3.2585	10.8251

By time $t = 400$, the larger wave has passed through the smaller to reach the point $x = 311.56$ whilst the smaller has reached $x = 281.68$. A very small wave of amplitude 0.63×10^{-4} has been left behind at $x = 233.8$. Undisturbed by an interaction, the larger wave would reach 303 and the smaller 293 by time $t = 400$. The interaction has caused a phase advance of $\delta x = 8.56$ in the larger wave and a phase retardation of $\delta x = -11.32$ in the smaller. This observation is in qualitative agreement with earlier numerical experiments on very much larger amplitude waves [18]. The accuracy of these results is expected to be effected by the relatively large space and time steps used.

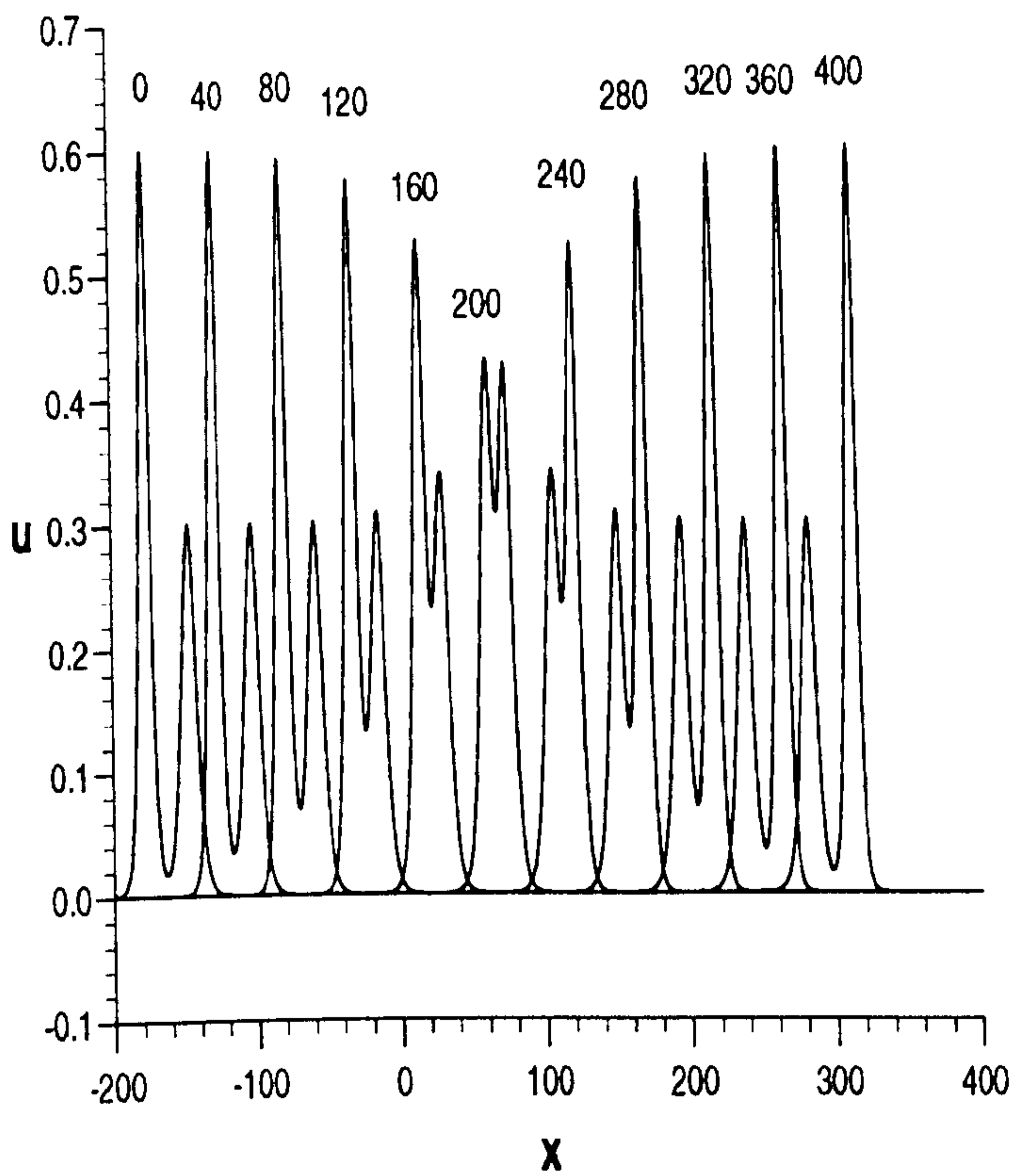


Figure 3.8 Interaction profiles of the solitary waves at times from $t = 0$ to $t = 400$ in the steps of 40.

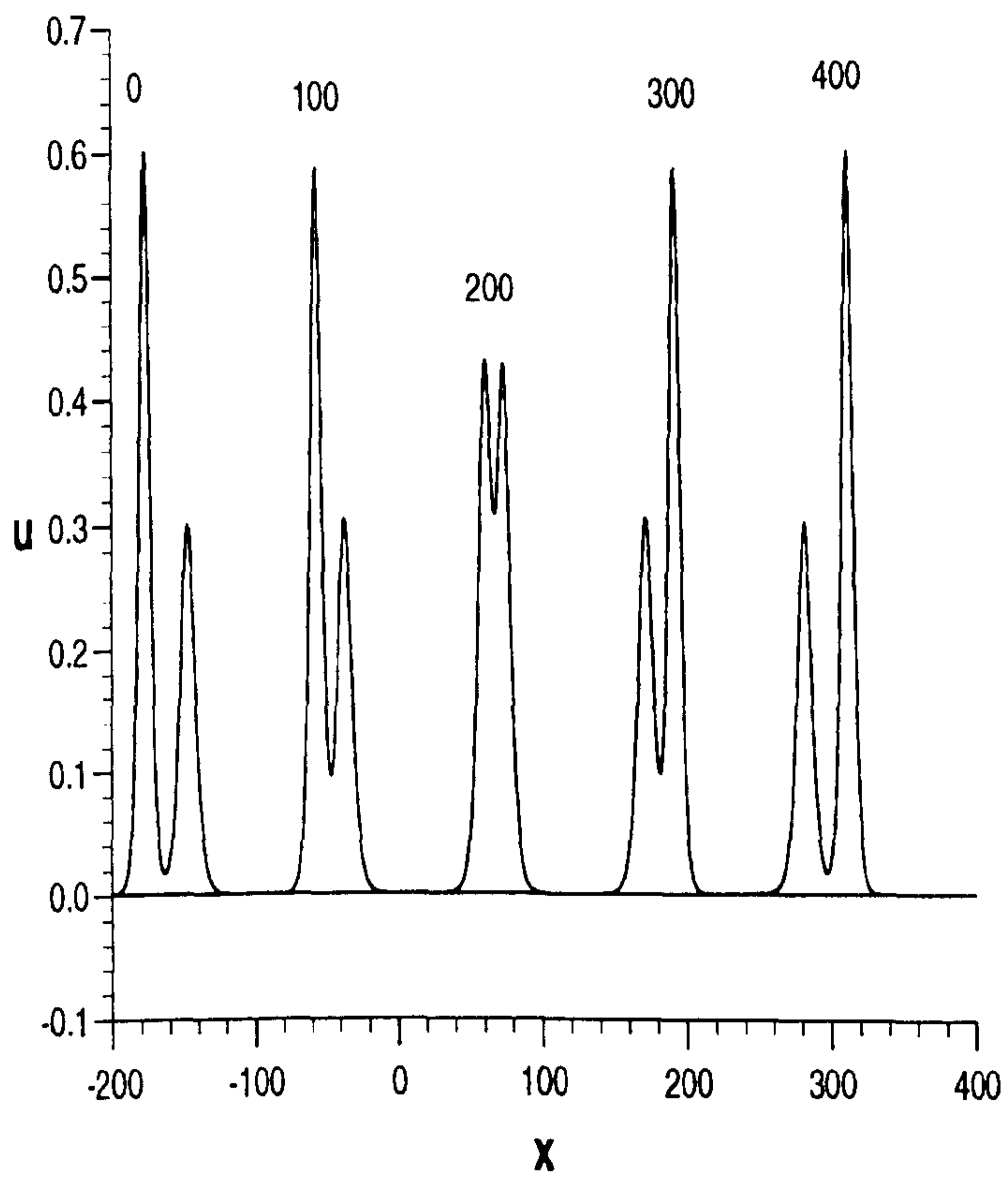


Figure 3.9 Interaction profiles of the solitary waves at times from $t = 0$ to $t = 400$ in the steps of 100.

3.4 Discussion

The Galerkin approach with linear finite elements set up in Section (3.2) leads to an unconditionally stable algorithm which models well the amplitude, position and velocity of a single solitary wave of small amplitude over an extended time scale.

The interaction of two solitary waves, both of small amplitude, is similarly simulated. By time $t = 400$ the interaction is virtually complete and the waves have emerged with, practically, their former amplitude and velocity. Phase shifts in line with those observed by earlier workers [18] are found.

Chapter 4

A Least-Squares Finite Element Scheme For The RLW Equation

4.1 Introduction

The RLW equation is solved by a least squares technique using linear space-time finite elements. In simulations of the migration of a single solitary wave this algorithm is shown to have higher accuracy and better conservation than a recent difference scheme based on cubic spline interpolation functions. In addition, for very small amplitude waves (≤ 0.09) it has higher accuracy than an approach using quadratic B-spline finite elements within Galerkin's method. The development of an undular bore is modelled.

The regularised long wave (RLW) equation plays a major role in the study of non-linear dispersive waves since it describes a large number of important physical phenomena, such as shallow water waves and ion acoustic plasma waves [19, 89]. There is experimental evidence to suggest that this description breaks down if the amplitude of any wave exceeds about 0.28 [89].

Numerical work on the RLW equation has been undertaken by, amongst

others, Eilbeck and McGuire [37], Bona et al [19] and, more recently, by Jain et al [64]. We have used the method of collocation and Galerkin's method within a B-spline finite element formulation to find stable, efficient and accurate numerical solutions to non-linear partial differential equations. In particular, we have studied the RLW equation using Galerkin's method with both cubic [40] and quadratic [46] B-spline finite elements. Here we use a least squares technique with space-time linear finite elements [83, 84] to construct a numerical solution. We discuss the properties and advantages of this method and compare its accuracy in modelling a solitary wave with that of numerical algorithms described in references [64] and [46]. Finally, simulations of the development of an undular bore are undertaken.

4.2 The finite element solution

We solve the normalised RLW equation

$$U_t + U_x + \epsilon U U_x - \mu U_{xxt} = 0, \quad (4.1)$$

where ϵ , μ are positive parameters and the subscripts x and t show differentiation. When the RLW equation is used to model waves generated in a shallow water channel the variables are normalised in the following way. Distance x and water elevation U are scaled to the water depth h and time t is scaled to $\sqrt{h/g}$, where g is the acceleration due to gravity. Physical boundary conditions require $U \rightarrow 0$ as $|x| \rightarrow \infty$.

When applying the least squares approach and using space-time finite elements, we consider the Variational Principle [83, 84]

$$\delta \int_0^t \int_0^L [U_t + U_x + \epsilon U U_x - \mu U_{xxt}]^2 dx dt = 0, \quad (4.2)$$

A uniform linear spatial array of linear finite elements is set up $0 = x_0 < x_1 \dots < x_N = L$. A typical finite element of size $\Delta x = (x_{m+1} - x_m)$, Δt mapped by local coordinates ξ, τ where $x = x_m + \xi \Delta x$, $0 \leq \xi \leq 1$, $t = \tau \Delta t$, $0 \leq \tau \leq 1$, makes, to integral (4.2), the

contribution

$$\delta \int_0^1 \int_0^1 \left[U_\tau + \frac{\Delta t}{\Delta x} U_\xi + \frac{\epsilon \Delta t}{\Delta x} \hat{U} U_\xi - \frac{\mu}{\Delta x^2} U_{\xi\xi\tau} \right]^2 d\xi d\tau, \quad (4.3)$$

where to simplify the integral, \hat{U} is taken to be constant over an element. This leads to

$$\int_0^1 \int_0^1 [U_\tau + v U_\xi - b U_{\xi\xi\tau}] \delta [U_\tau + v U_\xi - b U_{\xi\xi\tau}] d\xi d\tau, \quad (4.4)$$

where

$$b = \frac{\mu}{\Delta x^2},$$

and

$$v = \frac{\Delta t}{\Delta x} (1 + \epsilon \hat{U})$$

is taken as locally constant over each element. The variation of U over the element $[x_m, x_{m+1}]$ is given by

$$U^e = \sum_{j=1}^2 N_j (u_j + \tau \Delta u_j), \quad (4.5)$$

where N_1, N_2 are linear spatial basis functions. The u_1, u_2 are the nodal parameters which are temporally linear and change by the increments $\Delta u_1, \Delta u_2$ in time Δt . With the local coordinate system ξ defined above the basis functions have expressions [103]

$$N_1 = 1 - \xi,$$

$$N_2 = \xi.$$

Write the second term in the integrand of (4.4) as a weight function

$$\delta W = \sum_{j=1}^2 W_j \Delta u_j = \delta [U_\tau + v U_\xi - b U_{\xi\xi\tau}]. \quad (4.6)$$

Using, from (4.5), the result that

$$\delta U^e = \sum_{j=1}^2 N_j \tau \Delta u_j, \quad (4.7)$$

in (4.6) we have

$$W_j = N_j + \tau v N'_j. \quad (4.8)$$

Substituting into Equation (4.4) gives

$$\int_0^1 \int_0^1 [U_\tau + v U_\xi - b U_{\xi\xi\tau}] [N_j + \tau v N'_j] d\xi d\tau, \quad (4.9)$$

which can be interpreted as a Petrov-Galerkin approach with weight function W_j , as well as a least squares formulation. Integrating by parts leads to

$$\int_0^1 \int_0^1 [(U_\tau + v U_\xi)(N_j + \tau v N'_j) + b U_{\xi\tau} N'_j] d\xi d\tau. \quad (4.10)$$

Now if we substitute for U using Equation (4.5), an element's contribution is obtained in the form

$$\sum_{k=1}^2 \int_0^1 \int_0^1 [(N_k \Delta u_k + v N'_k (u_k + \tau \Delta u_k))(N_j + \tau v N'_j) + b N'_k N'_j \Delta u_k] d\xi d\tau. \quad (4.11)$$

Integrate (4.11) with respect to τ giving in matrix notation

$$\begin{aligned} [A^e + \frac{1}{2}(C^e + C^{eT}) + \frac{1}{3}B^e + bD^e] \Delta u^e \\ + [C^e + \frac{1}{2}B^e] u^e, \end{aligned} \quad (4.12)$$

where

$$u^e = (u_1, u_2)^T,$$

are the relevant nodal parameters. The element matrices are

$$A_{jk}^e = \int_0^1 N_j N_k d\xi,$$

$$B_{jk}^e = v^2 \int_0^1 N'_j N'_k d\xi,$$

$$C_{jk}^e = v \int_0^1 N_j N'_k d\xi,$$

$$D_{jk}^e = \int_0^1 N_j' N_k' d\xi,$$

where j, k take only the values 1 and 2. The matrices A^e, B^e, C^e and D^e are thus 2×2 , and have the explicit forms

$$A^e = \frac{1}{6} \begin{pmatrix} 2 & 1 \\ 1 & 2 \end{pmatrix},$$

$$B^e = v^2 \begin{pmatrix} 1 & -1 \\ -1 & 1 \end{pmatrix},$$

$$C^e = \frac{1}{2}v \begin{pmatrix} -1 & 1 \\ -1 & 1 \end{pmatrix},$$

$$D^e = \begin{pmatrix} 1 & -1 \\ -1 & 1 \end{pmatrix},$$

$$C^e + C^{eT} = v \begin{pmatrix} -1 & 0 \\ 0 & 1 \end{pmatrix},$$

and v given by

$$v = \frac{\Delta t}{\Delta x} (1 + \epsilon u_1),$$

is constant over the element.

Formally assembling together contributions from all elements leads to the matrix equation

$$[A + \frac{1}{2}(C + C^T) + \frac{1}{3}B + bD]\Delta u + [C + \frac{1}{2}B]u = 0, \quad (4.13)$$

and $u = (u_0, u_1, \dots, u_N)^T$, contains all the nodal parameters. The matrices A, B, C, D are tridiagonal and row m of each has the following form:

$$A : \frac{1}{6}(1, 4, 1)$$

$$D : (-1, 2, -1)$$

$$B : (-v_{m-1}^2, v_{m-1}^2 + v_m^2, -v_m^2)$$

$$\begin{aligned}
C &: \frac{1}{2}(-v_{m-1}, v_{m-1} - v_m, v_m) \\
(C + C^T) &: (0, v_{m-1} - v_m, 0) \\
(C^T - C) &: (v_{m-1}, 0, -v_m).
\end{aligned}$$

Hence identifying $u = u^n$ and $\Delta u = u^{n+1} - u^n$ we can write Equation (4.13) as

$$\begin{aligned}
& [A + \frac{1}{2}(C + C^T) + \frac{1}{3}B + bD]u^{n+1} \\
& = [A + \frac{1}{2}(C^T - C) - \frac{1}{6}B + bD]u^n,
\end{aligned} \tag{4.14}$$

a scheme for updating u^n to time level $t = (n + 1)\Delta t$. A typical member of (4.14) is

$$\begin{aligned}
& (\frac{1}{6} - b - \frac{1}{3}v_{m-1}^2)u_{m-1}^{n+1} \\
& + (\frac{2}{3} + 2b + \frac{1}{2}[v_{m-1} - v_m] + \frac{1}{3}[v_{m-1}^2 + v_m^2])u_m^{n+1} \\
& + (\frac{1}{6} - b - \frac{1}{3}v_m^2)u_{m+1}^{n+1} = \\
& (\frac{1}{6} - b + \frac{1}{2}v_{m-1} + \frac{1}{6}v_{m-1}^2)u_{m-1}^n \\
& + (\frac{2}{3} + 2b - \frac{1}{6}[v_{m-1}^2 + v_m^2])u_m^n \\
& + (\frac{1}{6} - b - \frac{1}{2}v_m + \frac{1}{6}v_m^2)u_{m+1}^n,
\end{aligned} \tag{4.15}$$

where v_m is given by

$$v_m = \frac{\Delta t}{\Delta x}(1 + \epsilon u_m^n).$$

The boundary conditions $U(0, t) = 0$ and $U(L, t) = 0$ require $u_0 = 0$ and $u_N = 0$. The above set of quasi-linear equations has a matrix which is tridiagonal in form so that a solution using the Thomas algorithm is direct and no iterations are necessary.

4.2.1 Stability Analysis

The growth factor g of the error ϵ_j^n in a typical Fourier mode of amplitude $\hat{\epsilon}^n$

$$\hat{\epsilon}_j^n = \hat{\epsilon}^n \exp(ijk\Delta x) \quad (4.16)$$

where k is the mode number and Δx the element size, is determined for a linearisation of the numerical scheme.

In the linearisation it is assumed that the quantity U in the nonlinear term is locally constant. Under these conditions the error ϵ_j^n satisfies the same finite difference scheme as the function δ_j^n and we find that a typical member of Equation (4.15) has the form

$$\begin{aligned} & \left(\frac{1}{6} - b - \frac{1}{3}r^2\right)\epsilon_{m-1}^{n+1} + \left(\frac{2}{3} + 2b + \frac{2}{3}r^2\right)\epsilon_m^{n+1} \\ & + \left(\frac{1}{6} - b - \frac{1}{3}r^2\right)\epsilon_{m+1}^{n+1} = \left(\frac{1}{6} - b + \frac{1}{2}r + \frac{1}{6}r^2\right)\epsilon_{m-1}^n \\ & + \left(\frac{2}{3} + 2b - \frac{1}{3}r^2\right)\epsilon_m^n + \left(\frac{1}{6} - b - \frac{1}{2}r + \frac{1}{6}r^2\right)\epsilon_{m+1}^n, \end{aligned} \quad (4.17)$$

where

$$b = \frac{\mu}{\Delta x^2}$$

and

$$r = \frac{\Delta t}{\Delta x}$$

substituting the above Fourier mode gives

$$|g|^2 = \frac{p+P}{p+Q},$$

where

$$\begin{aligned} p &= (\cos[k\Delta x] + 2)^2 + 36b^2(\cos[k\Delta x] - 1)^2 \\ & \quad + 12b(2 - \cos[k\Delta x] - \cos^2[k\Delta x]) \end{aligned}$$

$$P = (r^4 - 12br^2)(\cos[k\Delta x] - 1)^2 + r^2(1 - \cos[k\Delta x])(7\cos[k\Delta x] + 5)$$

$$Q = (4r^4 + 24br^2)(\cos[k\Delta x] - 1)^2 + 4r^2(1 - \cos[k\Delta x])(\cos[k\Delta x] + 2)$$

and $r = \frac{\Delta t}{\Delta x} \leq 1$, so that $|g| \leq 1$ and the scheme is unconditionally stable.

4.3 Test problems

With the boundary conditions $U \rightarrow 0$ as $x \rightarrow \pm\infty$ the solitary wave solution of the RLW equation is [89]

$$U(x, t) = 3c \operatorname{sech}^2(k[x - vt - x_0]), \quad (4.18)$$

where

$$k^2 = \frac{\epsilon c}{4\mu(1 + \epsilon c)},$$

and

$$v = 1 + \epsilon c,$$

is the wave velocity. It is expected that this solution will also be valid for sufficiently wide finite regions.

Table 4.1

Invariants and error norms for single solitary wave
amplitude=0.3, $\Delta x = 0.125$, $\Delta t = 0.1$, $-40 \leq x \leq 60$.

method	time	C_1	C_2	C_3	$L_2 \times 10^3$	$L_\infty \times 10^3$
	0	3.97993	0.810461	2.57901	0.002	0.007
	2	3.98017	0.810284	2.57842	0.550	0.252
	4	3.98041	0.810111	2.57785	1.090	0.487
	6	3.98064	0.809935	2.57726	1.610	0.699
Least	8	3.98085	0.809749	2.57666	2.109	0.892
Squares	10	3.98108	0.809574	2.57608	2.591	1.065
linear	12	3.98128	0.809390	2.57547	3.049	1.224
elements	14	3.98150	0.809217	2.57490	3.485	1.372
	16	3.98169	0.809030	2.57428	3.905	1.510
	18	3.98186	0.808830	2.57352	4.310	1.639
	20	3.98203	0.808650	2.57302	4.688	1.755
Galerkin						
quadratic [46]	20	3.97989	0.810467	2.57902	0.220	0.086
f.d [46],[64]						
cubic	20	4.41219	0.897342	2.85361	196.1	67.35

4.3.1 Solitary wave motion

In the following simulation of the motion of a single solitary wave $\epsilon = \mu = 1$. To make comparison with earlier simulation results [46, 64] Equation (4.18) is taken as initial condition with range $-40 \leq x \leq 60$, $\Delta x = 0.125$, $\Delta t = 0.1$ and $x_0 = 0$, with $c = 0.1$ so that solitary wave has amplitude 0.3. The simulation is run to time $t = 20$ and the L_2 and L_∞ error norms and the invariants C_1 , C_2 , C_3 , whose analytic values can be obtained as

$$C_1 = \frac{6c}{k} = 3.9799497,$$

$$C_2 = \frac{12c^2}{k} + \frac{48kc^2\mu}{5} = 0.81046249,$$

$$C_3 = \frac{36c^2}{k} \left(1 + \frac{4c}{5}\right) = 2.579007,$$

are recorded throughout the simulation: see Table (4.1). In Figure (4.1) the initial wave profile and that at $t = 20$ are compared. It is clear that, by $t = 20$, there has been little degradation of the wave amplitude and that any non-physical oscillations that may have developed on the wave are very small to be observed. The distribution of error along the wave profile is shown in Figure (4.2). The error is concentrated near the wave maximum and oscillates smoothly between -2×10^{-3} and $+2 \times 10^{-3}$. Results previously found, at time $t = 20$, with quadratic B-spline finite elements, of length $\Delta x = 0.1$, within a standard Galerkin approach [46] and also with a finite difference scheme based upon cubic spline interpolation functions [46, 64] with space step $\Delta x = 0.1$ are given for comparison.

In the simulation of a solitary wave of amplitude 0.3 the least squares algorithm leads, at time $t = 20$, to an L_∞ error norm with value 1.755×10^{-3} , while the quantities C_1, C_2, C_2 change by up to 0.25%. In a corresponding simulation using a B-spline method with quadratic spline elements the error norm at time $t = 20$ is only 0.086×10^{-3} and the quantities C_1, C_2, C_3 change by less than $8 \times 10^{-4}\%$.

The difference scheme used by Jain et al [64] is based upon cubic spline interpolation functions. We have implemented this algorithm to provide comparative results [46]. These have been checked against the Figures provided in reference [64] and show that for a solitary wave of amplitude 0.3 at $t = 20$ the L_∞ error norm has a value of about 68×10^{-3} , it is also obtained that the quantities C_1, C_2, C_3 increase from the analytic value by about 10% during the course of the experiment. These errors are considerably higher than those obtained with the present algorithm and conservation is correspondingly poor. We see that for solitary waves of amplitude 0.3 the least squares approach leads to a less accurate algorithm than Galerkin with quadratic splines but is more accurate than the finite difference scheme described.

In a second simulation involving the migration of a single solitary wave with the smaller amplitude 0.09 and using the same range and space/time steps as quoted in [64] and [46] the results given in Table (4.2) are obtained. The analytic values of the invariants are $C_1 = 2.109407$, $C_2 = 0.127302$, $C_3 = 0.388806$.

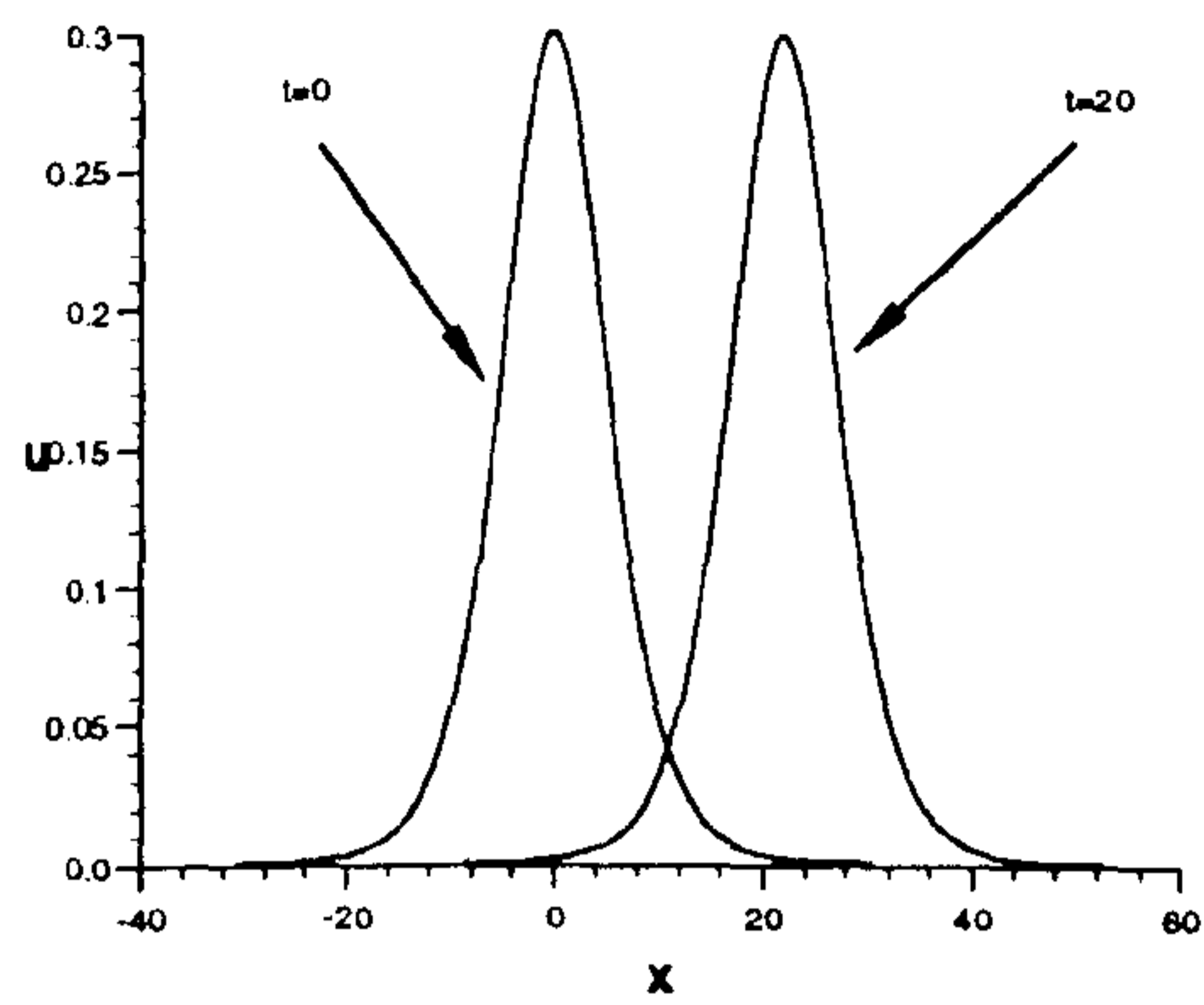


Figure 4.1 Profiles of the solitary wave at $t = 0$ and $t = 20$.

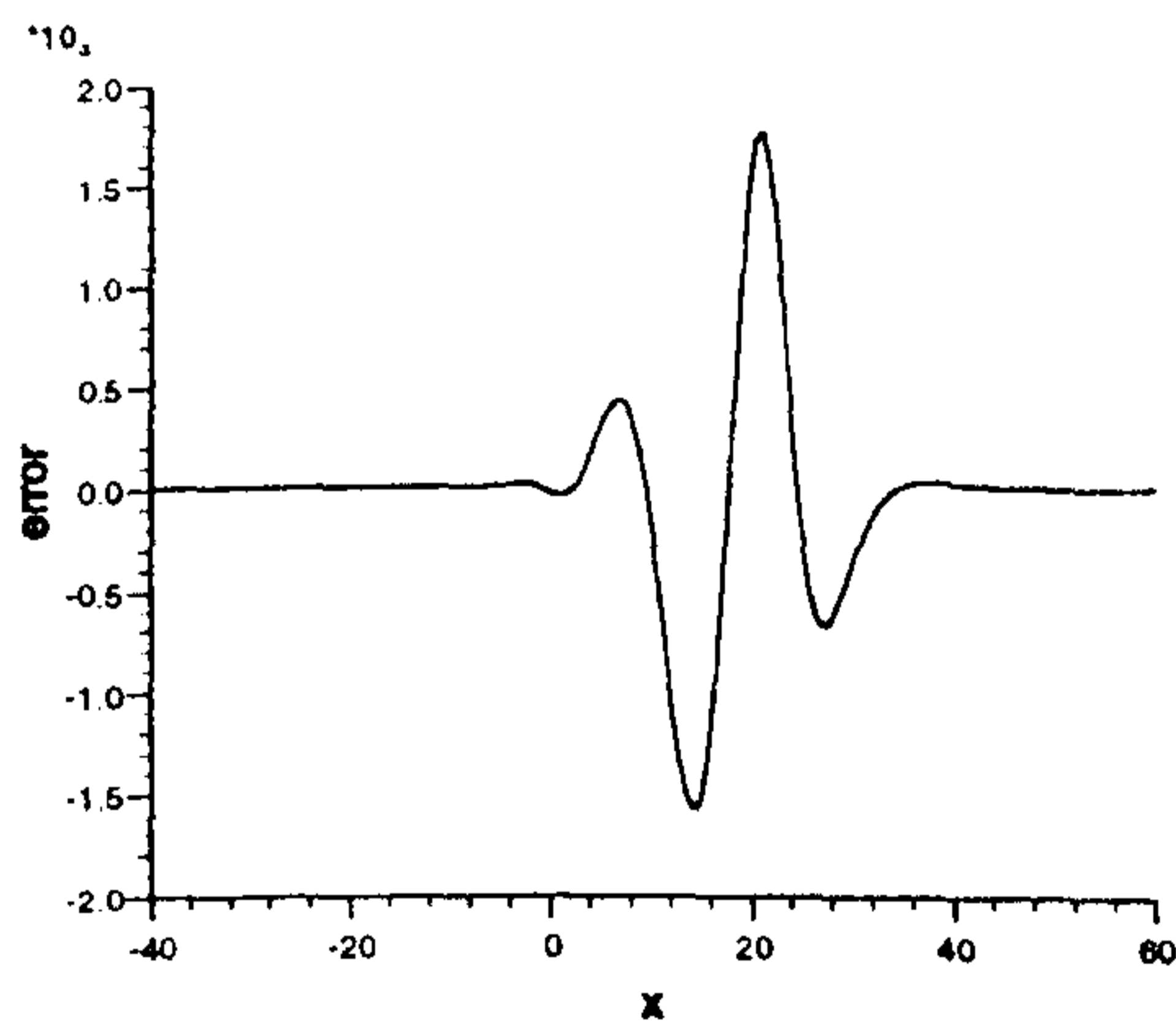


Figure 4.2 The error = exact - numerical solution at $t = 20$ for solitary wave in Figure (4.1) plotted on a larger scale

This simulation of a solitary wave of amplitude 0.09 leads, with the least squares algorithm, to an L_∞ error norm, at $t = 20$, of 0.24×10^{-3} , while the quantities C_2 , C_3 change by about 0.03%, C_1 changes by less 0.1%. In a corresponding simulation using a B-spline method with quadratic spline elements the error norm at $t = 20$ is 0.432×10^{-3} and while the quantities C_2 , C_3 change by less than $8 \times 10^{-4}\%$, C_1 changes by about 0.12%.

With the cubic finite difference scheme [64] it is obtained that $L_\infty = 4 \times 10^{-3}$ at time = 20 and that the quantities C_1, C_2, C_3 increase from the analytic value by about 10% during the course of the experiment. These errors are considerably higher than those found with the present algorithm and conservation is poor. We find that the least squares algorithm has the highest accuracy and also, for this smaller solitary wave, better conservation than exhibited in Table (4.1). Profiles of the solitary waves at times from $t = 0$ to $t = 20$ are shown in Figure (4.3).

Table 4.2

Invariants and error norms for single solitary wave
amplitude=0.09, $\Delta x = 0.125$, $\Delta t = 0.1$, $-40 \leq x \leq 60$.

method	time	C_1	C_2	C_3	$L_2 \times 10^3$	$L_\infty \times 10^3$
Least Squares linear elements	0	2.10702	0.127302	0.388804	0.138	0.390
	2	2.10773	0.127298	0.388792	0.106	0.274
	4	2.10825	0.127293	0.388776	0.110	0.193
	6	2.10864	0.127289	0.388765	0.138	0.136
	8	2.10892	0.127286	0.388757	0.172	0.096
	10	2.10907	0.127281	0.388742	0.205	0.067
	12	2.10911	0.127276	0.388726	0.237	0.067
	14	2.10903	0.127272	0.388714	0.265	0.082
	16	2.10880	0.127269	0.388704	0.292	0.118
18	2.10837	0.127264	0.388689	0.320	0.168	
20	2.10769	0.127260	0.388677	0.347	0.239	
Galerkin quadratic [46]	20	2.10460	0.127302	0.388803	0.563	0.432
f.d [46, 64] cubic	20	2.333	0.140815	0.430052	14.45	3.996

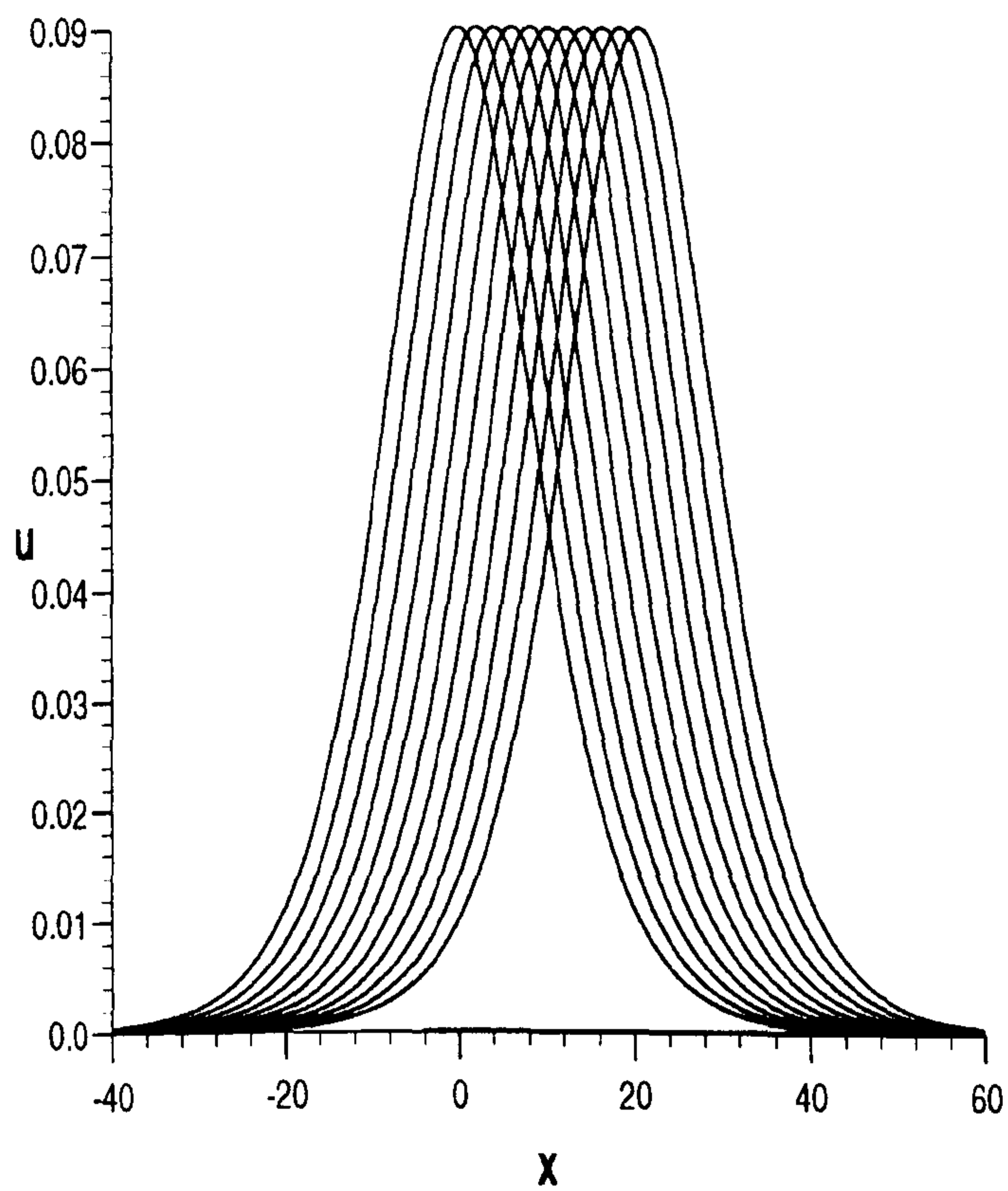


Figure 4.3 Profiles of the solitary waves at times from $t = 0$ to $t = 20$ amplitude=0.09, $\Delta x = 0.125$, $\Delta t = 0.1$.

Table 4.3

Invariants and error norms for single solitary wave
 amplitude=0.09, $\Delta x = 0.025$, $\Delta t = 0.025$, $-40 \leq x \leq 60$.

method	time	C_1	C_2	C_3	$L_2 \times 10^3$	$L_\infty \times 10^3$
Least Squares linear elements	0	2.10705	0.127306	0.388804	0.062	0.390
	2	2.10792	0.127319	0.388843	1.413	0.371
	4	2.10878	0.127346	0.388929	2.861	0.740
	6	2.10946	0.127358	0.388965	4.300	1.116
	8	2.11003	0.127366	0.388992	5.720	1.478
	10	2.11063	0.127391	0.389072	7.151	1.834
	12	2.11113	0.127413	0.389139	8.565	2.222
	14	2.11146	0.127426	0.389179	10.004	2.607
	16	2.11175	0.127462	0.389292	11.419	2.969
	18	2.11177	0.127489	0.389373	12.862	3.374
20	2.11151	0.127506	0.389425	14.289	3.759	

Table 4.4

Invariants and error norms for single solitary wave
amplitude=0.09, $\Delta x = 0.05$, $\Delta t = 0.05$, $-40 \leq x \leq 60$.

method	time	C_1	C_2	C_3	$L_2 \times 10^3$	$L_\infty \times 10^3$
Least Squares linear elements	0	2.10704	0.127304	0.388803	0.088	0.390
	2	2.10781	0.127302	0.388800	0.182	0.274
	4	2.10843	0.127298	0.388789	0.339	0.193
	6	2.10896	0.127296	0.388784	0.506	0.160
	8	2.10944	0.127296	0.388784	0.671	0.213
	10	2.10978	0.127289	0.388763	0.829	0.256
	12	2.11002	0.127283	0.388747	0.977	0.293
	14	2.11017	0.127283	0.388746	1.112	0.328
	16	2.11014	0.127278	0.388731	1.246	0.361
	18	2.10991	0.127271	0.388711	1.378	0.394
20	2.10940	0.127264	0.388686	1.503	0.426	

Table 4.5

Invariants and error norms for single solitary wave
 amplitude=0.09, $\Delta x = 0.25$, $\Delta t = 0.2$, $-40 \leq x \leq 60$.

method	time	C_1	C_2	C_3	$L_2 \times 10^3$	$L_\infty \times 10^3$
Least Squares linear elements	0	2.10700	0.127302	0.388804	0.195	0.390
	2	2.10764	0.127298	0.388794	0.147	0.274
	4	2.10806	0.127294	0.388782	0.141	0.193
	6	2.10829	0.127290	0.388772	0.166	0.136
	8	2.10841	0.127287	0.388761	0.205	0.096
	10	2.10841	0.127284	0.388751	0.247	0.075
	12	2.10831	0.127280	0.388740	0.290	0.089
	14	2.10812	0.127277	0.388730	0.333	0.101
	16	2.10779	0.127274	0.388719	0.375	0.114
	18	2.10729	0.127270	0.388708	0.419	0.127
20	2.10655	0.127267	0.388696	0.464	0.158	

Table 4.6

Invariants and error norms for single solitary wave
amplitude=0.09, $\Delta x = 0.5$, $\Delta t = 0.4$, $-40 \leq x \leq 60$.

method	time	C_1	C_2	C_3	$L_2 \times 10^3$	$L_\infty \times 10^3$
	0	2.10695	0.127301	0.388804	0.275	0.390
	2	2.10750	0.127294	0.388782	0.242	0.274
	4	2.10779	0.127286	0.388760	0.305	0.193
	6	2.10791	0.127279	0.388738	0.399	0.136
Least	8	2.10791	0.127272	0.388716	0.493	0.130
Squares	10	2.10785	0.127265	0.388694	0.584	0.155
linear	12	2.10771	0.127258	0.388671	0.672	0.184
elements	14	2.10750	0.127251	0.388649	0.760	0.212
	16	2.10718	0.127243	0.388627	0.847	0.239
	18	2.10668	0.127236	0.388604	0.935	0.265
	20	2.10595	0.127229	0.388581	1.024	0.290

Table 4.7

Invariants and error norms for single solitary wave
amplitude=0.09, $\Delta x = 1.0$, $\Delta t = 0.8$, $-40 \leq x \leq 60$.

method	time	C_1	C_2	C_3	$L_2 \times 10^3$	$L_\infty \times 10^3$
	0	2.10684	0.127300	0.388804	0.390	0.390
	1.6	2.10725	0.127286	0.388762	0.396	0.294
	3.2	2.10749	0.127273	0.388720	0.544	0.222
	4.8	2.10762	0.127259	0.388678	0.729	0.201
Least	6.4	2.10768	0.127246	0.388637	0.920	0.245
Squares	8	2.10770	0.127232	0.388595	1.111	0.305
linear	9.6	2.10768	0.127219	0.388554	1.301	0.367
elements	11.2	2.10763	0.127206	0.388513	1.490	0.428
	12.8	2.10753	0.127193	0.388472	1.679	0.491
	14.4	2.10738	0.127179	0.388431	1.868	0.548
	16	2.10715	0.127166	0.388391	2.056	0.614
	17.6	2.10681	0.127153	0.388350	2.243	0.668
	19.2	2.10631	0.127140	0.388310	2.429	0.733
	20.8	2.10563	0.127127	0.388269	2.614	0.789

Table 4.8

Invariants and error norms for single solitary wave
amplitude=0.09, $\Delta x = 4.0$, $\Delta t = 0.8$, $-40 \leq x \leq 60$.

method	time	C_1	C_2	C_3	$L_2 \times 10^3$	$L_\infty \times 10^3$
	0	2.10615	0.127281	0.388803	0.779	0.390
	1.6	2.10829	0.127411	0.389206	0.945	0.294
	3.2	2.11026	0.127542	0.389608	1.505	0.432
	4.8	2.11212	0.127672	0.390010	2.135	0.573
Least	6.4	2.11389	0.127802	0.390411	2.771	0.851
Squares	8	2.11560	0.127932	0.390811	3.399	1.072
linear	9.6	2.11727	0.128062	0.391210	4.016	1.090
elements	11.2	2.11889	0.128191	0.391608	4.621	1.489
	12.8	2.12047	0.128320	0.392005	5.215	1.631
	14.4	2.12198	0.128449	0.392402	5.798	1.717
	16	2.12341	0.128578	0.392797	6.370	2.077
	17.6	2.12472	0.128706	0.393192	6.933	2.079
	19.2	2.12588	0.128834	0.393586	7.487	2.345
	20.8	2.12684	0.128962	0.393979	8.033	2.578

Invariants and error norms for single solitary wave are given in Tables (4.3) to (4.8). In Table (4.9) we examine the effect of various space-step/time-step combinations and find that the highest accuracy is found with space steps between 0.125-0.25 combined with time steps in the range 0.1-0.2. Profile of solitary wave at time $t = 20$ is given in Figure (4.4).

Table 4.9

Error norms for single solitary wave at
 $t = 20$, amplitude=0.09, $-40 \leq x \leq 60$.

Δx	Δt	$L_2 \times 10^3$	$L_\infty \times 10^3$
0.025	0.025	14.3	3.76
0.05	0.05	1.50	0.426
0.125	0.1	0.347	0.239
0.25	0.2	0.464	0.158
0.5	0.4	1.02	0.290
1.0	0.8	2.61	0.789
4.0	0.8	8.03	2.58

Table 4.10

Invariants and error norms for single solitary wave
amplitude=0.09, $\Delta x = 0.05$, $\Delta t = 0.05$, $-80 \leq x \leq 120$.

method	time	C_1	C_2	C_3	$L_2 \times 10^3$	$L_\infty \times 10^3$
Least Squares linear elements	0	2.10940	0.127301	0.388805	0.008	0.002
	2	2.10942	0.127301	0.388805	0.140	0.050
	4	2.10942	0.127300	0.388803	0.288	0.104
	6	2.10942	0.127297	0.388792	0.430	0.155
	8	2.10948	0.127303	0.388811	0.565	0.207
	10	2.10943	0.127294	0.388782	0.699	0.246
	12	2.10939	0.127285	0.388755	0.833	0.285
	14	2.10939	0.127282	0.388744	0.961	0.321
	16	2.10935	0.127273	0.388718	1.085	0.351
18	2.10930	0.127264	0.388689	1.209	0.381	
20	2.10927	0.127257	0.388669	1.328	0.413	

Table 4.11

Invariants and error norms for single solitary wave
 amplitude=0.09, $\Delta x = 0.125$, $\Delta t = 0.1$, $-80 \leq x \leq 120$.

method	time	C_1	C_2	C_3	$L_2 \times 10^3$	$L_\infty \times 10^3$
	0	2.10940	0.127301	0.388805	0.000	0.000
	2	2.10941	0.127297	0.388793	0.027	0.011
	4	2.10941	0.127292	0.388777	0.055	0.022
	6	2.10941	0.127288	0.388765	0.081	0.031
Least	8	2.10943	0.127285	0.388755	0.105	0.040
Squares	10	2.10942	0.127280	0.388739	0.131	0.051
linear	12	2.10942	0.127275	0.388723	0.156	0.060
elements	14	2.10943	0.127271	0.388713	0.181	0.070
	16	2.10945	0.127269	0.388704	0.206	0.078
	18	2.10945	0.127264	0.388691	0.233	0.087
	20	2.10946	0.127261	0.388679	0.255	0.095

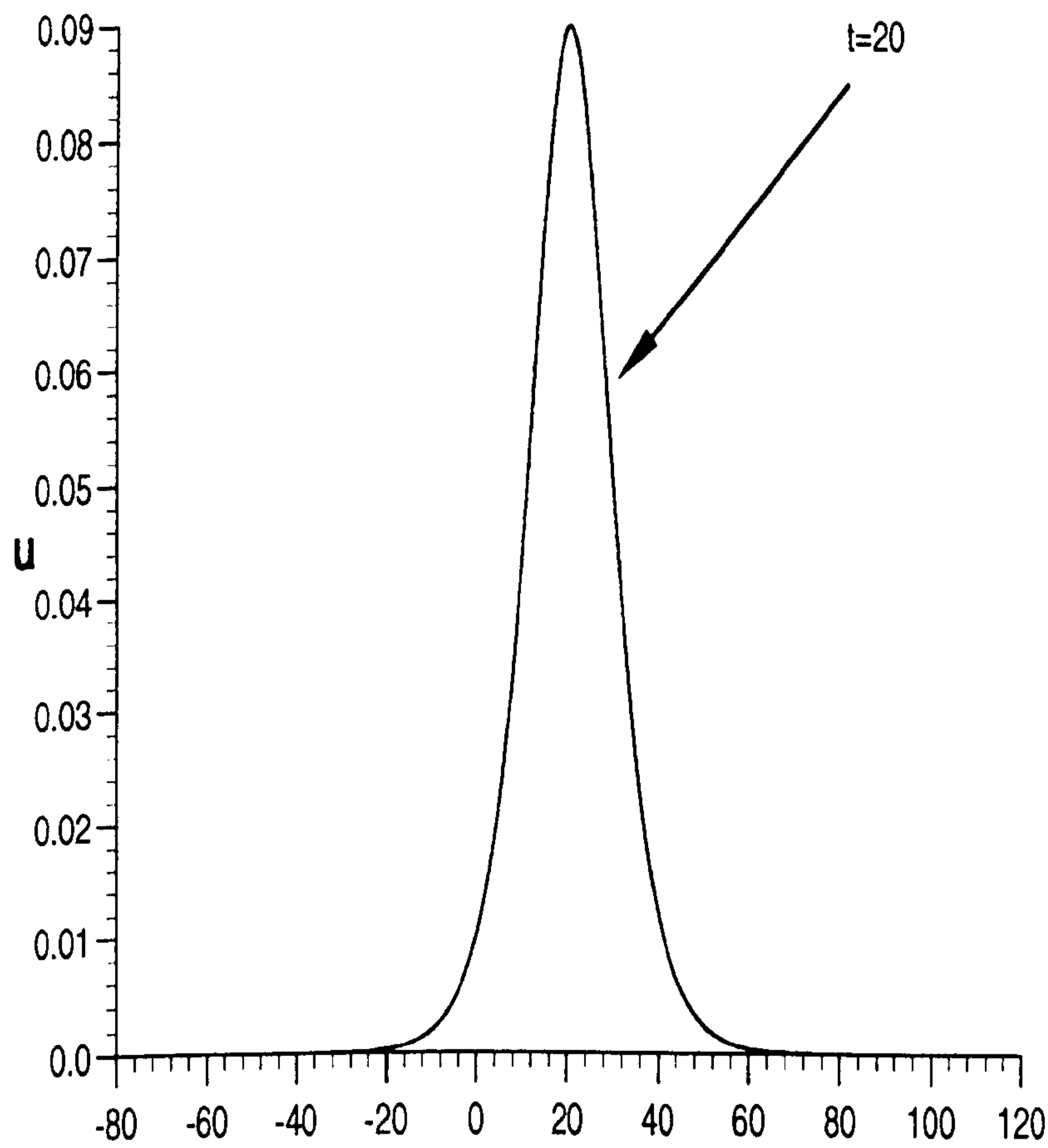


Figure 4.4 Profile of the solitary wave at $t = 20$
amplitude=0.09, $\Delta x = 0.125$, $\Delta t = 0.1$.

Table 4.12

Invariants and error norms for single solitary wave
amplitude=0.09, $\Delta x = 0.25$, $\Delta t = 0.2$, $-80 \leq x \leq 120$.

method	time	C_1	C_2	C_3	$L_2 \times 10^3$	$L_\infty \times 10^3$
	0	2.10940	0.127302	0.388806	0.000	0.000
	2	2.10944	0.127298	0.388794	0.045	0.015
	4	2.10947	0.127294	0.388783	0.091	0.031
	6	2.10950	0.127291	0.388772	0.136	0.046
Least	8	2.10953	0.127287	0.388762	0.181	0.061
Squares	10	2.10957	0.127284	0.388751	0.225	0.075
linear	12	2.10960	0.127280	0.388740	0.270	0.089
elements	14	2.10963	0.127277	0.388730	0.314	0.101
	16	2.10967	0.127274	0.388721	0.357	0.115
	18	2.10970	0.127270	0.388709	0.401	0.128
	20	2.10973	0.127267	0.388699	0.443	0.140

Table 4.13

Invariants and error norms for single solitary wave
 amplitude=0.09, $\Delta x = 0.5$, $\Delta t = 0.4$, $-80 \leq x \leq 120$.

method	time	C_1	C_2	C_3	$L_2 \times 10^3$	$L_\infty \times 10^3$
	0	2.10940	0.127301	0.388806	0.000	0.000
	2	2.10947	0.127294	0.388783	0.100	0.033
	4	2.10954	0.127287	0.388761	0.199	0.065
	6	2.10960	0.127280	0.388739	0.298	0.096
Least	8	2.10967	0.127272	0.388717	0.395	0.126
Squares	10	2.10973	0.127265	0.388695	0.493	0.155
linear	12	2.10980	0.127258	0.388672	0.589	0.184
elements	14	2.10986	0.127251	0.388650	0.685	0.212
	16	2.10993	0.127244	0.388628	0.780	0.239
	18	2.10999	0.127237	0.388606	0.874	0.265
	20	2.11005	0.127230	0.388584	0.967	0.290

Table 4.14

Error norms for single solitary wave at
 $t = 20$, amplitude=0.09, $-80 \leq x \leq 120$.

Δx	Δt	$L_2 \times 10^3$	$L_\infty \times 10^3$
0.05	0.05	1.328	0.413
0.125	0.1	0.255	0.095
0.25	0.2	0.443	0.140
0.5	0.4	0.967	0.290

Table 4.15

Invariants and error norms for single solitary wave
amplitude=0.03, $\Delta x = 0.125$, $\Delta t = 0.1$, $-80 \leq x \leq 120$.

method	time	C_1	C_2	C_3	$L_2 \times 10^3$	$L_\infty \times 10^3$
	0	1.20555	0.024167	0.072938	0.015	0.042
	2	1.20562	0.024167	0.072936	0.015	0.034
	4	1.20568	0.024166	0.072934	0.018	0.028
	6	1.20572	0.024166	0.072933	0.023	0.023
Least	8	1.20575	0.024165	0.072931	0.029	0.019
Squares	10	1.20577	0.024164	0.072929	0.035	0.015
linear	12	1.20578	0.024164	0.072927	0.042	0.013
elements	14	1.20579	0.024163	0.072925	0.047	0.014
	16	1.20579	0.024162	0.072922	0.054	0.016
	18	1.20578	0.024162	0.072920	0.060	0.020
	20	1.20577	0.024161	0.072918	0.067	0.023

Table 4.16

Invariants and error norms for single solitary wave
amplitude=0.03, $\Delta x = 0.25$, $\Delta t = 0.2$, $-80 \leq x \leq 120$.

method	time	C_1	C_2	C_3	$L_2 \times 10^3$	$L_\infty \times 10^3$
	0	1.20555	0.024167	0.072938	0.021	0.042
	2	1.20562	0.024167	0.072938	0.019	0.034
	4	1.20567	0.024167	0.072938	0.020	0.028
	6	1.20569	0.024167	0.072937	0.024	0.023
Least	8	1.20571	0.024167	0.072937	0.030	0.019
Squares	10	1.20572	0.024167	0.072937	0.034	0.015
linear	12	1.20573	0.024167	0.072937	0.038	0.013
elements	14	1.20573	0.024167	0.072937	0.041	0.013
	16	1.20572	0.024167	0.072936	0.043	0.013
	18	1.20572	0.024167	0.072936	0.045	0.013
	20	1.20571	0.024167	0.072936	0.047	0.013

Table 4.17

Invariants and error norms for single solitary wave
amplitude=0.03, $\Delta x = 0.5$, $\Delta t = 0.4$, $-80 \leq x \leq 120$.

method	time	C_1	C_2	C_3	$L_2 \times 10^3$	$L_\infty \times 10^3$
	0	1.20555	0.024167	0.072938	0.030	0.042
	2	1.20560	0.024167	0.072938	0.029	0.034
	4	1.20563	0.024167	0.072937	0.036	0.028
	6	1.20565	0.024167	0.072937	0.046	0.023
Least	8	1.20565	0.024167	0.072936	0.055	0.022
Squares	10	1.20566	0.024167	0.072936	0.062	0.022
linear	12	1.20566	0.024167	0.072936	0.068	0.022
elements	14	1.20565	0.024167	0.072935	0.073	0.022
	16	1.20565	0.024166	0.072935	0.077	0.022
	18	1.20565	0.024166	0.072934	0.081	0.021
	20	1.20564	0.024166	0.072934	0.086	0.021

As the amplitude of a solitary wave is reduced the pulse broadens and it may be necessary to increase the solution range in order to maintain accuracy. The effect of doubling the range from $-40 \leq x \leq 60$ to $-80 \leq x \leq 120$ is demonstrated in Table (4.14). The maximum improvement in accuracy is found for $\Delta x = 0.125$, $\Delta t = 0.1$ where the L_2 error norm is halved and the L_∞ error norm is reduced by more than half, from 0.24×10^{-3} down to 0.095×10^{-3} . In Tables from (4.10) to (4.13) invariants and error norms are demonstrated for single solitary wave.

Invariants and Error norms for single solitary wave are given in Tables (4.15) to (4.17) . The error norms and invariants for an even smaller solitary wave, amplitude =0.03, are given in Table (4.16) . With the range $-80 \leq x \leq 120$, $\Delta x = 0.25$ and $\Delta t = 0.2$ we find excellent results. Throughout the simulation the L_2 and L_∞ error norms remain less than 5×10^{-5} , while the invariants C_2 and C_3 change by less than $3 \times 10^{-3}\%$ and C_1 changes by about 0.013% by time $t = 20$. The effect of changes in the space and time

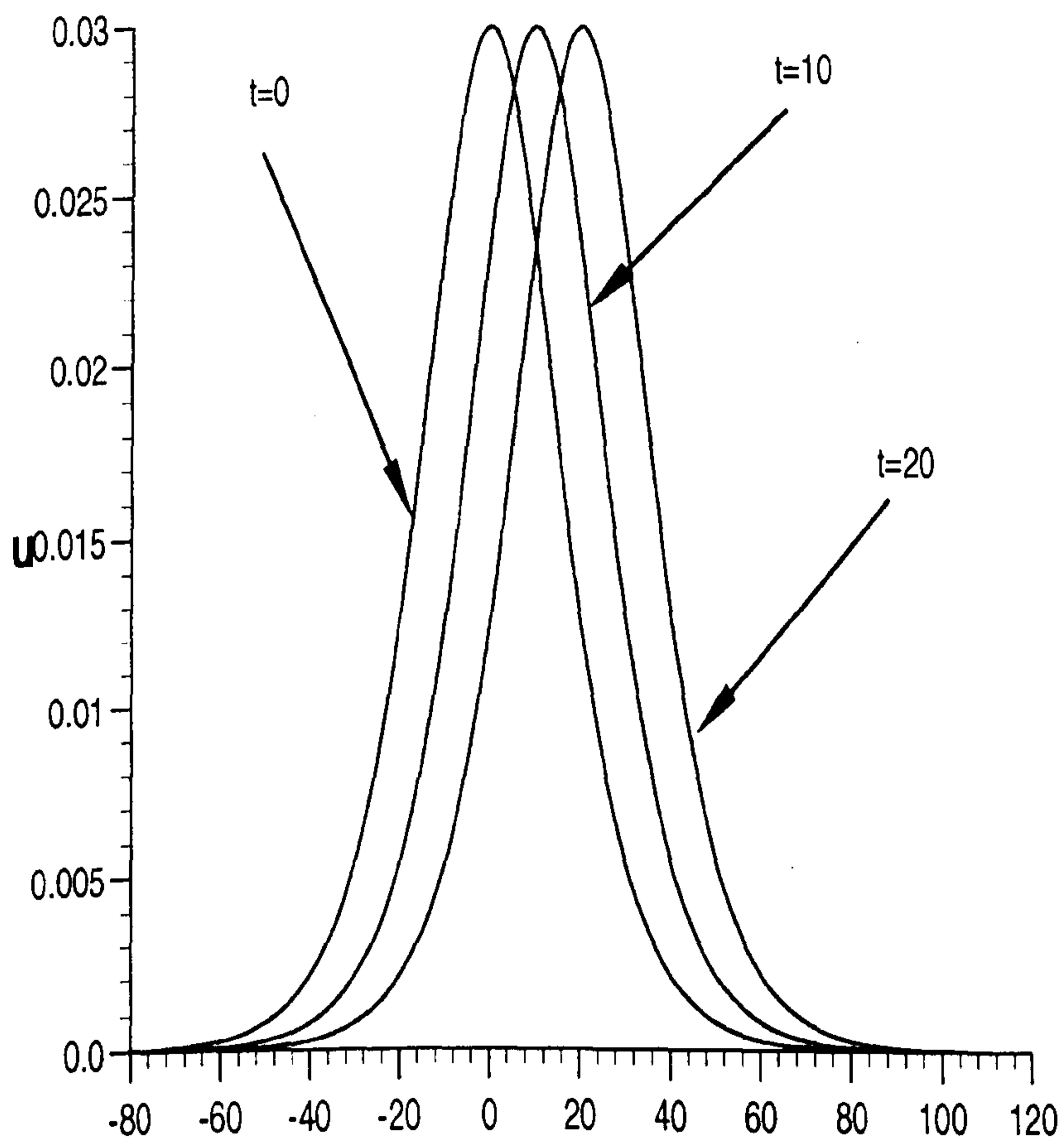


Figure 4.5 Profiles of the solitary waves at $t = 0, 10, 20$
amplitude=0.03, $\Delta x = 0.25$, $\Delta t = 0.2$.

steps is examined in Table (4.18). The smallest error norms are obtained with the choice $\Delta x = 0.25$ and $\Delta t = 0.2$. Profiles of the solitary wave at times $t = 0, 10, 20$ are shown in Figure (4.5).

Table 4.18
Error norms for single solitary
wave at $t = 20$ amplitude = 0.03,
 $-80 \leq x \leq 120$.

Δx	Δt	$L_2 \times 10^3$	$L_\infty \times 10^3$
0.125	0.1	0.067	0.023
0.25	0.2	0.047	0.013
0.5	0.4	0.086	0.021

4.4 Modelling an undular bore

A bore is formed when a deeper stream of water flows into an area of still water in a long horizontal channel. When the transition between the deeper stream and the still water has a very gentle slope, the slope will steepen and a bore will form. There is experimental evidence to show that when the ratio of the change in level to the depth of still water is less than 0.28 the bore is undular, otherwise one or more undulation is breaking [89].

To study the development of an undular bore we follow Peregrine [89] and use as initial condition

$$U(x, 0) = 0.5U_0 \left[1 - \tanh \frac{(x - x_c)}{d} \right], \quad (4.19)$$

where $U(x, 0)$ denotes the elevation of the water above the equilibrium surface at time $t = 0$. The change in water level of magnitude U_0 is centred on $x = x_c$, and d measures the steepness of the change. The smaller the value of d the steeper is the slope. To compare with earlier studies of water waves we take the parameters to have the following values: $\epsilon = 1.5$, $\mu = 0.16666667$, $U_0 = 0.1$ and $d = 5.0$. The physical boundary conditions require that $U \rightarrow 0$ as $x \rightarrow \infty$ and $U \rightarrow U_0$ as $x \rightarrow -\infty$. To limit the effect of boundaries

on the numerical solution we take $x_0 = -60$ and $x_N = 300$ together with $\Delta x = 0.24$, $\Delta t = 0.1$ and run the simulation until $t = 200$.

As the simulation proceeds undulations begin to develop and grow, moving back along the profile as the leading edge moves to the right. The function profile at time $t = 200$ is the shown in Figure (4.6). This profile is consistent with those for other time slots shown in references [89] and [46]. The temporal development of the amplitude of the leading undulation is given in Figure (4.7). There is quantitative agreement between this graph and the appropriate graph shown in Figure 5 of [89]. As we see, after a short incubation period lasting until about $t = 28$, the leading undulation begins to grow and reaches a height of 0.125 at $t = 80$ and subsequently 0.161 at $t = 160$. This agrees with the results reported by Peregrine [89] who observes an incubation period lasting until $t = 27$ and finds an amplitude of 0.126 at $t = 80$. A space/time curve for the leading undulation is given in Figure (4.8). After time $t = 30$ the velocity of the wave is, within the experimental error, constant at 1.080 ± 0.002 throughout the simulation (to $t = 200$). This velocity is consistent with that of a solitary wave of height 0.16; an observation also made by Peregrine [89]. For times in excess of 400 the leading undulation, which is almost a detached solitary wave, has an amplitude of 0.186 and a velocity of 1.093 which are appropriate for such a solitary wave. Results for undular bore until $t = 200$ by taking $d = 5.0$ are demonstrated in Table (4.19).

The steeper initial profile obtained by taking $d = 2.0$ has also been studied. The leading undulation begins growing almost as soon as the simulation starts and proceeds smoothly attaining an amplitude of 0.177 at $t = 160$, in good agreement with Peregrine's observation [89] of 0.175 at $t = 160$, thereafter growth continues in a smooth monotonic manner. Results for undular bore until $t = 200$, with $d = 2.0$ are given in Table (4.20).

Table 4.19

Results for undular bore until
 $t = 200$, $\epsilon = 1.5$, $\mu = 0.16666667$,
 $U_0 = 0.1$, $d = 5.0$.

time	Ubig	ibig * Δx
0	0.1000	-7.6800
20	0.1000	38.6400
40	0.1047	87.6000
60	0.1149	109.2000
80	0.1255	130.8000
100	0.1358	152.4000
120	0.1453	174.0000
140	0.1539	195.8400
160	0.1614	217.4400
180	0.1681	239.2800
200	0.1739	261.1200

Table 4.20

Results for undular bore until
 $t = 200$, $\epsilon = 1.5$, $\mu = 0.16666667$,
 $U_0 = 0.1$, $d = 2.0$.

time	Ubig	ibig * Δx
0	0.1000	-32.8800
20	0.1198	67.4400
40	0.1330	88.5600
60	0.1433	109.9200
80	0.1519	131.2800
100	0.1594	153.1200
120	0.1662	174.7200
140	0.1721	196.5600
160	0.1774	218.4000
180	0.1822	240.2400
200	0.1865	262.3200

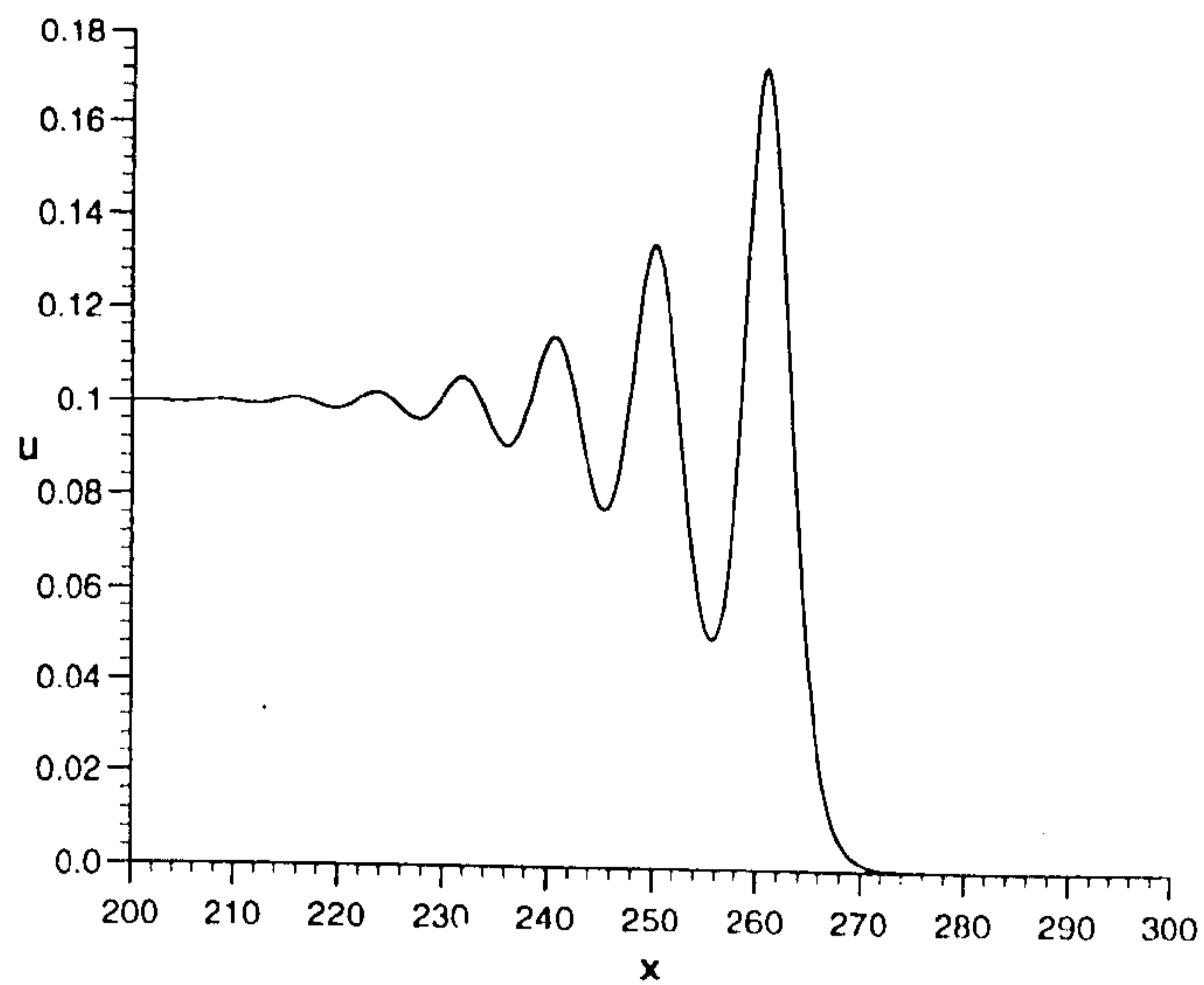


Figure 4.6 The undulation profile at time $t = 200$ for a gentle slope $d = 5$.

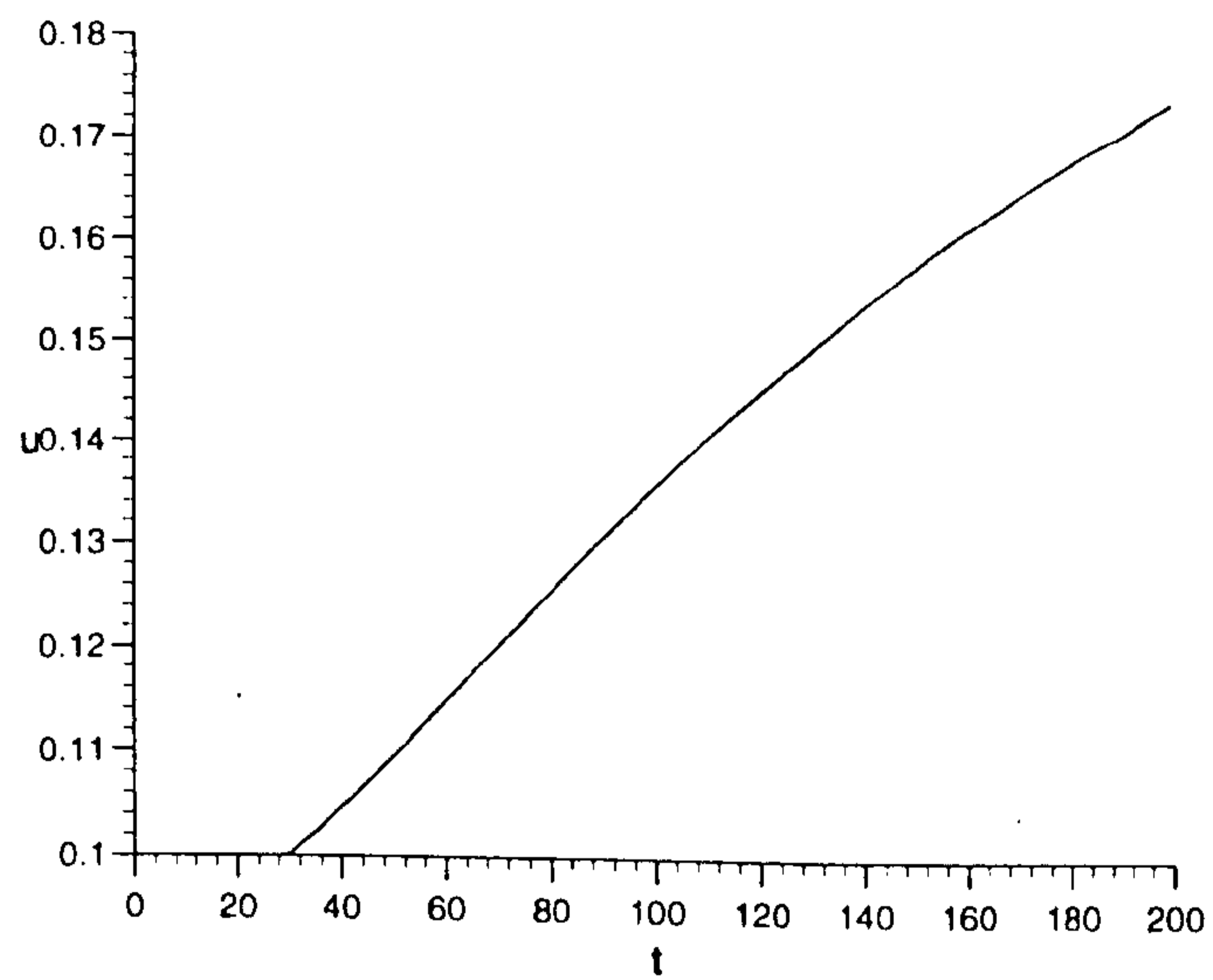


Figure 4.7 The growth in the amplitude of the leading undulation $d = 5$.

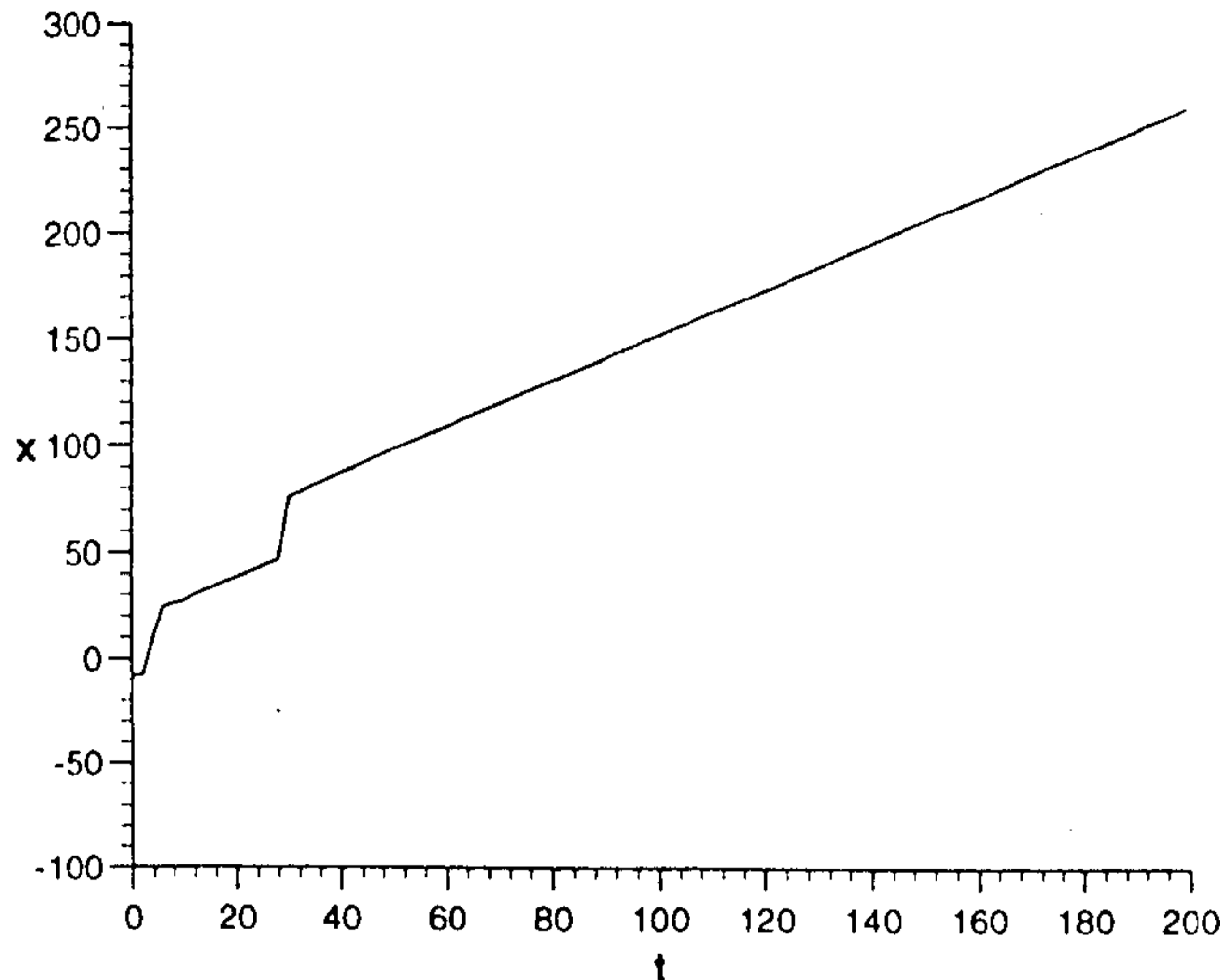


Figure 4.8 A space/time graph for the leading undulation $d = 5$.

4.5 Discussion

The space/time least squares approach with linear finite elements set up in Section (4.2) leads to an unconditionally stable algorithm which faithfully models the amplitude, position and velocity of a single solitary wave over an extended time scale.

The development of an undular bore from an appropriate initial condition is simulated. The undulations develop smoothly. During the experiment the leading undulation has the expected characteristics. Its shape, height and velocity are consistent with earlier work [46, 89]. With the steeper initial condition $d = 2$ and $U_0 = 0.1$ we find that, at time $t = 200$ the leading undulation has an amplitude of 0.186 and a velocity of 1.092 ± 0.002 . These results are not dissimilar to those obtained by boundary forcing the RLW equation with $U_0 = 0.1$ [48], where at $t = 200$ the leading solitary wave has an amplitude 0.178 and a velocity 1.089. As the simulation proceeds to

longer times the undulations continue to develop smoothly and monotonically into a train of independent solitary waves. By time $t = 400$ the leading undulation in both simulations has become virtually a solitary wave with amplitude 0.186 and velocity 1.093. None of the instabilities found by Jain et al [64] are observed.

Chapter 5

A Petrov-Galerkin Algorithm For The RLW Equation

5.1 Introduction

The regularised long wave equation is solved by a Petrov-Galerkin method using quadratic B-spline spatial finite elements. A linear recurrence relationship for the numerical solution of the resulting system of ordinary differential equations is obtained via a Crank-Nicolson approach involving a product approximation. The motion of solitary waves is studied to assess the properties of the algorithm. The development of an undular bore is studied

Peregrine [89] was the first to derive the regularised long wave (RLW) equation

$$U_t + U_x + UU_x - \mu U_{xxt} = 0, \quad (5.1)$$

where t is time, x is the space coordinate, $U(x, t)$ is the wave amplitude and μ is a constant, as the governing equation for the lossless propagation of long wavelength water waves along a long straight channel. It is also used to model the development of an undular bore.

The RLW equation has the solitary wave solution

$$U(x, t) = 3\text{csech}^2(k[x - x_0 - vt]), \quad (5.2)$$

where

$$k = \sqrt{\frac{c}{4\mu(1+c)}}, \quad v = 1 + c. \quad (5.3)$$

The RLW solitary waves may not have velocities lying in the range $0 \leq v \leq 1$.

We have previously studied the interaction of RLW solitary waves [40] using a Galerkin algorithm based on linear elements [46]. In the following we will set up a Petrov-Galerkin solution using quadratic B-spline finite elements. The numerical algorithm so obtained is validated by modelling the motion of solitary waves. The algorithm is then used to model an undular bore.

5.2 The finite element solution

A uniform linear spatial array of linear finite elements is set up $0 = x_0 < x_1 < \dots < x_N = L$ covering the simulation region. A typical finite element of size $\Delta x = (x_{m+1} - x_m)$ is mapped by local coordinates ξ related to the global coordinates x by $\Delta x \xi = x - x_m$, $0 \leq \xi \leq 1$. The trial function for a quadratic B-spline finite element is

$$U = (1 - 2\xi + \xi^2)\delta_{m-1} + (1 + 2\xi - 2\xi^2)\delta_m + \xi^2\delta_{m+1}, \quad (5.4)$$

where the quantities δ_m are nodeless element parameters. At the node x_m the nodal variables U_m and U'_m are given in terms of the parameters δ_m by

$$U_m = \delta_m + \delta_{m-1}, \quad \Delta x U'_m = 2(\delta_m - \delta_{m-1}), \quad (5.5)$$

where the prime denotes differentiation with respect to x .

When a Petrov-Galerkin method [103] is applied to Equation (5.1) with weight functions W_m the weak form

$$\int_{x_0}^{x_N} W_m (U_t + U_x + UU_x - \mu U_{xxt}) dx = 0, \quad (5.6)$$

where $m = 0, 1, \dots, N - 1$, is produced. With weight functions of the form

$$W_m = \begin{cases} 1, & x_m \leq x \leq x_{m+1}, \\ 0, & x < x_m, \quad x > x_{m+1}, \end{cases}$$

Equation (5.6) becomes for a single element $[x_m, x_{m+1}]$

$$\int_{x_m}^{x_{m+1}} (U_t + U_x + UU_x - \mu U_{xxt}) dx = 0. \quad (5.7)$$

Integrating leads to

$$\int_{x_m}^{x_{m+1}} U_t dx + [U]_{x_m}^{x_{m+1}} + \frac{1}{2}[U^2]_{x_m}^{x_{m+1}} - \mu[U_{xt}]_{x_m}^{x_{m+1}} = 0. \quad (5.8)$$

With a Crank-Nicolson approach in time we centre on $(n + \frac{1}{2})\Delta t$ and obtain the well known *second order accurate* expression for $U^{n+\frac{1}{2}}$ and its time derivative as

$$U = \frac{1}{2}(U^n + U^{n+1}),$$

$$\frac{\partial U}{\partial t} = \frac{1}{\Delta t}(U^{n+1} - U^n).$$

where the superscripts n and $n + 1$ are time labels. Using Taylor expansions for U^{n+1} and U^n about $(n + \frac{1}{2})\Delta t$ enables us to find for U^2 at $(n + \frac{1}{2})\Delta t$ the expression

$$U^2 = U^{n+1}U^n,$$

which is also *second order accurate* in time.

Substituting these expressions into Equation (5.8) produces

$$\frac{1}{\Delta t} \int_{x_m}^{x_{m+1}} (U^{n+1} - U^n) dx + \frac{1}{2}[U^{n+1} + U^n]_{x_m}^{x_{m+1}}$$

$$+ \frac{1}{2}[U^{n+1}U^n]_{x_m}^{x_{m+1}} - \frac{\mu}{\Delta t}[U_x^{n+1} - U_x^n]_{x_m}^{x_{m+1}} = 0, \quad (5.9)$$

which with (5.5) leads to the quasi-linear recurrence relationship

$$(1 - \alpha - \beta - \alpha[\delta_{m-1}^n + \delta_m^n])\delta_{m-1}^{n+1} +$$

$$(4 + 2\beta + \alpha[\delta_{m+1}^n - \delta_{m-1}^n])\delta_m^{n+1} +$$

$$(1 + \alpha - \beta + \alpha[\delta_m^n + \delta_{m+1}^n])\delta_{m+1}^{n+1} =$$

$$(1 + \alpha - \beta)\delta_{m-1}^n + (4 + 2\beta)\delta_m^n +$$

$$(1 - \alpha - \beta)\delta_{m+1}^n, \quad (5.10)$$

where

$$\alpha = \frac{3\Delta t}{2\Delta x}, \quad \beta = \frac{6\mu}{\Delta x^2}, \quad (5.11)$$

and $m = 0, 1, \dots, N-1$, $n = 0, 1, \dots$.

With boundary conditions U_0, U_N prescribed, leading to $\delta_{-1}^n + \delta_0^n = U_0$ and $\delta_{N-1}^n + \delta_N^n = U_N$, the first and last equations corresponding to $m = 0, N-1$ have the reduced forms

$$\begin{aligned} & (3 + \alpha + 3\beta + \alpha[\delta_0^n + \delta_1^n])\delta_0^{n+1} + (1 + \alpha - \beta + \alpha[\delta_0^n + \delta_1^n])\delta_1^{n+1} \\ & = (3 - \alpha + 3\beta)\delta_0^n + (1 - \alpha - \beta)\delta_1^n + \alpha U_0^2 + 2\alpha U_0, \end{aligned}$$

and

$$\begin{aligned} & (1 - \alpha - \beta - \alpha[\delta_{N-2}^n + \delta_{N-1}^n])\delta_{N-2}^{n+1} + (3 - \alpha + 3\beta - \alpha[\delta_{N-2}^n + \delta_{N-1}^n])\delta_{N-1}^{n+1} \\ & = (1 + \alpha - \beta)\delta_{N-2}^n + (3 + \alpha + 3\beta)\delta_{N-1}^n - \alpha U_N^2 - 2\alpha U_N. \end{aligned}$$

The above set of quasi-linear equations has a matrix which is tridiagonal in form so that a solution using the Thomas algorithm is direct and no iterations are necessary.

5.2.1 Stability Analysis

The growth factor g of the error ϵ_j^n in a typical Fourier mode of amplitude $\hat{\epsilon}^n$

$$\hat{\epsilon}_j^n = \hat{\epsilon}^n \exp(ijk\Delta x) \quad (5.12)$$

where k is the mode number and Δx the element size, is determined for a linearisation of the numerical scheme.

In the linearisation it is assumed that the quantity U in the nonlinear term is locally constant. Under these conditions the error ϵ_j^n satisfies the

same finite difference scheme as the function δ_j^n and we find that a typical member of Equation (5.10) has the form

$$\begin{aligned} & (1 - \alpha - \beta)\epsilon_{m-1}^{n+1} + (4 + 2\beta)\epsilon_m^{n+1} \\ & + (1 + \alpha - \beta)\epsilon_{m+1}^{n+1} = (1 + \alpha - \beta)\epsilon_{m-1}^n \\ & + (4 + 2\beta)\epsilon_m^n + (1 - \alpha - \beta)\epsilon_{m+1}^n, \end{aligned} \quad (5.13)$$

where

$$\alpha = \frac{3\Delta t}{2\Delta x}$$

and

$$\beta = \frac{6\mu}{\Delta x^2}$$

substituting the above Fourier mode gives

$$(p + iq)\epsilon^{\hat{n}+1} = (p - iq)\epsilon^{\hat{n}}$$

where

$$p = (2 - 2\beta) \cos[k\Delta x] + (4 + 2\beta)$$

and

$$q = 2\alpha \sin[k\Delta x].$$

Writing $\epsilon^{\hat{n}+1} = g\epsilon^{\hat{n}}$, it is observed that $g = \frac{p-iq}{p+iq}$ and so has unit modulus therefore scheme is unconditionally stable.

5.3 Validation

In the following simulation of the motion of a single solitary wave $\epsilon = \mu = 1$. To make comparison with earlier simulation results [46, 49, 64] Equation (5.2) is taken as initial condition with range $-40 \leq x \leq 60$, $\Delta x = 0.125$, $\Delta t = 0.1$ and $x_0 = 0$, with $c = 0.1$ so that the solitary wave has amplitude 0.3. The simulation is run to time $t = 20$ and the L_2 and L_∞ error norms and the invariants C_1 , C_2 , C_3 , whose analytic values can be found as

$$C_1 = \frac{6c}{k} = 3.9799497,$$

$$C_2 = \frac{12c^2}{k} + \frac{48kc^2\mu}{5} = 0.81046249,$$

$$C_3 = \frac{36c^2}{k} \left(1 + \frac{4c}{5}\right) = 2.579007,$$

are recorded throughout the simulation: see Table (5.1).

Table 5.1

Invariants and error norms for single solitary wave
amplitude=0.3, $\Delta x = 0.125$, $\Delta t = 0.1$, $-40 \leq x \leq 60$.

method	time	C_1	C_2	C_3	$L_2 \times 10^3$	$L_\infty \times 10^3$
Petrov Galerkin quadratic elements	0	3.97993	0.810461	2.57901	0.002	0.007
	2	3.97994	0.810460	2.57901	0.022	0.009
	4	3.97995	0.810459	2.57900	0.045	0.018
	6	3.97996	0.810455	2.57899	0.067	0.027
	8	3.97995	0.810445	2.57895	0.090	0.034
	10	3.97996	0.810442	2.57895	0.115	0.043
	12	3.97995	0.810435	2.57892	0.137	0.052
	14	3.97993	0.810425	2.57889	0.162	0.061
	16	3.97992	0.810418	2.57887	0.183	0.069
	18	3.97989	0.810408	2.57883	0.206	0.074
20	3.97986	0.810399	2.57880	0.227	0.081	
Galerkin quadratic [46]	20	3.97989	0.810467	2.57902	0.220	0.086
f.d [46] [64] cubic	20	4.41219	0.897342	2.85361	196.1	67.35
l.s linear [49]	20	3.98203	0.808650	2.57302	4.688	1.755

The quantity C_1 is constant to 4 and C_3 to 3 decimal places, while C_2 changes by up to 1 in the 4th decimal place. This degree of conservation is not as good as that obtained with Galerkin's method with quadratic B-spline elements but is superior to that obtained with the other methods listed. The errors, at time $t = 20$, found with the present method are comparable with those obtained using Galerkin and smaller than those obtained with the other 2 methods.

In Figure (5.1) the initial wave profile and that at $t = 20$ are compared. It is clear that, by $t = 20$, there has been little degradation of the wave amplitude. The distribution of error along the wave profile is shown in Figure (5.2); the maximum error is located on either side of the pulse maximum and varies up to about $\pm 9 \times 10^{-5}$.

In a second simulation involving the migration of a single solitary wave with the smaller amplitude 0.09 and using the same range and space/time steps as quoted in [46] and [64] the results given in Table (5.2) are obtained. The analytic values of the invariants are $C_1 = 2.109407$, $C_2 = 0.127302$, $C_3 = 0.388806$.

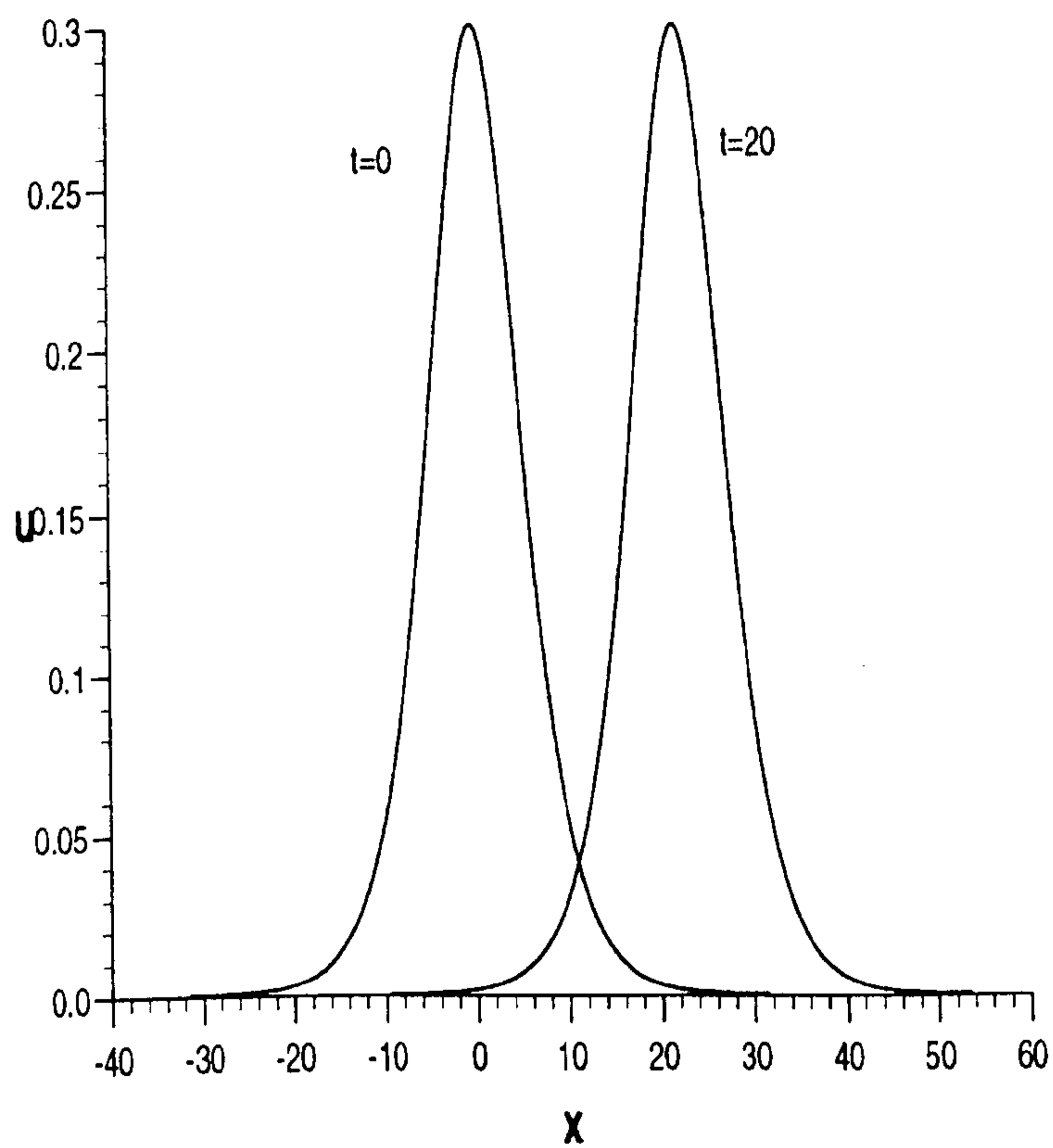


Figure 5.1 Profiles of the solitary wave at $t = 0$ and $t = 20$.

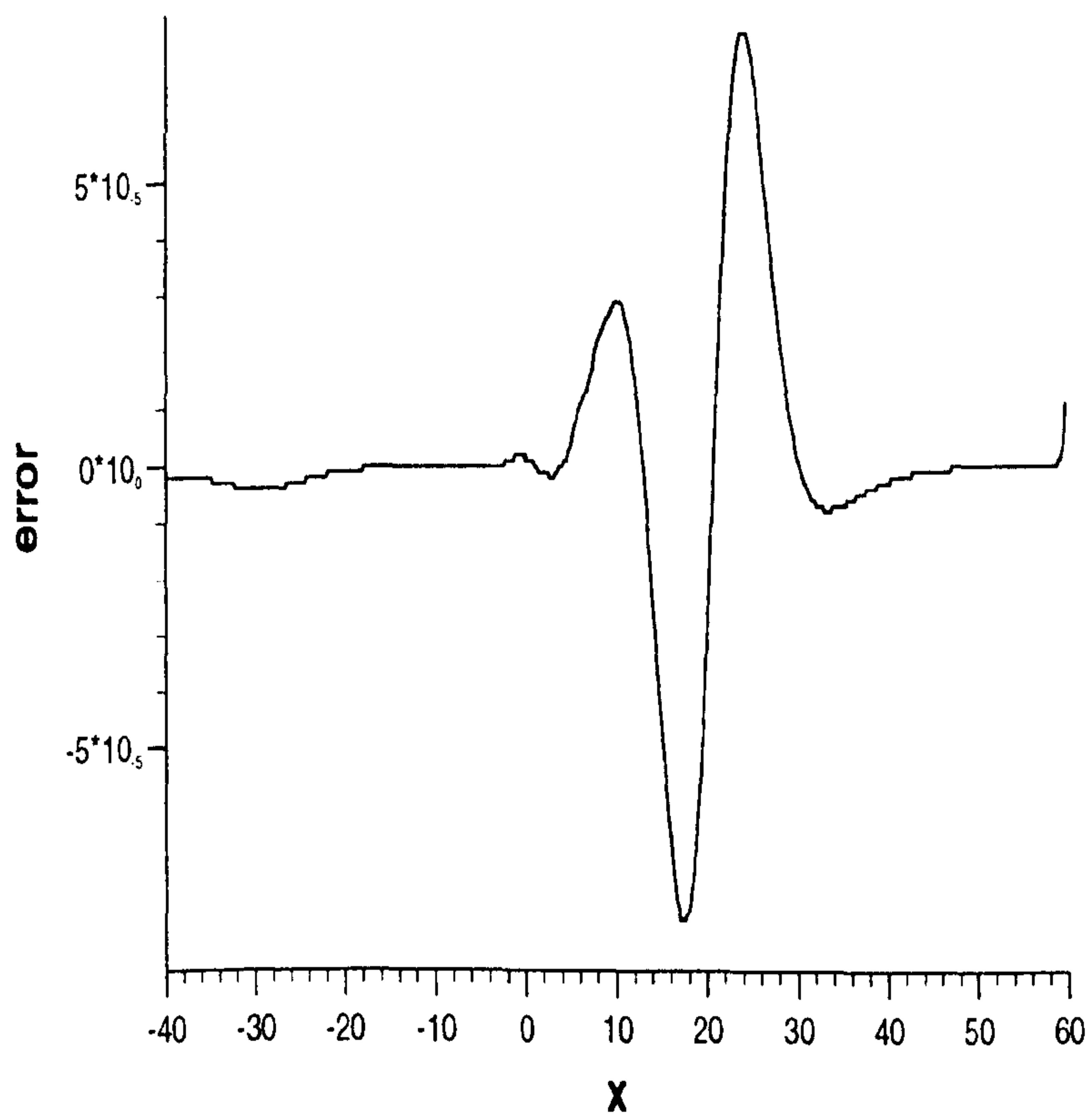


Figure 5.2 The error=exact-numerical solution at $t = 20$ for the solitary wave in Figure (5.1) plotted on a larger scale.

(5.10) to (5.13). Now it is found that the smallest errors are obtained with space steps between 0.125-0.25 combined with the time steps 0.1-0.2.

The error norms and the invariants for an even smaller solitary wave, amplitude = 0.03, are given in the Tables (5.15) to (5.17). Now the lowest errors are found when $\Delta x = 0.25$, $\Delta t = 0.2$. With the range $-80 \leq x \leq 120$ error norms for single solitary wave at $t = 20$, amplitude = 0.03, are demonstrated in the Table (5.18).

Table 5.3

Invariants and Error norms for single solitary wave
amplitude=0.09, $\Delta x = 0.025$, $\Delta t = 0.025$, $-40 \leq x \leq 60$.

method	time	C_1	C_2	C_3	$L_2 \times 10^3$	$L_\infty \times 10^3$
	0	2.107050	0.127306	0.388804	0.062	0.390
	2	2.084932	0.124578	0.380376	3.906	1.042
	4	2.062838	0.121896	0.372093	7.795	2.090
	6	2.041034	0.119285	0.364032	11.627	3.122
Petrov	8	2.019413	0.116728	0.356142	15.425	4.145
Galerkin	10	2.002002	0.114685	0.349842	18.522	5.010
quadratic	12	2.002191	0.114667	0.349786	18.742	5.161
elements	14	2.002268	0.114651	0.349736	18.995	5.339
	16	2.002206	0.114631	0.349676	19.285	5.522
	18	2.002002	0.114614	0.349622	19.593	5.692
	20	2.001500	0.114588	0.349542	19.944	5.868

Table 5.4

Invariants and Error norms for single solitary wave
amplitude=0.09, $\Delta x = 0.05$, $\Delta t = 0.05$, $-40 \leq x \leq 60$.

method	time	C_1	C_2	C_3	$L_2 \times 10^3$	$L_\infty \times 10^3$
Petrov Galerkin quadratic elements	0	2.107036	0.127304	0.388803	0.088	0.390
	2	2.107366	0.127210	0.388515	0.268	0.274
	4	2.107547	0.127114	0.388219	0.521	0.240
	6	2.107695	0.127023	0.387937	0.775	0.388
	8	2.107791	0.126931	0.387656	1.027	0.434
	10	2.107823	0.126840	0.387374	1.274	0.524
	12	2.107763	0.126748	0.387089	1.517	0.609
	14	2.107567	0.126654	0.386799	1.752	0.689
	16	2.107238	0.126562	0.386515	1.983	0.766
	18	2.106703	0.126466	0.386220	2.216	0.846
	20	2.105908	0.126370	0.385922	2.446	0.922

Table 5.5

Invariants and Error norms for single solitary wave
amplitude=0.09, $\Delta x = 0.25$, $\Delta t = 0.2$, $-40 \leq x \leq 60$.

method	time	C_1	C_2	C_3	$L_2 \times 10^3$	$L_\infty \times 10^3$
Petrov Galerkin quadratic elements	0	2.106995	0.127302	0.388804	0.195	0.390
	2	2.107695	0.127302	0.388805	0.139	0.274
	4	2.108199	0.127302	0.388805	0.110	0.193
	6	2.108551	0.127302	0.388805	0.104	0.136
	8	2.108789	0.127302	0.388806	0.114	0.096
	10	2.108913	0.127302	0.388806	0.128	0.067
	12	2.108921	0.127302	0.388806	0.142	0.061
	14	2.108803	0.127302	0.388806	0.155	0.088
	16	2.108535	0.127302	0.388806	0.169	0.125
	18	2.108073	0.127302	0.388806	0.186	0.179
20	2.107357	0.127301	0.388804	0.211	0.254	

Table 5.6

Invariants and Error norms for single solitary wave
amplitude=0.09, $\Delta x = 0.5$, $\Delta t = 0.4$, $-40 \leq x \leq 60$.

method	time	C_1	C_2	C_3	$L_2 \times 10^3$	$L_\infty \times 10^3$
	0	2.106945	0.127301	0.388804	0.275	0.390
	2	2.107553	0.127301	0.388805	0.199	0.274
	4	2.107916	0.127301	0.388805	0.160	0.193
	6	2.108101	0.127301	0.388806	0.155	0.136
Petrov	8	2.108149	0.127301	0.388806	0.169	0.096
Galerkin	10	2.108090	0.127301	0.388806	0.189	0.067
quadratic	12	2.107939	0.127301	0.388806	0.210	0.057
elements	14	2.107688	0.127301	0.388806	0.232	0.064
	16	2.107307	0.127301	0.388805	0.255	0.091
	18	2.106751	0.127301	0.388805	0.282	0.130
	20	2.105952	0.127301	0.388804	0.315	0.184

Table 5.7

Invariants and Error norms for single solitary wave
amplitude=0.09, $\Delta x = 1.0$, $\Delta t = 0.8$, $-40 \leq x \leq 60$.

method	time	C_1	C_2	C_3	$L_2 \times 10^3$	$L_\infty \times 10^3$
	0	2.106840	0.127300	0.388804	0.390	0.390
	4	2.107557	0.127300	0.388805	0.341	0.193
Petrov	8	2.107506	0.127300	0.388805	0.510	0.146
Galerkin	12	2.107127	0.127300	0.388804	0.682	0.174
quadratic	16	2.106422	0.127300	0.388804	0.853	0.234
elements	20	2.104989	0.127299	0.388802	1.034	0.293

Table 5.8

Invariants and Error norms for single solitary wave
amplitude=0.09, $\Delta x = 4.0$, $\Delta t = 0.8$, $-40 \leq x \leq 60$.

method	time	C_1	C_2	C_3	$L_2 \times 10^3$	$L_\infty \times 10^3$
	0	2.106151	0.127281	0.388803	0.779	0.390
Petrov	3.2	2.106648	0.127281	0.388803	0.913	0.234
Galerkin	6.4	2.106617	0.127281	0.388803	1.537	0.406
quadratic	9.6	2.106304	0.127281	0.388803	2.200	0.727
elements	12.8	2.105791	0.127281	0.388802	2.849	0.961
	16.0	2.104991	0.127281	0.388801	3.479	1.048
	19.2	2.103634	0.127281	0.388799	4.091	1.159
	20.8	2.102606	0.127281	0.388797	4.390	1.409

Table 5.9

Error norms for single solitary wave at $t = 20$
amplitude=0.09, $-40 \leq x \leq 60$.

Δx	Δt	$L_2 \times 10^3$	$L_\infty \times 10^3$
0.025	0.025	19.9	5.87
0.05	0.05	2.45	0.922
0.125	0.1	0.537	0.316
0.25	0.2	0.211	0.254
0.5	0.4	0.315	0.184
1.0	0.8	1.03	0.293
4.0	0.8	4.39	1.41

Table 5.10

Invariants and Error norms for single solitary wave
 amplitude=0.09, $\Delta x = 0.05$, $\Delta t = 0.05$, $-80 \leq x \leq 120$.

method	time	C_1	C_2	C_3	$L_2 \times 10^3$	$L_\infty \times 10^3$
Petrov Galerkin quadratic elements	0	2.109396	0.127301	0.388805	0.008	0.002
	2	2.108924	0.127207	0.388516	0.248	0.136
	4	2.108437	0.127111	0.388217	0.488	0.240
	6	2.107983	0.127020	0.387938	0.716	0.340
	8	2.107496	0.126926	0.387645	0.944	0.437
	10	2.107028	0.126833	0.387357	1.168	0.528
	12	2.106534	0.126737	0.387062	1.388	0.613
	14	2.106031	0.126641	0.386763	1.612	0.692
	16	2.105555	0.126548	0.386477	1.831	0.765
	18	2.105078	0.126454	0.386188	2.054	0.846
20	2.104596	0.126360	0.385896	2.276	0.924	

Table 5.11

Invariants and Error norms for single solitary wave
amplitude=0.09 , $\Delta x = 0.125$, $\Delta t = 0.1$, $-80 \leq x \leq 120$.

method	time	C_1	C_2	C_3	$L_2 \times 10^3$	$L_\infty \times 10^3$
	0	2.109400	0.127301	0.388805	0.000	0.000
	2	2.109412	0.127303	0.388811	0.007	0.004
	4	2.109426	0.127305	0.388817	0.013	0.007
	6	2.109435	0.127307	0.388822	0.019	0.009
Petrov	8	2.109448	0.127309	0.388828	0.025	0.012
Galerkin	10	2.109456	0.127310	0.388831	0.030	0.014
quadratic	12	2.109474	0.127312	0.388838	0.035	0.015
elements	14	2.109483	0.127314	0.388843	0.040	0.018
	16	2.109491	0.127315	0.388846	0.044	0.019
	18	2.109499	0.127316	0.388851	0.048	0.021
	20	2.109505	0.127317	0.388854	0.053	0.023

Table 5.12

Invariants and Error norms for single solitary wave
amplitude=0.09, $\Delta x = 0.25$, $\Delta t = 0.2$, $-80 \leq x \leq 120$.

method	time	C_1	C_2	C_3	$L_2 \times 10^3$	$L_\infty \times 10^3$
	0	2.109402	0.127302	0.388806	0.000	0.000
	2	2.109403	0.127301	0.388805	0.006	0.002
	4	2.109405	0.127302	0.388806	0.012	0.004
	6	2.109403	0.127302	0.388805	0.018	0.006
Petrov	8	2.109406	0.127302	0.388806	0.024	0.007
Galerkin	10	2.109408	0.127302	0.388806	0.030	0.009
quadratic	12	2.109407	0.127302	0.388806	0.036	0.011
elements	14	2.109407	0.127302	0.388807	0.042	0.013
	16	2.109407	0.127302	0.388807	0.048	0.015
	18	2.109405	0.127301	0.388805	0.054	0.017
	20	2.109408	0.127302	0.388806	0.060	0.018

Table 5.13

Invariants and Error norms for single solitary wave
amplitude=0.09, $\Delta x = 0.5$, $\Delta t = 0.4$, $-80 \leq x \leq 120$.

method	time	C_1	C_2	C_3	$L_2 \times 10^3$	$L_\infty \times 10^3$
Petrov Galerkin quadratic elements	0	2.109404	0.127301	0.388806	0.000	0.000
	2	2.109405	0.127301	0.388806	0.024	0.007
	4	2.109406	0.127301	0.388806	0.048	0.014
	6	2.109407	0.127301	0.388806	0.072	0.021
	8	2.109407	0.127302	0.388807	0.096	0.029
	10	2.109406	0.127301	0.388806	0.120	0.036
	12	2.109405	0.127301	0.388806	0.144	0.043
	14	2.109406	0.127301	0.388806	0.167	0.051
	16	2.109406	0.127302	0.388806	0.191	0.058
	18	2.109406	0.127301	0.388807	0.215	0.066
20	2.109407	0.127301	0.388806	0.238	0.073	

Table 5.14

Error norms for single solitary wave at $t = 20$,
amplitude=0.09, $-80 \leq x \leq 120$.

Δx	Δt	$L_2 \times 10^3$	$L_\infty \times 10^3$
0.05	0.05	2.276	0.924
0.125	0.1	0.053	0.023
0.25	0.2	0.060	0.018
0.5	0.4	0.238	0.073

Table 5.15

Invariants and Error norms for single solitary wave
amplitude=0.03, $\Delta x = 0.125$, $\Delta t = 0.1$, $-80 \leq x \leq 120$.

method	time	C_1	C_2	C_3	$L_2 \times 10^3$	$L_\infty \times 10^3$
Petrov Galerkin quadratic elements	0	1.205554	0.024167	0.072938	0.015	0.042
	2	1.205617	0.024166	0.072934	0.014	0.034
	4	1.205669	0.024165	0.072931	0.017	0.028
	6	1.205710	0.024164	0.072927	0.022	0.023
	8	1.205743	0.024163	0.072924	0.028	0.019
	10	1.205771	0.024162	0.072921	0.035	0.015
	12	1.205791	0.024161	0.072917	0.041	0.013
	14	1.205806	0.024160	0.072914	0.047	0.014
	16	1.205811	0.024158	0.072910	0.053	0.016
	18	1.205817	0.024157	0.072907	0.059	0.018
20	1.205814	0.024156	0.072903	0.065	0.020	

Table 5.16

Invariants and Error norms for single solitary wave
amplitude=0.03, $\Delta x = 0.25$, $\Delta t = 0.2$, $-80 \leq x \leq 120$.

method	time	C_1	C_2	C_3	$L_2 \times 10^3$	$L_\infty \times 10^3$
	0	1.205551	0.024167	0.072938	0.021	0.042
	2	1.205625	0.024167	0.072938	0.017	0.034
	4	1.205682	0.024167	0.072938	0.014	0.028
	6	1.205726	0.024167	0.072938	0.013	0.023
Petrov	8	1.205758	0.024168	0.072938	0.012	0.019
Galerkin	10	1.205783	0.024168	0.072938	0.012	0.015
quadratic	12	1.205799	0.024167	0.072938	0.012	0.013
elements	14	1.205809	0.024167	0.072938	0.012	0.010
	16	1.205816	0.024167	0.072938	0.013	0.008
	18	1.205817	0.024168	0.072938	0.013	0.007
	20	1.205815	0.024168	0.072938	0.014	0.006

Table 5.17

Invariants and Error norms for single solitary wave
 amplitude=0.03, $\Delta x = 0.5$, $\Delta t = 0.4$, $-80 \leq x \leq 120$.

method	time	C_1	C_2	C_3	$L_2 \times 10^3$	$L_\infty \times 10^3$
	0	1.205545	0.024167	0.072938	0.030	0.042
	2	1.205608	0.024167	0.072938	0.025	0.034
	4	1.205651	0.024167	0.072938	0.025	0.028
	6	1.205677	0.024167	0.072938	0.029	0.023
Petrov	8	1.205688	0.024167	0.072938	0.034	0.019
Galerkin	10	1.205693	0.024167	0.072938	0.038	0.015
quadratic	12	1.205694	0.024167	0.072938	0.042	0.015
elements	14	1.205691	0.024167	0.072938	0.045	0.015
	16	1.205685	0.024167	0.072938	0.047	0.015
	18	1.205667	0.024167	0.072938	0.048	0.015
	20	1.205668	0.024167	0.072938	0.050	0.015

Table 5.18

Error norms for single solitary wave at $t = 20$
 amplitude=0.03, $-80 \leq x \leq 120$.

Δx	Δt	$L_2 \times 10^3$	$L_\infty \times 10^3$
0.125	0.1	0.065	0.020
0.25	0.2	0.014	0.006
0.5	0.4	0.050	0.015

5.4 Modelling an undular bore

To study the development of an undular bore we follow Peregrine [89] and use as initial condition

$$U(x, 0) = 0.5U_0[1 - \tanh(\frac{x - x_c}{d})] \quad (5.14)$$

where $U(x, 0)$ denotes the elevation of the water above the equilibrium surface at time $t = 0$. The change in water level of magnitude U_0 is centred on $x = x_c$, and d measures the steepness of the change. The smaller the value of d the steeper is the slope. For the simulation we take the parameters to have the following values: $\epsilon = 1.0$, $\mu = 0.16666667$, $U_0 = 0.1$ and $d = 5.0$. The physical boundary conditions require that $U \rightarrow 0$ as $x \rightarrow \infty$ and $U \rightarrow U_0$ as $x \rightarrow -\infty$. To limit the effect of boundaries on the numerical solution we take $x_0 = -100$ and $x_N = 500$ together with $\Delta x = 0.15$, $\Delta t = 0.15$ and run the simulation until $t = 400$. These step sizes were chosen following the results given in Section (5.3) which appear to imply that these will lead to optimum accuracy.

Table 5.19
Results for an undular bore $U_0 = 0.1$.

time	C_1	C_2	C_3	U_{max}	X_{max}
0	10.0074	0.9759	3.0235		
50	15.2670	1.5101	4.6800	0.1049	46.40
100	20.5262	2.0442	6.3362	0.1215	99.05
150	25.7860	2.5785	7.9929	0.1367	151.55
200	31.0460	3.1128	9.6497	0.1495	204.35
250	36.3064	3.6472	11.3068	0.1596	257.15
300	41.5670	4.1816	12.9639	0.1671	310.10
350	46.8272	4.7160	14.6209	0.1727	363.05
400	52.0872	5.2503	16.2777	0.1768	416.15

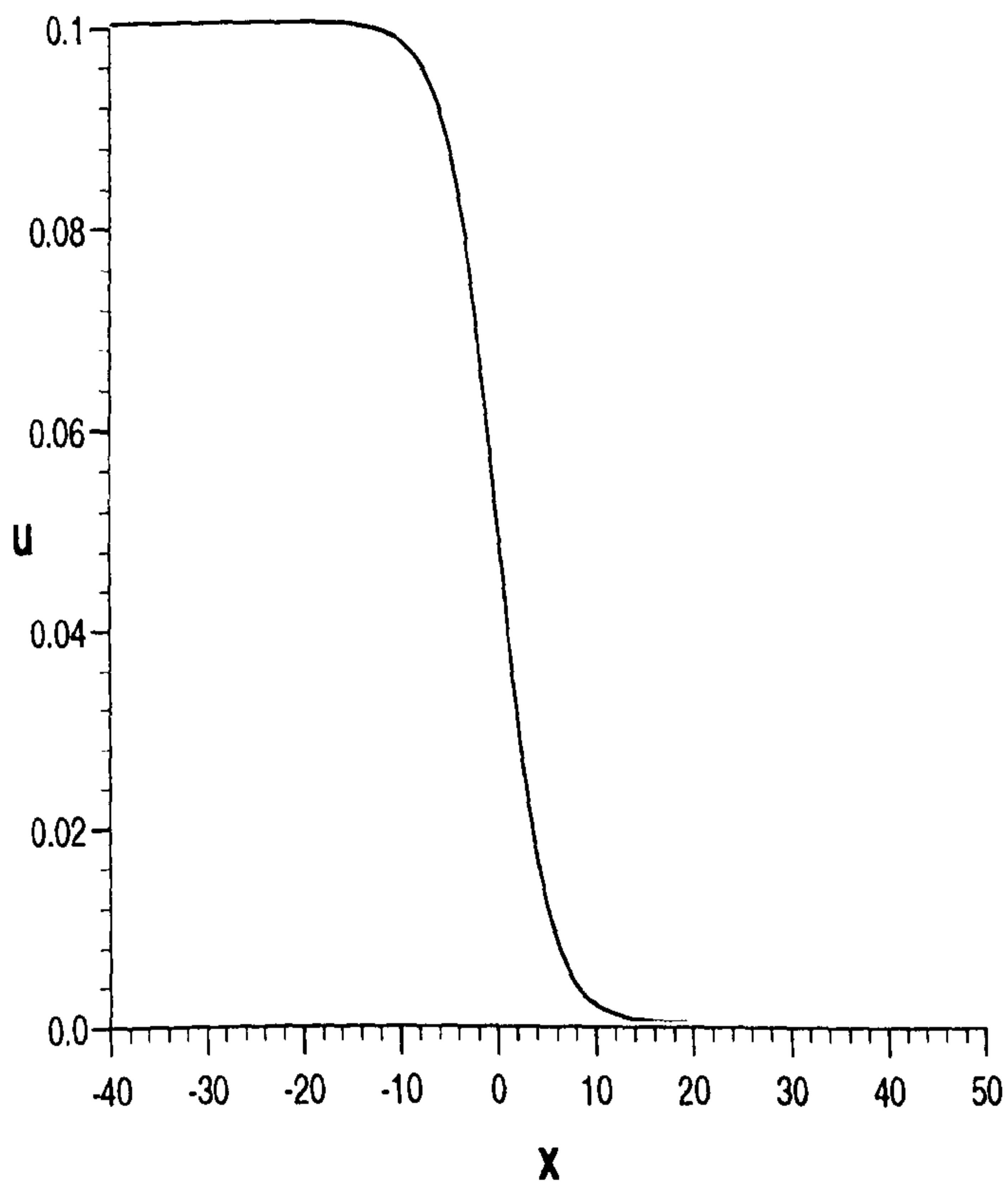


Figure 5.3 The undulation profile
at time $t = 0$ for a gentle slope $d = 5$.

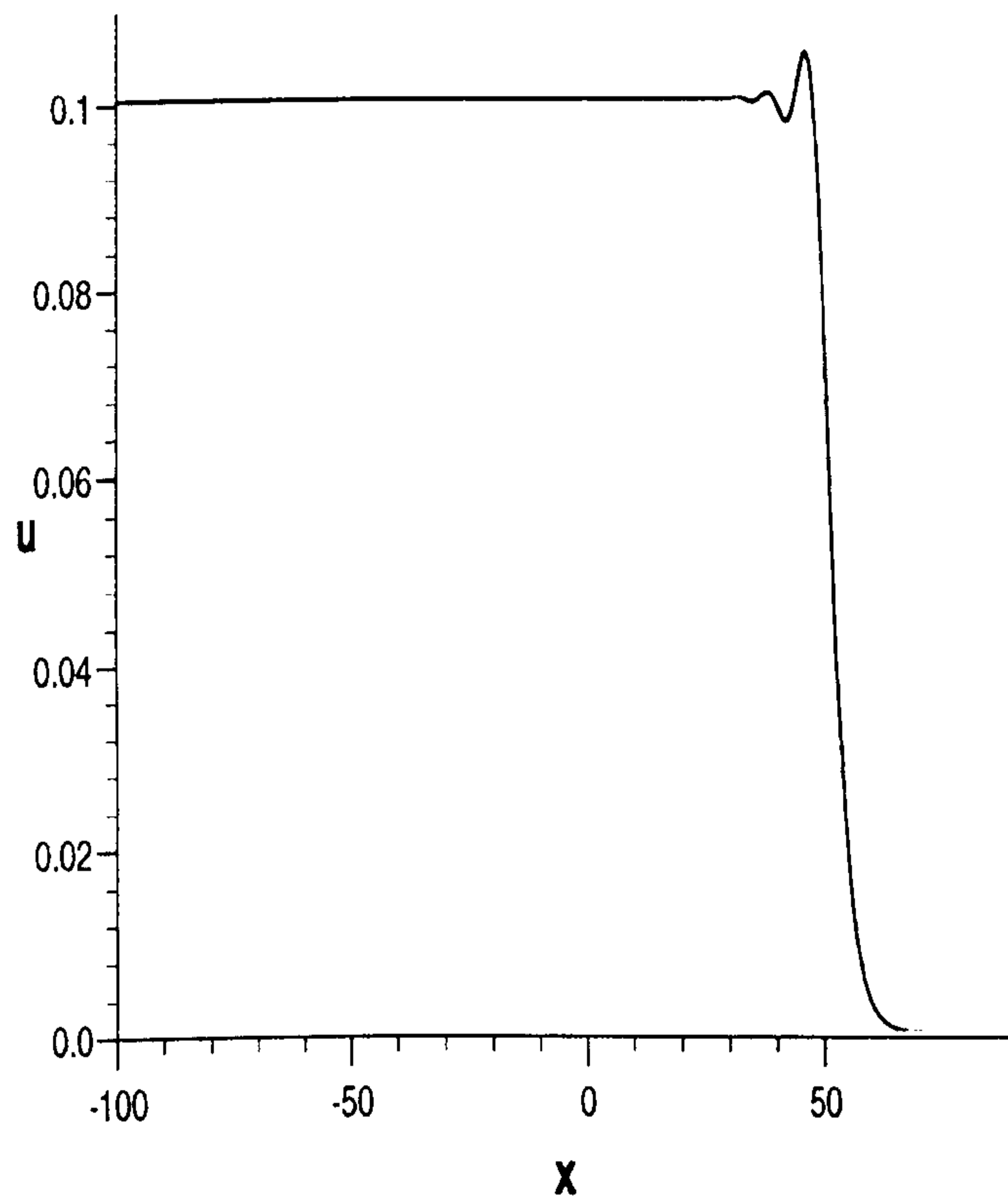


Figure 5.4 The undulation profile
at time $t = 50$ for a gentle slope $d = 5$.

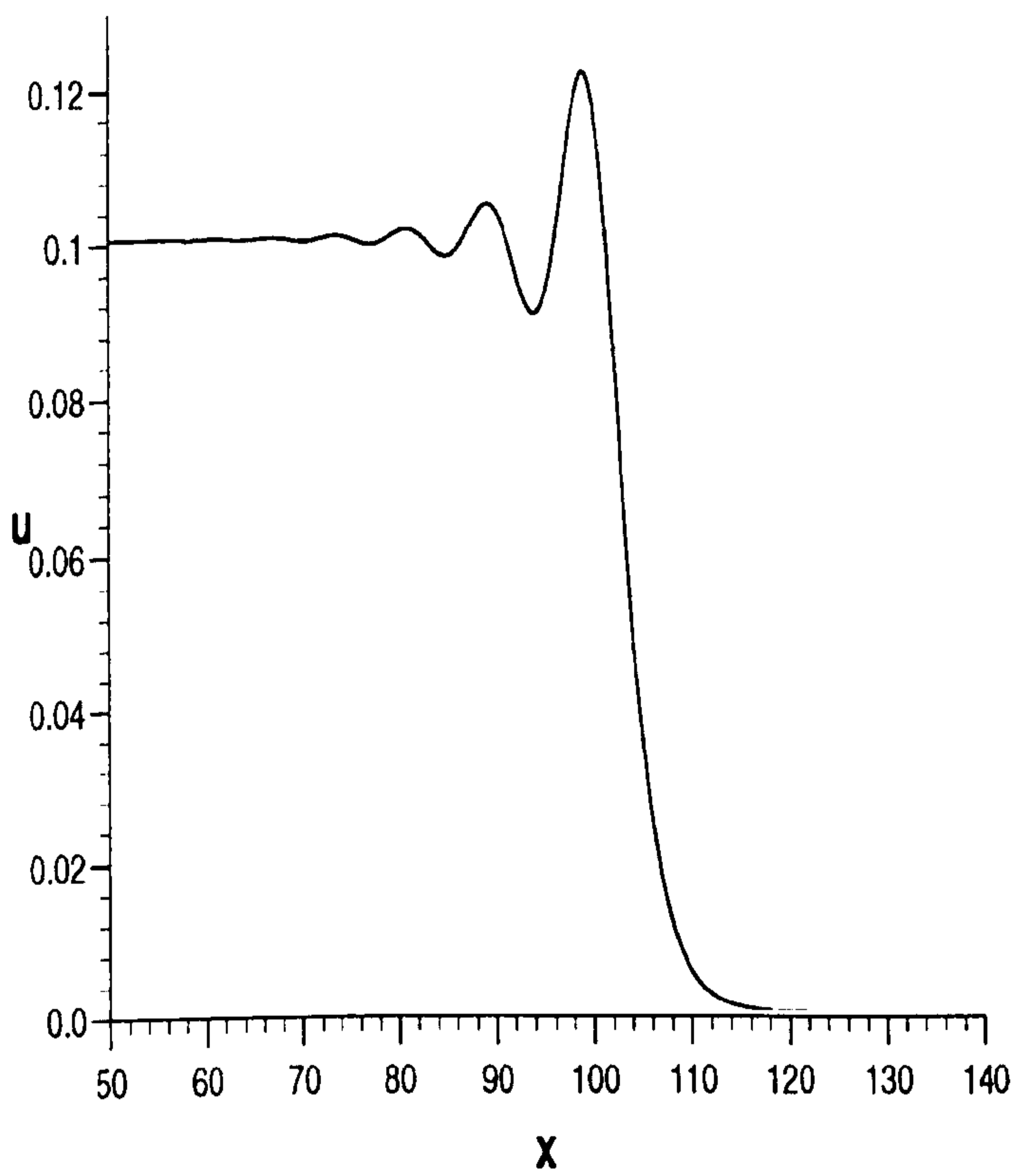


Figure 5.5 The undulation profile
at time $t = 100$ for a gentle slope $d = 5$.

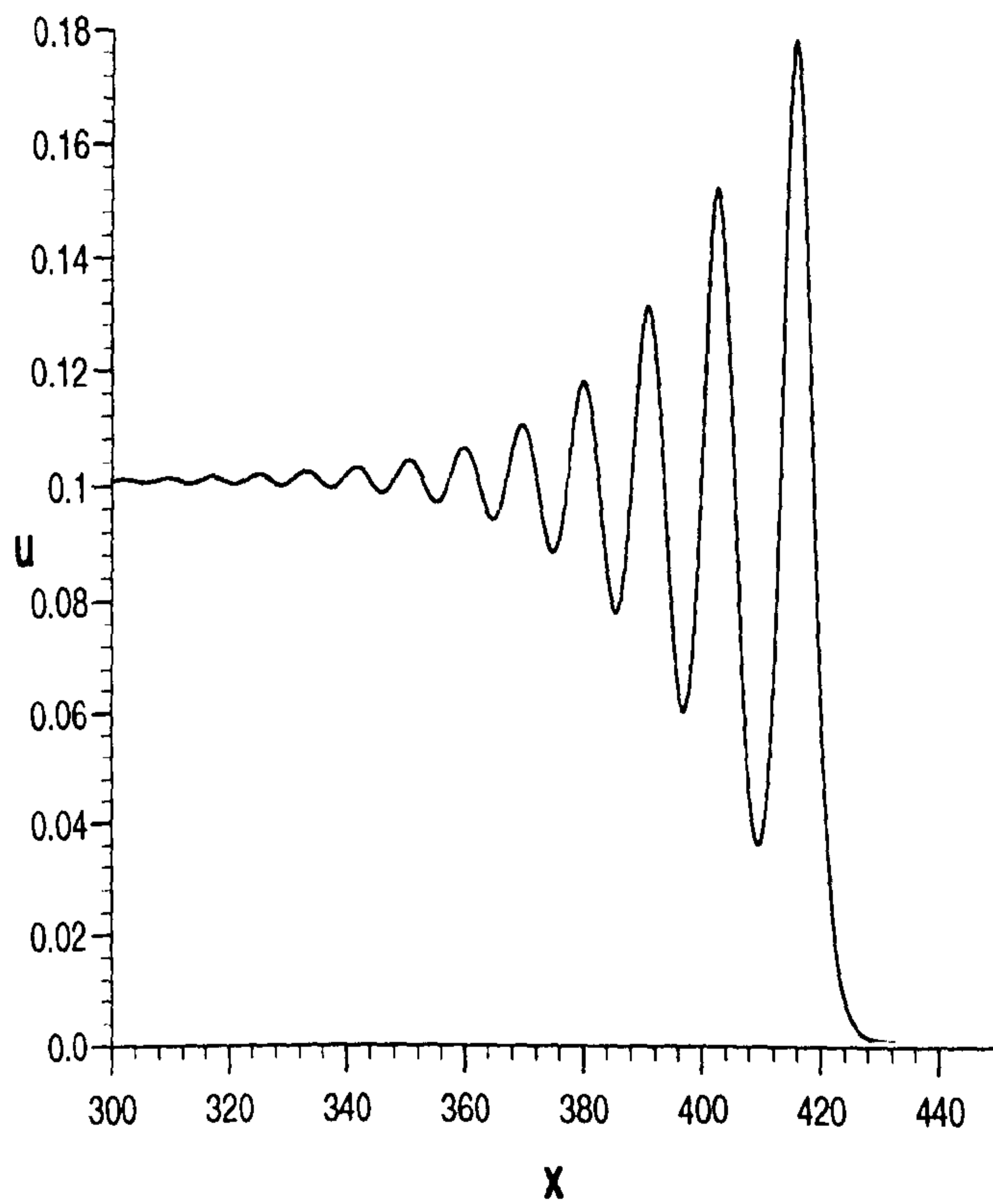


Figure 5.6 The undulation profile
at time $t = 400$ for a gentle slope $d = 5$.

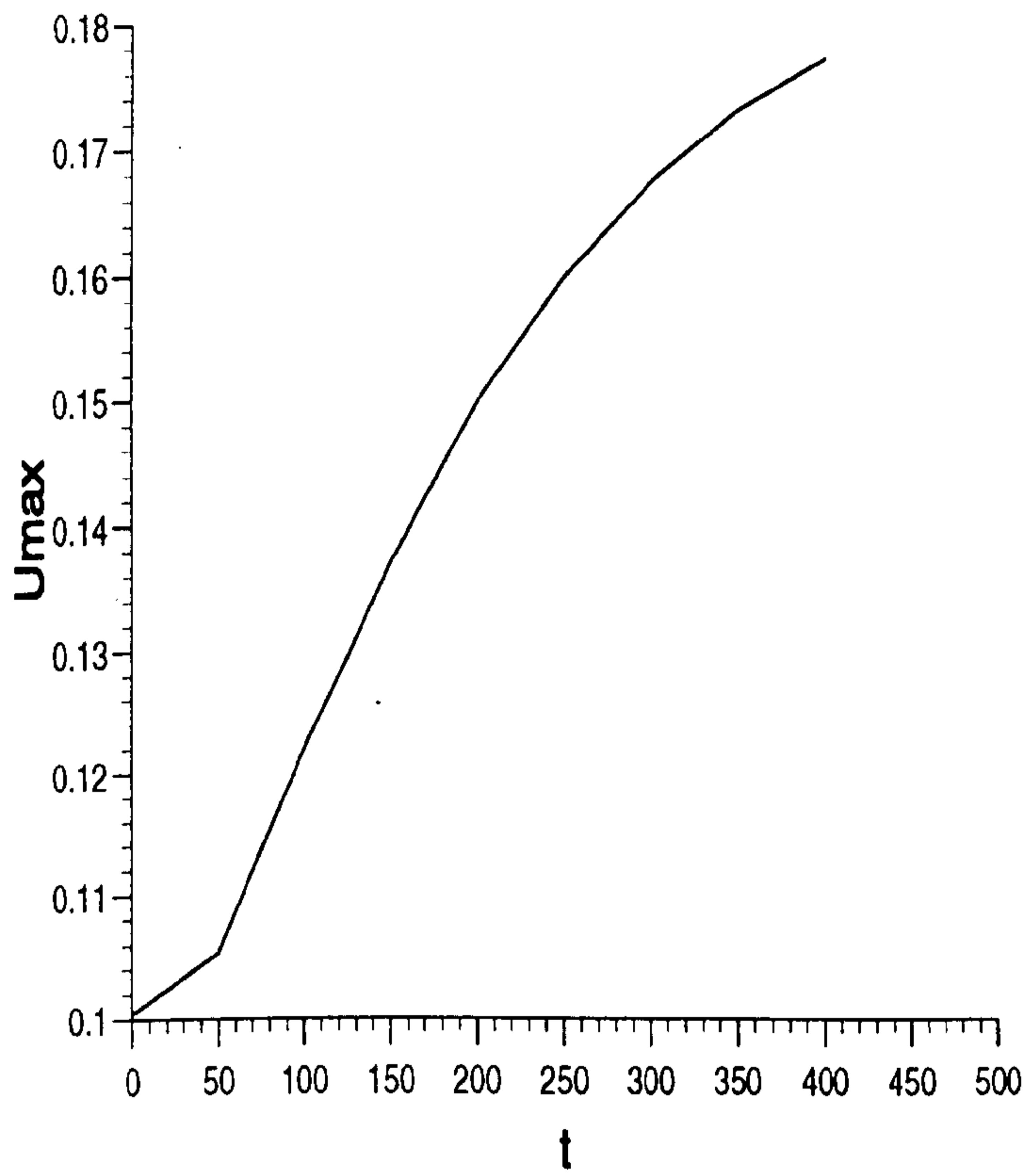


Figure 5.7 The growth in the amplitude of the leading undulation $d = 5$.

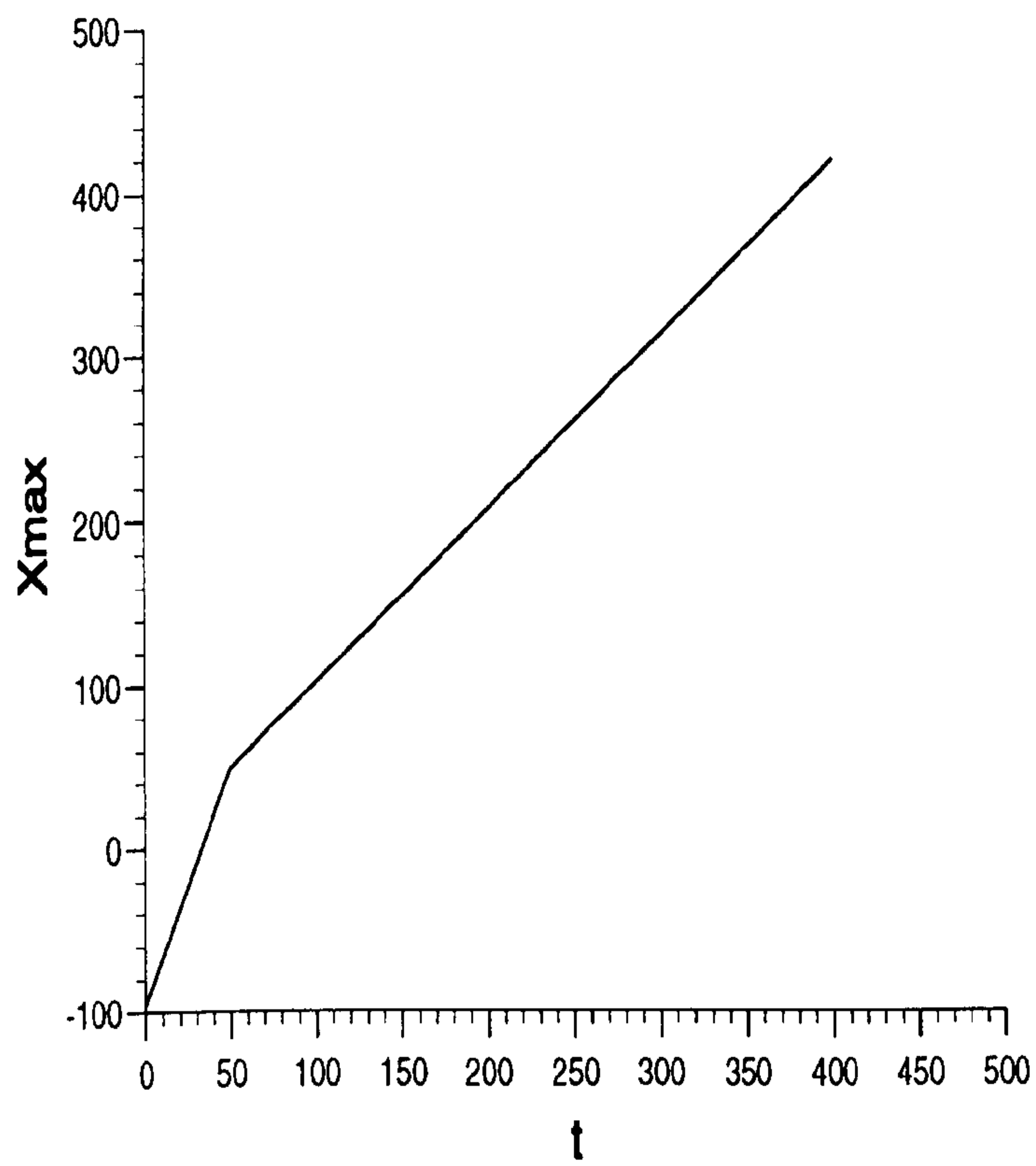


Figure 5.8 A space/time graph for the leading undulation $d = 5$.

Table 5.20

Results for an undular bore $U_0 = 0.1$, $d = 2.0$,
 $t_{max} = 400$, $\Delta x = 0.15$, $\Delta t = 0.15$, $\mu = 0.16666667$.

time	C_1	C_2	C_3
0	10.0074	0.9910	3.0708
50	15.2671	1.5253	4.7274
100	20.5267	2.0595	6.3839
150	25.7863	2.5937	8.0404
200	31.0459	3.1280	9.6971
250	36.3057	3.6622	11.3537
300	41.5654	4.1965	13.0103
350	46.8252	4.7308	14.6670
400	52.0851	5.2650	16.3237

Table 5.21

Results for an undular bore $U_0 = 0.1$, $d = 2.0$.

time	U_{max}	X_{max}
0	0.1000	-100
50	0.1310	47.30
100	0.1452	99.35
150	0.1557	152.00
200	0.1638	204.80
250	0.1698	257.75
300	0.1745	310.70
350	0.1779	363.80
400	0.1806	416.90

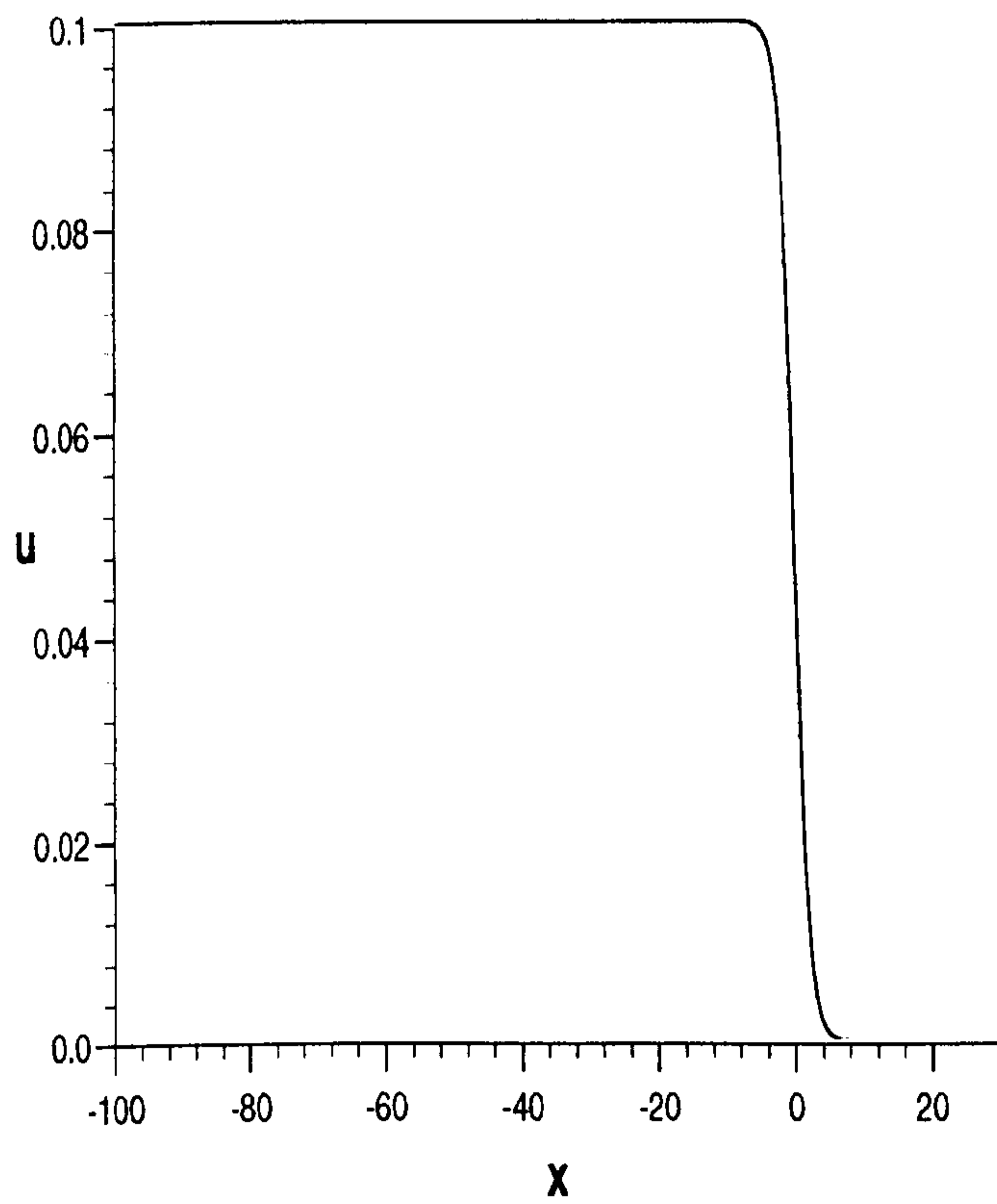


Figure 5.9 The undulation profile at time $t = 0$ for a gentle slope $d = 2$.

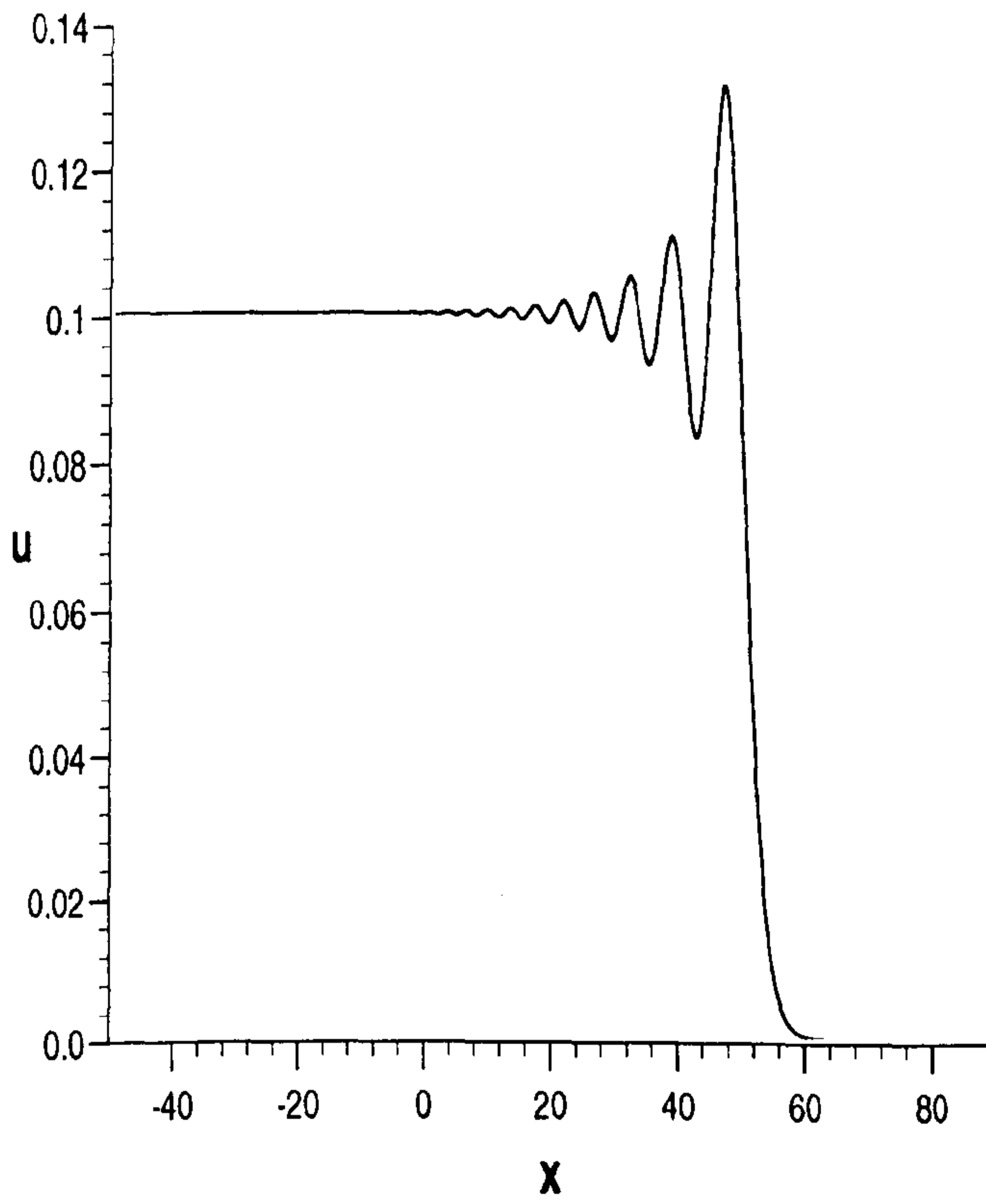


Figure 5.10 The undulation profile at time $t = 50$ for a gentle slope $d = 2$.

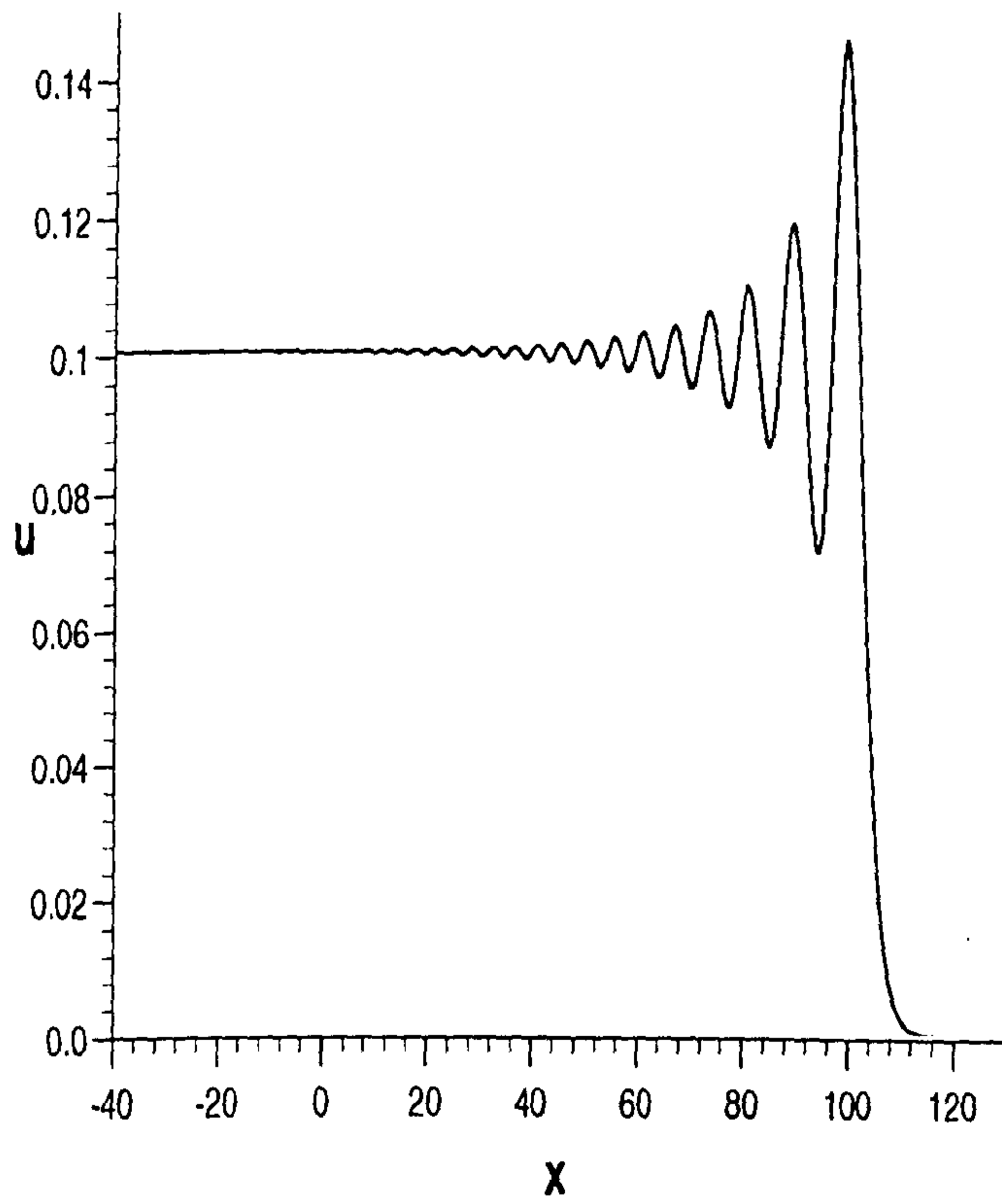


Figure 5.11 The undulation profile at time $t = 100$ for a gentle slope $d = 2$.

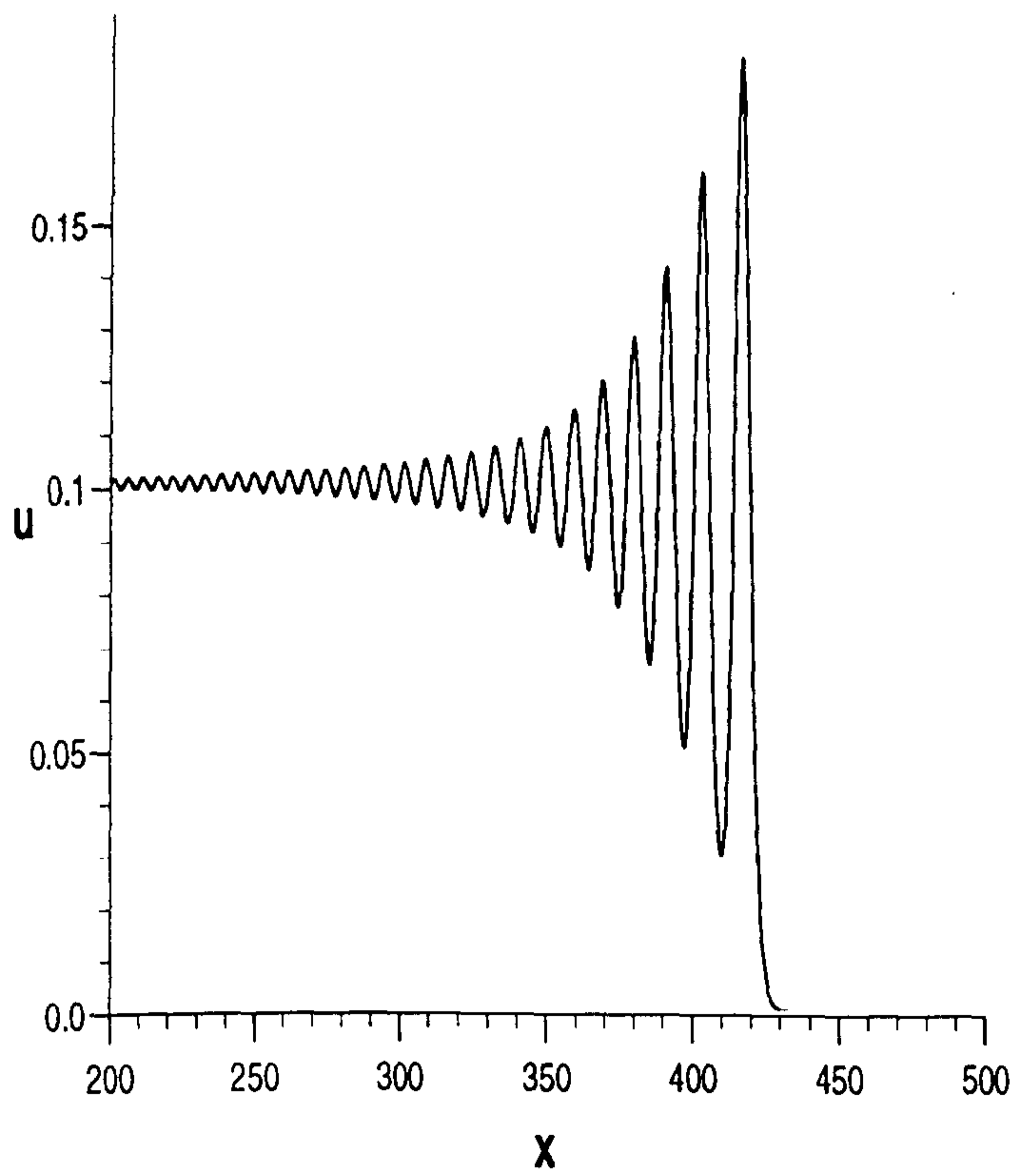


Figure 5.12 The undulation profile
at time $t = 400$ for a gentle slope $d = 2$.

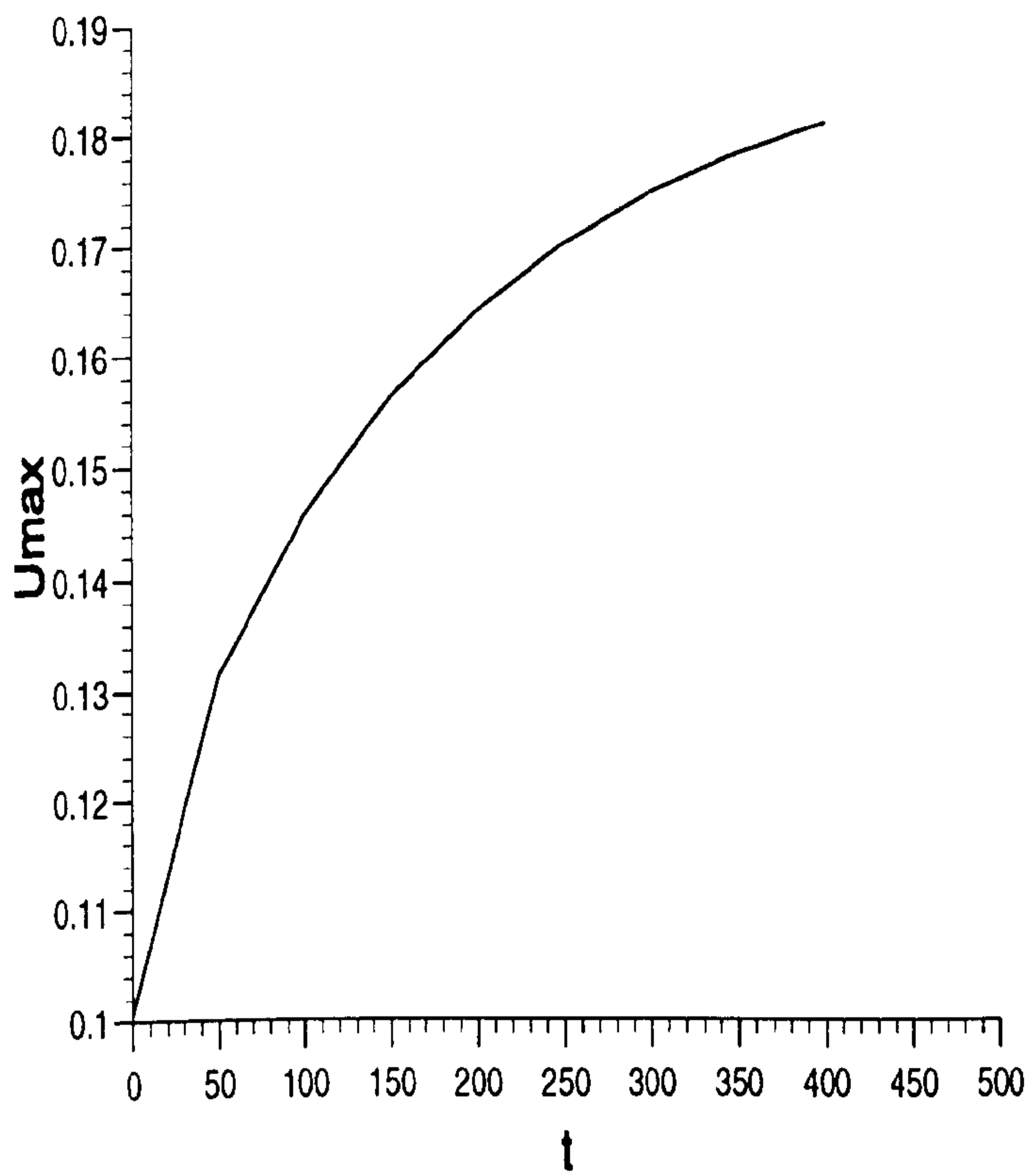


Figure 5.13 The growth in the amplitude of the leading undulation $d = 2$.

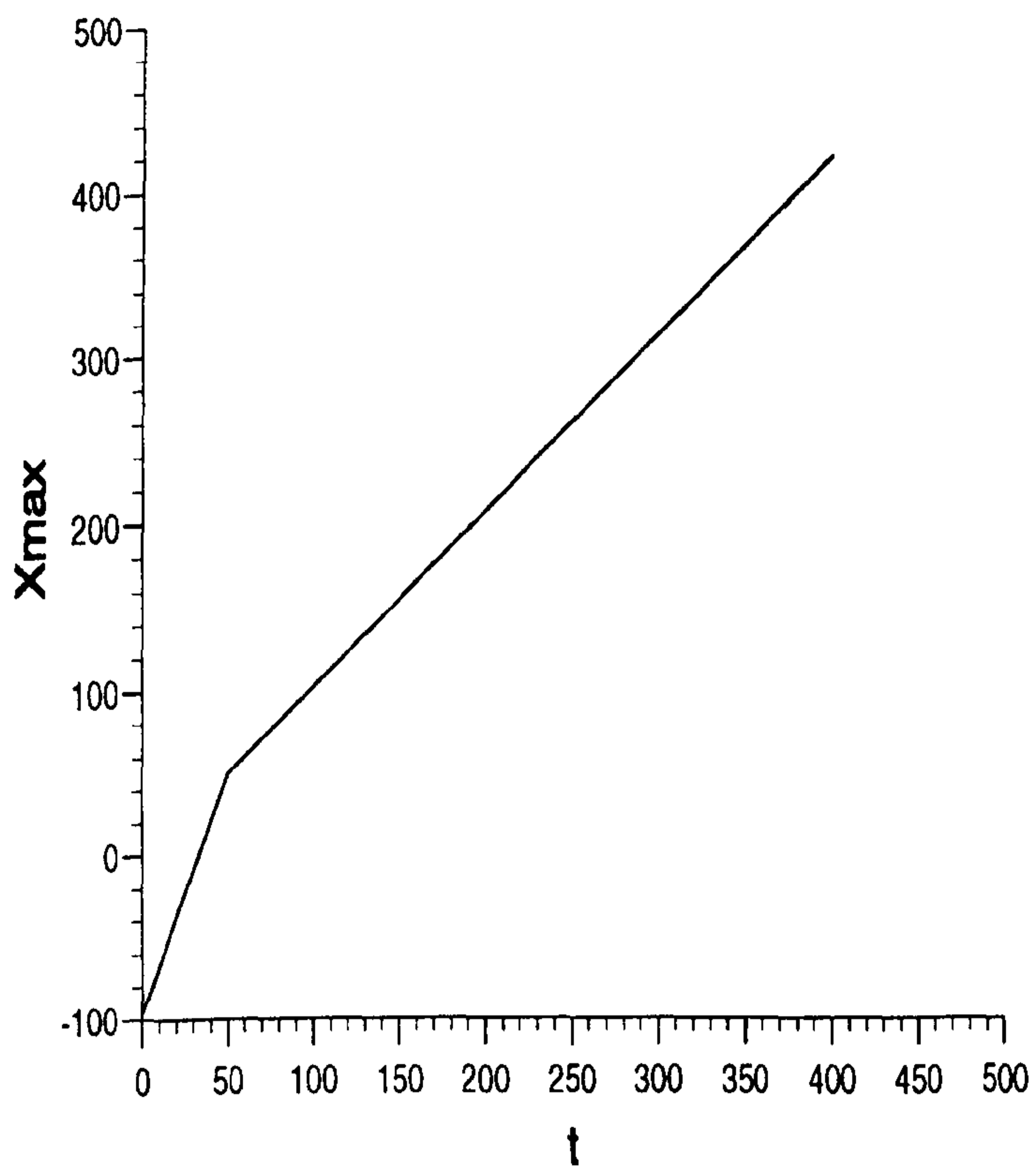


Figure 5.14 A space/time graph
for the leading undulation $d = 2$.

The undulation profile at times $t = 0, 50, 100$ for a gentle slope $d = 5.0$ is given in Figures (5.3), (5.4), (5.5). By time $t = 400$ the fully developed undular bore of Figure (5.6) is obtained. The temporal growth and space/time graph for the leading undulation are given in Figures (5.7) and (5.8). The amplitude of the leading undulation has stabilised at about 0.177 when it has a velocity of 1.062. The values are fully consistent with those for an RLW solitary wave.

From the results given in Table (5.19) we calculate that the growth rates in the quantities C_j are $M_1 = 0.1052$, $M_2 = 0.01069$, $M_3 = 0.02899$ which compare well with the theoretical values $M_1 = 0.1050$, $M_2 = 0.01067$, $M_3 = 0.03375$.

In Table (5.20) is demonstrated results for an undular bore with $U_0 = 0.1$, $d = 2.0$. We give results for an undular bore with $U_0 = 0.1$, $d = 2.0$ in Table (5.21). The undulation profile at times $t = 0, 50, 100, 400$ for a gentle slope $d = 2.0$ is shown in Figures (5.9) to (5.12). The growth in the amplitude and a space/time graph for the leading undulation $d = 2.0$ are given in Figures (5.13) and (5.14).

5.5 Discussion

The Petrov-Galerkin approach with quadratic B-spline finite elements set up in Section (5.2) leads to an unconditionally stable algorithm which faithfully models the amplitude, position and velocity of a single solitary wave over an extended time scale.

An undular bore is also modelled well and the results obtained agree well with earlier work.

Chapter 6

A Least-Squares Finite Element Scheme For Burgers' Equation

6.1 Introduction

Burgers' equation may be considered as model equation for the decay of turbulence within a box of length L . In the form [22, 32]

$$U_t + UU_x - \nu U_{xx} = 0, \quad (6.1)$$

the subscripts t and x denote differentiation. Here t is time, x is a space coordinate and $U(x, t)$ is velocity. The quantity ν measures the fluid viscosity and is related to the Reynolds number R_e defined with reference to a representative velocity U_0 and the scale length of the turbulent field L by

$$R_e = \frac{U_0 L}{\nu}. \quad (6.2)$$

Physical boundary conditions require U to be zero at the ends of the box, so that $U \rightarrow 0$ as $x \rightarrow 0, L$

Burgers' equation is one of very few non-linear partial differential equations which can be solved analytically for arbitrary initial data [61]. These

solutions, in many cases, involve infinite series which for small values of ν may converge very slowly.

Numerical algorithms for the solution of Burgers' equation have been proposed by many authors. Varoglu and Finn [99] set up space-time finite elements incorporating characteristics with which to obtain a numerical solution via a weighted residual method. Caldwell and Smith [24] use cubic spline finite elements, Evans and Abdullah [39] a group explicit finite difference method, Kakuda and Tosaka [67] a generalised boundary element approach, Mittal and Singhal [79] a technique of finitely reproducing nonlinearities to obtain a set of stiff ordinary differential equations which are solved by a Runge-Kutta-Chebyshev method while Ali et al [5] use collocation over cubic B-spline finite elements and Nguyen and Reynen [83] developed a Petrov-Galerkin method based on a least squares approach. Some of them are very successful in modelling the solutions. In this paper we apply a space-time least-squares finite element algorithm, based on the work of Nguyen and Reynen [83], to the numerical solution of Burgers' equation. Some standard problems are studied and comparisons are made with published results.

6.2 The finite element solution

When applying the least squares approach and using space-time finite elements, we consider the Variational Principle [83]

$$\delta \int_0^t \int_0^L [U_t + UU_x - \nu U_{xx}]^2 dx dt = 0, \quad (6.3)$$

A uniform linear spatial array of linear finite elements is set up $0 = x_0 < x_1 < \dots < x_N = L$. A typical finite element of size $\Delta x = (x_{m+1} - x_m)$, Δt mapped by local coordinates ξ , τ where $x = x_m + \xi \Delta x$, $0 \leq \xi \leq 1$, $t = \tau \Delta t$, $0 \leq \tau \leq 1$, makes, to integral (6.3), the contribution

$$\delta \int_0^1 \int_0^1 [U_\tau + \frac{\Delta t}{\Delta x} \hat{U} U_\xi - \frac{\nu \Delta t}{\Delta x^2} U_{\xi\xi}]^2 d\xi d\tau, \quad (6.4)$$

where to simplify the integral, \hat{U} is taken to be constant over an element. This leads to

$$\int_0^1 \int_0^1 [U_\tau + vU_\xi - bU_{\xi\xi}] \delta[U_\tau + vU_\xi - bU_{\xi\xi}] d\xi d\tau, \quad (6.5)$$

where

$$b = \frac{\nu \Delta t}{\Delta x^2},$$

and the Courant number

$$v = \frac{\hat{U} \Delta t}{\Delta x}$$

is taken as locally constant over each element. The variation of U over the element $[x_m, x_{m+1}]$ is given by

$$U^e = \sum_{j=1}^2 N_j(u_j + \tau \Delta u_j), \quad (6.6)$$

where N_1, N_2 are linear spatial basis functions. The u_1, u_2 are the nodal parameters which are temporally linear and change by the increments $\Delta u_1, \Delta u_2$ in time Δt . With the local coordinate system ξ defined above, the basis functions have expressions [83]

$$N_1 = 1 - \xi,$$

$$N_2 = \xi.$$

Write the second term in the integrand of (6.5) as a weight function

$$\delta W = \sum_{j=1}^2 W_j \Delta u_j = \delta[U_\tau + vU_\xi - bU_{\xi\xi}]. \quad (6.7)$$

Using, from (6.6), the result that

$$\delta U^e = \sum_{j=1}^2 N_j \tau \Delta u_j, \quad (6.8)$$

in (6.7) we have

$$W_j = N_j + \tau v N_j'. \quad (6.9)$$

Substituting into Equation (6.5) gives

$$\int_0^1 \int_0^1 [U_\tau + vU_\xi - bU_{\xi\xi}][N_j + \tau v N'_j] d\xi d\tau, \quad (6.10)$$

which can be interpreted as a Petrov-Galerkin approach with weight function W_j , as well as a least squares formulation. Integrating by parts leads to

$$\int_0^1 \int_0^1 [(U_\tau + vU_\xi)(N_j + \tau v N'_j) + bU_\xi N'_j] d\xi d\tau. \quad (6.11)$$

Now if we substitute for U using Equation (6.6), an element's contribution is obtained in the form

$$\begin{aligned} \sum_{k=1}^2 \int_0^1 \int_0^1 [(N_k \Delta u_k + v N'_k (u_k + \tau \Delta u_k))(N_j + \tau v N'_j) \\ + b N'_k N'_j (u_k + \tau \Delta u_k)] d\xi d\tau. \end{aligned} \quad (6.12)$$

Integrate (6.12) with respect to τ giving in matrix notation

$$\begin{aligned} [A^e + \frac{1}{2}(C^e + C^{eT}) + \frac{1}{3}B^e + \frac{b}{2}D^e] \Delta u^e \\ + [C^e + \frac{1}{2}B^e + bD^e] u^e, \end{aligned} \quad (6.13)$$

where

$$u^e = (u_1, u_2)^T,$$

are the relevant nodal parameters. The element matrices are

$$\begin{aligned} A_{jk}^e &= \int_0^1 N_j N_k d\xi, \\ B_{jk}^e &= v^2 \int_0^1 N'_j N'_k \xi d\xi, \\ C_{jk}^e &= v \int_0^1 N_j N'_k d\xi, \\ D_{jk}^e &= \int_0^1 N'_j N'_k d\xi, \end{aligned}$$

where j, k take only the values 1 and 2. The matrices A^e, B^e, C^e and D^e are thus 2×2 and have the explicit forms

$$A_{jk}^e = \frac{1}{6} \begin{pmatrix} 2 & 1 \\ 1 & 2 \end{pmatrix},$$

$$B_{jk}^e = v^2 \begin{pmatrix} 1 & -1 \\ -1 & 1 \end{pmatrix},$$

$$C_{jk}^e = \frac{1}{2}v \begin{pmatrix} -1 & 1 \\ -1 & 1 \end{pmatrix},$$

$$D_{jk}^e = \begin{pmatrix} 1 & -1 \\ -1 & 1 \end{pmatrix},$$

and v given by

$$v = u_1 \frac{\Delta t}{\Delta x},$$

is constant over the element.

Formally assembling together contributions from all elements leads to the matrix equation

$$\begin{aligned} [A + \frac{1}{2}(C + C^T) + \frac{1}{3}B + \frac{b}{2}D]\Delta u \\ + [C + \frac{1}{2}B + bD]u = 0, \end{aligned} \quad (6.14)$$

and $u = (u_0, u_1, \dots, u_N)^T$, contains all the nodal parameters. The matrices A, B, C, D are tridiagonal and row m of each has the following form:

$$A : \frac{1}{6}(1, 4, 1)$$

$$D : (-1, 2, -1)$$

$$B : (-v_{m-1}^2, v_{m-1}^2 + v_m^2, -v_m^2)$$

$$C : \frac{1}{2}(-v_{m-1}, v_{m-1} - v_m, v_m)$$

Hence identifying $u = u^n$ and $\Delta u = u^{n+1} - u^n$ we can write Equation (6.14) as

$$\begin{aligned} & [A + \frac{1}{2}(C + C^T) + \frac{1}{3}B + \frac{b}{2}D]u^{n+1} \\ & = [A + \frac{1}{2}(C^T - C) - \frac{1}{6}B - \frac{b}{2}D]u^n, \end{aligned} \quad (6.15)$$

a scheme for updating u^n to time level $t = (n + 1)\Delta t$. A typical member of (6.15) is

$$\begin{aligned} & (\frac{1}{6} - \frac{b}{2} - \frac{1}{3}v_{m-1}^2)u_{m-1}^{n+1} + (\frac{2}{3} + b + \frac{1}{2}[v_{m-1} - v_m] \\ & \quad + \frac{1}{3}[v_{m-1}^2 + v_m^2])u_m^{n+1} \\ & \quad + (\frac{1}{6} - \frac{b}{2} - \frac{1}{3}v_m^2)u_{m+1}^{n+1} = \\ & (\frac{1}{6} + \frac{b}{2} + \frac{1}{2}v_{m-1} + \frac{1}{6}v_{m-1}^2)u_{m-1}^n \\ & \quad + (\frac{2}{3} - b - \frac{1}{6}[v_{m-1}^2 + v_m^2])u_m^n \\ & \quad + (\frac{1}{6} + \frac{b}{2} - \frac{1}{2}v_m + \frac{1}{6}v_m^2)u_{m+1}^n, \end{aligned} \quad (6.16)$$

where v_m is given by

$$v_m = \frac{\Delta t}{\Delta x} u_m^n.$$

The boundary conditions $U(0, t) = 0$ and $U(L, t) = 0$ require $u_0 = 0$ and $u_N = 0$. The above set of quasi-linear equations has a matrix which is tridiagonal in form so that a solution using the Thomas algorithm is direct and no iterations are necessary.

6.2.1 Stability Analysis

The growth factor g of the error ϵ_j^n in a typical Fourier mode of amplitude $\hat{\epsilon}^n$

$$\hat{\epsilon}_j^n = \hat{\epsilon}^n \exp(ijk\Delta x) \quad (6.17)$$

where k is the mode number and Δx the element size, is determined for a linearisation of the numerical scheme.

In the linearisation it is assumed that the quantity U in the nonlinear term is locally constant. Under these conditions the error ϵ_j^n satisfies the same finite difference scheme as the function δ_j^n and we find that a typical member of Equation (6.16) has the form

$$\begin{aligned} & \left(\frac{1}{6} - \frac{b}{2}\right)\epsilon_{m-1}^{n+1} + \left(\frac{2}{3} + b\right)\epsilon_m^{n+1} \\ & + \left(\frac{1}{6} - \frac{b}{2}\right)\epsilon_{m+1}^{n+1} = \left(\frac{1}{6} + \frac{b}{2}\right)\epsilon_{m-1}^n \\ & + \left(\frac{2}{3} - b\right)\epsilon_m^n + \left(\frac{1}{6} + \frac{b}{2}\right)\epsilon_{m+1}^n, \end{aligned} \quad (6.18)$$

where

$$b = \frac{\nu\Delta t}{\Delta x^2}$$

substituting the above Fourier mode gives

$$|g| = \frac{P - Q}{P + Q}$$

where

$$P = \frac{2}{3}\cos^2\left[\frac{k\Delta x}{2}\right] + \frac{1}{3}$$

and

$$Q = 2b\left(1 - \cos^2\left[\frac{k\Delta x}{2}\right]\right),$$

and $\cos^2\left[\frac{k\Delta x}{2}\right] \leq 1$ so that $|g| \leq 1$ and the scheme is unconditionally stable.

6.3 Test problems

Simulations arising from three different initial conditions will be described and the results of these experiments compared with published data. We use boundary conditions $U = 0$ at the ends of the box $x = 0$ and $x = L$.

- (a) Take as initial condition [5, 83]

$$U(x, t) = \left(\frac{x}{t}\right)\left[\frac{1}{1 + \left(\frac{t}{t_0}\right)^{\frac{1}{2}} \exp\left(\frac{x^2}{4\nu t}\right)}\right],$$

where

$$t_0 = \exp\left(\frac{1}{8\nu}\right),$$

evaluated at $t = 1$. This is a very useful initial condition as the resulting analytic solution is expressed in closed form so that the L_2 and L_∞ error norms are easily calculated for any value of ν . To test convergence we set $\nu = 0.5$ and vary Δt and Δx and run simulations to time $t = 3.25$ over a region of length $L = 8.0$. In Table (6.5) the L_2 and L_∞ error norms are quoted. We observe that as the magnitudes of the space and time steps are reduced the error norms become progressively smaller. Even with the smallest step values used we do not achieve minimum values of these norms. Accuracy is high, however, we cannot reproduce the accuracy for $\nu = 0.005$ of $L_2 = 0.000235$ and $L_\infty = 0.000688$ at $t = 3.25$ found by Ali et al [5] using cubic B-spline finite elements of length $\Delta x = 0.02$ with a time step $\Delta t = 0.1$.

Table 6.1

Problem (a). Error norms

$$\nu = 0.5, \Delta t = 0.05,$$

$$\Delta x = 0.08, 0 \leq x \leq 8.$$

time	L_2	L_∞
1.00	0.000000	0.000000
1.75	0.001715	0.001644
2.50	0.001901	0.001496
3.25	0.001900	0.001321

Table 6.2

Problem (a). Error norms

$$\nu = 0.05, \Delta t = 0.05,$$

$$\Delta x = 0.03, 0 \leq x \leq 3.$$

time	L_2	L_∞
1.00	0.000000	0.000000
1.75	0.001170	0.002022
2.50	0.001366	0.001947
3.25	0.001420	0.001787

Table 6.3

Problem (a). Error norms

$$\nu = 0.005, \Delta t = 0.05,$$

$$\Delta x = 0.012, 0 \leq x \leq 1.2.$$

time	L_2	L_∞
1.00	0.000000	0.000001
1.75	0.004479	0.019973
2.50	0.005511	0.021157
3.25	0.006295	0.021901

Table 6.4

Problem (a). Error norms

$$\nu = 0.001, \Delta t = 0.025,$$

$$\Delta x = 0.005, 0 \leq x \leq 1.$$

time	L_2	L_∞
1.00	0.000001	0.000010
1.75	0.003240	0.024452
2.50	0.002048	0.018070
3.25	0.005888	0.046279

Table 6.5
 Problem (a). Error norms
 at time $t = 3.25$, $\nu = 0.5$.

Δx	Δt	L_2	L_∞
0.16	0.05	0.003685	0.002376
0.08	0.05	0.001900	0.001321
0.04	0.025	0.000950	0.000656
0.02	0.0125	0.000475	0.000326
0.01	0.0125	0.000255	0.000194
0.01	0.00625	0.000241	0.000164
0.005	0.00625	0.000128	0.000095

Table 6.6
 Problem (a). Error norms at time $t = 3.25$
 various values of ν and L .

ν	$x_{max} = L$	Δx	Δt	L_2	L_∞
0.5	8	0.08	0.05	0.001900	0.001321
0.05	3	0.03	0.05	0.001420	0.001787
0.005	1.2	0.012	0.05	0.006295	0.021901
0.001	1.0	0.005	0.025	0.005888	0.046279

Table 6.7

Problem(a). Analytic and numerical solutions

$$\nu = 0.5, \Delta t = 0.05, \Delta x = 0.08.$$

t	1.0	1.0	1.75	1.75	2.5	2.5	3.25	3.25
x	exact	numeric	exact	numeric	exact	numeric	exact	numeric
0.00	0.0000	0.0000	0.0000	0.0000	0.0000	0.0000	0.0000	0.0000
0.80	0.3611	0.3611	0.1903	0.1905	0.1237	0.1242	0.0893	0.0898
1.60	0.3833	0.3833	0.2669	0.2677	0.1923	0.1931	0.1466	0.1473
2.40	0.1435	0.1435	0.1945	0.1961	0.1773	0.1787	0.1520	0.1532
3.20	0.0215	0.0215	0.0803	0.0809	0.1083	0.1095	0.1133	0.1146
4.00	0.0015	0.0015	0.0201	0.0201	0.0454	0.0458	0.0626	0.0633
4.80	0.0001	0.0001	0.0032	0.0032	0.0136	0.0137	0.0263	0.0265
5.60			0.0004	0.0003	0.0030	0.0030	0.0087	0.0087
6.40					0.0005	0.0005	0.0023	0.0023
7.20							0.0005	0.0005

A second set of simulations using this initial condition with various values of ν have been run up to time $t = 3.25$ and the error norms given in Table (6.6). In Tables from (6.1) to (6.4) we examine error norms. The length of the region L is dictated by the spread of the solution.

In Figures (6.1) to (6.4) we compare the numerical solution for $\nu = 0.5, 0.05, 0.005, 0.001$, shown by continuous curves, with the analytic solutions represented by circular points. In all cases the agreement is very close and compares well with that obtained by Nguyen and Reynen [83]; see their Figures 1 and 2. To enable a more quantitative assessment to be made the numerical and analytic solutions are compared at various points and times in Tables (6.7) to (6.10). These show that, in general, the largest error is observed on the steeper downward parts of the curve, particularly at later times.

Table 6.8
 Problem(a). Analytic and numerical solutions
 $\nu = 0.05, \Delta t = 0.05, \Delta x = 0.03.$

t	1.0	1.0	1.75	1.75	2.5	2.5	3.25	3.25
x	exact	numeric	exact	numeric	exact	numeric	exact	numeric
0.0	0.0000	0.0000	0.0000	0.0000	0.0000	0.0000	0.0000	0.0000
0.3	0.2070	0.2070	0.1150	0.1154	0.0778	0.0783	0.0579	0.0585
0.6	0.2195	0.2195	0.1664	0.1672	0.1243	0.1251	0.0972	0.0981
0.9	0.0516	0.0516	0.1064	0.1083	0.1095	0.1113	0.0990	0.1006
1.2	0.0031	0.0031	0.0283	0.0287	0.0529	0.0542	0.0644	0.0660
1.5	0.0000	0.0000	0.0036	0.0036	0.0144	0.0146	0.0264	0.0271
1.8			0.0003	0.0003	0.0024	0.0024	0.0072	0.0074
2.1					0.0003	0.0003	0.0014	0.0014
2.4							0.0002	0.0002

Table 6.9
 Problem (a). Analytic and numerical solutions
 $\nu = 0.005, \Delta t = 0.05, \Delta x = 0.012.$

t	1.0	1.0	1.75	1.75	2.5	2.5	3.25	3.25
x	exact	numeric	exact	numeric	exact	numeric	exact	numeric
0.00	0.0000	0.0000	0.0000	0.0000	0.0000	0.0000	0.0000	0.0000
0.12	0.1200	0.1200	0.0686	0.0697	0.0480	0.0492	0.0369	0.0379
0.24	0.2400	0.2400	0.1371	0.1380	0.0960	0.0972	0.0738	0.0750
0.36	0.3591	0.3591	0.2057	0.2059	0.1440	0.1448	0.1108	0.1118
0.48	0.3490	0.3490	0.2733	0.2719	0.1919	0.1921	0.1477	0.1484
0.60	0.0024	0.0024	0.2996	0.2981	0.2381	0.2369	0.1843	0.1845
0.72	0.0000	0.0000	0.0287	0.0309	0.2425	0.2455	0.2173	0.2165
0.84			0.0002	0.0002	0.0376	0.0459	0.1918	0.2024
0.96					0.0006	0.0007	0.0277	0.0359
1.08							0.0008	0.0009

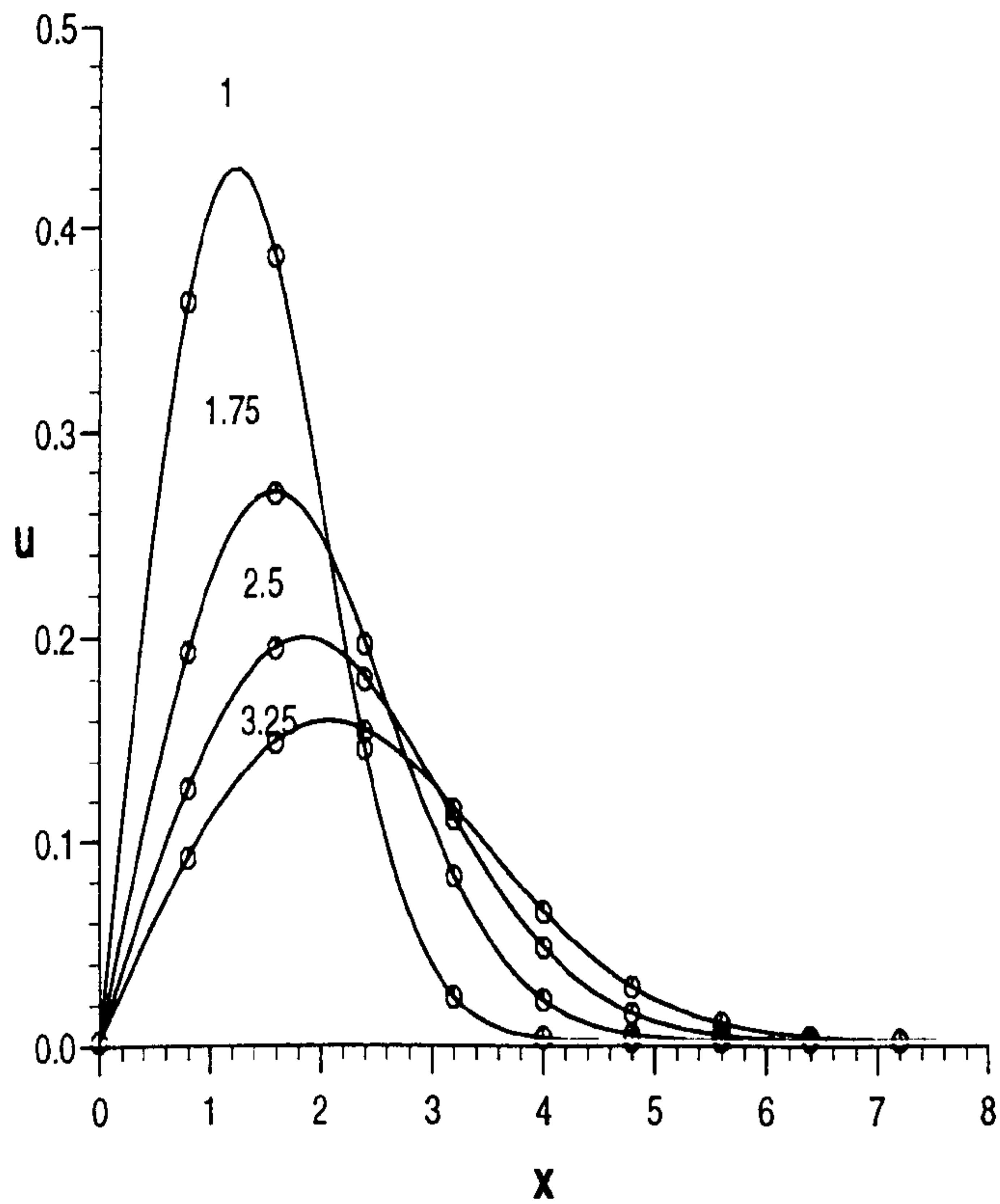


Figure 6.1 Problem (a). Numerical solutions for $\nu = 0.5$, $\Delta x = 0.08$, $\Delta t = 0.05$, shown by continuous curves for times $t = 1, 1.75, 2.5, 3.25$. Analytic solutions are shown by circular points.

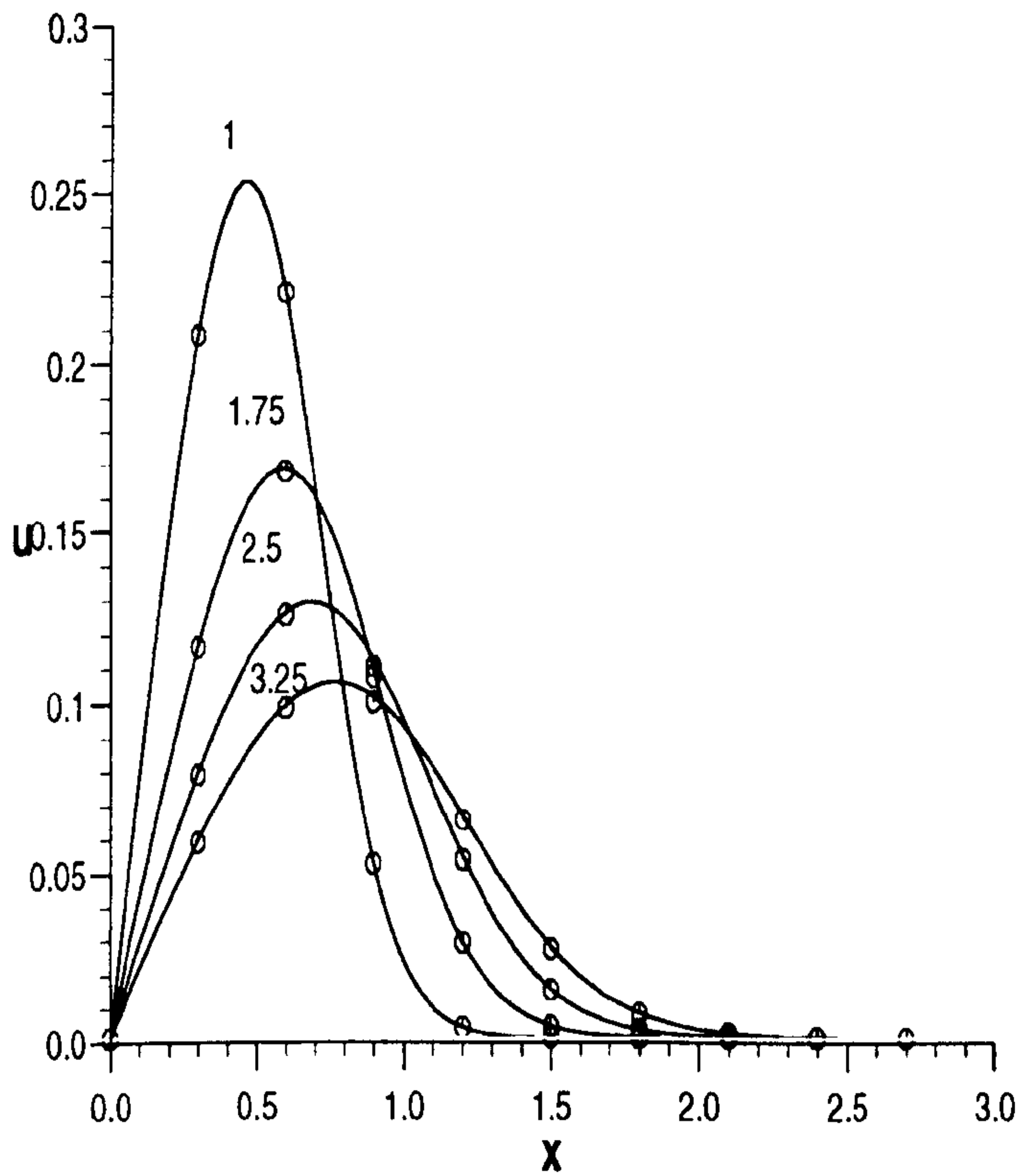


Figure 6.2 Problem (a). Numerical solutions for $\nu = 0.05$, $\Delta x = 0.03$, $\Delta t = 0.05$, shown by continuous curves for times $t = 1, 1.75, 2.5, 3.25$. Analytic solutions are shown by circular points.

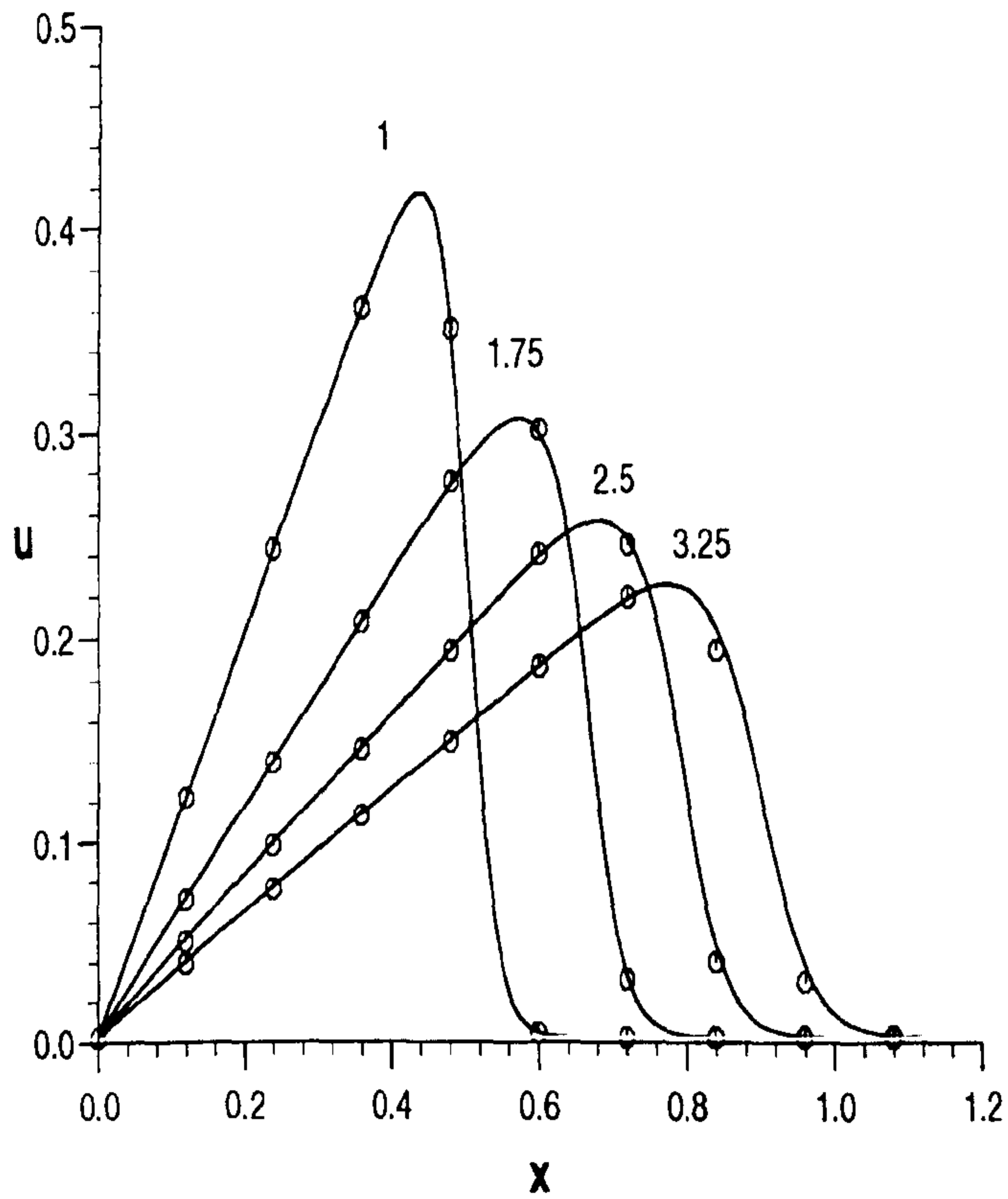


Figure 6.3 Problem (a). Numerical solutions for $\nu = 0.005$, $\Delta x = 0.012$, $\Delta t = 0.05$, shown by continuous curves for times $t = 1, 1.75, 2.5, 3.25$. Analytic solutions by circular points.

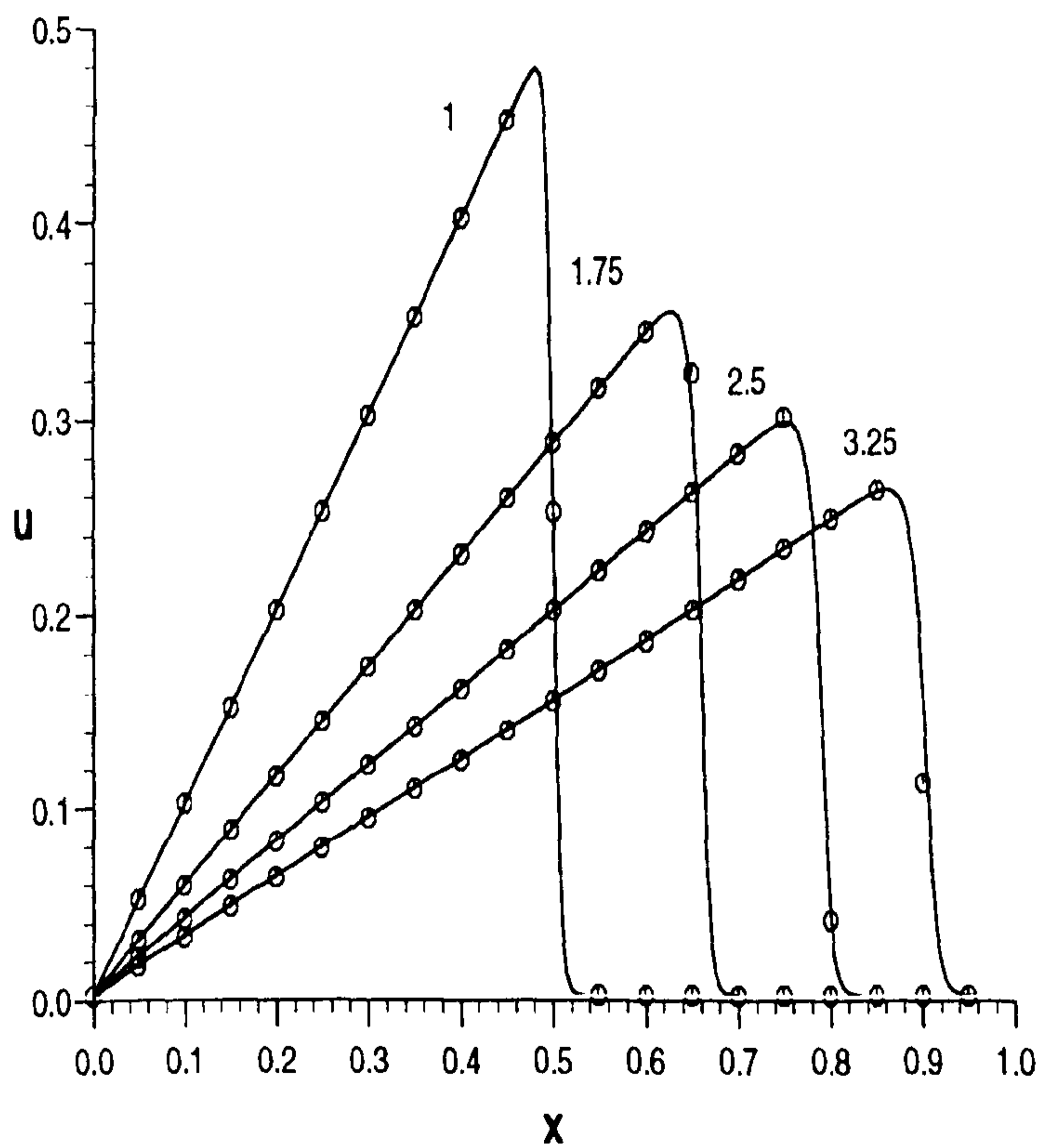


Figure 6.4 Problem (a). Numerical solutions for $\nu = 0.001$, $\Delta x = 0.005$, $\Delta t = 0.025$, shown by continuous curves for times $t = 1, 1.75, 2.5, 3.25$. Analytic solutions by circular points.

Table 6.10

Problem (a). Analytic and numerical solutions

$$\nu = 0.001, \Delta t = 0.025, \Delta x = 0.005.$$

t	1.0	1.0	1.75	1.75	2.5	2.5	3.25	3.25
x	exact	numeric	exact	numeric	exact	numeric	exact	numeric
0.0	0.0000	0.0000	0.0000	0.0000	0.0000	0.0000	0.0000	0.0000
0.1	0.1000	0.1000	0.0571	0.0577	0.0400	0.0407	0.0308	0.0314
0.2	0.2000	0.2000	0.1143	0.1146	0.0800	0.0806	0.0615	0.0622
0.3	0.3000	0.3000	0.1714	0.1715	0.1200	0.1204	0.0923	0.0928
0.4	0.4000	0.4000	0.2286	0.2285	0.1600	0.1602	0.1231	0.1234
0.5	0.2500	0.2500	0.2857	0.2854	0.2000	0.2000	0.1538	0.1541
0.6	0.0000	0.0000	0.3429	0.3420	0.2400	0.2398	0.1846	0.1847
0.7			0.0002	0.0001	0.2800	0.2796	0.2154	0.2153
0.8					0.0396	0.0416	0.2462	0.2459
0.9							0.1113	0.1576
1.0							0.0000	0.0000

(b) Sine curve initial condition

$$U(x, 0) = \sin(\pi x), \quad (6.19)$$

over $0 < x < 1$. This problem has been widely studied [83, 99]. To compare with previous work, in particular with the most detailed solution given by Kakuda and Tosaka [67], let ν have the values 1, 0.1, 0.01. The results of our computations are given in Figures (6.5), (6.6) and (6.7) as continuous lines and are compared with analytic values taken from [67]. Agreement is good.

Quantitative comparisons can be made using the point values of the solutions given in Tables from (6.11) to (6.13). Solutions obtained here are seen to be as accurate as those obtained by Kakuda and Tosaka [67].

Table 6.11

Problem (b). Analytic and numerical solutions for $\nu = 1$,
 $\Delta x = 0.005$, $\Delta t = 0.005$.

t	0.02	0.02	0.04	0.04	0.10	0.10	0.22	0.22
x	numeric	exact	numeric	exact	numeric	exact	numeric	exact
0.1	0.2430	0.2437	0.1963	0.1970	0.1092	0.1095	0.0345	0.0345
0.2	0.4650	0.4662	0.3764	0.3776	0.2092	0.2098	0.0658	0.0659
0.4	0.7690	0.7699	0.6272	0.6283	0.3474	0.3479	0.1074	0.1075
0.6	0.7911	0.7904	0.6521	0.6514	0.3593	0.3591	0.1087	0.1087
0.8	0.5009	0.4994	0.4168	0.4151	0.2285	0.2278	0.0678	0.0678
0.9	0.2653	0.2643	0.2213	0.2202	0.1212	0.1207	0.0358	0.0357

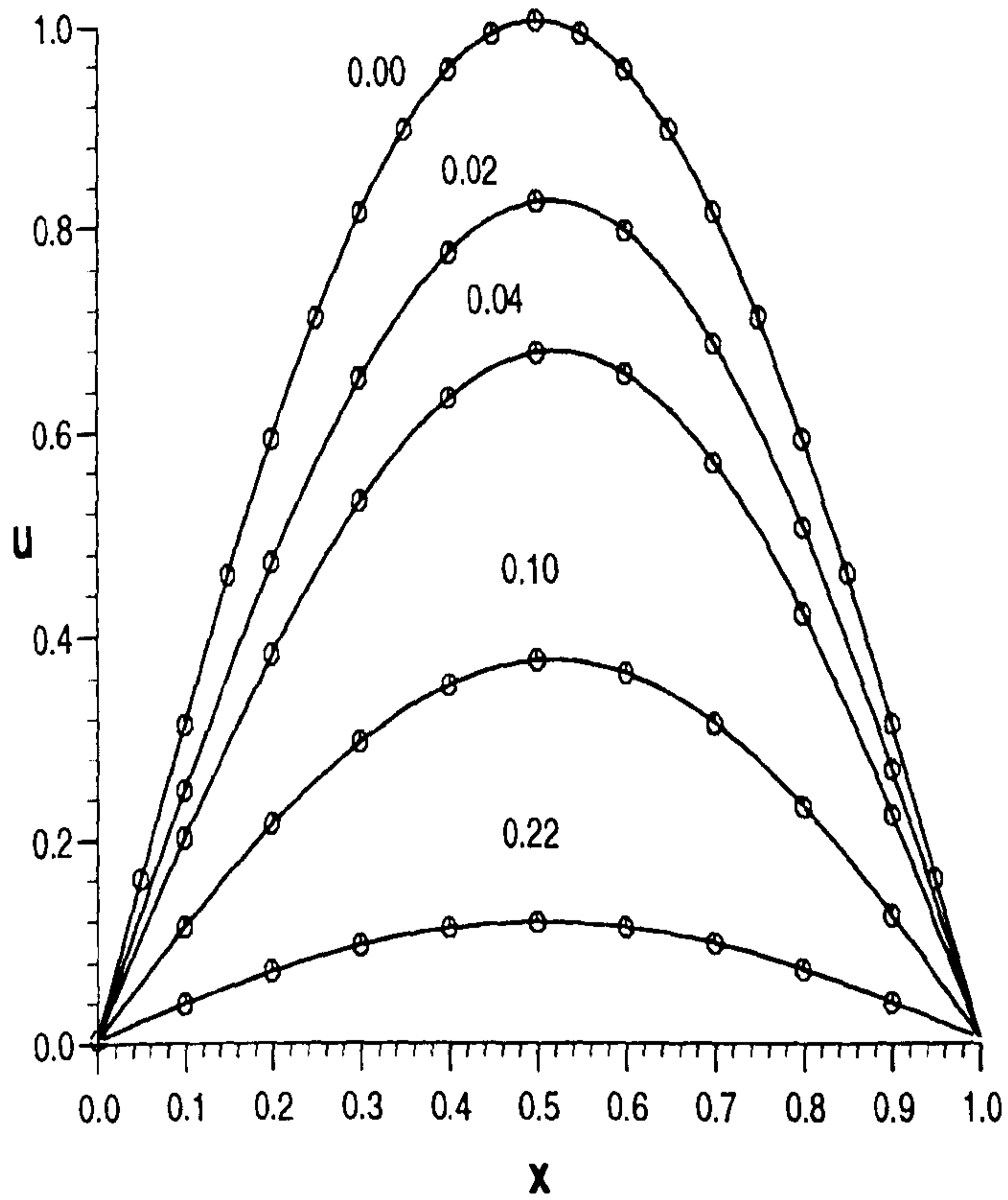


Figure 6.5 Problem (b). Numerical solution for $\nu = 1.0$, $\Delta x = 0.005$, $\Delta t = 0.005$, shown by continuous curves for various labelled times. Analytic solutions are shown by circular points [67].

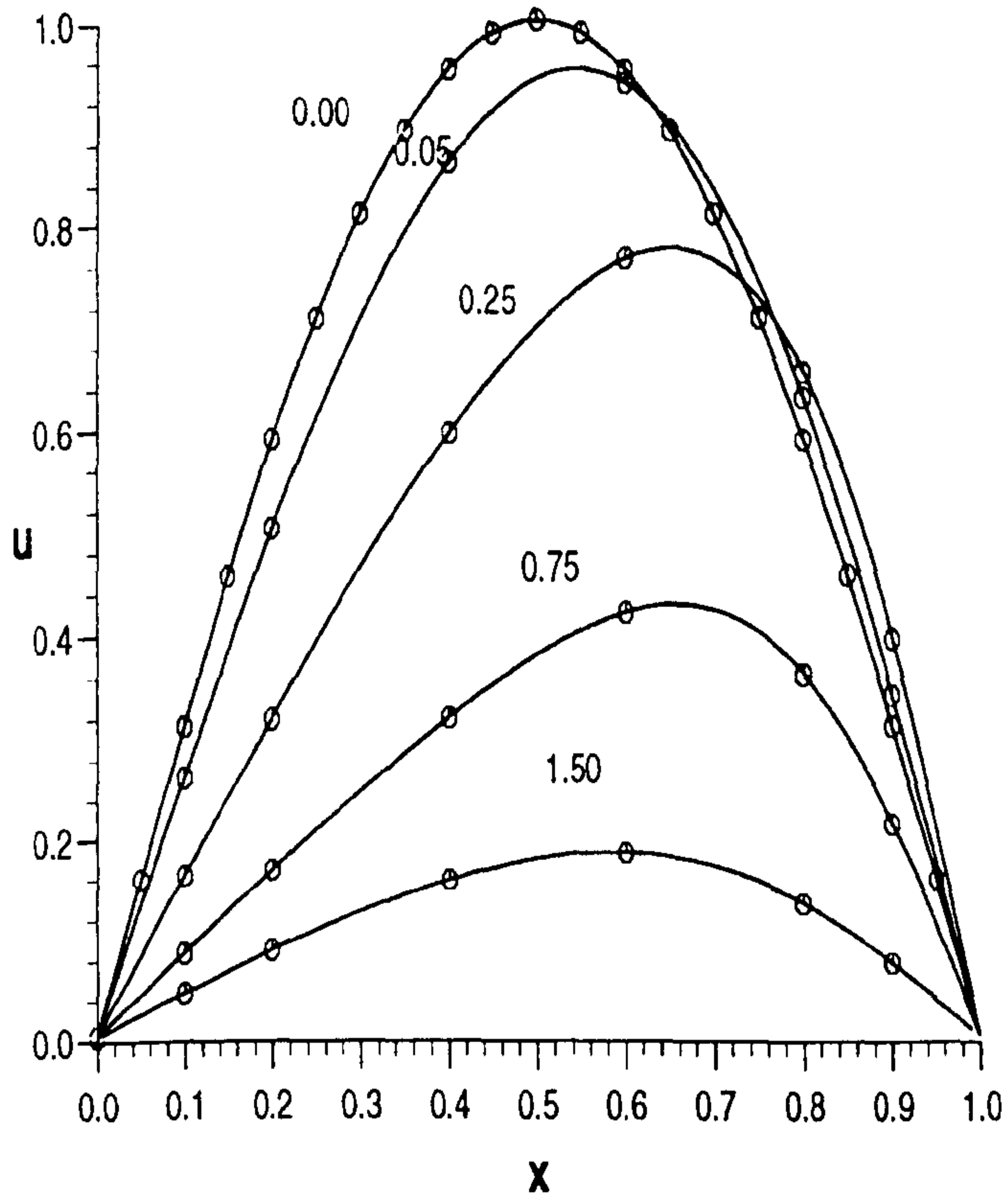


Figure 6.6 Problem (b). Numerical solution for $\nu = 0.1$, $\Delta x = 0.005$, $\Delta t = 0.005$, shown by continuous curves for various labelled times. Analytic solutions are shown by circular points [67].

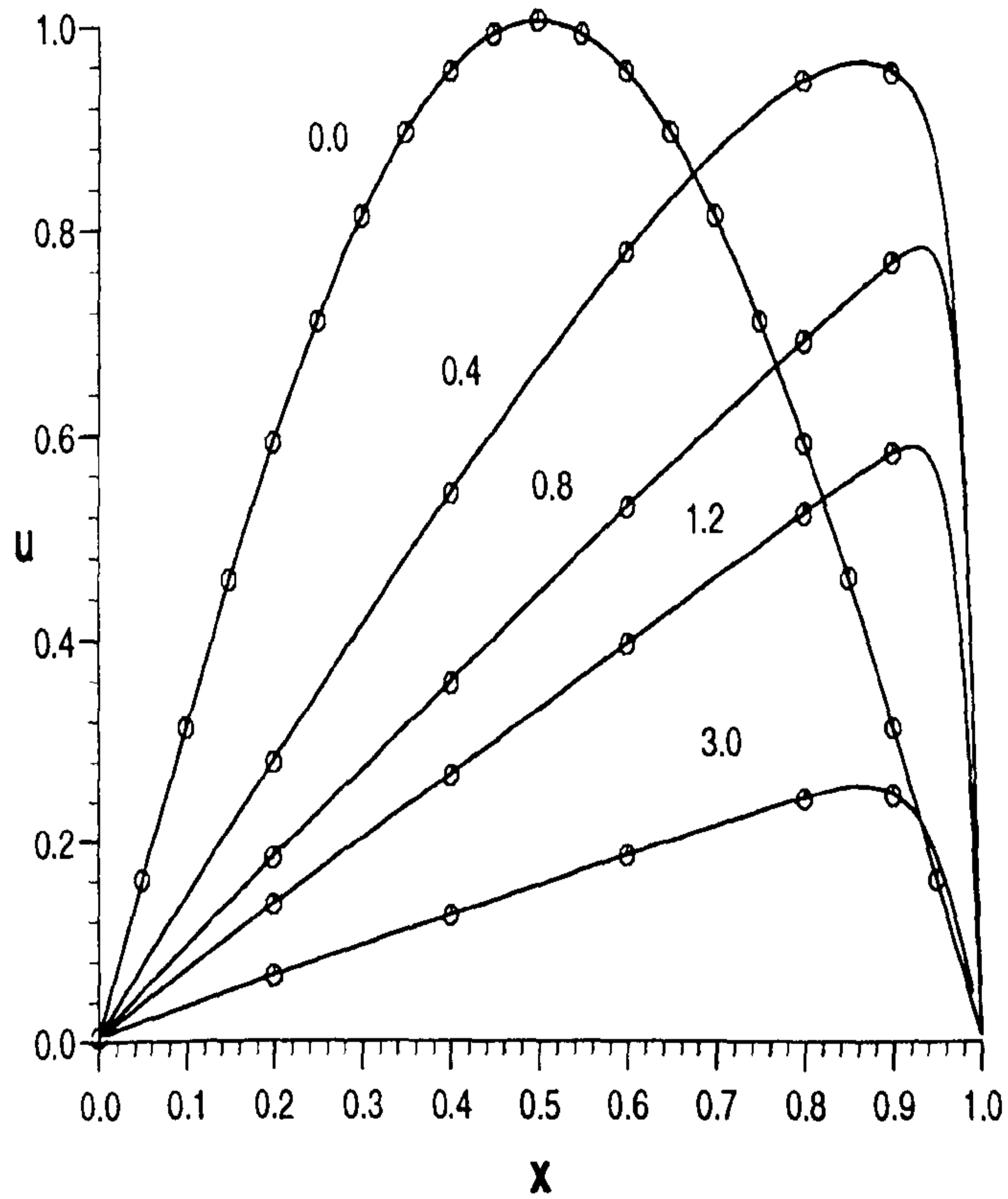


Figure 6.7 Problem (b). Numerical solutions for $\nu = 0.01$, $\Delta x = 0.005$, $\Delta t = 0.005$ shown by continuous curves for the labelled times. Analytic solutions are shown by circular points [67].

Table 6.12

Problem (b). Analytic and numerical solutions for
 $\nu = 0.1, \Delta x = 0.005, \Delta t = 0.005.$

t	0.05	0.05	0.25	0.25	0.75	0.75	1.50	1.50
x	numeric	exact	numeric	exact	numeric	exact	numeric	exact
0.1	0.2590	0.2587	0.1606	0.1603	0.0836	0.0834	0.0438	0.0438
0.2	0.5001	0.5001	0.3166	0.3162	0.1658	0.1655	0.0859	0.0858
0.4	0.8596	0.8599	0.5937	0.5941	0.3174	0.3174	0.1557	0.1556
0.6	0.9376	0.9374	0.7646	0.7653	0.4190	0.4192	0.1835	0.1833
0.8	0.6299	0.6290	0.6560	0.6537	0.3601	0.3590	0.1330	0.1325
0.9	0.3405	0.3394	0.3965	0.3926	0.2147	0.2131	0.0736	0.0732

Table 6.13

Problem (b). Analytic and numerical solutions for
 $\nu = 0.01, \Delta x = 0.005, \Delta t = 0.005.$

t	0.4	0.4	0.8	0.8	1.2	1.2	3.0	3.0
x	numeric	exact	numeric	exact	numeric	exact	numeric	exact
0.1	0.2590	0.2587	0.1606	0.1603	0.0836	0.0834	0.0438	0.0438
0.2	0.2763	0.2745	0.1791	0.1774	0.1324	0.1309	0.0608	0.0601
0.4	0.5389	0.5379	0.3544	0.3528	0.2629	0.2613	0.1212	0.1202
0.6	0.7737	0.7735	0.5251	0.5240	0.3918	0.3904	0.1813	0.1802
0.8	0.9408	0.9410	0.6876	0.6871	0.5186	0.5175	0.2397	0.2386
0.9	0.9516	0.9489	0.7627	0.7630	0.5779	0.5778	0.2433	0.2416

(c) Initial condition [67, 79]

$$U(x, 0) = \begin{cases} \sin(\pi x), & 0 < x \leq 1 \\ -\frac{1}{2} \sin(\pi x), & 1 < x \leq 2 \\ 0, & 2 < x \leq 5. \end{cases}$$

Use boundary conditions $U(0, t) = U(6, t) = 0$. Values of ν are 0.1, 0.01. The solution curves are given in Figures (6.8) and (6.9). Both solution sets tend to zero smoothly as $x \rightarrow 6$. Comparing Figure (6.8), for $\nu = 0.1$, with Figure 1 of Mittal and Singhal [79] indicates that there is complete agreement at earlier times, up to about $t = 6$, but thereafter some slight deviation occurs since these authors force their solution to become zero at $t = 5$. Again if we compare Figure (6.9), for $\nu = 0.01$, with Figure 11 of [67] and Figure 2 of [79] we see that the right hand extremity of the curve for time $t = 10$ has reached $x = 5$ in [67] whereas in Figure (6.9) and [79], it has only reached $x = 4.5$. In addition, our curve for $t = 2$ tends to confirm the solutions of this problem obtained in [79] rather than those in [67].

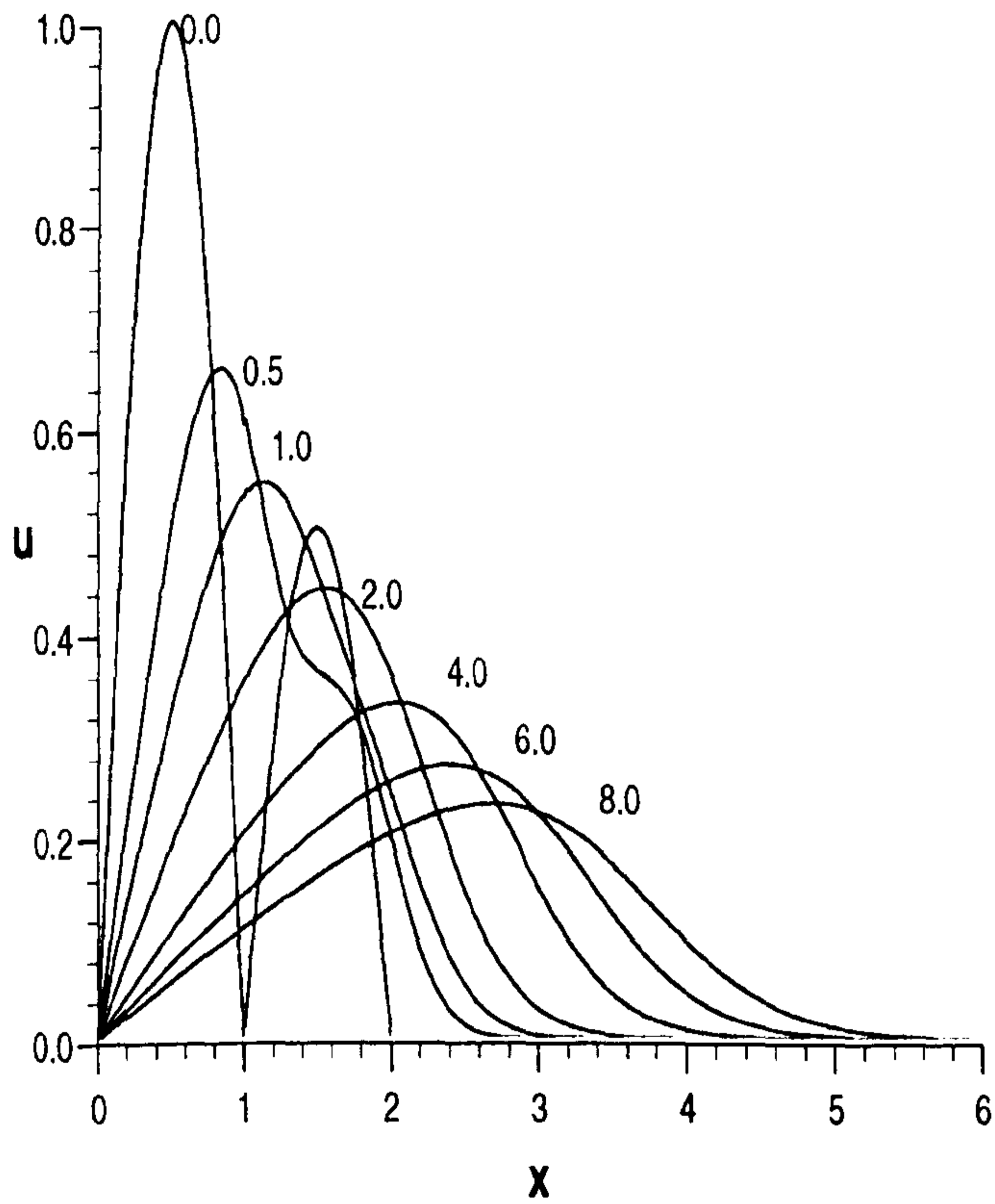


Figure 6.8 Problem (c). Numerical solutions for $\nu = 0.1$, $\Delta x = 0.01$, $\Delta t = 0.05$, shown at times $t = 0.0, 0.5, 1, 2, 4, 6$ and 8 by continuous curves.

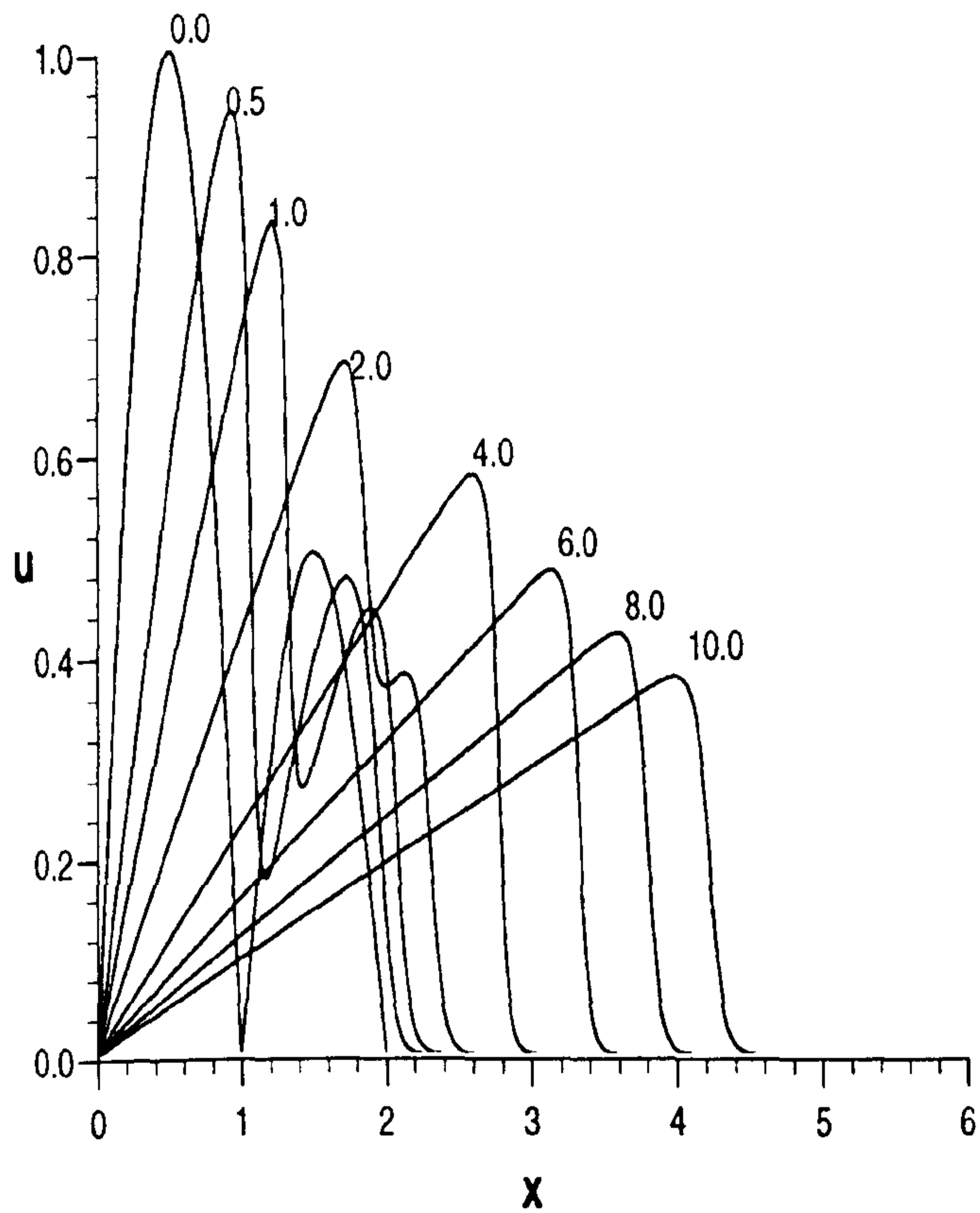


Figure 6.9 Problem (c). Numerical solutions for $\nu = 0.01$, $\Delta x = 0.01$, $\Delta t = 0.05$, shown at times $t = 0.0, 0.5, 1, 2, 4, 6, 8$ and 10 by continuous curves.

6.4 Discussion

The space/time least squares approach with linear finite elements set up in Section (6.2) leads to an unconditionally stable algorithm which faithfully models known solutions for Burgers' equation.

Superficially this algorithm may appear identical with that used by Nguyen and Reynen [83] upon which it is based, however, the linearisation employed is very different.

Although we both approximate the non-linear term by $UU_x = \hat{U}U_x$, where \hat{U} is a constant, the present authors then assume that \hat{U} has the form of a simple step function that is constant over each finite element $[x_m, x_{m+1}]$, $[t^n, t^{n+1}]$ taking the value to be U_m^n leading to the algorithm given at the end of Section (6.2). Nguyen and Reynen [83] do not describe their assumptions explicitly but we can deduce from the text and the equation they derive for u_m^{n+1}

$$\begin{aligned} & \left(\frac{1}{6} - \frac{b}{2} - \frac{1}{3}v^2\right)u_{m-1}^{n+1} + \left(\frac{2}{3} + b + \frac{2}{3}v^2\right)u_m^{n+1} \\ & + \left(\frac{1}{6} - \frac{b}{2} - \frac{1}{3}v^2\right)u_{m+1}^{n+1} = \left(\frac{1}{6} + \frac{b}{2} + \frac{1}{2}v + \frac{1}{6}v^2\right)u_{m-1}^n \\ & + \left(\frac{2}{3} - b - \frac{1}{3}v^2\right)u_m^n + \left(\frac{1}{6} + \frac{b}{2} - \frac{1}{2}v + \frac{1}{6}v^2\right)u_{m+1}^n, \end{aligned}$$

that they assume \hat{U} is constant over two adjacent spatial elements $[x_{m-1}, x_m]$, $[x_m, x_{m+1}]$, $[t^n, t^{n+1}]$, taking the value $\frac{1}{2}(U_m^n + U_m^{n+1})$, implying an overlapping step function leading to

$$v = \frac{\Delta t}{\Delta x} \frac{1}{2}(U_m^n + U_m^{n+1}).$$

From the evidence of the results presented here and in [83] either assumption appears equally valid and to produce similar results.

Chapter 7

A Petrov-Galerkin Finite Element Scheme For Burgers' Equation

7.1 Introduction

Burgers' equation is solved by a Petrov-Galerkin method using quadratic B-spline spatial finite elements. A linear recurrence relationship for the numerical solution of the resulting system of ordinary differential equations is obtained via a Crank-Nicolson approach involving a product approximation. Standard problems are solved to assess the properties of the algorithm.

As a model of flow through a shock wave, based upon the Navier-Stokes equations for one-dimensional non-stationary flow of a compressible viscous fluid, we obtain [32]

$$W_t + \beta W W_x = \frac{4}{3} \nu^* W_{xx}, \quad (7.1)$$

where the subscripts t and x denote differentiation; W is the excess of flow velocity over sonic velocity, $\beta = (\gamma + 1)/2$, γ is the ratio of specific heats C_p/C_v and ν^* is the kinematic viscosity at sonic conditions. With the nor-

malisations

$$U = \beta W, \quad \nu = \frac{4}{3}\nu^*$$

the one dimensional Burgers' equation is obtained

$$U_t + UU_x - \nu U_{xx} = 0. \quad (7.2)$$

Here t is time, x is the space coordinate and $U(x, t)$ is velocity. The initial conditions are

$$U(x, 0) = f_0(x), \quad 0 \leq x \leq L,$$

and the boundary conditions are

$$U(0, t) = U_0, \quad U(L, t) = U_L,$$

where L is the length of the channel.

Burgers' equation may also be treated as a model equation for the decay of turbulence in a box, where U is velocity and [22]

$$\nu = \frac{1}{Re}.$$

The quantity Re is the Reynolds number defined with reference to a representative velocity U_0 and the scale length of the turbulent field L by

$$Re = \frac{U_0 L}{\nu^*}. \quad (7.3)$$

Physical boundary conditions require U to be zero at the ends of the box, so that $U \rightarrow 0$ as $x \rightarrow 0, L$.

Burgers' equation is one of very few non-linear partial differential equations which can be solved analytically for arbitrary initial data [61]. These solutions, in many cases, involve infinite series which for small values of ν may converge very slowly.

Numerical algorithms for the solution of Burgers' equation have been proposed by many authors. Varoglu and Finn [99] set up space-time finite elements incorporating characteristics with which to obtain a numerical solution via a weighted residual method. Caldwell and Smith [24] use cubic

spline finite elements, Evans and Abdullah [39] a group explicit finite difference method, Kakuda and Tosaka [67] a generalised boundary element approach, Mittal and Singhal [79] a technique of finitely reproducing nonlinearities to obtain a set of stiff ordinary differential equations which are solved by a Runge-Kutta-Chebyshev method, while Ali et al [5] use collocation over cubic B-spline finite elements and Nguyen and Reynen [83] developed a least squares approach with linear elements. We have applied a similar space-time least-squares finite element algorithm, based on the work of Nguyen and Reynen [83], to the numerical solution of Burgers' equation [50].

Here we develop a Petrov-Galerkin solution to Burgers' equation using quadratic B-spline finite elements. Some standard problems are studied and comparisons are made with published results.

7.2 The finite element solution

A uniform linear spatial array of linear finite elements is set up $0 = x_0 < x_1 \dots < x_N = L$. A typical finite element of size $\Delta x = (x_{m+1} - x_m)$ is mapped by local coordinates ξ given by $\Delta x \xi = x - x_m$, $0 \leq \xi \leq 1$, see Figure (7.1) [43]. The trial function for a quadratic B-spline finite element is

$$U = (1 - 2\xi + \xi^2)\delta_{m-1} + (1 + 2\xi - 2\xi^2)\delta_m + \xi^2\delta_{m+1}. \quad (7.4)$$

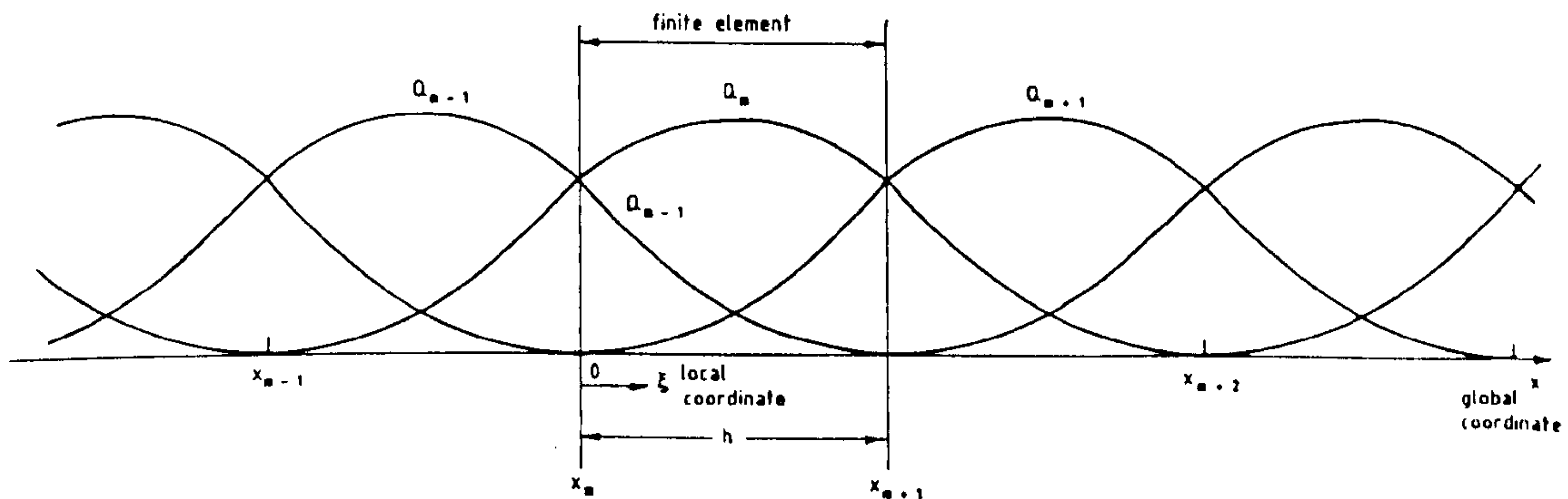


Figure 7.1 Quadratic B-Splines covering a uniform mesh. Spline Q_m extends over three elements $[x_{m-1}, x_m]$, $[x_m, x_{m+1}]$, $[x_{m+1}, x_{m+2}]$. The splines Q_{m-1} , Q_m , Q_{m+1} cover the element $[x_m, x_{m+1}]$; all other splines are zero over this element [43].

The quantities δ_m are nodeless element parameters. The nodal variables U_m and U'_m , at the node $x = x_m$, are given in terms of the parameters δ_m by

$$U_m = \delta_m + \delta_{m-1}, \quad (7.5)$$

$$\Delta x U'_m = 2(\delta_m - \delta_{m-1}), \quad (7.6)$$

where the prime denotes differentiation with respect to x .

When a Petrov-Galerkin method is applied to Equation (7.2) with weight functions W_m the weak form

$$\int_{x_0}^{x_N} W_m (U_t + UU_x - \nu U_{xx}) dx = 0, \quad (7.7)$$

where $m = 0, 1, \dots, N - 1$, is produced. With weight functions of the form

$$W_m = \begin{cases} 1, & x_m \leq x \leq x_{m+1}, \\ 0, & x < x_m, \quad x > x_{m+1}, \end{cases}$$

Equation (7.7) becomes for a single element $[x_m, x_{m+1}]$

$$\int_{x_m}^{x_{m+1}} (U_t + UU_x - \nu U_{xx}) dx = 0. \quad (7.8)$$

Integrating leads to

$$\int_{x_m}^{x_{m+1}} U_t dx + \frac{1}{2} [U^2]_{x_m}^{x_{m+1}} - \nu [U_x]_{x_m}^{x_{m+1}} = 0. \quad (7.9)$$

Employing a Crank-Nicolson approach in time by centring on $(n + \frac{1}{2})\Delta t$ to obtain second order accurate expressions for $U^{n+\frac{1}{2}}$, its time derivative and $(U^2)^{n+\frac{1}{2}}$ as

$$\begin{aligned} U &= \frac{1}{2}(U^n + U^{n+1}), \\ \frac{\partial U}{\partial t} &= \frac{1}{\Delta t}(U^{n+1} - U^n), \\ U^2 &= U^{n+1}U^n, \end{aligned}$$

where the superscripts n and $n + 1$ are time labels.

Substituting into Equation (7.9) produces

$$\begin{aligned} \frac{1}{\Delta t} \int_{x_m}^{x_{m+1}} (U^{n+1} - U^n) dx + \frac{1}{2} [U^{n+1}U^n]_{x_m}^{x_{m+1}} \\ - \frac{\nu}{2} [U_x^{n+1} + U_x^n]_{x_m}^{x_{m+1}} = 0, \end{aligned} \quad (7.10)$$

which with (7.4)-(7.6) leads to the quasi-linear recurrence relationship

$$\begin{aligned} (1 - \beta - \alpha[\delta_{m-1}^n + \delta_m^n])\delta_{m-1}^{n+1} \\ + (4 + 2\beta + \alpha[\delta_{m+1}^n - \delta_{m-1}^n])\delta_m^{n+1} \\ + (1 - \beta + \alpha[\delta_m^n + \delta_{m+1}^n])\delta_{m+1}^{n+1} = (1 + \beta)\delta_{m-1}^n \\ + (4 - 2\beta)\delta_m^n + (1 + \beta)\delta_{m+1}^n, \end{aligned} \quad (7.11)$$

where

$$\alpha = \frac{3\Delta t}{2\Delta x}, \quad \beta = \frac{3\nu\Delta t}{\Delta x^2}, \quad (7.12)$$

and $m = 0, 1, \dots, N - 1$, $n = 0, 1, \dots$.

With boundary conditions U_0, U_N prescribed, leading to $\delta_{-1}^n + \delta_0^n = U_0$ and $\delta_{N-1}^n + \delta_N^n = U_N$, the first and last equations corresponding to $m = 0, N - 1$ have the reduced forms

$$\begin{aligned} & (3 + 3\beta + \alpha[\delta_0^n + \delta_1^n])\delta_0^{n+1} + (1 - \beta + \alpha[\delta_0^n + \delta_1^n])\delta_1^{n+1} \\ & = (3 - 3\beta)\delta_0^n + (1 + \beta)\delta_1^n + (2\beta + \alpha U_0)U_0, \end{aligned}$$

and

$$\begin{aligned} & (1 - \beta - \alpha[\delta_{N-2}^n + \delta_{N-1}^n])\delta_{N-2}^{n+1} + (3 + 3\beta - \alpha[\delta_{N-2}^n + \delta_{N-1}^n])\delta_{N-1}^{n+1} \\ & = (1 + \beta)\delta_{N-2}^n + (3 - 3\beta)\delta_{N-1}^n + (2\beta - \alpha U_N)U_N. \end{aligned}$$

Alternative boundary conditions $\frac{\partial U}{\partial x} = 0$ at both ends of the region imply $\delta_{-1} = \delta_0$ and $\delta_N = \delta_{N-1}$ and the first and last equations are replaced by

$$\begin{aligned} & (5 + \beta + \alpha[\delta_1^n - 3\delta_0^n])\delta_0^{n+1} + (1 - \beta + \alpha[\delta_0^n + \delta_1^n])\delta_1^{n+1} \\ & = (5 - \beta)\delta_0^n + (1 + \beta)\delta_1^n, \end{aligned}$$

and

$$\begin{aligned} & (1 - \beta - \alpha[\delta_{N-2}^n + \delta_{N-1}^n])\delta_{N-2}^{n+1} + (5 + \beta + \alpha[3\delta_{N-1}^n - \delta_{N-2}^n])\delta_{N-1}^{n+1} \\ & = (1 + \beta)\delta_{N-2}^n + (5 - \beta)\delta_{N-1}^n. \end{aligned}$$

The above set of quasi-linear equations has a matrix which is tridiagonal in form so that a solution using the Thomas algorithm is direct and no iterations are necessary.

7.2.1 Stability Analysis

The growth factor g of the error ϵ_j^n in a typical Fourier mode of amplitude $\hat{\epsilon}^n$

$$\hat{\epsilon}_j^n = \hat{\epsilon}^n \exp(ijk\Delta x) \quad (7.13)$$

where k is the mode number and Δx the element size, is determined for a linearisation of the numerical scheme.

In the linearisation it is assumed that the quantity U in the nonlinear term is locally constant. Under these conditions the error ϵ_j^n satisfies the same finite difference scheme as the function δ_j^n and we find that a typical member of Equation (7.11) has the form

$$\begin{aligned} & (1 - \beta)\epsilon_{m-1}^{n+1} + (4 + 2\beta)\epsilon_m^{n+1} \\ & + (1 - \beta)\epsilon_{m+1}^{n+1} = (1 + \beta)\epsilon_{m-1}^n \\ & + (4 - 2\beta)\epsilon_m^n + (1 + \beta)\epsilon_{m+1}^n, \end{aligned} \quad (7.14)$$

where

$$\beta = 3 \frac{\nu \Delta t}{\Delta x^2}$$

substituting the above Fourier mode gives

$$|g| = \frac{P - Q}{P + Q}$$

where

$$P = 4 \cos^2 \left[\frac{k\Delta x}{2} \right] + 2$$

and

$$Q = 4\beta \left(1 - \cos^2 \left[\frac{k\Delta x}{2} \right] \right) \geq 0,$$

and $\cos^2 \left[\frac{k\Delta x}{2} \right] \leq 1$ so that $|g| \leq 1$ and the scheme is unconditionally stable.

$$\delta^0 = \begin{bmatrix} \delta_{-1}^0 \\ \delta_0^0 \\ \delta_1^0 \\ \star \\ \star \\ \star \\ \delta_{N-1}^0 \\ \delta_N^0 \end{bmatrix},$$

and

$$b = \begin{bmatrix} U_0^0 \\ U_1^0 \\ U_2^0 \\ \star \\ \star \\ \star \\ U_N^0 \\ \Delta x U_N'^0 \end{bmatrix}.$$

These equations may be solved recursively as

$$\delta_N^0 = \frac{1}{2}(U_N^0 + \frac{1}{2}\Delta x U_N'^0),$$

$$\delta_{N-1}^0 = \frac{1}{2}(U_N^0 - \frac{1}{2}\Delta x U_N'^0),$$

and

$$\delta_{j-1}^0 = U_j^0 - \delta_j^0,$$

for $j = N - 1, \dots, 0$.

7.4 Test problems

Simulations arising from four different initial conditions will be described and the results of these experiments compared with published data. Problems (a) and (b) model the decay of turbulence within a box and we use boundary conditions $U = 0$ at the ends of the box $x = 0$ and $x = L$. Problems (c) and (d) describe the flow through a shock wave and for these the boundary conditions are $U \rightarrow 1$ as $x \rightarrow x_0$ and (c) $U \rightarrow 0.2$, (d) $U \rightarrow 0.0$, as $x \rightarrow x_N$.

To make quantitative comparisons between solutions obtained by different methods we use the L_2 and L_∞ error norms which measure the mean and maximum errors respectively in each numerical solution.

- (a) Take as initial condition [5, 50]

$$U(x, t) = \left(\frac{x}{t}\right) \left[\frac{1}{1 + \left(\frac{t}{t_0}\right)^{\frac{1}{2}} \exp\left(\frac{x^2}{4\nu t}\right)} \right], \quad (7.17)$$

where

$$t_0 = \exp\left(\frac{1}{8\nu}\right),$$

evaluated at $t = 1$. This is a very useful initial condition as the resulting analytic solution is expressed in closed form so that the L_2 and L_∞ error norms are easily calculated for any value of ν . To test convergence we set $\nu = 0.5$ and vary Δt and Δx and run simulations to time $t = 3.25$ over a region of length $L = 8.0$. In Table (7.1) the L_2 and L_∞ error norms are quoted. We observe that the smallest values for the error norms $L_2 = 0.0001$ and $L_\infty = 0.00008$ at time $t = 3.25$, are achieved with $\Delta x = 0.08$ and $\Delta t = 0.05$. These error norms are similar in size to those obtained earlier by Ali et al [5] $L_2 = 0.000235$ and $L_\infty = 0.000688$ at $t = 3.25$ using cubic B-spline finite elements of length $\Delta x = 0.02$ with a time step $\Delta t = 0.1$. It is clear from Table (7.1) that if the space and time steps are increased or reduced in size from the optimum values the magnitudes of both error norms increase. In Tables from (7.2) to (7.5) we demonstrate error norms with various values of ν .

Table 7.1
 Problem (a). Error norms
 at time $t = 3.25$, $\nu = 0.5$.

Δx	Δt	L_2	L_∞
0.32	0.2	0.0013	0.0010
0.16	0.1	0.00038	0.00029
0.16	0.05	0.00032	0.00024
0.08	0.05	0.0001	0.00008
0.06	0.04	0.0025	0.0045
0.04	0.025	0.4786	1.9280

Table 7.2
 Problem (a). Error norms
 $\nu = 0.5$, $\Delta x = 0.08$, $\Delta t = 0.05$.

time	L_2	L_∞
1.00	0.000000	0.000000
1.75	0.000147	0.000125
2.50	0.000117	0.000095
3.25	0.000100	0.000082

Table 7.3

Problem (a). Error norms
 $\nu = 0.05$, $\Delta x = 0.03$, $\Delta t = 0.05$.

time	L_2	L_∞
1.00	0.000000	0.000000
1.75	0.001136	0.002705
2.50	0.001010	0.001751
3.25	0.000912	0.001281

Table 7.4

Problem (a). Error norms
 $\nu = 0.005$, $\Delta x = 0.012$, $\Delta t = 0.05$.

time	L_2	L_∞
1.00	0.000000	0.000001
1.75	0.000346	0.000843
2.50	0.000232	0.000578
3.25	0.000185	0.000450

Table 7.5

Problem (a). Error norms
 $\nu = 0.001$, $\Delta x = 0.005$, $\Delta t = 0.025$.

time	L_2	L_∞
1.00	0.000000	0.000000
1.75	0.001028	0.007245
2.50	0.000411	0.002439
3.25	0.000214	0.001223

Table 7.6

Problem(a). Error norms at time
 $t = 3.25$ various values of ν and L .

ν	$x_{max} = L$	Δx	Δt	L_2	L_∞
0.5	8	0.08	0.05	0.0001	0.00008
0.05	3	0.03	0.05	0.0009	0.0013
0.05	8	0.16	0.1	0.0008	0.0009
0.005	1.2	0.012	0.05	0.0002	0.0005
0.001	1.0	0.005	0.025	0.0002	0.0012

Table 7.7

Problem (a). Analytic and numerical solutions
 $\nu = 0.5, \Delta t = 0.05, \Delta x = 0.08$.

t	1.0	1.0	1.75	1.75	2.5	2.5	3.25	3.25
x	exact	numeric	exact	numeric	exact	numeric	exact	numeric
0.00	0.0000	0.0000	0.0000	0.0000	0.0000	0.0000	0.0000	0.0000
0.80	0.3611	0.3611	0.1903	0.1902	0.1237	0.1237	0.0893	0.0893
1.60	0.3833	0.3833	0.2669	0.2668	0.1923	0.1922	0.1466	0.1465
2.40	0.1435	0.1435	0.1945	0.1945	0.1773	0.1773	0.1520	0.1519
3.20	0.0215	0.0215	0.0803	0.0804	0.1083	0.1084	0.1133	0.1133
4.00	0.0015	0.0015	0.0201	0.0201	0.0454	0.0454	0.0626	0.0626
4.80	0.0001	0.0001	0.0032	0.0032	0.0136	0.0136	0.0263	0.0263
5.60			0.0004	0.0003	0.0030	0.0030	0.0087	0.0086
6.40					0.0005	0.0005	0.0023	0.0023
7.20							0.0005	0.0005

Table 7.8

Problem(a). Analytic and numerical solutions

$$\nu = 0.05, \Delta t = 0.05, \Delta x = 0.03.$$

t	1.0	1.0	1.75	1.75	2.5	2.5	3.25	3.25
x	exact	numeric	exact	numeric	exact	numeric	exact	numeric
0.00	0.0000	0.0000	0.0000	0.0000	0.0000	0.0000	0.0000	0.0000
0.30	0.2070	0.2070	0.1150	0.1150	0.0778	0.0778	0.0579	0.0579
0.60	0.2195	0.2195	0.1664	0.1664	0.1243	0.1243	0.0972	0.0972
0.90	0.0516	0.0516	0.1064	0.1064	0.1095	0.1094	0.0990	0.0990
1.20	0.0031	0.0031	0.0283	0.0283	0.0529	0.0530	0.0644	0.0644
1.50	0.0001	0.0001	0.0036	0.0036	0.0144	0.0144	0.0264	0.0265
1.80	0.0000	0.0000	0.0003	0.0003	0.0024	0.0024	0.0072	0.0072
2.10					0.0003	0.0003	0.0014	0.0014
2.40							0.0002	0.0002

Table 7.9

Problem(a). Analytic and numerical solutions

$$\nu = 0.005, \Delta t = 0.05, \Delta x = 0.012.$$

t	1.0	1.0	1.75	1.75	2.5	2.5	3.25	3.25
x	exact	numeric	exact	numeric	exact	numeric	exact	numeric
0.00	0.0000	0.0000	0.0000	0.0000	0.0000	0.0000	0.0000	0.0000
0.12	0.1200	0.1200	0.0686	0.0686	0.0480	0.0480	0.0369	0.0369
0.24	0.2400	0.2400	0.1371	0.1371	0.0960	0.0960	0.0738	0.0738
0.36	0.3591	0.3591	0.2057	0.2057	0.1440	0.1440	0.1108	0.1108
0.48	0.3490	0.3490	0.2733	0.2734	0.1919	0.1919	0.1477	0.1477
0.60	0.0024	0.0024	0.2996	0.3004	0.2381	0.2382	0.1843	0.1843
0.72			0.0287	0.0280	0.2425	0.2428	0.2173	0.2174
0.84			0.0002	0.0002	0.0376	0.0373	0.1917	0.1918
0.96					0.0006	0.0006	0.0277	0.0275
1.08							0.0008	0.0008

Table 7.10
 Problem (a). Analytic and numerical solutions
 $\nu = 0.001, \Delta t = 0.025, \Delta x = 0.005.$

t	1.0	1.0	1.75	1.75	2.5	2.5	3.25	3.25
x	exact	numeric	exact	numeric	exact	numeric	exact	numeric
0.0	0.0000	0.0000	0.0000	0.0000	0.0000	0.0000	0.0000	0.0000
0.1	0.1000	0.1000	0.0571	0.0571	0.0400	0.0400	0.0308	0.0308
0.2	0.2000	0.2000	0.1143	0.1143	0.0800	0.0800	0.0615	0.0615
0.3	0.3000	0.3000	0.1714	0.1714	0.1200	0.1200	0.0923	0.0923
0.4	0.4000	0.4000	0.2286	0.2286	0.1600	0.1600	0.1231	0.1231
0.5	0.2500	0.2500	0.2857	0.2857	0.2000	0.2000	0.1538	0.1538
0.6	0.0000	0.0000	0.3429	0.3429	0.2400	0.2400	0.1846	0.1846
0.7			0.0002	0.0001	0.2800	0.2800	0.2154	0.2154
0.8					0.0396	0.0377	0.2462	0.2462
0.9							0.1113	0.1103
1.0							0.0000	0.0000

A second set of simulations using this initial condition with various values of ν have been run up to time $t = 3.25$ and the error norms given in Table (7.6). The length of the region L is dictated by the spread of the solution.

In Figures (7.2) to (7.5) we compare the numerical solution for $\nu = 0.5, 0.05, 0.005, 0.001$, shown by continuous curves, with the analytic solutions represented by circular points. In all cases the agreement is very close and compares well with that obtained by Nguyen and Reynen [83]; see their Figures 1 and 2. To enable a more quantitative assessment to be made the numerical and analytic solutions are compared at various points and times in Tables (7.7) to (7.10). These show that, in general, the largest error is observed on the steeper downward parts of the curve, particularly at later times.

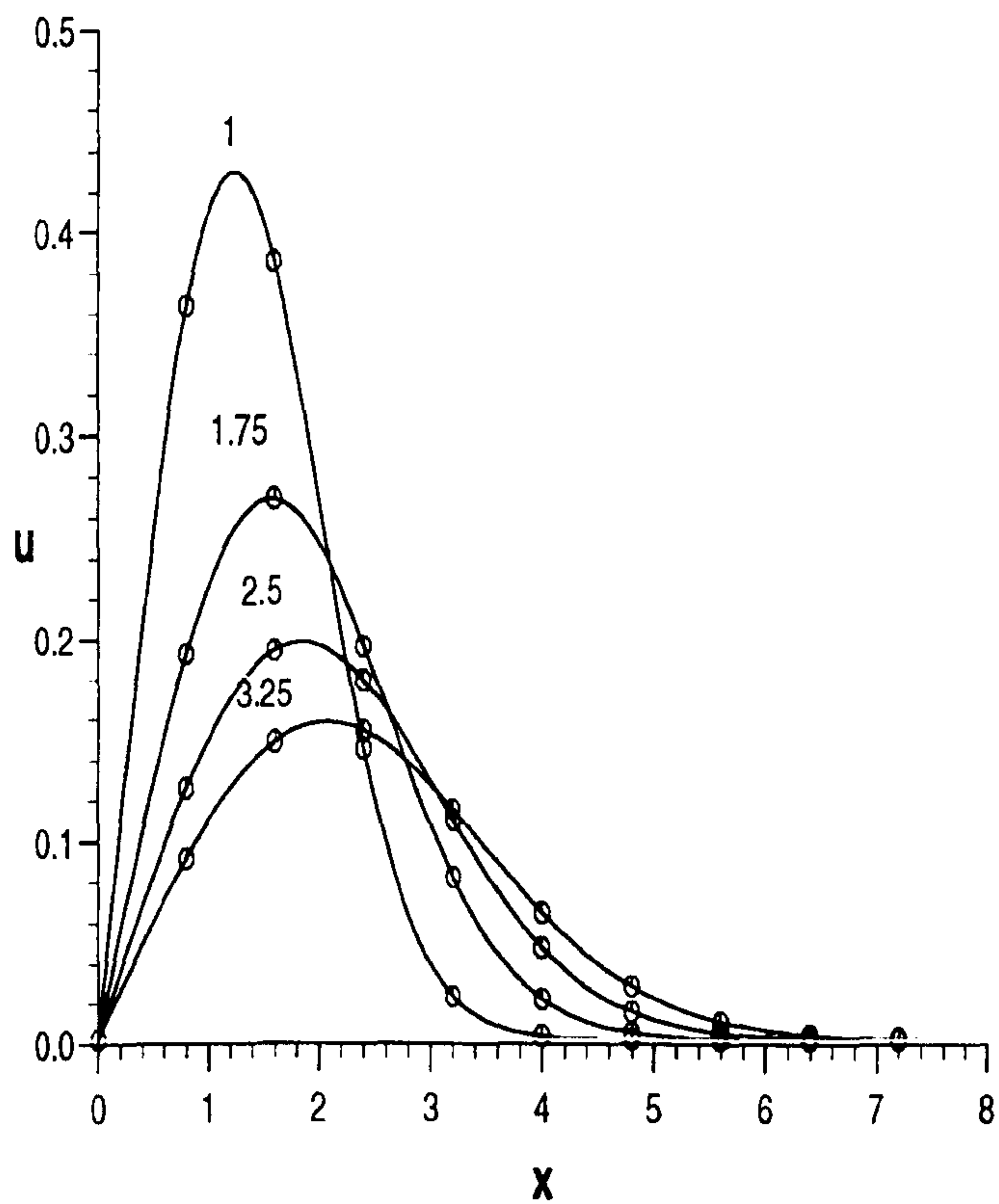


Figure 7.2 Problem (a). Numerical solutions for $\nu = 0.5$, $\Delta x = 0.08$, $\Delta t = 0.05$, shown by continuous curves for times $t = 1, 1.75, 2.5, 3.25$. Analytic solutions are shown by circular points.

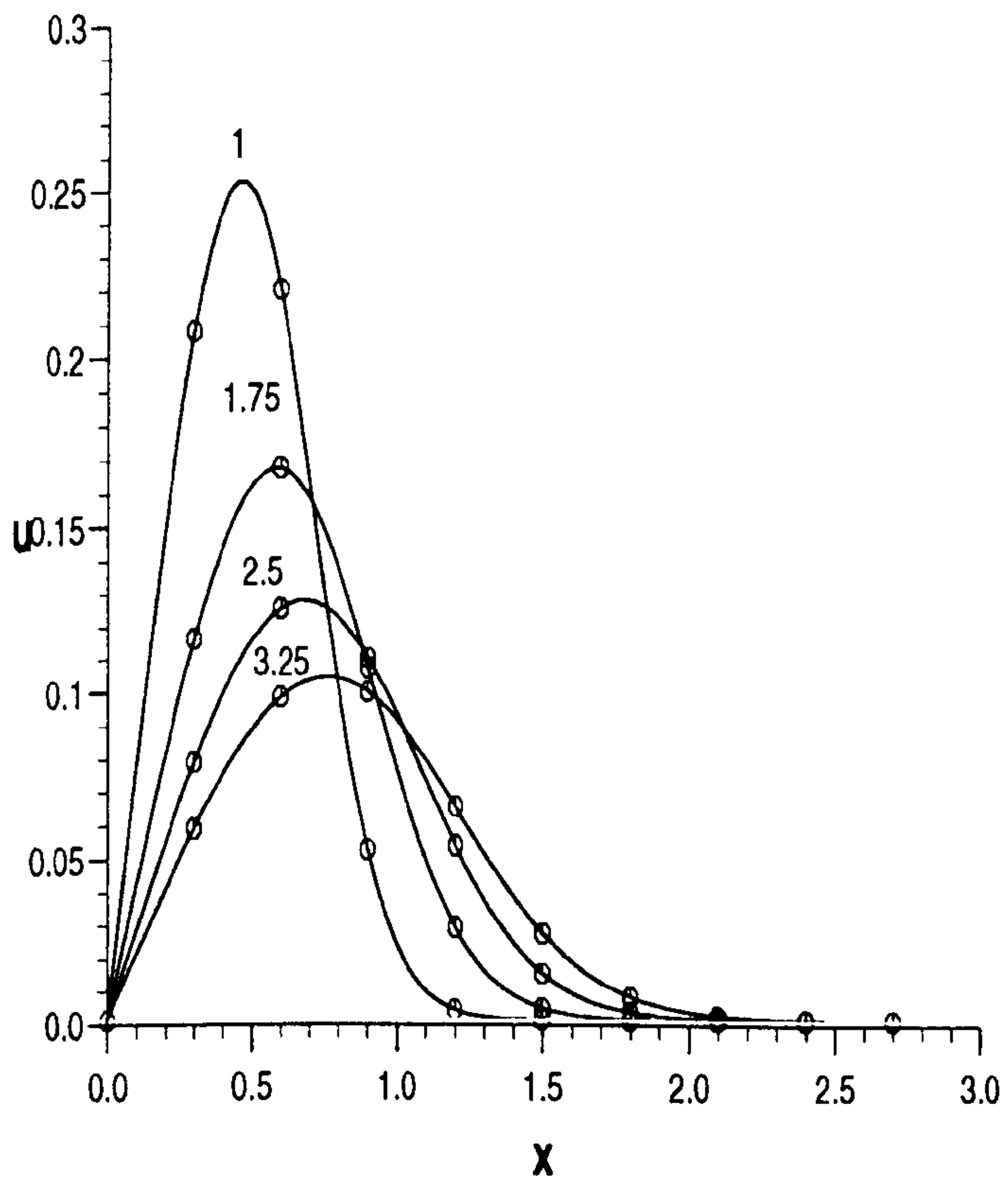


Figure 7.3 Problem (a). Numerical solutions for $\nu = 0.05$, $\Delta x = 0.03$, $\Delta t = 0.05$, shown by continuous curves for times $t = 1, 1.75, 2.5, 3.25$. Analytic solutions are shown by circular points.

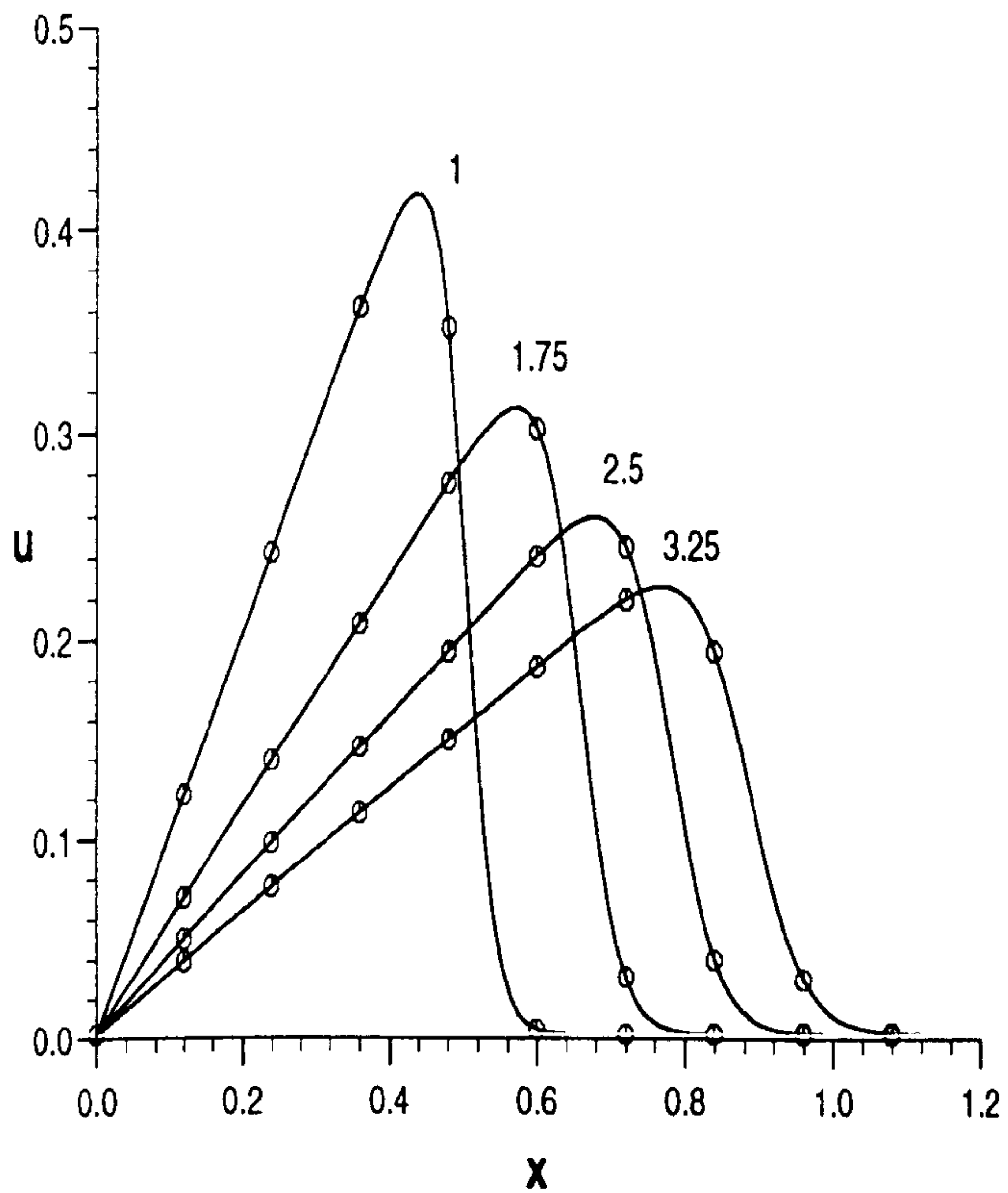


Figure 7.4 Problem (a). Numerical solutions for $\nu = 0.005$, $\Delta x = 0.012$, $\Delta t = 0.05$, shown by continuous curves for times $t = 1, 1.75, 2.5, 3.25$. Analytic solutions shown by circular points.

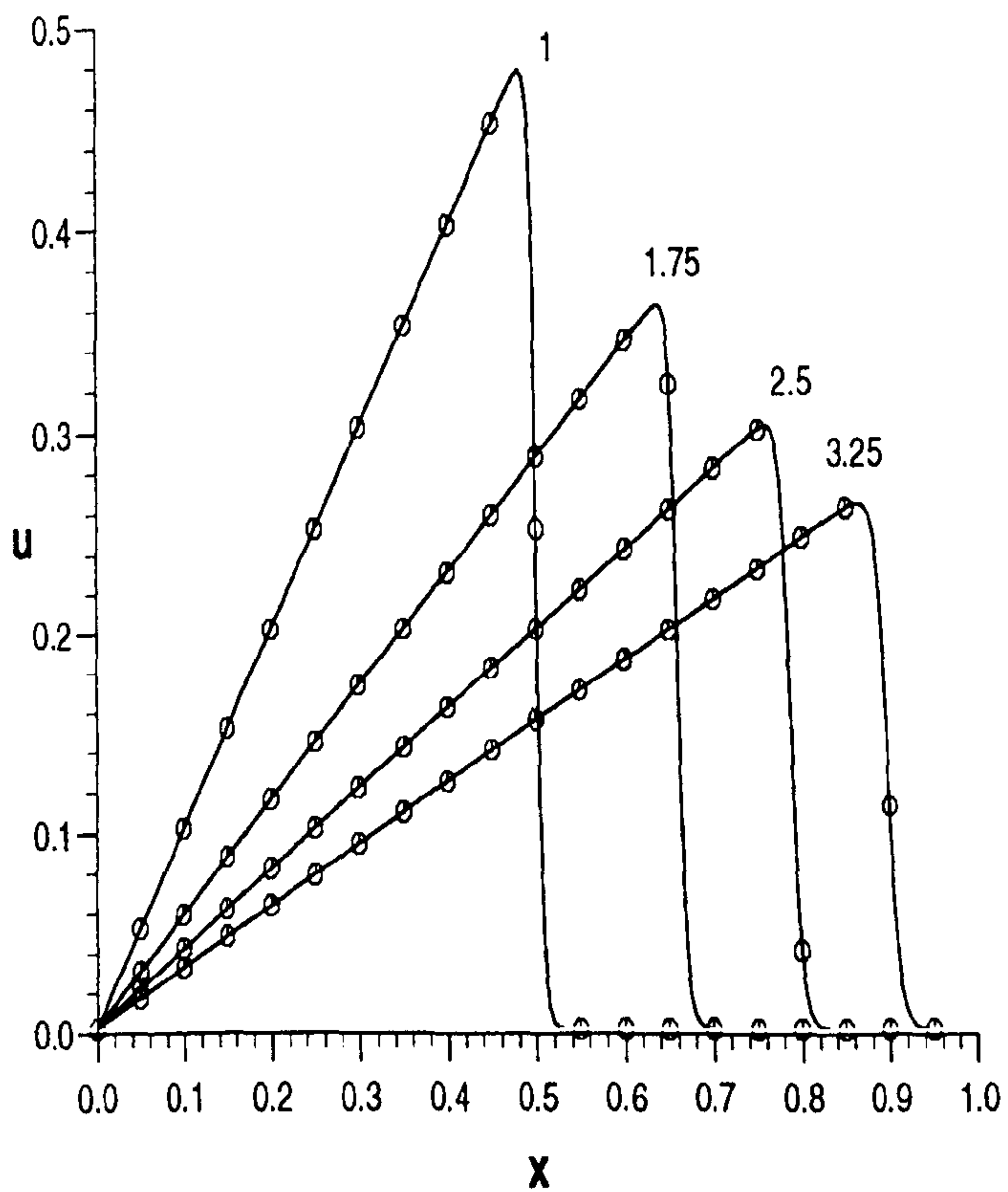


Figure 7.5 Problem (a). Numerical solutions for $\nu = 0.001$, $\Delta x = 0.005$, $\Delta t = 0.025$, shown by continuous curves for times $t = 1, 1.75, 2.5, 3.25$.

Analytic solutions shown by circular points.

(b) Sine curve initial condition

$$U(x, 0) = \sin(\pi x), \quad (7.18)$$

over $0 < x < 1$. This problem has been studied widely [50, 99]. Simulations for ν with values $\nu = 1.0, 0.1, 0.01$ are undertaken and the results compared with the detailed solution given by Kakuda and Tosaka [67]. The results of our computations are shown in Figures (7.6), (7.7) and (7.8) as continuous lines and are compared with analytic values (\circ) taken from [67]. Agreement is good. In Figure (7.9) numerical solutions are shown at times $t = 0.0, 0.2, 0.4, 0.6, 0.8, 1.0$ by continuous curves.

Quantative comparisons can be made using the point values of the solutions given in Tables from (7.11) to (7.13).

Table 7.11
 Problem(b). Analytic and numerical solutions
 for $\nu = 1, \Delta x = 0.02, \Delta t = 0.01$.

t	0.02	0.02	0.04	0.04	0.10	0.10	0.22	0.22
x	numeric	exact	numeric	exact	numeric	exact	numeric	exact
0.1	0.2435	0.2437	0.1968	0.1970	0.1092	0.1095	0.0346	0.0345
0.2	0.4659	0.4662	0.3773	0.3776	0.2090	0.2098	0.0661	0.0659
0.4	0.7695	0.7699	0.6275	0.6283	0.3464	0.3479	0.1087	0.1075
0.6	0.7898	0.7904	0.6492	0.6514	0.3570	0.3591	0.1120	0.1087
0.8	0.4946	0.4994	0.4101	0.4151	0.2270	0.2278	0.0748	0.0678
0.9	0.2554	0.2643	0.2129	0.2202	0.1214	0.1207	0.0455	0.0357

Table 7.12
 Problem (b). Analytic and numerical solutions
 for $\nu = 0.1$, $\Delta x = 0.01$, $\Delta t = 0.05$.

t	0.05	0.05	0.25	0.25	0.75	0.75	1.50	1.50
x	numeric	exact	numeric	exact	numeric	exact	numeric	exact
0.1	0.2583	0.2587	0.1601	0.1603	0.0834	0.0834	0.0437	0.0438
0.2	0.4996	0.5001	0.3159	0.3162	0.1654	0.1655	0.0856	0.0858
0.4	0.8601	0.8599	0.5938	0.5941	0.3170	0.3174	0.1552	0.1556
0.6	0.9380	0.9374	0.7654	0.7653	0.4180	0.4192	0.1829	0.1833
0.8	0.6283	0.6290	0.6512	0.6537	0.3552	0.3590	0.1333	0.1325
0.9	0.3364	0.3394	0.3849	0.3926	0.2089	0.2131	0.0755	0.0732

For $\nu = 1.0$ the solution curves remain almost symmetric about $x = 0.5$ as the function decays away. As ν is decreased in value the solution curves tend to skew more and more to the right as time proceeds.

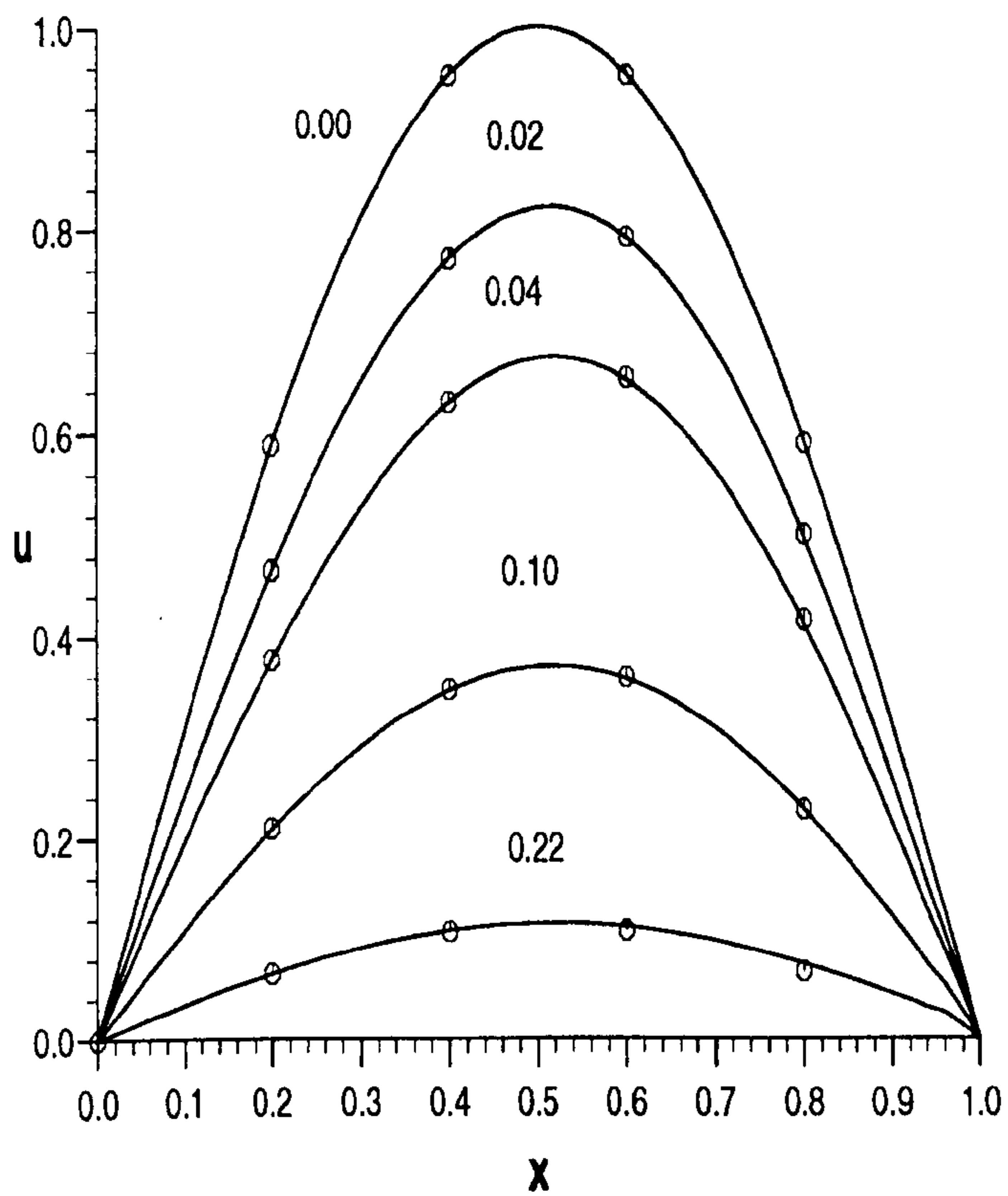


Figure 7.6 Problem (b). Numerical solutions for $\nu = 1.0$, $\Delta x = 0.02$, $\Delta t = 0.01$, shown by continuous curves for various labelled times. Analytic solutions are shown by circular points [67].

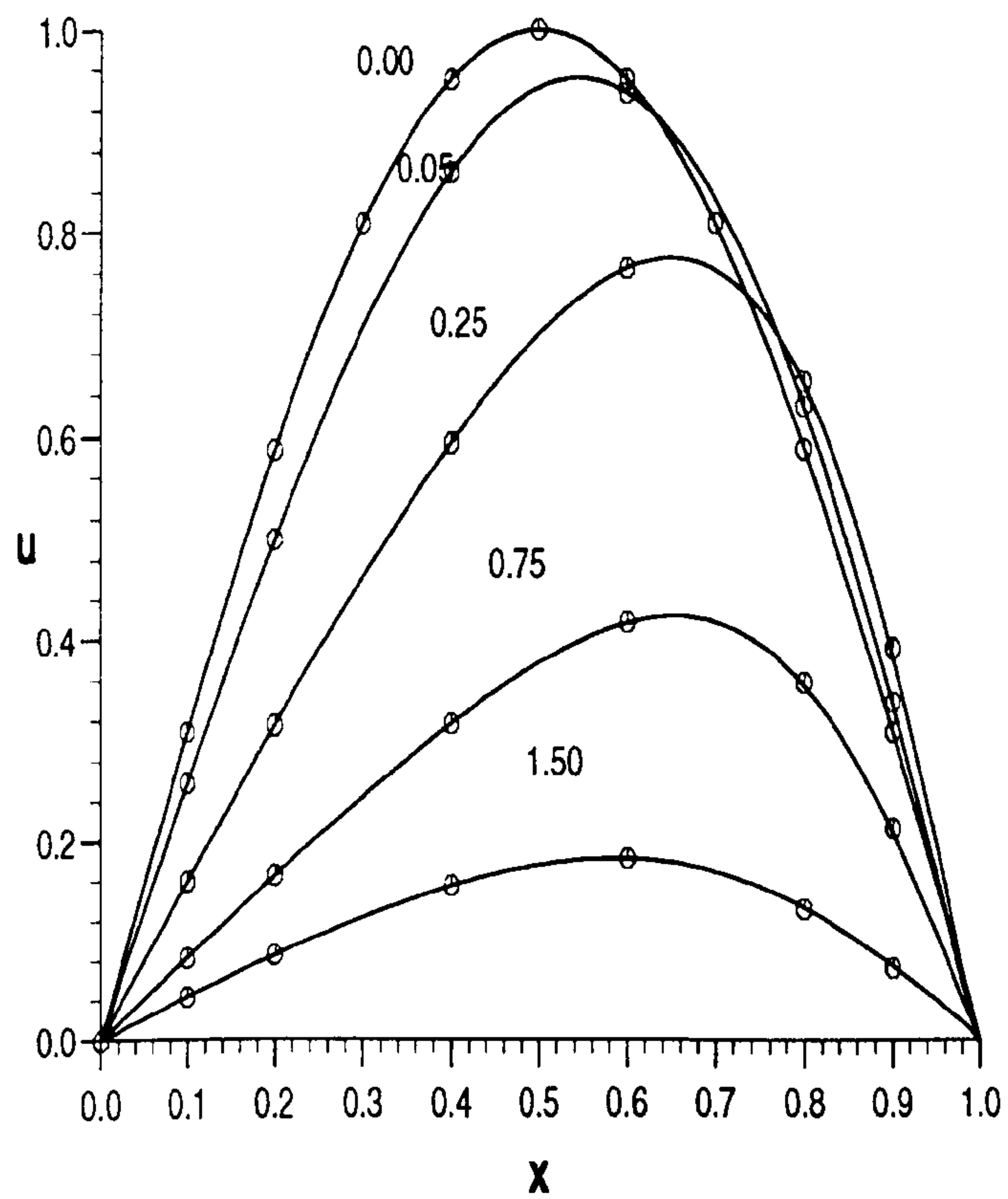


Figure 7.7 Problem (b). Numerical solutions for $\nu = 0.1$, $\Delta x = 0.01$, $\Delta t = 0.05$, shown by continuous curves for various labelled times. Analytic solutions are shown by circular points [67].

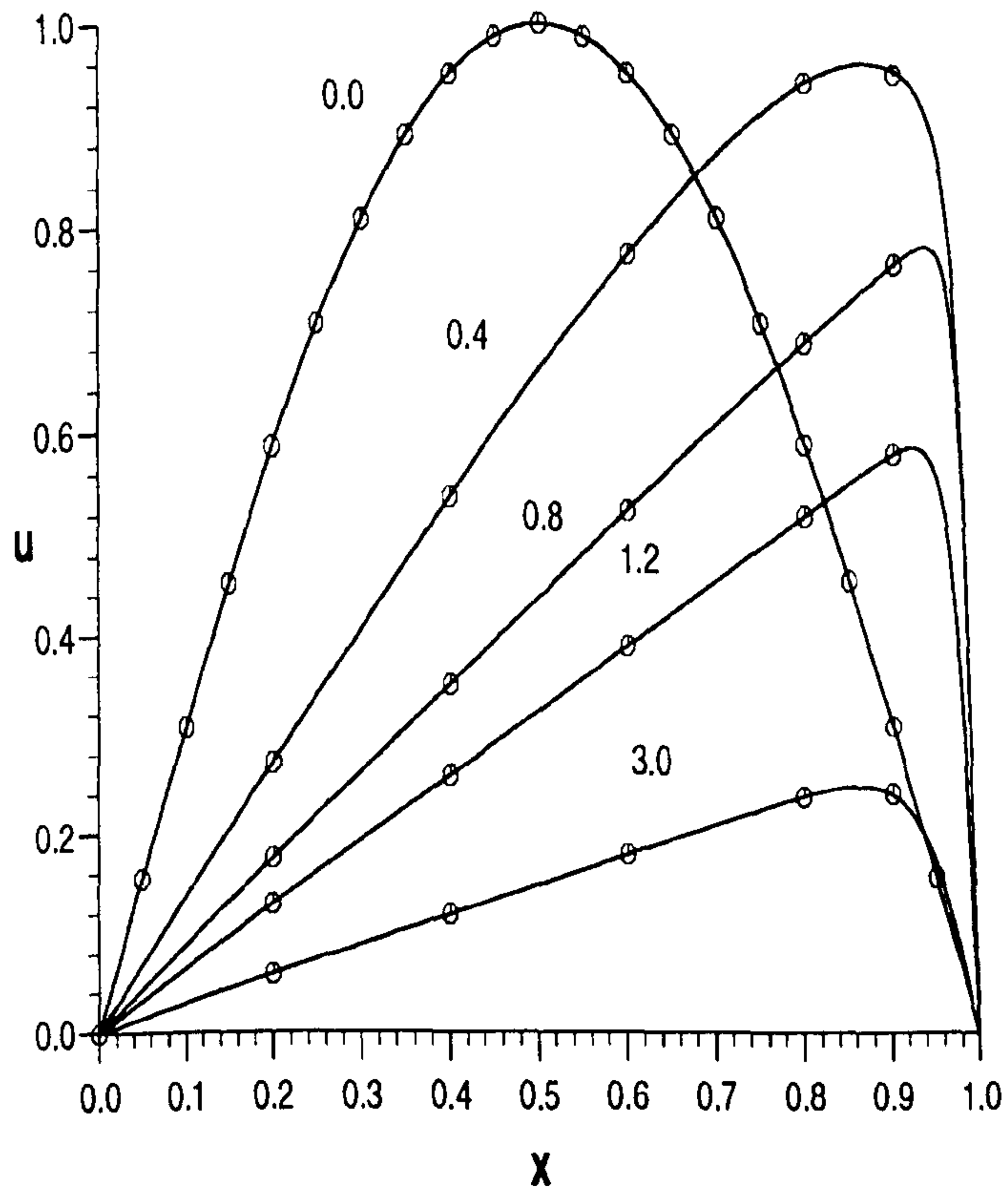


Figure 7.8 Problem (b). Numerical solutions for $\nu = 0.01$, $\Delta x = 0.005$, $\Delta t = 0.005$, shown by continuous curves for the labelled times. Analytic solutions are shown by circular points [67].

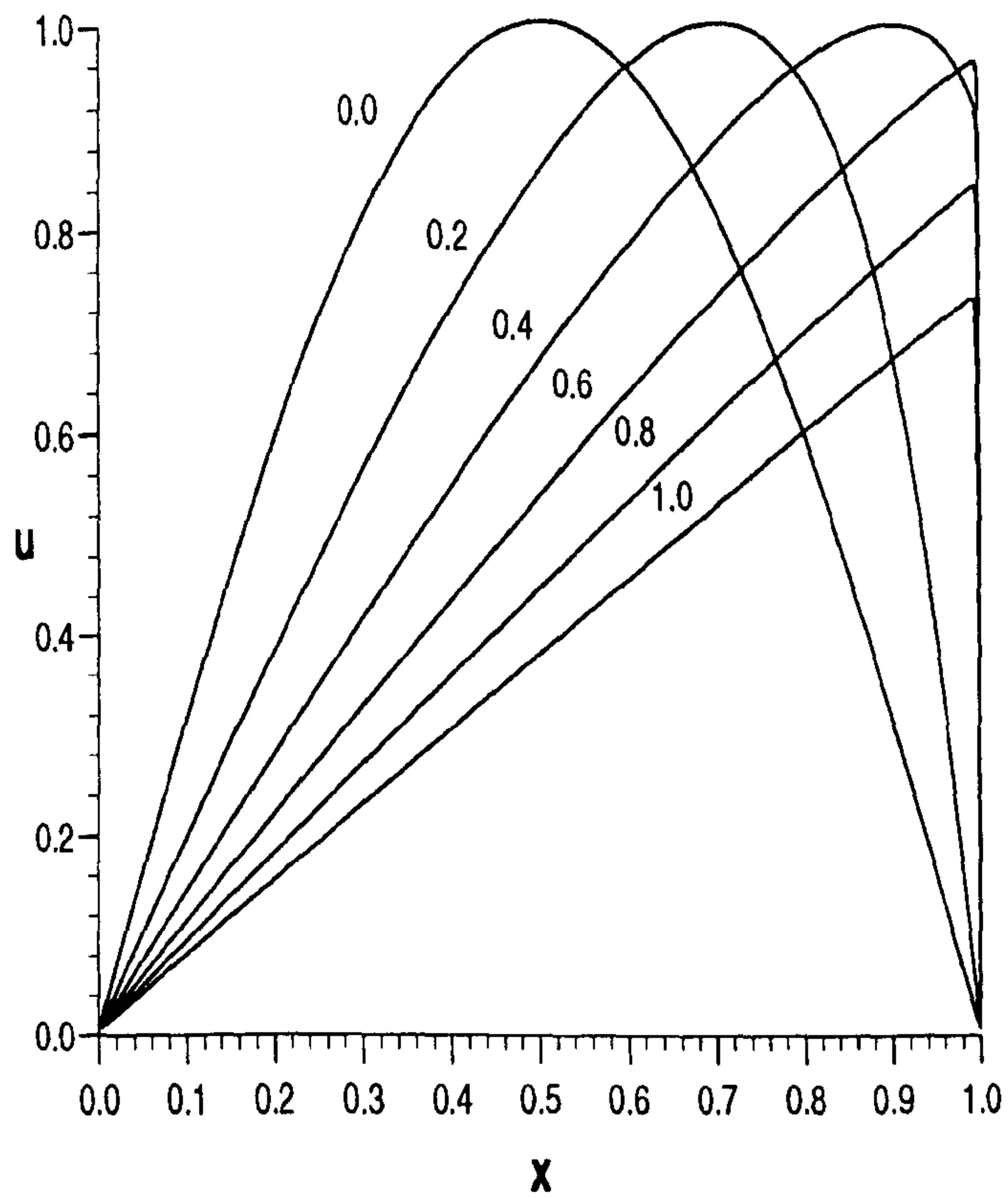


Figure 7.9 Problem (b). Numerical solutions for $\nu = 0.001$, $\Delta x = 0.001$, $\Delta t = 0.001$, shown by continuous curves for the labelled times.

Table 7.13

Problem (b). Analytic and numerical solutions
for $\nu = 0.01$, $\Delta x = 0.005$, $\Delta t = 0.005$.

t	0.4	0.4	0.8	0.8	1.2	1.2	3.0	3.0
x	numeric	exact	numeric	exact	numeric	exact	numeric	exact
0.2	0.2745	0.2745	0.1774	0.1774	0.1309	0.1309	0.601	0.0601
0.4	0.5379	0.5379	0.3528	0.3528	0.2613	0.2613	0.1202	0.1202
0.6	0.7735	0.7735	0.5240	0.5240	0.3904	0.3904	0.1802	0.1802
0.8	0.9411	0.9410	0.6871	0.6871	0.5175	0.5175	0.2386	0.2386
0.9	0.9525	0.9489	0.7629	0.7630	0.5775	0.5778	0.2402	0.2416

For $\nu = 0.01$ a very steep front develops for times greater than 0.4. As time increases beyond 1.2 the front becomes progressively less steep as the function decays away. When $\nu = 0.001$ the steep front again develops for times in excess of 0.4, and does not become less steep as the simulation proceeds.

Errors increase slowly during the simulations. By the end of each experiment we have, comparing with earlier work,

(i) for $\nu = 1$, at time $t = 0.22$, $L_\infty = 0.0098$, $L_\infty = 0.0001$ [50] and $L_\infty = 0.0053$ [67].

(ii) for $\nu = 0.1$, at time $t = 1.5$, $L_\infty = 0.0023$, $L_\infty = 0.00051$ [50] and $L_\infty = 0.0013$ [67].

(iii) for $\nu = 0.01$, at time $t = 3$, $L_\infty = 0.0014$, $L_\infty = 0.0017$ [50] and $L_\infty = 0.0039$ [67].

Solutions obtained using the present Petrov-Galerkin algorithm show similar accuracy to those obtained by Kakuda and Tosaka [67] while the least-squares approach [50] produces higher accuracy for the larger values of ν .

(c) As a model of flow through a shock wave we use the initial condition [5, 29, 60]

$$U(x, t) = \frac{1}{1 + \exp(\eta)} [\alpha + \mu + (\mu - \alpha) \exp(\eta)], \quad (7.19)$$

where $\eta = \frac{\alpha}{\nu}(x - \mu t - \beta)$. The initial condition is obtained by evaluating Equation (7.19) at $t = 0$. For this function $U \rightarrow 1$ as $x \rightarrow -\infty$ and $U \rightarrow 0.2$ as $x \rightarrow +\infty$. Use boundary conditions $U(-2, t) = 1$, and $U(5, t) = 0.2$. The parameters have the following values, $\alpha = 0.4$, $\beta = 0.125$, $\mu = 0.6$ and $\nu = 0.1, 0.01$.

This is another very useful problem to study since the exact analytic solution is known. The solution curves are given in Figure (7.10), for $\nu = 0.1$, and (7.11) for $\nu = 0.01$. The analytic solution is shown by circular points. For both values of ν the accuracy of the numerical solution is very good; the fronts move to the right with constant speed and retain their original profile. With the prescribed parameters the shock wave profile remains smooth and does not develop any non-physical wiggles; the errors are very small. Over the region $-2 \leq x \leq 4$ the maximum error is measured as $L_\infty = 0.00005$ for $\nu = 0.1$ and $L_\infty = 0.00066$ for $\nu = 0.01$.

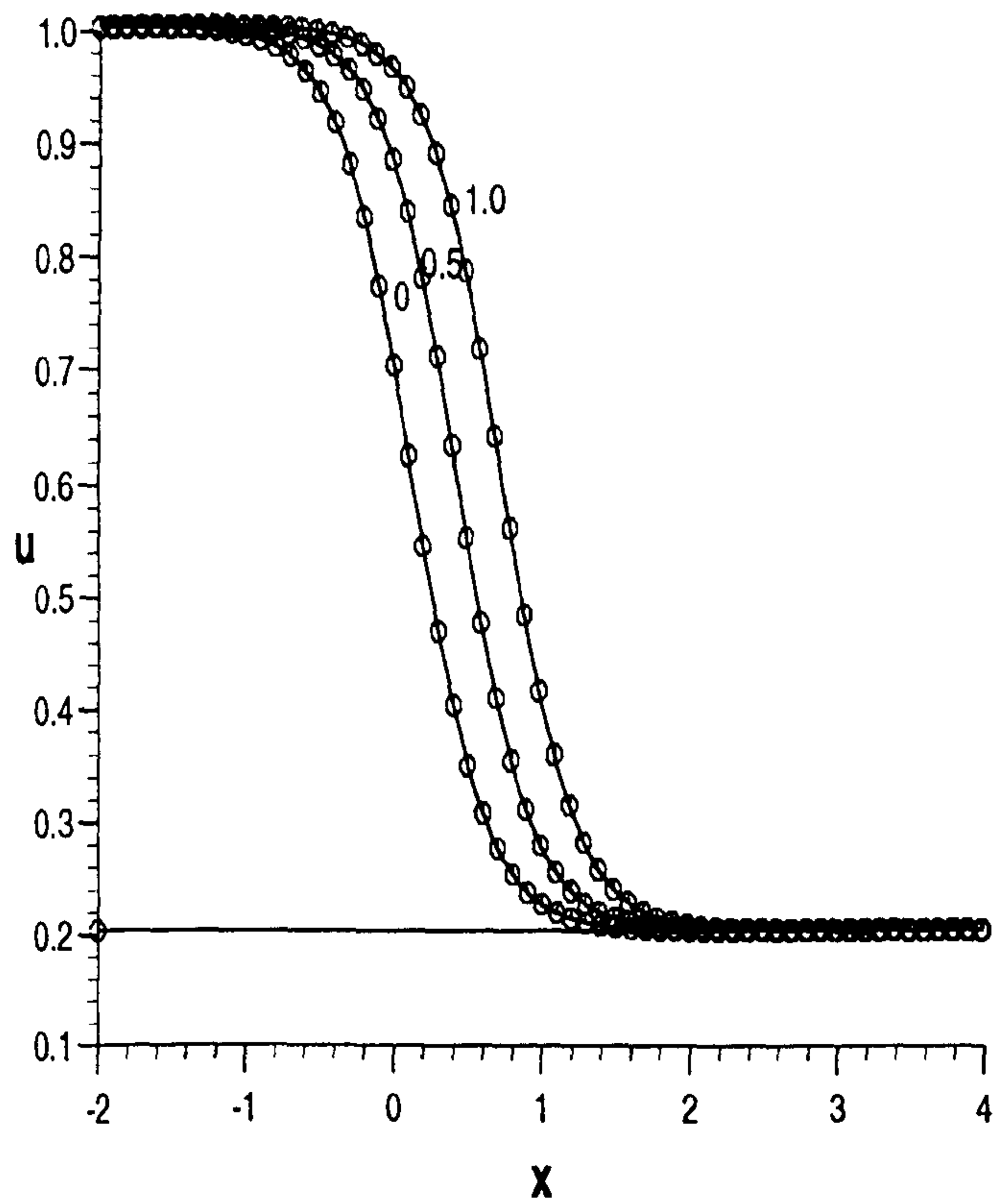


Figure 7.10 Problem(c). Numerical solutions for $\nu = 0.1$, $\Delta x = 0.01$, $\Delta t = 0.005$, shown at times $t = 0.0, 0.5, 1$ by continuous curves, and the analytic solution by circular points.

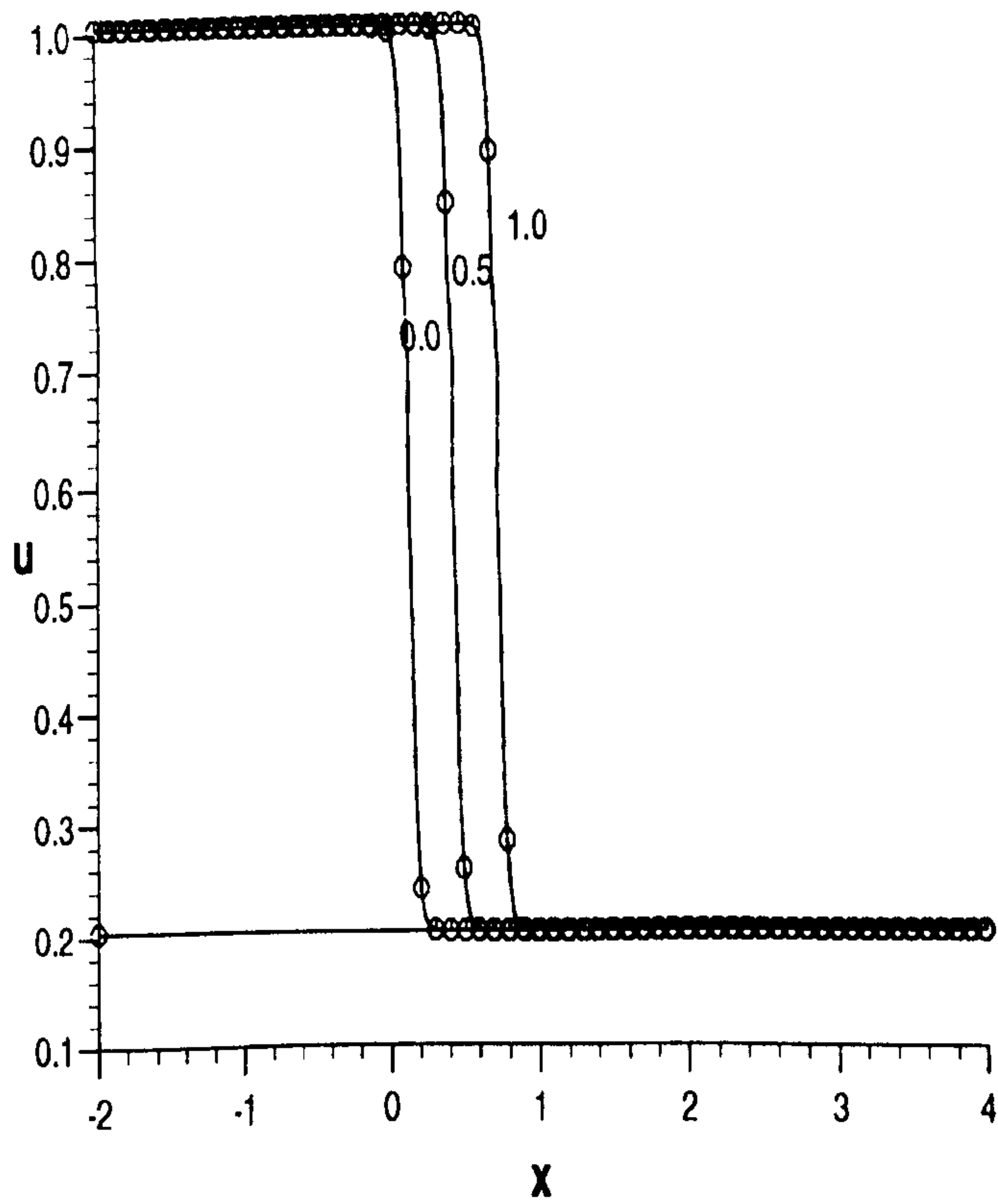


Figure 7.11 Problem(c). Numerical solutions for $\nu = 0.01$, $\Delta x = 0.01$, $\Delta t = 0.005$, shown at times $t = 0.0, 0.5, 1$ by continuous curves, and the analytic solution by circular points.

(d) As a second model of flow through a shock wave we use the initial condition [79, 99]

$$U(x, 0) = \begin{cases} 1, & -2 < x < 5, \\ (6 - x), & 5 \leq x < 6, \\ 0, & 6 \leq x \leq 16. \end{cases}$$

The numerical solutions at times $t = 0, 1, 2, 3, 4$, for $\nu = 1.0, 0.1, 0.01$ are given in Figures (7.12) to (7.14).

For $\nu = 1$ the viscosity rapidly smooths out the initial discontinuity and the front becomes less and less steep with time. With $\nu = 0.1$ the transition zones become smoothed out while the front remains at the initial steep angle and moves to the right with a constant speed of 0.5. The wave fronts shown here reflect those obtained by Varoglu and Finn [99], see their Figure 10, rather than the irregularly spaced fronts obtained by Mittal and Singhal [79], see their Figure 4. When $\nu = 0.01$ as the simulation proceeds the wave front steepens becoming practically vertical by time $t = 1$. It moves to the right with a uniform speed 0.5. This numerical solution agrees almost exactly with the analytic solution obtained when $\nu = 0$ and $t \geq 1$.

$$U(x, t) = \begin{cases} 1, & x < 5.5 + 0.5t, \\ 0, & x > 5.5 + 0.5t. \end{cases}$$

The major differences in the solution graphs arise in the transition zones where the curves for the numerical solution are smoothed out by the small viscosity. With the space and time steps chosen the wave profiles remain smooth throughout the simulations.

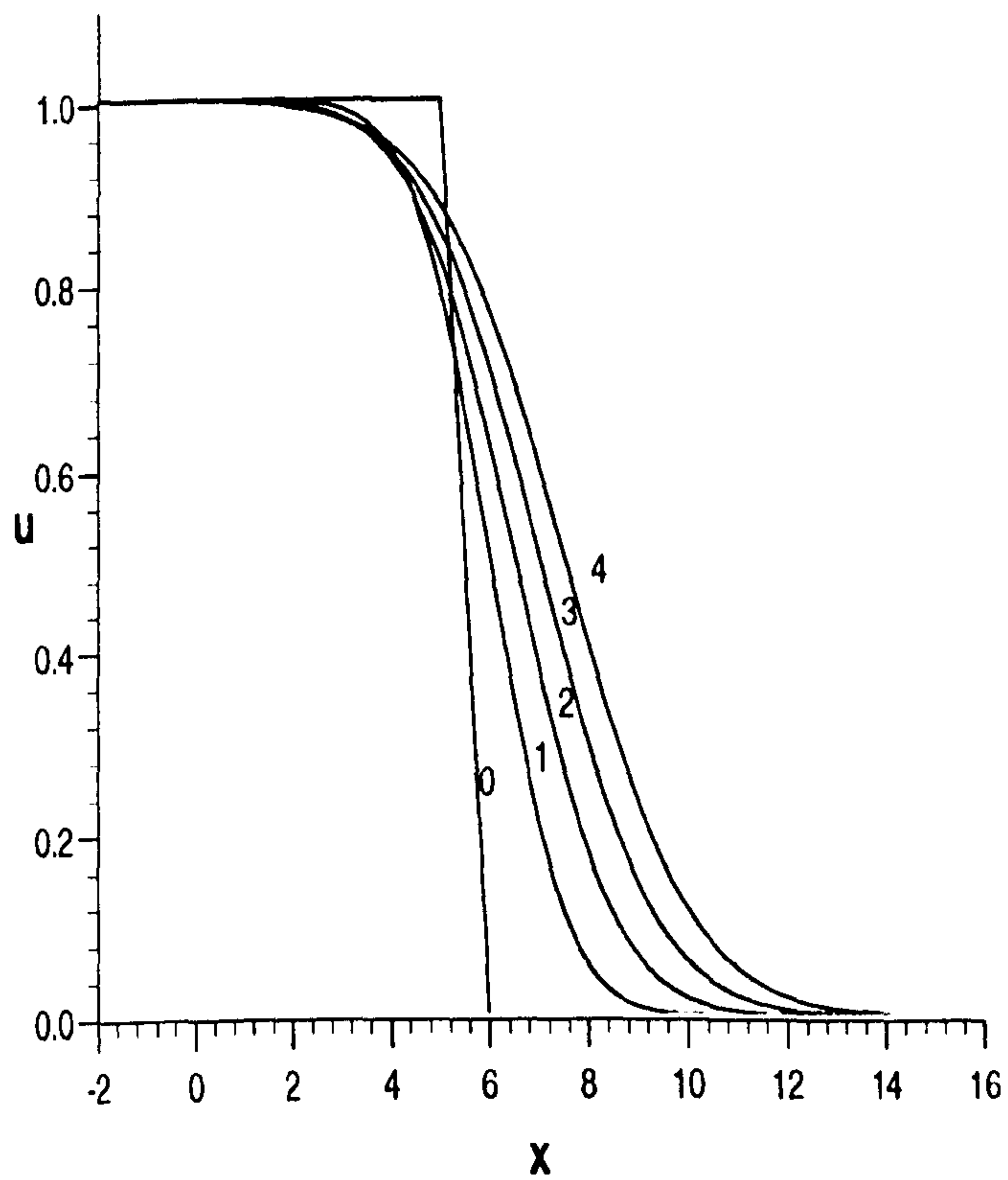


Figure 7.12 Problem (d). Numerical solutions for $\nu = 1$, $\Delta x = 0.1$, $\Delta t = 0.04$, shown at times $t = 0, 1, 2, 3, 4$ by continuous curves.

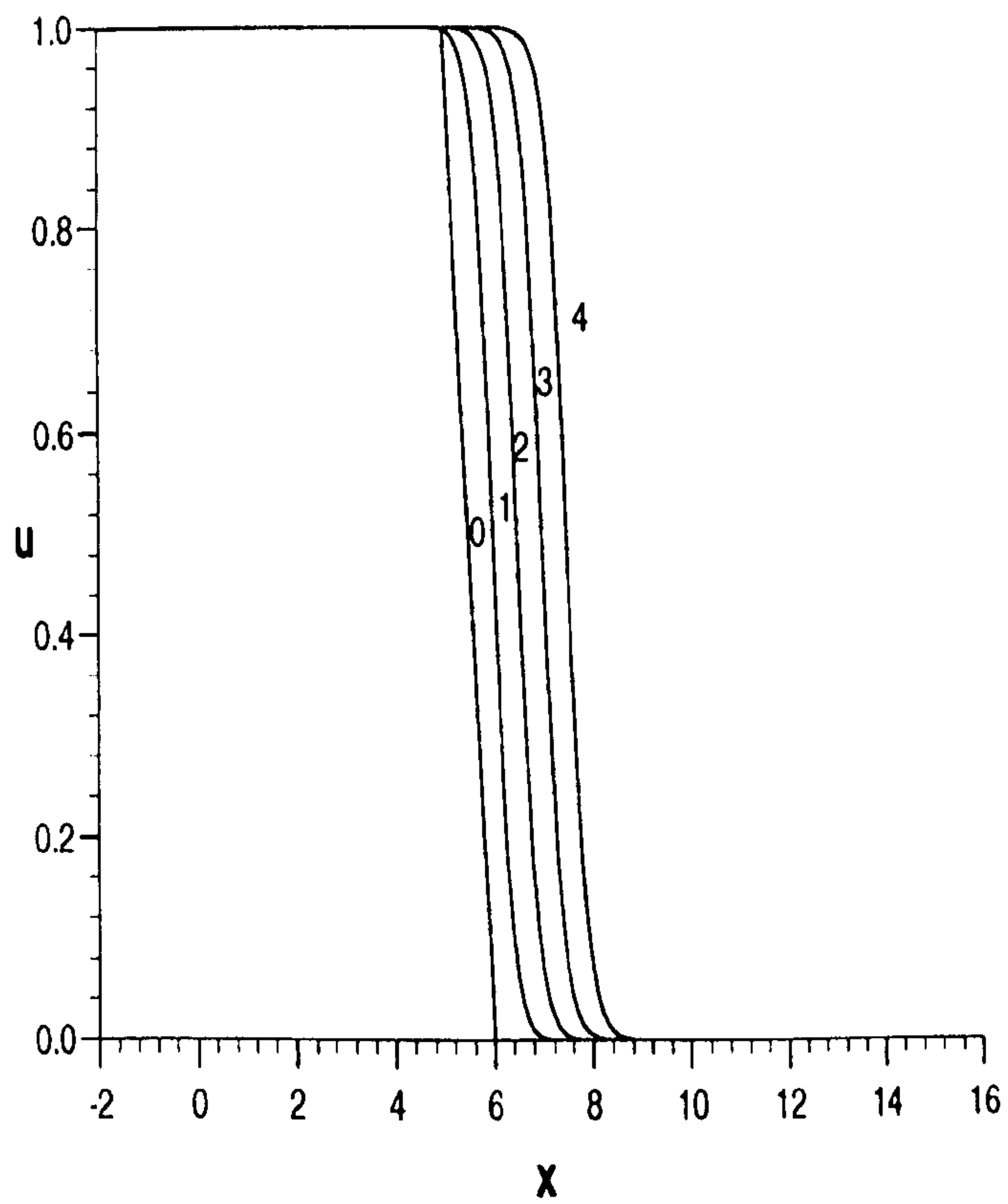


Figure 7.13 Problem (d). Numerical solutions for $\nu = 0.1$, $\Delta x = 0.1$, $\Delta t = 0.04$, shown at times $t = 0, 1, 2, 3, 4$, by continuous curves.

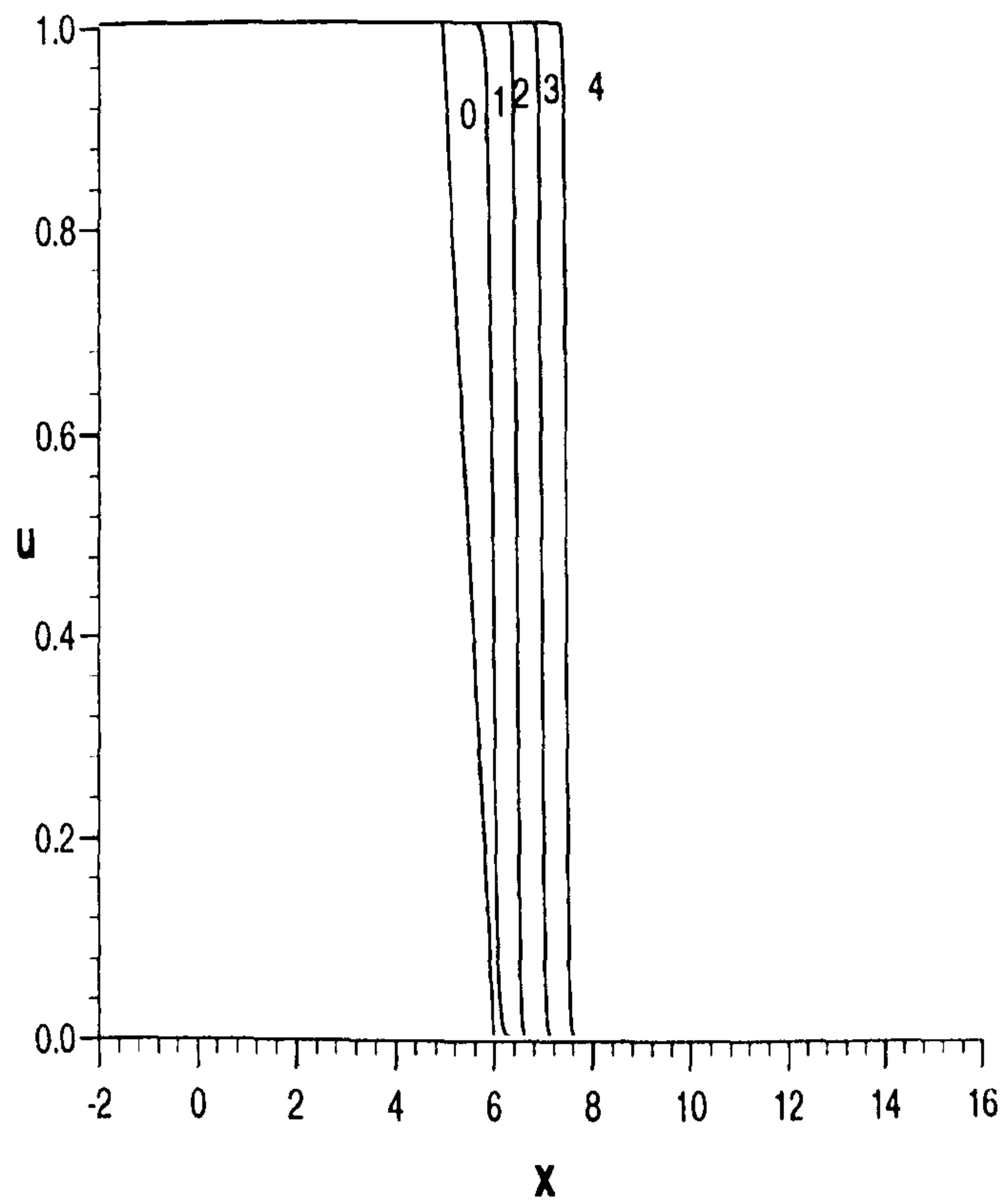


Figure 7.14 Problem (d). Numerical solutions for $\nu = 0.01$, $\Delta x = 0.01$, $\Delta t = 0.01$, shown at times $t = 0, 1, 2, 3, 4$, by continuous curves.

7.5 Discussion

The Petrov-Galerkin method using quadratic B-spline finite elements leads to a quasi-linear numerical algorithm the solution of which is direct so no iterations are necessary. The accuracy of the method, which faithfully models standard solutions of Burgers' equation, is even higher than achieved by Ali et al using cubic elements [5]. In modelling flow through a shock wave no spurious non-physical wiggles are observed on the solution profile. This method is a useful addition to those available for the solution of transient initial value problems governed by the non-linear Burgers' equation.

Chapter 8

A Least-Squares Quadratic B-Spline Finite Element Scheme For The RLW Equation

8.1 Introduction

As an extension to the least squares method we have in this Chapter replaced the linear finite element used in the previous discussion by a quadratic B-spline element. The analysis is then somewhat complicated as will be seen in the following Section. This work is at an early stage and we will not complete it until much later this year.

8.2 The B-spline finite element solution

We solve the normalised RLW equation

$$U_t + U_x + cUU_x - \mu U_{xxt} = 0 \quad (8.1)$$

where c, μ are positive parameters and the subscripts x and t denote differentiation. Boundary conditions require $U \rightarrow 0$ as $|x| \rightarrow \infty$.

When applying the least squares approach and using space-time finite elements, we consider the Variational Principle [83, 84]

$$\delta \int_0^t \int_0^L [U_t + U_x + \epsilon U U_x - \mu U_{xxt}]^2 dx dt = 0, \quad (8.2)$$

A uniform spatial array of linear finite elements is set up $0 = x_0 < x_1 \dots < x_N = L$. A typical finite element of size $\Delta x = (x_{m+1} - x_m)$, Δt , mapped by local coordinates ξ , τ where $x = x_m + \xi \Delta x$, $0 \leq \xi \leq 1$, $t = \tau \Delta t$, $0 \leq \tau \leq 1$, makes, to integral (8.2), the contribution

$$\delta \int_0^1 \int_0^1 [U_\tau + \frac{\Delta t}{\Delta x} U_\xi + \frac{\epsilon \Delta t}{\Delta x} \hat{U} U_\xi - \frac{\mu}{\Delta x^2} U_{\xi\xi\tau}]^2 d\xi d\tau, \quad (8.3)$$

where to simplify the integral, \hat{U} is taken to be constant over an element. This leads to

$$\int_0^1 \int_0^1 [U_\tau + v U_\xi - b U_{\xi\xi\tau}] \delta [U_\tau + v U_\xi - b U_{\xi\xi\tau}] d\xi d\tau, \quad (8.4)$$

where

$$b = \frac{\mu}{\Delta x^2},$$

and

$$v = \frac{\Delta t}{\Delta x} (1 + \epsilon \hat{U}),$$

is taken as locally constant over each element. The variation of U over the element $[x_m, x_{m+1}]$ is given by

$$U^e = \sum_{j=m-1}^{m+1} Q_j (a_j + \tau \Delta a_j), \quad (8.5)$$

where Q_{m-1} , Q_m , Q_{m+1} are quadratic B-spline spatial basis functions. The a_{m-1} , a_m , a_{m+1} are nodeless parameters which are temporally linear and change by the increments Δa_{m-1} , Δa_m , Δa_{m+1} in time Δt . With the local coordinate system ξ defined above the basis functions have expressions [103]

$$\begin{aligned}
Q_{m-1} &= (1 - \xi)^2, \\
Q_m &= 1 + 2\xi - 2\xi^2, \\
Q_{m+1} &= \xi^2.
\end{aligned}$$

The nodal values at $x = x_m$ are $U_m = U(x_m)$ and $\theta_m = \frac{\partial U}{\partial x}(x_m) = \frac{1}{\Delta x} \frac{\partial U}{\partial \xi}(x_m) = \frac{1}{\Delta x} U'(x_m)$, where the prime denotes differentiation with respect to ξ , are given in terms of the parameters a_i by

$$U_m = a_{m-1} + a_m, \quad (8.6)$$

$$\begin{aligned}
\theta_m &= \frac{\partial U}{\partial x}(x_m) = \frac{1}{\Delta x} \frac{\partial U}{\partial \xi}(x_m) \\
&= \frac{1}{\Delta x} U'(x_m) = \frac{2}{\Delta x} (a_m - a_{m-1}).
\end{aligned} \quad (8.7)$$

The quadratic B-spline finite element description possesses the same nodal parameters U_m, U'_m as does the cubic hermite element and so has similar continuity properties.

Write the second term in the integrand of (8.4) as a weight function

$$\delta W = \sum_{j=m-1}^{m+1} W_j \Delta a_j = \delta[U_\tau + vU_\xi - bU_{\xi\xi\tau}]. \quad (8.8)$$

Using, from (8.5), the result that

$$\delta U^c = \sum_{j=m-1}^{m+1} Q_j \tau \Delta a_j, \quad (8.9)$$

in (8.8) we have

$$W_j = Q_j + \tau v Q'_j - b Q''_j. \quad (8.10)$$

Substituting into Equation (8.4) gives

$$\int_0^1 \int_0^1 [U_\tau + vU_\xi - bU_{\xi\xi\tau}] [Q_j + \tau v Q'_j - b Q''_j] d\xi d\tau, \quad (8.11)$$

which can be interpreted as a Petrov-Galerkin approach with weight function W_j , as well as a least squares formulation. Rearrange as

$$\int_0^1 \int_0^1 [(U_\tau - bU_{\xi\xi\tau})(Q_j + \tau v Q'_j - bQ''_j) + vU_\xi(Q_j + \tau v Q'_j - bQ''_j)] d\xi d\tau, \quad (8.12)$$

Now if we substitute for U using Equation (8.5), integrate with respect to τ and integrate by parts as required, we obtain an element's contribution in the form

$$\sum_{j=m-1}^{m+1} \Delta a_j \int_0^1 [Q_i Q_j + 2bQ'_i Q'_j + \frac{1}{3}v^2 Q'_i Q'_j + b^2 Q''_i Q''_j + \frac{v}{2}(Q_i Q'_j + Q'_i Q_j) - \frac{bv}{2}(Q'_i Q''_j + Q''_i Q'_j)] d\xi + \sum_{j=m-1}^{m+1} a_j \int_0^1 [vQ_i Q'_j + \frac{1}{2}v^2 Q'_i Q'_j - bvQ''_i Q'_j] d\xi.$$

In matrix notation this becomes

$$[A^e + 2bB^e + \frac{1}{3}v^2 B^e + b^2 C^e + \frac{v}{2}(D^e + D^{eT}) - \frac{bv}{2}(E^e + E^{eT})] \Delta \mathbf{a}^e + [vD^e + \frac{1}{2}v^2 B^e - bvE^e] \mathbf{a}^e,$$

where

$$\mathbf{a}^e = (a_{m-1}, a_m, a_{m+1})^T,$$

are the relevant nodal parameters. The element matrices are

$$A_{ij}^e = \int_0^1 Q_i Q_j d\xi,$$

$$B_{ij}^e = \int_0^1 Q'_i Q'_j d\xi,$$

$$C_{ij}^e = \int_0^1 Q''_i Q''_j d\xi,$$

$$D_{ij}^e = \int_0^1 Q_i Q'_j d\xi,$$

$$E_{ij}^e = \int_0^1 Q_i'' Q_j' d\xi,$$

where i, j take only the values $m-1$, m and $m+1$ for the element $[x_m, x_{m+1}]$. The matrices A^e, B^e, C^e, D^e and E^e are thus 3x3, and have the explicit forms

$$A^e = \frac{1}{30} \begin{bmatrix} 6 & 13 & 1 \\ 13 & 54 & 13 \\ 1 & 13 & 6 \end{bmatrix},$$

$$B^e = \frac{2}{3} \begin{bmatrix} 2 & -1 & -1 \\ -1 & 2 & -1 \\ -1 & -1 & 2 \end{bmatrix},$$

$$C^e = 4 \begin{bmatrix} 1 & -2 & 1 \\ -2 & 4 & -2 \\ 1 & -2 & 1 \end{bmatrix},$$

$$D^e = \frac{1}{6} \begin{bmatrix} -3 & 2 & 1 \\ -8 & 0 & 8 \\ -1 & -2 & 3 \end{bmatrix},$$

$$E^e = 2 \begin{bmatrix} -1 & 0 & 1 \\ 2 & 0 & -2 \\ -1 & 0 & 1 \end{bmatrix},$$

and the element constant value for v is given by

$$v_m = \frac{\Delta t}{\Delta x} (1 + \epsilon[a_{m-1} + a_m]).$$

Formally assembling together contributions from all elements leads to the matrix equation

$$\begin{aligned} [A + 2bB + \frac{1}{3}B_1 + b^2C + \frac{1}{2}(D_1 + D_1^T) - \frac{b}{2}(E_1 + E_1^T)]\Delta\mathbf{a} \\ + [D_1 + \frac{1}{2}B_1 - bE_1]\mathbf{a} = 0, \end{aligned} \quad (8.13)$$

and $\mathbf{a} = (a_{-1}, a_0, \dots, a_N)^T$, contains all the nodal parameters. The matrices A, B, B_1, C, D_1 and E_1 are pentadiagonal and row m of each has the following form:

$$\begin{aligned}
A &: \frac{1}{30}(1, 26, 66, 26, 1) \\
B &: \frac{2}{3}(-1, -2, 6, -2, -1) \\
B_1 &: \frac{2}{3}(-v_{m-1}^2, -v_{m-1}^2 - v_m^2, 2[v_{m-1}^2 + v_m^2 + v_{m+1}^2], -v_m^2 - v_{m+1}^2, -v_{m+1}^2) \\
C &: 4(1, -4, 6, -4, 1) \\
D_1 &: \frac{1}{6}(-v_{m-1}, -2v_{m-1} - 8v_m, 3v_{m-1} - 3v_{m+1}, 8v_m + 2v_{m+1}, v_{m+1}) \\
E_1 &: 2(-v_{m-1}, 2v_m, v_{m-1} - v_{m+1}, -2v_m, v_{m+1}) \\
(D_1 + D_1^T) &: (0, v_{m-1} - v_m, v_{m-1} - v_{m+1}, v_m - v_{m+1}, 0) \\
(E_1^T + E_1) &: 4(0, v_m - v_{m-1}, v_{m-1} - v_{m+1}, v_{m+1} - v_m, 0).
\end{aligned}$$

Hence identifying $\mathbf{a} = \mathbf{a}^n$ and $\Delta \mathbf{a} = \mathbf{a}^{n+1} - \mathbf{a}^n$ we can write Equation (8.13) as

$$\begin{aligned}
& [A + 2bB + \frac{1}{3}B_1 + b^2C + \frac{1}{2}(D_1 + D_1^T) - \frac{b}{2}(E_1 + E_1^T)] \mathbf{a}^{n+1} \\
& = [A + 2bB + \frac{1}{3}B_1 + b^2C + \frac{1}{2}(D_1 + D_1^T) \\
& \quad - \frac{b}{2}(E_1 + E_1^T) - D_1 - \frac{1}{2}B_1 + bE_1] \mathbf{a}^n, \quad (8.14)
\end{aligned}$$

and $\mathbf{a} = (a_{-1}, a_0, \dots, a_N)^T$, contains all the nodal parameters, a scheme for updating u^n to time level $t = (n + 1)\Delta t$. A typical member of (8.14) is

$$\begin{aligned}
& (\frac{1}{5} - 8b - \frac{4}{3}v_{m-1}^2 + 24b^2)a_{m-2}^{n+1} \\
& + (\frac{26}{5} - 16b - \frac{4}{3}[v_{m-1}^2 + v_m^2] - 96b^2 - 12b[v_m - v_{m-1}]) \\
& + 3[v_{m-1} - v_m]a_{m-1}^{n+1} + (\frac{66}{5} + 48b + \frac{8}{3}[v_{m-1}^2 + v_m^2 + v_{m+1}^2] \\
& \quad + 144b^2 + 3[v_{m-1} - v_{m+1}] - 12b[v_{m-1} - v_{m+1}])a_m^{n+1} \\
& + (\frac{26}{5} - 16b - \frac{4}{3}[v_m^2 + v_{m+1}^2] - 96b^2 - 12b[v_{m+1} - v_m])
\end{aligned}$$

$$\begin{aligned}
& +3[v_m - v_{m+1}]a_{m+1}^{n+1} + \left(\frac{1}{5} - 8b - \frac{4}{3}v_{m+1}^2 + 24b^2\right)a_{m+2}^{n+1} \\
= & \left(\frac{1}{5} - 8b - \frac{4}{3}v_{m-1}^2 + 24b^2 + v_{m-1} + 2v_{m-1}^2 - 12bv_{m-1}\right)a_{m-2}^n \\
& + \left(\frac{26}{5} - 16b - \frac{4}{3}[v_{m-1}^2 + v_m^2] - 96b^2 - 12b[v_m - v_{m-1}]\right. \\
& \quad \left.+ 3[v_{m-1} - v_m] + 2v_{m-1} + 8v_m + 2[v_{m-1}^2 + v_m^2]\right. \\
& \quad \left.+ 24bv_m\right)a_{m-1}^n + \left(\frac{66}{5} + 48b + \frac{8}{3}[v_{m-1}^2 + v_m^2 + v_{m+1}^2]\right. \\
& \quad \left.+ 144b^2 + 3[v_{m-1} - v_{m+1}] - 12b[v_{m-1} - v_{m+1}]\right. \\
& \quad \left.+ 3[v_{m+1} - v_{m-1}] - 4[v_{m-1}^2 + v_m^2 + v_{m+1}^2] - 12b[v_{m+1} - v_{m-1}]\right)a_m^n \\
& \quad + \left(\frac{26}{5} - 16b - \frac{4}{3}[v_m^2 + v_{m+1}^2] - 96b^2 - 12b[v_{m+1} - v_m]\right. \\
& \quad \left.+ 3[v_m - v_{m+1}] - 8v_m - 2v_{m+1} + 2[v_m^2 + v_{m+1}^2] - 24bv_m\right)a_{m+1}^n \\
& \quad + \left(\frac{1}{5} - 8b - \frac{4}{3}v_{m+1}^2 + 24b^2 - v_{m+1} + 2v_{m+1}^2 + 12bv_{m+1}\right)a_{m+2}^n
\end{aligned}$$

where v_m is given by

$$v_m = \frac{\Delta t}{\Delta x}(1 + \epsilon[a_m^n + a_{m-1}^n])$$

The boundary conditions $U(0, t) = 0$ and $U(L, t) = 0$ require $u_0 = 0$ and $u_N = 0$. The above set of quasi-linear equations has a matrix which is pentadiagonal in form.

Chapter 9

General Conclusions

In Chapters III, IV and V we have presented a series of numerical algorithms for the solution of the RLW equation. All are based on Petrov-Galerkin finite element methods and include a Galerkin method using linear finite elements, a least squares method also using linear elements and a Petrov-Galerkin method based on quadratic B-spline finite elements together with a piecewise constant weight function. Each approach is validated through a study of the motion of a single solitary wave. Results of other simulations undertaken using the algorithms are discussed in the relevant Sections and in the concluding Sections of each Chapters.

In Chapters VI and VII two numerical algorithms for the solution of Burgers' Equation are described. These are a least squares method using linear elements and a Petrov-Galerkin method based on quadratic B-spline finite elements and a piecewise constant weight function. Each is used to study the evolution of initial conditions for which the analytic solutions are known. Again results are discussed within each Chapter.

All five algorithms lead to recurrence relationships which may be expressed as tridiagonal matrix equations. We would therefore not expect the accuracy of any two methods to differ significantly for the same problem using the same parameters. Our general conclusion, is however, that amongst the schemes examined in this study, the highest accuracy for both the RLW and Burgers' equations is obtained with the Petrov-Galerkin method us-

B-spline finite elements and piecewise constant weight functions, the least accurate is the least squares method with linear elements.

We would therefore recommend using the Petrov-Galerkin method for the solution of the transient non-linear partial differential equation in preference to the least squares method.

The material of Chapters IV and VII have formed the basis for 2 scientific papers. That on the RLW equation has been published already [49], the second on the Burgers' equation is being refereed.

We have begun setting up the least squares method with quadratic B-spline finite elements in Chapter VIII. This work is in progress.

Appendix

Algorithm for the solution of tridiagonal system of equations

Assume the tridiagonal systems of equations has the general form:

$$-a_i\delta_{i-1} + b_i\delta_i - c_i\delta_{i+1} = d_i \quad 0 \leq i \leq N$$

with:

$$a_0 = c_N = 0$$

$$\alpha_0 = b_0, \quad \beta_0 = d_0$$

Then compute the following parameters:

$$\alpha_i = b_i - a_i \frac{c_{i-1}}{\alpha_{i-1}}$$

$$\beta_i = d_i + a_i \frac{\beta_{i-1}}{\alpha_{i-1}}$$

for $i = 1, 2, \dots, n$

Then the solution is given by:

$$\delta_N = \frac{\beta_N}{\alpha_N}$$

$$\delta_i = \frac{(\beta_i + c_i\delta_{i+1})}{\alpha_i}$$

for $i = N - 1, N - 2, \dots, 0$

Bibliography

- [1] ABLOWITZ, M. J., and LADIK, J. F., "Nonlinear Differential-Difference Equations and Fourier Analysis", *J. Math. Phys.*, **17**, 1011-1018, (1976).
- [2] ABLOWITZ, M. J., and CLARKSON, P. A., "Solitons, Nonlinear Evolution Equations and Inverse Scattering", Cambridge University Press, (1991).
- [3] AKIN, J. E., "Application and Implementation of Finite Element Methods", Academic Press, (1982).
- [4] ALEXANDER, M. E., and MORRIS, J. L., "Galerkin Methods Applied to Some Model Equations for Non-Linear Dispersive Waves", *J. Comp. Phys.*, **30**, 428-481, (1979).
- [5] ALI, A. H. A., GARDNER, G. A., and GARDNER, L. R. T., "A Collocation Solution for Burgers' Equation Using Cubic B-Spline Finite Elements", *Comp. Meth. Appl. Mech. Eng.*, **100**, 325-337, (1992).
- [6] ALI, A. H. A., GARDNER, L. R. T., and GARDNER, G. A., "Numerical Studies of the Korteweg-de Vries Burgers Equation using B-Spline Finite Elements", *J. Math. Phys.*, **27**, 37-53, (1993).
- [7] ARCHILLA, B. G., "A Spectral Method for the Equal Width Equation", *J. Comp. Phys.*, **125**, 395-402, (1996).

- [8] BARRETT, K. E., "A Variational Principle for the Stream Function-Vorticity Formulation of the Navier-Stokes Equations Incorporating No-Slip Conditions", *J. Comp. Phys.*, **26**, 153-161, (1978).
- [9] BEAM, R. M., WARMING, R. F., and YEE, H. C., "Stability Analysis of Numerical Boundary Conditions and Implicit Difference Approximations for Hyperbolic Equations", *J. Comp. Phys.*, **48**, 200-222, (1982).
- [10] BEER, G., and MEEK, J. L., "Infinite Domain Elements", *Int. J. Num. Meth. Engng.*, **17**, 43-52, (1981).
- [11] BENJAMIN, T. B., F. R. S., "The Stability of Solitary Waves", *Proc. Roy. Soc., London*, **A328**, 153-183, (1972).
- [12] BENJAMIN, T. B., BONA, J. L., and MAHONY, J. J., "Model Equations for Long Waves in Nonlinear Dispersive Systems", *Phil. Trans. Roy. Soc., London*, **272**, 47-78, (1972).
- [13] BETTESS, P., "Infinite Elements", *Int. J. Num. Meth. Engng.*, **11**, 53-64, (1977).
- [14] BHATTACHARYA, M. C., "Finite-Difference Solutions of the Partial Differential Equations", *Comm. in Appl. Num. Meth.*, **6**, 173-184, (1990).
- [15] BIHARI, B. L., "Multiresolution Schemes for Conservation Laws With Viscosity", *J. Comp. Phys.*, **123**, 207-225, (1996).
- [16] BONA, J. L., and SMITH, R., "The Initial-Value Problem for the Korteweg-de Vries Equation", *Phil. Trans. Roy. Soc., London*, **278**, 555-601, (1975).
- [17] BONA, J. R., and DOUGALIS, V. A., "An Initial and Boundary-Value Problem for a Model Equation for Propagation of Long Waves", *J. Math. Anal. Appl.*, **75**, 503-522, (1980).
- [18] BONA, J. L., PRITCHARD, W. G., and SCOTT, L. R., "Solitary Wave Interaction", *Phys. Fluids*, **23**, 438-441, (1980).

- [19] BONA, J. L., PRITCHARD, W. G., and SCOTT, L. R., "Numerical Schemes for a Model of Nonlinear Dispersive Waves", *J. Comp. Phys.*, **60**, 167-186, (1985).
- [20] BOYD, J. P., "Numerical Computations of a Nearly Singular Nonlinear Equation: Weakly Nonlocal Bound States of Solitons for Fifth-Order Korteweg-de Vries Equation", *J. Comp. Phys.*, **124**, 55-70, (1996).
- [21] BURDEN, R. L., and FAIRES, J. D., "Numerical Analysis", 3rd ed., Prindle, Weber & Schmidt, (1985).
- [22] BURGERS, J., "A Mathematical Model Illustrating the Theory of Turbulence", *Advances in Applied Mechanics*, 171-199, (Academic Press, New York, 1948).
- [23] CALDWELL, J., WANLESS, P., and COOK, A.E., "A Finite Element Approach to Burgers' Equation", *Appl. Math. Modelling*, **5**, 189-193, (1981).
- [24] CALDWELL, J., and SMITH, P., "Solution of Burgers' Equation with a Large Reynolds Number", *Appl. Math. Modelling*, **6**, 381-385, (1982).
- [25] CANOSA, J., and GOZDAG, J., "The Korteweg-de Vries Burgers Equation", *J. Comp. Phys.*, **23**, 393-403, (1977).
- [26] CARDLE, J. A., "A Modification of the Petrov-Galerkin Method for the Transient Convection-Diffusion Equation", *Int. J. Num. Meth. Engng.*, **38**, 171-181, (1995).
- [27] CARRANO, C. S., YEH, G., "A Fourier Analysis and Dynamic optimization of the Petrov-Galerkin Finite Element Method", *Int. J. Num. Meth. Engng.*, **38**, 4123-4155, (1995).
- [28] CHOW, Y. K., and SMITH, I. M., "Static and Periodic Infinite Solid Elements", *Int. J. Num. Meth. Engng.*, **17**, 503-526, (1981).

- [29] CHRISTIE, I., GRIFFITHS, D. F., and MITCHELL, A. R., SANZ-SERNA, J. M., "Product Approximation for Non-linear Problems in the Finite Element Method", *IMA J. Num. Anal.*, **1**, 253-266, (1981).
- [30] CHU, C. K., XIANG, L. W., and BARANSKY, Y., "Solitary Waves Induced by Boundary Motion", *Comm. Pure Appl. Math.*, **36**, 495-504, (1983).
- [31] CLOUGH, R. W., "The Finite Element Method in Plane Stress Analysis", *J. Struct. Div., ASCE, Proc. 2nd Conf. Electronic Computation*, 345-378, (1960).
- [32] COLE, J. D., "On a Quasi-Linear Parabolic Equation Occurring in Aerodynamics", *Quart. J. Appl. Math.*, **9**, 225-236, (1951).
- [33] CURNIER, A., "A Static Infinite Element", *Int. J. Num. Meth. Engng.*, **19**, 1479-1488, (1983).
- [34] DAVIES, A. M., "The Use of the Galerkin Method with a Basis of B-Splines for the Solution of the One-Dimensional Primitive Equations", *J. Comp. Phys.*, **27**, 123-137, (1978).
- [35] DAVIES, A. J., "The Finite Element Method: A First Approach", Clarendon Press Oxford, (1980).
- [36] DHATT, G., and TOUZOT, G., "The Finite Element Method Displayed", John Wiley & Sons, (1984).
- [37] EILBECK, J. C., and MCGUIRE, G. R., "Numerical Study of the Regularized Long-Wave Equation I: Numerical Methods", *J. Comp. Phys.*, **19**, 43-62, (1945).
- [38] EILBECK, J. C., and MCGUIRE, G. R., "Numerical Study of the Regularized Long-Wave Equation. II: Interaction of Solitary Waves", *J. Comp. Phys.*, **23**, 63-73, (1977).
- [39] EVANS, D. J., and ABDULLAH, A. R., "The Group Explicit Method for the Solution of Burgers' Equation", *Computing*, **32**, 239-253, (1984).

- [40] GARDNER, L. R. T., and GARDNER, G. A., "Solitary Waves of the Regularised Long Wave Equation", *J. Comp. Phys.*, **91**, 441-459, (1990).
- [41] GARDNER, L. R. T., and GARDNER, G. A., ZAKI S. I., and EL SAHRAWI Z., "B-Spline Finite Element Studies of the Non-linear Schrodinger Equation", *Comp. Meth. Appl. Mech. Eng.*, **108**, 303-318, (1993).
- [42] GARDNER, L. R. T., GARDNER, G. A., and ZAKI, S. I., "Collisional Effects in Plasmas Modelled by a Simplified Fokker-Planck Equation", *J. Comp. Phys.*, **107**, 40-50, (1993).
- [43] GARDNER, L. R. T., GARDNER, G. A., and DAG, I., "Hermite Infinite and Graded Quadratic B-Spline Finite Elements", *Int. J. Num. Meth. Engng.*, **36**, 3317-3332, (1993).
- [44] GARDNER, L. R. T., GARDNER, G. A., GEYIKLI, T., "Solitary Wave Solutions of the MKdV-Equation", *Comp. Meth. Appl. Mech. Eng.*, **124**, 321-333, (1995).
- [45] GARDNER, L. R. T., GARDNER, G. A., and DAG, I., "The Boundary-Forced Regularised Long-Wave Equation", *Nuovo Cimento*, **10B**, 1487-1496, (1995).
- [46] GARDNER, L. R. T., GARDNER, G. A., and DAG, I., "A B-Spline Finite Element Method for the RLW Equation", *Comm. Num. Meth. Eng.*, **11**, 59-68, (1995).
- [47] GARDNER, L. R. T., GARDNER, G. A., "A two dimensional bi-cubic B-Spline Finite Element: Used in a Study of MHD-duct flow", *Comp. Meth. Appl. Mech. Eng.*, **124**, 365-375, (1995).
- [48] GARDNER, L. R. T., GARDNER, G. A., and DAG, I., "The Boundary Forced RLW Equation", *Nuovo Cimento*, **110B**, 1487-1496, (1995).

- [49] GARDNER, L. R. T., GARDNER, G. A., and DOGAN, A., "A Least-Squares Finite Element Scheme for the RLW Equation", *Comm. Num. Meth. Eng.*, **12**, 795-804, (1996).
- [50] GARDNER, L. R. T., GARDNER, G. A., and DOGAN, A., "A Least Squares Finite Element Scheme for Burgers' Equation", *U.C.N.W. Maths Preprint*, 96.01.
- [51] GARDNER, L. R. T., GARDNER, G. A., and DOGAN, A., "A Least Squares Finite Element Scheme for the RLW Equation", *U.C.N.W. Maths Preprint*, 96.02.
- [52] GARDNER, L. R. T., GARDNER, G. A., and DOGAN, A., "A Galerkin Finite Element Scheme for the RLW Equation", *U.C.N.W. Maths Preprint*, 96.03
- [53] GARDNER, L. R. T., GARDNER, G. A., and DOGAN, A., "A Petrov-Galerkin Scheme for Burgers' Equation", *U.C.N.W. Maths Preprint*, 96.06
- [54] GARDNER, L. R. T., GARDNER, G. A., and DOGAN, A., "A Petrov-Galerkin Algorithm for the RLW Equation", *U.C.N.W. Maths Preprint*, 96.09.
- [55] GARDNER, L. R. T., GARDNER, G. A., and DOGAN, A., "A Petrov-Galerkin Scheme for Burgers' Equation", *The Arab. J. Science and Eng.*, in press.
- [56] GREIG, I. S., and MORRIS, J. L., "A Hopscotch Method for the Korteweg-de-Vries Equation", *J. Comp. Phys.*, **20**, 64-80, (1976).
- [57] HALD, O. H., "Convergence of Fourier Methods for Navier-Stokes Equations", *J. Comp. Phys.*, **40**, 305-317, (1981).
- [58] HAMMACK, J. L., "A Note on Tsunamis: Their Generation and Propagation in an Ocean of Uniform Depth", *J. Fluid Mech.*, **60**, 769-799, (1973).

- [59] HENDREY, J. A., and DELVES, L. M., "The Global Element Method Applied to a Harmonic Mixed Boundary Value Problem", *J. Comp. Phys.*, **33**, 33-44, (1979).
- [60] HERBEST, B. M., SCHOOMBIE, S. W., and MITCHELL, A. R., "A Moving Petrov-Galerkin Method for Transport Equations", *Int. J. Num. Meth. Engng.*, **18**, 1321-1336, (1982).
- [61] HOPF, E., "The Partial Differential Equation $u_t + uu_x = \mu u_{xx}$ ", *Comm. Pure Appl. Math.*, **9**, 201-230, (1950).
- [62] HUNG, T., and BROWN, T. D., "An Implicit Finite-Difference Method for Solving the Navier-Stokes Equation Using Orthogonal Curvilinear Coordinates", *J. Comp. Phys.*, **23**, 343-363, (1977).
- [63] IDELSOHN, S. R., HEINRICH, J. C., and ONATE E., "Petrov-Galerkin Methods for the Transient Advective-Diffusive Equation with Sharp Gradients", *Int. J. Num. Meth. Engng.*, **39**, 1455-1473, (1996).
- [64] JAIN, P. C., SHANKAR, R., and SINGH, T. V., "Numerical Solutions of Regularized Long Wave Equation", *Comm. Num. Meth. Eng.* **9**, 579-586, (1993).
- [65] JEFFREY, A., and KAKUTANI, T., "Weak Nonlinear Dispersive Waves: A Discussion Centered Around the Korteweg-de Vries Equation", *Siam Review*, **14**, 582-643, (1972).
- [66] JOHNSON, R. S., "Some Numerical Solutions of a Variable-Coefficient Korteweg-de Vries Equation", *J. Fluid Mech.*, **54**, 81-91, (1972).
- [67] KAKUDA, K., and TOSAKA, N., "The Generalized Boundary Element Approach to Burgers' Equation", *Int. J. Num. Meth. Engng.*, **29**, 245-261, (1990).
- [68] KNICKERBOCKER, C. J., and NEWELL, A. C., "Shelves and The Korteweg-de Vries Equation", *J. Fluid Mech.*, **98**, 803-818, (1980).

- [69] KRUSKAL, M. D., MIURA, R. M., and GARDNER, C. S., and ZABUSKY, N. J., "Korteweg-de Vries Equation and Generalizations. V. Uniqueness and Nonexistence of Polynomial Conservation Laws", *J. Math. Phys.*, **11**, 952-960, (1970).
- [70] LAX, P. D., "Integrals of Nonlinear Equations of Evolution and Solitary Waves", *Comm. Pure Appl. Math.*, **21**, 467-490, (1968).
- [71] LAX, P. D. , "Almost Periodic Solutions of the KdV Equation", *Siam Review*, **18**, 351-375, (1976).
- [72] LOHAR, B. L., and JAIN, P. C., "Variable Mesh Cubic Spline Technique for N-Wave Solution of Burgers' Equation", *J. Comp. Phys.*, **39**, 433-442, (1981).
- [73] LYNN, P. P., HADID, H. A., "Infinite Elements with $\frac{1}{r^n}$ Type Decay", *Int. J. Num. Meth. Engng.*, **17**, 347-355, (1981).
- [74] MANORANJAN, V. S., MITCHELL, A. R., and MORRIS, J. L., "Numerical Solutions of the Good Boussinesq Equation", *SIAM J. Stat. Comput.*, **5**, 946-957, (1984).
- [75] MANORANJAN, V. S., ORTEGA, T., and SANZ-SERNA, J. M., "Soliton and Antisoliton Interactions in the "good" Boussinesq Equation ", *J. Math. Phys.*, **29**, 1964-1968, (1988).
- [76] MEDINA, F., TAYLOR, R. L., "Finite Element Techniques for Problems of Unbounded Domains", *Int. J. Num. Meth. Engng.*, **19**, 1209-1226, (1983).
- [77] MENIKOFF, A., "The Existence of Unbounded Solutions of the Korteweg-De Vries Equation", *Comm. Pure Appl. Math.*, **25**, 407-432, (1972).
- [78] MILLER, K., and MILLER, R. N., "Moving Finite Elements.", *Siam J. Numer. Anal.*, **18**, 1019-1032, (1981).

- [79] MITTAL, R. C., and SINGHAL, P., "Numerical Solution of Burgers' Equation", *Comm. Num. Meth. Eng.*, **9**, 397-406, (1993).
- [80] MIURA, R. M., "Korteweg-de Vries Equation and Generalizations. I. A Remarkable Explicit Nonlinear Transformation", *J. Math. Phys.*, **9**, 1202-1204, (1968).
- [81] MIURA, R. M., "The Korteweg-de Vries Equation : A Survey of Results", *SIAM Review*, **18**, 412-459, (1976).
- [82] MORTON, K. W., and PARROTT, A. K., "Generalised Galerkin Methods for First-Order Hyperbolic Equations", *J. Comp. Phys.*, **36**, 249-270, (1980).
- [83] NGUYEN N. and REYNEN J., "A Space-Time Finite Element Approach to Burgers' Equation", in *Numerical Methods for non-linear problems*, **2**, (Ed. C. Taylor, E. Hinton, D. R. J. Owen and E. Onate), 718-728 (Pineridge, 1982).
- [84] NGUYEN, N., and REYNEN, J., "A Space-Time Least-Square Finite Element Scheme for Advection-Diffusion Equations", *Comp. Meth. Appl. Mech. Engng.*, **42**, 331-342, (1984).
- [85] OLVER, P. J., "Evolution Equations Possessing Infinitely Many Symmetries", *J. Math. Phys.*, **18**, 1212-1215, (1977).
- [86] OLVER, P. J., "Euler Operators and Conservation Laws of the BBM Equation", *Math. Proc. Camb. Phil. Soc.*, **85**, 143-159, (1979).
- [87] PATRICIO, F., "Implicit Methods for Diffusion-Convection Equations", *Comm. in Appl. Num. Meth.*, **6**, 27-33, (1990).
- [88] PAYNE, L. E., "On the Stability of Solutions of the Navier-Stokes Equations and Convergence to Steady State", *Siam J. Appl. Math.*, **15**, 392-405, (1967).
- [89] PEREGRINE, D. H., "Calculations of the Development of an Undular Bore", *J. Fluid Mech.*, **25**, 321-330, (1966).

- [90] PISSANETZKY, S., "An Infinite Element and a Formula for Numerical Quadrature over an Infinite Interval", *Int. J. Num. Meth. Engng.*, **19**, 913-927, (1983).
- [91] POWELL, M. J. D., "The Local Dependence of Least Squares Cubic Splines", *SIAM J. Numer. Anal.*, **6**, 398-413, (1969).
- [92] REDDY, J. N., "An Introduction to the Finite Element Method", McGraw-Hill, Inc., (1985).
- [93] SANZ-SERNA, J. M., and Christie, I., "Petrov-Galerkin Methods for Nonlinear Dispersive Waves", *J. Comp. Phys.*, **39**, 94-102, (1981).
- [94] SJOBERG, A., "On the Korteweg-de Vries Equation: Existence and Uniqueness", *J. Math. Anal. Appl.*, **29**, 569-579, (1970).
- [95] SU, C. H., and GARDNER, C. S., "Korteweg-de Vries Equation and Generalizations. III. Derivation of the Korteweg-de Vries Equation and Burgers Equation", *J. Math. Phys.*, **10**, 536-539, (1969).
- [96] SULLIVAN, J. M., O'NEILL, K., "Application of Infinite Elements to Phase Change Situations On Deforming Meshes", *Int. J. Num. Meth. Engng.*, **33**, 1861-1874, (1992).
- [97] VAN ERP, G. M., and MENKEN C. M., "The Spline Finite Strip Method in the Buckling Analyses of Thin-Walled Structures", *Comm. in Appl. Num. Meth.*, **6**, 477-484, (1990).
- [98] VAROGLU, E., and FINN, W. D. L., "Finite Elements Incorporating Characteristics for One-Dimensional Diffusion-Convection Equation", *J. Comp. Phys.*, **34**, 371-389, (1980).
- [99] VAROGLU, E., and FINN, W. D. L., "Space Time Finite Elements Incorporating Characteristics Burgers' Equation", *Int. J. Num. Meth. Engng.*, **16**, 171-184, (1980).